

# **SILICA-SILANE REINFORCED PASSENGER CAR TIRE TREADS**

EFFECT OF SILICA MORPHOLOGY, SILICA-POLYMER  
INTERFACE STRUCTURE AND RUBBER MATRIX NETWORK  
ON TIRE-PERFORMANCE INDICATORS

Silica-silane reinforced passenger car tire treads

Effect of silica morphology, silica-polymer interface structure and rubber matrix network  
on tire-performance indicators

By Ernest Cichomski

Ph.D thesis, University of Twente, Enschede, the Netherlands, 2015.

With references – With summary in English and Dutch.

Copy right © Ernest Cichomski, 2015.

All right reserved.

Cover design by Ernest Cichomski

Printed by Print Partners Ipskamp, P.O. Box 333, 7500 AH Enschede, the  
Netherlands.

ISBN: 978-90-365-3890-9

# **SILICA-SILANE REINFORCED PASSENGER CAR TIRE TREADS**

**EFFECT OF SILICA MORPHOLOGY, SILICA-POLYMER  
INTERFACE STRUCTURE AND RUBBER MATRIX NETWORK  
ON TIRE-PERFORMANCE INDICATORS**

DISSERTATION

to obtain

the degree of doctor at the University of Twente,

on the authority of the rector magnificus

Prof.dr. H. Brinksma

on account of the decision of the graduation committee,

to be publicly defended

on Friday 29<sup>th</sup> of May 2015 at 12:45

by

Ernest Michał Cichowski

born on 22<sup>nd</sup> of September 1981

in Łódź, Poland

This dissertation has been approved by:

Promotor: prof. dr. ir. J. W. M. Noordermeer

Co-promotor: Dr. Wilma K. Dierkes

*Learn from yesterday, live for today, hope for tomorrow. The important thing is not to stop questioning.*

**Albert Einstein**

*To Rima*

# **SILICA-SILANE REINFORCED PASSENGER CAR TIRE TREADS**

**EFFECT OF SILICA MORPHOLOGY, SILICA-POLYMER  
INTERFACE STRUCTURE AND RUBBER MATRIX NETWORK  
ON TIRE-PERFORMANCE INDICATORS**

DISSERTATION

to obtain

the degree of doctor at the University of Twente,

on the authority of the rector magnificus

Prof.dr. H. Brinksma

on account of the decision of the graduation committee,

to be publicly defended

on Friday 29<sup>th</sup> of May 2015 at 12:45

by

**Ernest Michał Cichomski**

born on 22<sup>nd</sup> of September 1981

in Łódź, Poland

## *Table of contents*

---

|                         |  |     |
|-------------------------|--|-----|
| <b>Chapter 1</b>        | Introduction .....   | 1   |
| <b>Chapter 2</b>        | Tire properties and performance and correlations<br>with rubber properties .....   | 7   |
| <b>Chapter 3</b>        | Influence of the silica specific surface area and structure<br>on rolling and wet skid resistance of a passenger car tire<br>tread compound .....  | 63  |
| <b>Chapter 4</b>        | Influence of physical and chemical polymer-filler bonds<br>on tire wet traction performance indicators for passenger<br>car tire tread materials .....   | 97  |
| <b>Chapter 5</b>        | Influence of modification of the silane coupling agent on<br>wet-traction and rolling resistance performance indicators<br>for passenger car tire tread materials: Influence of number<br>of ethoxy groups ..... | 117 |
| <b>Chapter 6</b>        | Modification of the silane coupling agent for improvement<br>of wet traction and rolling resistance: Influence of the length<br>of the aliphatic linker .....  | 140 |
| <b>Chapter 7</b>        | Modification of the silane coupling agent for improvement<br>of wet traction and rolling resistance: Influence of the type<br>of alkoxy group.....   | 159 |
| <b>Chapter 8</b>        | Effect of the crosslink density and sulfur-length on wet-traction<br>and rolling resistance performance indicators for passenger<br>car tire tread materials .....   | 180 |
| <b>Chapter 9</b>        | Summary.....   | 202 |
|                         | Samenvatting .....   | 208 |
| <b>Annex 1</b>          | Publications and papers.....   | 215 |
| <b>Annex 2</b>          | Symbols and abbreviations .....  | 218 |
| <b>Curriculum vitae</b> | .....  | 221 |
| <b>Acknowledgments</b>  | .....  | 222 |





### Introduction

---

Identifying the inventor of the vulcanization process is complex. Charles Goodyear (1800–1860) is generally credited as the first to formulate the basic concept. However, he never fully understood the process. On the other hand, Thomas Hancock (1786–1865), a British scientist and engineer, was the first to patent vulcanization of rubber and indeed, he understood vulcanization better than Goodyear and was likely inspired by seeing Goodyear's earlier samples. Hancock was awarded a British patent on May 21, 1844. Three weeks later, Goodyear was awarded a patent in the United States <sup>1</sup>

The history of synthetic rubber started with Michael Faraday who had shown in 1829 that rubber had the empirical formula  $C_5H_8$ . In 1860, Greville Williams obtained a liquid with the same formula by dry distillation of natural rubber; he called it “isoprene”. Synthetic rubber technology started further in 1879, when Gustave Bouchardat found that heating isoprene with hydrochloric acid produced a rubberlike polymer. However, Bouchardat had obtained isoprene from natural rubber; the first truly synthetic rubber was made by William Tilden three years later. Tilden obtained isoprene by cracking turpentine, but the process of converting it to rubber took several weeks. In 1911 Francis Matthews and Carl Harries discovered, independently, that isoprene could be polymerized more rapidly by sodium <sup>2</sup>.

Through the 1920's, synthetic rubber research was influenced by fluctuations of the price of natural rubber. Prices were generally low, but export restrictions of natural rubber from British Malaya introduced by the British in 1922, coupled with the resultant price increase, sparked the establishment of modest synthetic rubber research programs in the Soviet Union, Germany and the United States between 1925 and 1932. Researchers at I. G. Farben, a German conglomerate that included Bayer, focused on the sodium polymerization of the monomer butadiene to produce a synthetic rubber called “Buna” (“bu” for butadiene and “na” for natrium, the chemical symbol for sodium).

The brake-tough came with the discovery in 1929 that Buna S (butadiene and styrene randomly co-polymerized in emulsion), when compounded with carbon black, was significantly more durable than natural rubber.

Carbon black can be considered as a one of the oldest manufactured products and its usage as a pigment of India inks and mural paints can be traced back to the ancient Chinese and Egyptians. The most important event which had the greatest influence on the usage of carbon black occurred at the beginning of the former century and involved the discovery of the reinforcing effect of carbon blacks when added to natural rubber, a discovery that was to become one of the most significant milestones in the rubber and automotive industry. By using carbon black as a reinforcing filler the service life of a tire was greatly increased, ultimately making it possible to achieve a range of several ten thousand kilometers.<sup>3</sup>

Since the early nineteen-forties, carbon blacks have been complemented by the group of highly active silicas. Technological reasons have long prevented silicas from being used in tire compounds. Conventionally, carbon black is considered to be a more effective reinforcing filler for rubber tire treads than silica, if the silica is used without a coupling agent. In comparison with carbon black there tends to be a lack of, or at least an insufficient degree of physical and/or chemical bonding between the silica particles and the rubber. This is necessary to enable the silica to become a reinforcing filler for the rubber for most purposes, including tire treads. To overcome such deficiencies, additives capable of reacting with both the silica surface and the rubber molecules, generally known as coupling agents became a necessity during compounding<sup>4</sup>. Silica offers several advantages over carbon black. In tire treads, silica yields a comparable wear resistance and better wet grip in combination with a lower rolling resistance than carbon black when used in combination with a coupling agent<sup>5,6</sup>.

Since rubber and carbon black are both hydrophobic substances, problems rarely arise when the two are mixed. When silica is mixed however with the commonly used non-polar, olefinic hydrocarbon rubbers, there will be a greater occurrence of hydrogen-bond interactions between surface silanol groups in silica agglomerates than of interactions between polar siloxane or silanol groups and the rubber, so mixing silica with rubber involves major problems<sup>7</sup>. For this reason there is great interest in the

possibility of enhancing the compatibility of hydrocarbon rubbers and precipitated silica by modifying the surface of the silica. Bifunctional organosilanes are commonly used to chemically modify the silica surface in order to promote interactions with hydrocarbon rubbers. The most widely used organo-silane for tire applications nowadays is bis(triethoxysilylpropyl) tetrasulfide (TESPT)<sup>8</sup>. In the late 60's of last century a silane coupling agent such as 3-mercaptopropyltrimethoxyl silane was applied in silica filled rubber to improve the reinforcing properties. This silane had a scorch problem: the tendency to prematurely vulcanize during processing. Therefore, the new silane bis-(3-triethoxysilylpropyl) tetrasulfide was introduced by Degussa in 1972<sup>9,10,11</sup>. Michelin was the pioneer in the silica technology and the partial substitution of carbon black by silica in 1992 helped launch its first generation of low fuel consumption 'Green Tires'.

The use of silica can result in a reduction in rolling resistance of 20 % and more, relative to carbon black. Assuming correct tire pressures are maintained and making allowance for varying speeds and different driving characteristics, a 20 % reduction in rolling resistance according to Michelin corresponds to appr. 5 % fuel savings<sup>12</sup>.

Due to the increased use of silica for reinforcement in tire technology and its potential in other rubber applications, it is generally felt that a further study of the mechanism of silica adhesion, or compatibilization with the rubber matrix by coupling agents, is appropriate.

## **1.2 AIM OF THIS THESIS**

The aim of the investigations in the present thesis is to aid the understanding of the underlying mechanisms involved in rubber-filler interactions for the wet skid and rolling resistances of tires, a dynamic viscoelastic phenomenon. Despite many studies on the performance of tire tread compounds, thorough knowledge of the influence of the characteristics of silica reinforcing fillers on wet skid and rolling resistance is still limited. Another important element is the chemical structure of the silane coupling agent which determines the polymer-filler interactions and influences the wet skid and rolling resistances. The chemical structure of the coupling agent determines the silanization kinetics and reactivity towards the polymer. The use of silane coupling agents is related

with the application of chemistry in equipment which is designed for physical processes only: the mixing of carbon black, and this causes limitations during processing. One of the main obstacles is the generation of ethanol from the reaction of the silane with the silanol moieties on the silica surface during the mixing process. Another problem is related with the adsorption of byproducts of the silanization onto the silica surface and their negative effects on the final properties.

### **1.3 STRUCTURE OF THIS THESIS**

Chapter 2: briefly describes the influence of major compounding ingredients: diverse filler systems, polymer functionalization and type of silane coupling agent on the reinforcement mechanisms of rubbers with emphasis on tire wet skid and rolling resistance related properties.

This thesis encompasses 6 experimental chapters:

Chapter 3: Is a comparative study of five different reinforcing silica types concerning their influence on properties related to tire performance. The silicas are characterized by different specific surface areas, aggregate sizes and structure, but with otherwise comparable properties. The value of the dynamic loss tangent,  $\tan \delta$  at 60 °C is used to assess the influence on rolling resistance, and a Laboratory Abrasion Tester (LAT 100) is used to evaluate the wet skid resistance of the tested compounds

Chapter 4: In this chapter a series of compounds with two fundamentally different polymer-filler interphases is examined: one with chemical bonds, another with physical interaction. These interphases are obtained by two different silane coupling agents from which one is unable to form chemical bonds between filler and polymer. This leads to changes in macroscopic material properties including wet skid resistance.

Chapter 5: A study of the effect of the number of ethoxy-groups in the silane coupling agent on the macroscopic dynamic compound properties as indicators for tire performance. Silanes with just one ethoxy-group instead of three as commonly used, are

expected to decrease rolling resistance and to improve wet skid resistance, based on the changes in hysteresis caused by the structural changes of the silane.

Chapter 6: Deals with the hydrocarbon-chain or simply the linker within the silane coupling agent. In order to investigate the influence of the linker length on the wet skid and rolling resistance indicators, a silane with a decyl-linker, bis-(triethoxysilyldecyl)-tetrasulfide (TESDeT), is compared with bis-(triethoxysilylpropyl) tetrasulfide (TESPT) on equimolar basis.

Chapter 7: The type of alkoxy-groups of the silane coupling agent determines the silanization rate and the kind of alcohol evolved during the silanization reaction. Therefore, independent of the reactivity of the silane towards the silica surface and of the reactivity towards the polymer chain, the physical and chemical properties of byproducts of the silanization reaction are of great importance for the material performance. To investigate the influence of the alkoxy-group on the wet skid and rolling resistance related properties, two silanes differing in type of alkoxy-group but with otherwise comparable structures are synthesized. One silane with methoxy-groups, bis-(dimethylmethoxysilylpropyl) tetrasulfide (MMeOS), was chosen due to its high silanization rate, and bis-(dimethylmethoxyethoxysilylpropyl) tetrasulfide (MMeOEtOS) for its increased affinity of the hydrolysable group towards the silica surface. Both silanes are compared with the reference silane TESPT.

Chapter 8: The scope of this chapter is to study the influence of different sulfur vulcanization systems for silica reinforced SBR/BR blends on the performance indicators of tire treads made thereof. Three series of compounds are prepared: with conventional, semi-efficient and efficient vulcanization systems. Each vulcanization system results in a specific overall crosslink density and different sulfur rank distribution: mono-, di- and polysulfidic of nature.

Chapter 9 contains the summary of this thesis.

## REFERENCES

---

- [1] 1493: Uncovering the New World Columbus Created. Random House Digital, Inc., Knopf (2013) 244.
- [2] U.S. Synthetic Rubber Program, University of Akron, Ohio (1998).
- [3] Carbon Black: Science and Technology, Second Edition, Jean-Baptiste Donnet, CRC Press (1993).
- [4] D. J. Zanzig, P. H. Sandstrom, M. J. Crawford, J. J. A. Verthe and C. A. Losey (to The Goodyear Tire & Rubber Company), EP 0 638 610 A1 (27-07-1994).
- [5] Degussa, Organosilanes for the rubber industry, technical inf. (1995).
- [6] M. P. Wagner, Rubber Chem. Technol., 49 (1976) 703.
- [7] R. W. Cruse et al., Rubber & Plastics News, (17 April 1997) 14.
- [8] US. Pat. 3,768,537 PPG industries Inc., R.H. Hess et al. (1973).
- [9] S. Wolff, Rubber Chem. Technol., 69 (1996) 325.
- [10] S. Wolff, Kautsch. Gummi Kunstst., 34 (1981) 280.
- [11] F. Thum, S. Wolff, Kautsch. Gummi Kunstst., 28 (1975) 733.
- [12] Internet Page, [www.tyres-online.co.uk/technology/silica.asp](http://www.tyres-online.co.uk/technology/silica.asp).



## Tire properties and performance and correlations with rubber properties

### 2.1.1 Rolling resistance

Rolling resistance can be expressed as a resistance (force directed opposite to movement direction) that occurs during rolling of circular objects on surfaces. About thirty percent of energy released during combustion of fuel in the engine of a vehicle is used to overcome the rolling resistance of the tire (Figure 1). The main reason for this energy loss is a phenomenon known as hysteresis <sup>1</sup>.

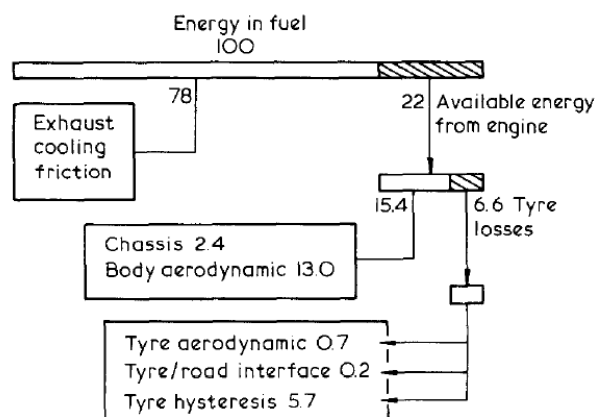


Figure 1: Energy losses of a medium size car travelling at an average speed of 80 km/h <sup>1</sup>

There is a good correlation between rolling resistance of a tire and the loss tangent ( $\tan \delta$ ) at 60 – 80°C of the rubber used for the tire tread material <sup>2</sup>. For that reason, rolling resistance can be predicted from the dynamic mechanical analysis data, which are measured in a temperature sweep mode. A low  $\tan \delta$  value at temperatures of the rolling tire is an indication for low rolling resistance. In contrast to wet skid resistance, rolling resistance is a low frequency phenomenon: <sup>1</sup>

- Rolling conditions (rolling resistance)



- relatively low frequency (up to 120 Hz)
- relatively low temperature (50°C for passenger tires)
- Sliding conditions (wet skid)
  - relatively high frequency (50 kHz – 1 MHz)
  - relatively high temperature (100 – 150°C)

The rolling resistance of a tire depends on several parameters:

- Surface texture of the road
- Tire composition
- Tire service temperature
- Weather conditions

Surface roughness of the road on which the tire moves is an important factor. The frequencies for rolling and sliding given above are the result of the speed of a vehicle and texture roughness of the surface on which the tire is moving <sup>3</sup>. Micro and macro texture roughness act as contact points between the surface of the tire tread and the road. There are two scales of road texture: <sup>1</sup>

- Macro-texture levels
  - aggregate particle size 6 – 12 mm
  - interparticle spacing 1 – 4 mm
  - absolute texture depth 1 – 3 mm
- Micro-texture levels
  - 10 – 100 μm

From the material point of view, the hysteresis (H) is the most important characteristic for the energetic balance. It is defined as energy loss divided by the total energy in a kinematic deformation cycle (Equation 1).

$$H = \frac{\text{Energy loss}}{\text{Total energy}} \quad \text{Equation 1}$$

During dynamic stress, a part of the energy applied to rubber is converted into heat (heat buildup of a tire) as a result of internal friction between filler particles and filler and polymer chains. Because of the heat buildup, the temperature of the moving tire rises until it reaches equilibrium with a cooling medium (environmental conditions). In most of the cases, the temperature of a moving tire is 60 – 80°C.

The energy input into a viscoelastic material can be described in a sinusoidal shear deformation  $\gamma(t)$  of angular frequency  $\omega$ . The shear stress response of a material  $\sigma(t)$  is also sinusoidal, but out of phase with the strain:

$$\gamma(t) = \gamma_0 \sin(\omega t) \quad \text{Equation 2}$$

$$\sigma(t) = \sigma_0 \sin(\omega t + \delta) = (\sigma_0 \cos \delta) \sin \omega t + (\sigma_0 \sin \delta) \cos \omega t \quad \text{Equation 3}$$

Where  $\gamma_0$  is the maximum strain amplitude,  $\sigma_0$  is the shear response at maximum strain, and  $t$  is the time. A delayed response on shear stress of a rubbery material is shown in Figure 2.

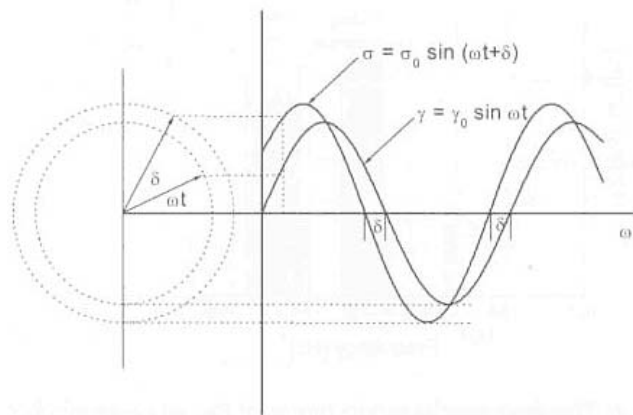


Figure 2: Illustration of the phase angle for the delay of the stress response on sinusoidal deformation

The shear stress signal can be divided into two contributions: one in phase with the strain and one 90° out of phase with the strain. These components are called storage ( $G'$ ) and loss modulus ( $G''$ ) and can be expressed as follows:

$$G' = \frac{\sigma_0}{\gamma_0} \cos \delta \quad \text{Equation 4}$$

$$G'' = \frac{\sigma_0}{\gamma_0} \sin \delta \quad \text{Equation 5}$$

The ratio of the above mentioned loss modulus and storage modulus is called the mechanical loss tangent (Equation 6). This material parameter represents its ability for energy storage or dissipation.

$$\tan \delta = \frac{G''}{G'} \quad \text{Equation 6}$$

In a  $\tan \delta$  – temperature plot as shown in Figure 3, the maximum of the curve is easy to detect; it represents the temperature at which the energy loss of a compound has a maximum.

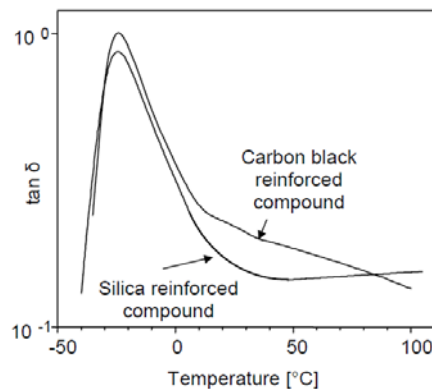


Figure 3: The loss tangent vs. temperature curve obtained for carbon black and silica filled compounds <sup>4</sup>.

For low rolling resistance, the tire tread material should have hysteretic energy losses as low as possible. The main cause of hysteresis is breakdown and reformation of the filler aggregates (the filler-filler network) under dynamic strain and sliding of polymer chains along the filler surface due to weak interactions between filler and elastomer. The filler-filler network is also relatively weak and breaks easily under the influence of strain, causing energy losses. In order to decrease the  $\tan \delta$  value at higher

temperatures, the network between the filler agglomerates should be less developed and the filler-elastomer interaction should be increased, preferably by a chemical interaction. It must clearly be stated that these two conditions should be satisfied at once. This means that for example for rubber, in which the filler is very well dispersed but which has only physical interactions with the elastomer matrix, hysteresis still will be high. This is the case for carbon black.

In rubber compounds, there are three parameters that can be varied in order to change the dynamic properties of the material: *the filler, the polymer and the crosslink type and density*. A lower hysteresis can be obtained by adjusting these parameters.

Concerning the filler, a good dispersion and filler-polymer interaction are required.

Decreased rolling resistance can be also obtained by using polymer blends. Thanks to a low glass transition temperature of  $-90^{\circ}\text{C}$ , butadiene rubber will reduce the hysteresis when it is blended with SBR, resulting in lower rolling resistance. However, unfortunately the wet skid resistance will also suffer. Polymers with a high primary chain molecular weight also contribute to reduced hysteresis <sup>4</sup>. High values of molecular weight, meaning long polymer chains, result in a more restricted polymer chain movement than in case of shorter and more plastic polymers.

### **2.1.2 Wet skid resistance**

While rolling resistance is a very important property from an economical point of view, the performance during braking is a safety issue. Therefore, a shorter breaking distance significantly improves the safety of traffic, on dry as well as on wet roads. There is a fundamental difference between breaking on dry and breaking on wet surfaces: The distance of breaking on wet surfaces is significantly longer than on dry surfaces. This is the result of the lubrication influence of water. It has been widely accepted that the dynamic properties of tread compounds, namely  $\tan \delta$  at low temperatures and high frequencies, are an indicator of wet skid resistance due to the high frequency nature of the dynamic strain involved <sup>5</sup>.

When the *green tire*, a tire with a tread of a low hysteresis material, was commercialized, it was found that besides low rolling resistance, this tire featured better wet skid

resistance <sup>5</sup>. This was achieved by replacing carbon black by a silica-coupling agent system. This improvement in tire performance can be explained in two ways:

- (I) As a consequence of the dynamic properties of the silica filled tire tread material;
- (II) As a consequence of the hydrophilic surface properties of the tire tread material filled with silica.

The first phenomenon is explained by the differences in dynamic properties of silica filled and carbon black filled rubber. The main difference between these two materials lays in a higher hysteresis at lower temperatures, and a lower hysteresis at higher temperatures of silica filled compounds. As can be seen in Figure 4, wet skid resistance improves along with increasing glass transition temperature.

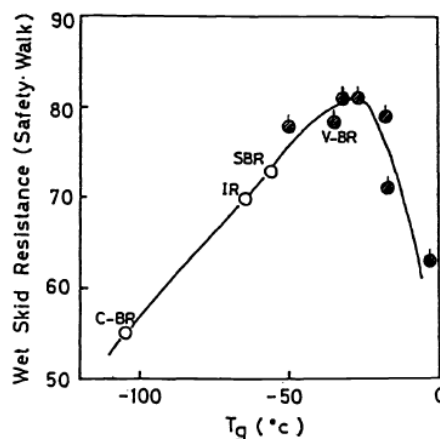


Figure 4: Relation between glass transition temperature and wet skid resistance C-BR, V-BR (respectively conventional vinyl content and high vinyl content polybutadiene rubber), IR and SBR <sup>3</sup>

However, a maximum is visible implying that there is only one optimal glass transition temperature for wet skid resistance. Therefore polymers with very high glass transition temperatures perform worse in terms of wet skid resistance, as they are beyond the optimum range. When the frequency of deformation reaches the natural resonance

frequency of the polymer, energy dissipation shows maximum; this point is called the glass transition. There is also a specific range which coincides with the frequency of the tire under service conditions.

Considering the two facts that

- (1) There is only one, more and less specific frequency and temperature of the tire during wet skid, which is probably higher than the temperature of the rolling tire;
- (2) An increasing frequency shifts the glass transition temperature towards higher values, the well known frequency – temperature superposition principle as shown in Figure 5; the behavior of a tire tread during wet skid can be easier understood.

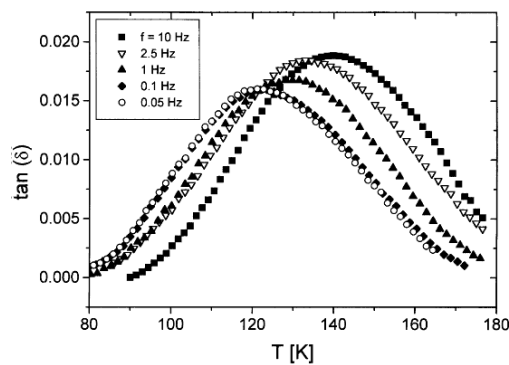


Figure 5: Frequency influence on glass transition temperature of E-SBR <sup>6</sup>

Assuming that the temperature of a rolling tire is constant, a higher frequency during wet skid conditions shifts the maximum of the mechanical loss angle to higher temperatures.

This implicates that there are two different modes:

- (1) During rolling, energy dissipation is relatively low compared to wet skid conditions
- (2) During wet skid conditions, energy dissipation is high.

This change in elastic behavior is caused by the frequency change from low frequencies during rolling to high frequencies during breaking <sup>3</sup>.

Returning to the second phenomenon that is hydrophilic surface properties of the tire tread, the three zone concept of wet skid (Figure 6) must be explained. The area under a tire during wet skid can be divided into three zones <sup>5,7</sup>:

**Zone 1:** Squeeze – film zone: In this region of contact area, a water wedge is formed due to the displacement inertia of the intercepted water film.

**Zone 2:** Transition zone: This is the region in which partial breakdown of the water film, now considerable reduced in thickness, is occurring. The friction coefficient varies widely from a very low value of viscous hydroplaning at the leading edge of this zone to almost dry friction at the end of the transition zone.

**Zone 3:** Traction zone: In this rear part of the contact area, the lubrication water film has almost been removed and dry friction is dominant.

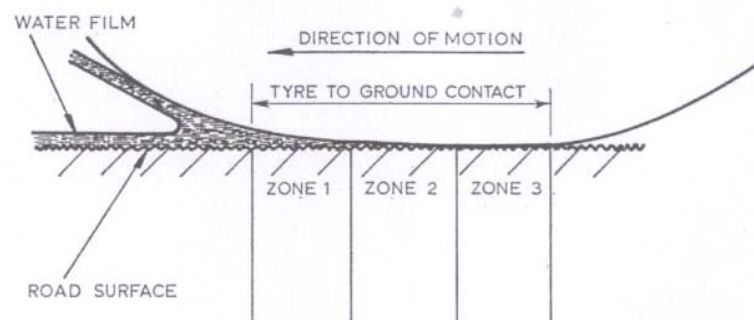


Figure 6: Three zone concept <sup>7</sup>

The three zone concept gives also one of the explanations why tire treads containing silica instead of carbon black as a filler show better wet skid performance: The silica filled compound contains bare silica particles at the interface rubber – water film (Figure 7). Due to the polar silica surface, the water film breaks easier compared to a carbon black containing surface, and the transition zone is reduced simultaneously increasing the traction zone. Consequently, local dry patches are formed creating a much higher friction coefficient and thus higher skid resistance between water and the rubber surface. Another consequence of this phenomenon is that higher silica loadings lead to

improvements of the wet skid resistance, as a higher particle density at the interface increases its polarity and hydrophilicity<sup>5,8</sup>.

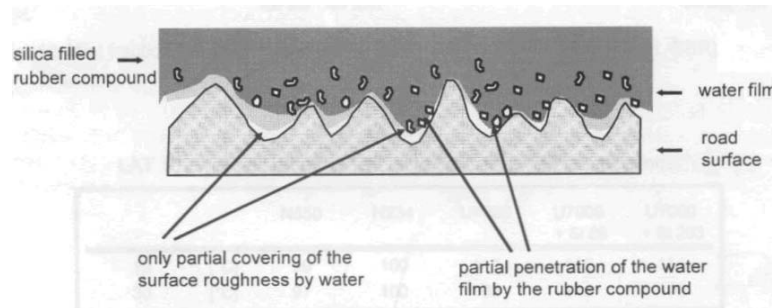


Figure 7: Partial penetration of a water film by silica particles in the material surface<sup>5</sup>.

### 2.1.3 Wear resistance

Wear is one of the consequences of the relative motion of two contacting surfaces under conditions that produce frictional work or energy. It is defined as a loss of material from one (or both) surfaces during the sliding contact that generates the frictional work<sup>9</sup>. Wear of materials can be divided into several types: adhesive, abrasive, erosive, corrosive and fatigue. It is a very complex phenomenon in which pavement roughness, temperature and interface contaminants (water, sand or mud) also play an important role. However, the above mentioned factors can not easily be adjusted, so the only way to improve wear resistance is to change the material properties.

The tire tread during rolling and especially during braking is subjected to mainly abrasive wear. Abrasive wear is governed by the abrasion of the surface layer of materials by the sharp edges of hard projections from the rough surface of the abradant. The ability of a tire to resist abrasive wear or abrasion resistance determines the tire life time or mileage<sup>9</sup>.

Glass transition temperature, reinforcing system and the cure system are factors determining the absolute wear rate of the tread compound. Generally, wear resistance is increasing with decreasing glass transition temperature, as shown in Figure 8<sup>10</sup>. SBR is blended with butadiene rubber ( $T_g = -90^\circ\text{C}$ ) to increase wear resistance and decrease



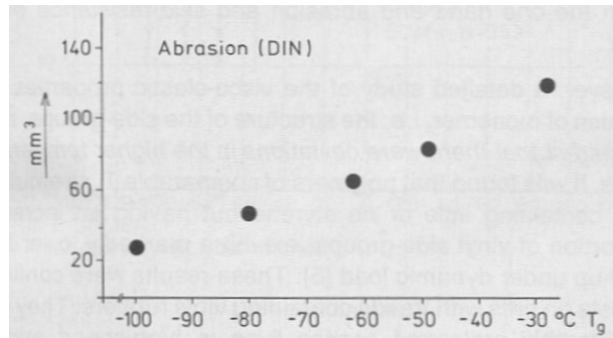


Figure 8: Glass transition temperature influence on abrasive wear <sup>11</sup>

rolling resistance. Polymers with higher molecular weight and a narrow molecular weight distribution have also higher wear resistance <sup>4, 11, 12</sup>.

Abrasion or wear of rubber composites is a property which is strongly affected by the filler. Adding a reinforcing filler to rubber considerably increases the wear resistance of the compound in comparison to gum rubber (Figure 9). However, with a further increasing filler amount, filler-filler interactions are getting stronger than polymer-filler interactions. This leads to release of filler particles from the surface exposed to friction.

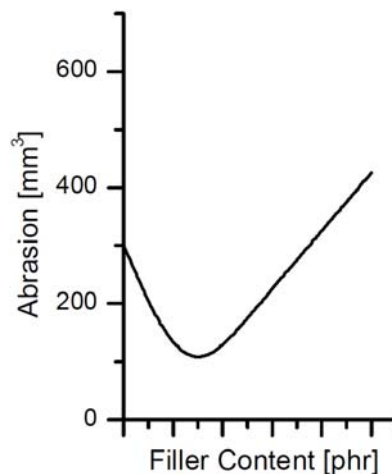


Figure 9: Wear resistance as a function of filler content <sup>13</sup>

Abrasion resistance is greatly influenced by filler dispersion in the elastomer matrix and by the polymer – filler interaction. The combination of fillers with a better dispersion, e.g.

carbon black, and non-polar rubbers such as SBR, give high abrasion resistance. Figure 10 compares the abrasion index of a carbon black compound with the abrasion index of a silica compound with and without coupling agent in two slip modes (obtained on a laboratory wear testing machine, LAT 100). From this figure, two conclusions can be drawn:

First, the filler – polymer compatibility has a higher contribution to wear resistance than the coupling phenomenon. The second conclusion is a low efficiency of silanisation, which is confirmed by the calculations of the silanization yield: the silanization of 8 phr coupling agent (triethoxysilylpropyl tetrasulfide, TESPT) with 80 phr silica with a specific surface area of 170 m<sup>2</sup>/g leads to the reaction of only 1 Si-OH per nm<sup>2</sup> out of 4 to 8 silanol groups per nm<sup>2</sup> available on silica surface <sup>5</sup>.

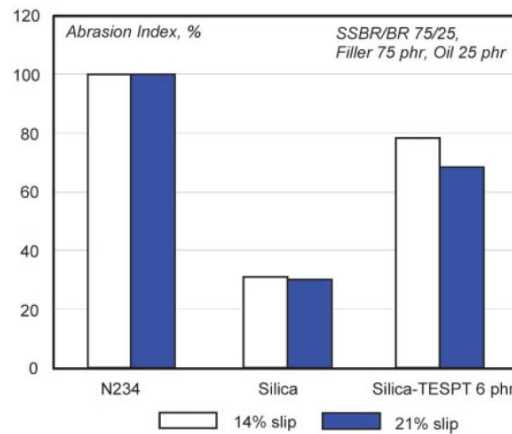


Figure 10: Abrasion resistance of carbon black (N234), silica and silica/TESPT compounds in two slip angles – 14% and 21% <sup>14</sup>

The specific surface area of a filler also has a contribution to wear resistance: along with an increasing surface area, the polymer – filler interaction is also increasing, leading to improved wear resistance. Unfortunately, with increasing specific surface area, the filler – filler interactions rise more rapidly than the polymer – filler interactions, so during mixing dispersion is more difficult, leading to inferior wear resistance (Figure 11).

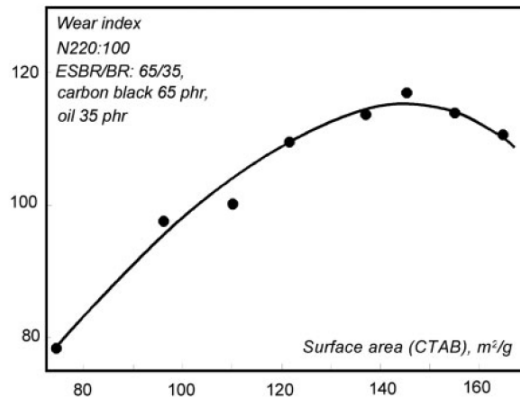


Figure 11: Wear resistance as a function of surface area of carbon black <sup>14</sup>

Because of the locally relatively high temperatures in places where friction occurs, wear resistance of a tire tread also depends, to a large extent, on its resistance to high temperatures.

Hardness is a factor as it makes cutting and ploughing processes more difficult. Wear of polymers has been shown to depend on the surface roughness of the road, but poor correlations exist between hardness and wear in polymers. Hutchins<sup>15</sup> suggested that this may be due to a significant elastic deformation during hardness testing in polymers. Furthermore, the mechanisms of wear in polymers may involve fatigue crack growth rather than the plastic deformation process common in metals.

For soft rubber sliding over a smooth, hard counterface (Figure 12), relative motion between the two surfaces was due to “waves of detachment”. These waves move as “folds” across the rubber surface in the direction of sliding. Schallamach<sup>16</sup> associated them with tangential and compressive stress gradients and the resulting elastic strain.

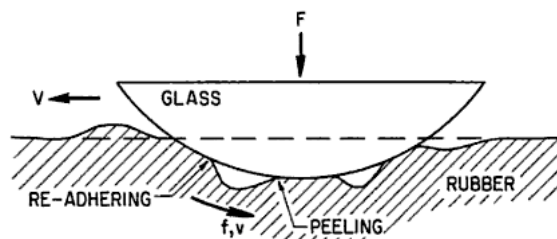


Figure 12: Rubber deformation by a hard asperity – Schallamach waves <sup>16</sup>

Because of this elastic deformation of rubber, the fatigue wear mechanism leads to a wear scar in which a pattern of ridges is observed perpendicular to the sliding direction. This pattern is shown in Figure 13, and it is probably caused by micro-tearing of the surface due to frictional forces between the abrasive and the surface. These micro-cracks initially grew downwards into the sample but as the tongue or ridge grew, the crack propagated upwards to form a loose wear particle, with growth and detachment occurring repeatedly <sup>17,18</sup>.

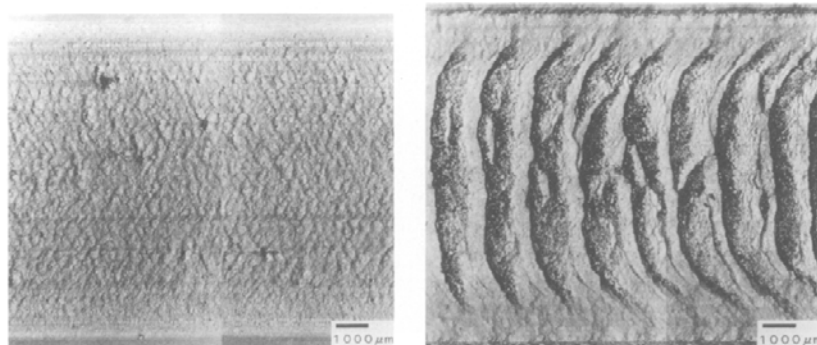


Figure 13: Surface of abraded natural rubber: after 10 000 cycles (left); and after 82 000 cycles (right) <sup>19</sup>

To counteract this process, the elasticity and tear strength of a rubber material should be as high as possible.<sup>20</sup>

## 2.2 REINFORCING THEORIES AND MECHANISMS

Applying fillers which can interact with the polymer matrix in a physical or chemical way leads to improvement of mechanical properties of the material. Interactions between filler and polymer can be mainly physical like in case of carbon black or chemical like in case of silica with a coupling agent. The most important requirement for a strong reinforcing effect is a strong interaction on the interface between filler and polymer. However, if the above-mentioned interactions are weak, namely if there are large polarity differences between the polymer and the filler, the

polymer chains are easily sliding over the filler particles and the reinforcing effect is limited to physically anchored polymer chains only. Mixing carbon black with a non-polar rubber like SBR leads to strong physical interactions causing improvement of mechanical properties. Silica interacts with above-mentioned non-polar rubbers only weakly due to the high polarity of its surface. Therefore, reinforcing capabilities of pure silica in non-polar elastomers are weak. This problem was solved by using coupling agents that create a bond between a non-polar polymer and the high polar surface of silica. Dispersion of fillers in a polymer matrix equally plays an important role in polymer reinforcement.

### **2.2.1 Filler-filler interactions**

When fillers are dispersed in a polymer matrix, they form aggregates which can be connected in a filler-filler network. Between the adherent, not covalently connected filler particles, there is a strong energy dissipation due to friction. Because of physical or weak chemical interactions between the filler particles, the filler-filler network is rather weak, which means that it can be broken under strain. This effect is called Payne effect, and it is an indication of the degree of filler-filler interaction.

The Payne effect is observed in filled rubbers under low shear conditions. The loss and storage modulus of filled rubbers are amplitude-dependent. There is a specific value of shear amplitude at which the loss modulus reaches a maximum and the storage modulus has an inflection point. This effect is independent of the type of polymer but is dependent on the type of filler. Silica filled rubbers, in which the silane coupling agent was not introduced, show a much stronger Payne effect than the rubbers filled with carbon black <sup>21</sup>.

### **2.2.2 Filler-polymer interactions**

When elastomers and reinforcing fillers are mixed, interactions occur and polymer chains are immobilized on the filler surface. This results in a thin layer of polymer (2 – 5 nm), which encapsulates filler particles and aggregates <sup>22</sup>. These interactions can be so strong that even a good solvent for the polymer can not extract it. The part of rubber that can not be extracted is called bound rubber. According to Medalia <sup>22</sup>, besides a

classification in chemically and physically bound rubber, there are two other types (Figure 14): A part of the rubber is trapped in the cavities of the filler structure; this part is called occluded rubber. The other part of the rubber, which is adsorbed onto the external aggregate surface, is called shell rubber. Under increasing deformation, these filler-polymer structures can successfully release the rubber which can further transfer the applied load. The filler-polymer interaction depends on the filler particle size: smaller filler particles have a higher contact surface with the polymer, and therefore a higher amount of bound rubber. However, applying very high specific surface area fillers in elastomers leads to difficulties during processing due to an increased blend viscosity.

Error! Bookmark not defined.

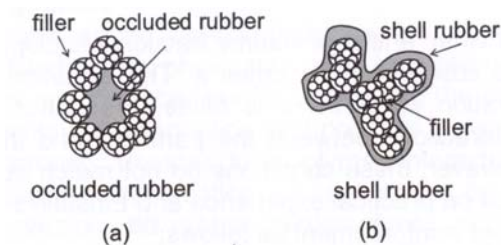


Figure 14: Schematic view of bond rubber:

(a) – Occluded rubber model <sup>23</sup>, (b) – Shell rubber model <sup>24</sup>

### 2.2.3 Hydrodynamic effect

This effect explains the viscosity increase of a liquid by the addition of rigid particles. In 1906, Einstein proposed the first straight theoretical model for viscosity increase in Newtonian flow (Equation 7) with the following assumptions:

- Particles are dispersed perfectly
- No interactions between particles
- Particles are rigid
- Particles are perfectly spherical
- Particles are perfectly wetted by the liquid

In Equation 7,  $\phi$  is the volumetric concentration of the particles and  $\eta_0$  and  $\eta$  are the viscosity of the pure liquid and the suspension respectively <sup>25</sup>.

$$\eta = \eta_0(1 + 2.5\phi) \quad \text{Equation 7}$$

In polymer technology, some of Einstein's assumptions are rather unusual, in particular that filler particles are perfect spheres and that there are strong filler-polymer interactions. The latter deficiency was taken into account in the equation introduced by Guth and Gold: <sup>26</sup>

$$\eta = \eta_0(1 + 2.5\phi + 14.1\phi^2) \quad \text{Equation 8}$$

By changing the viscosity for the elastic modulus  $E$ , this equation can easily be converted for elastic materials (Equation 9):

$$E = E_0(1 + 2.5\phi + 14.1\phi^2) \quad \text{Equation 9}$$

However, in actual practice different kind of fillers have different particle shapes. To take different shapes into consideration, a form factor  $f$  was introduced. This factor is the ratio of the longest dimension of the reinforcing particle to the shortest dimension. The modernized version of the Guth and Gold equation becomes then:

$$E = E_0(1 + 0.67f\phi + 1.62f^2\phi^2) \quad \text{Equation 10}$$

Nevertheless, all published results indicate that the above-mentioned equations cannot precisely predict the experimental values of the modulus when the filler concentration is in the practical range unless empirical coefficients are used <sup>20, 25</sup>.

#### **2.2.4 Polymer network**

The polymer network, especially crosslinks formed during vulcanization, has its own contribution to the modulus of the material. According to Equation 11, the static modulus of rubber is proportional to the concentration of elastically active network chains  $\nu$  and

the absolute temperature  $T$ , with the Boltzmann constant  $k_B$  fulfilling the role of the proportionality constant <sup>27</sup>:

$$E_0 = \nu \cdot k_B \cdot T \quad \text{Equation 11}$$

The crosslink density of the vulcanized rubber has a strong impact on the dynamic properties of the material. Along with an increasing number of crosslinks in rubber, the energy dissipation is decreasing, which can be easily noticed from the tangent  $\delta$  – crosslink density graph as shown in Figure 15.

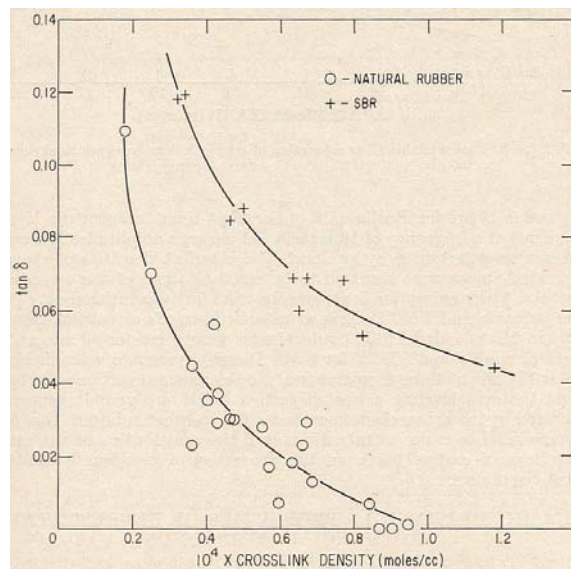


Figure 15: Influence of crosslink density on the loss angle <sup>23</sup>

Unfortunately, mechanical properties deteriorate when the crosslink density increases: rubber starts to be more brittle and hard.

Another major factor that has a significant contribution on the rubber properties is the type of the crosslink's. Sulfidic crosslinks in rubber can be analyzed by the distribution of polysulfidic, disulfidic and monosulfidic bonds. The crosslink distribution can be adjusted by using different ratios of accelerator to sulfur. Three types of vulcanization systems are to be distinguished <sup>28</sup>:



1. Conventional vulcanization (CV) with accelerator/sulfur ratio in range of 0.1-0.6:  
In this system there is only approx. 5% of monosulfidic crosslinks
2. Semi-efficient vulcanization (S-EV) with accelerator/sulfur ratio in the range of 0.7-2.5:  
In this system there is approx. 50% of monosulfidic crosslinks
3. Efficient vulcanization (EV) with accelerator/sulfur ratio in range 2.5-12:  
In this system, the content of monosulfidic crosslinks is increased to 80%

Rubber with a high content of monosulfidic crosslink's is less elastic, but the energy dissipation is also lower, which makes this type of crosslinks preferable for low rolling resistance tire tread material. Unfortunately, rubber which has a high elastic modulus is not desirable during wet skid, because less deformation means less grip. As a consequence, semi-efficient vulcanization systems are chosen for tire tread material.

## **2.3 FILLERS**

Except for natural rubber, which has the ability to strain-crystallize, other types of rubber in most of the cases can not be used in pure form and need to be reinforced by fillers.

### **2.3.1 Conventional fillers**

Fillers can be classified according to their reinforcing capabilities in reinforcing, semi-reinforcing and non-reinforcing fillers, though the differences between these classes cannot be sharply defined. A general rule is that the smaller the primary particles are and the higher the aspect ratio of the aggregates, the greater the reinforcing power of the filler. The term 'reinforcing' means ameliorating the mechanical properties such as modulus, tensile strength, abrasion and tear strength. In the case of elastomers, using reinforcing fillers leads simultaneously to an increase of the modulus and strain at break. This phenomenon is not fully understood but explains the ability of reinforced elastomers to provide distinctive material properties and justify their success

in different branches of the industry, especially in the tire industry where specific material properties are necessary<sup>29</sup>.

### 2.3.1.1 Carbon black

Historically, the first filler used in the rubber industry on large scale was carbon black. Applying reinforcing types of carbon in rubber increases the following properties: tensile strength, elasticity modulus, wear resistance and hysteresis. However, increasing the latter property is not desired for tire tread applications, especially as it increases rolling resistance.

Because of the high dispersive component of the surface energy, dispersibility of carbon black in nonpolar rubbers is high compared to silica. Silica is an amorphous material and the silanol groups are randomly located on its surface. Conversely, the aggregates of carbon black consist four different energetic sites (Figure 16):

- I: graphitic planes (16 kJ/mol),
- II: amorphous carbon (20 kJ/mol),
- III: crystallite edges (25 kJ/mol), and
- IV slit shaped cavities (30 kJ/mol)<sup>30</sup>.

Therefore distribution of functional groups on carbon black and silica are also different. In the case of carbon black, the functional groups are located only on the edges of the graphitic basal planes of the crystallites as shown in Figure 16.

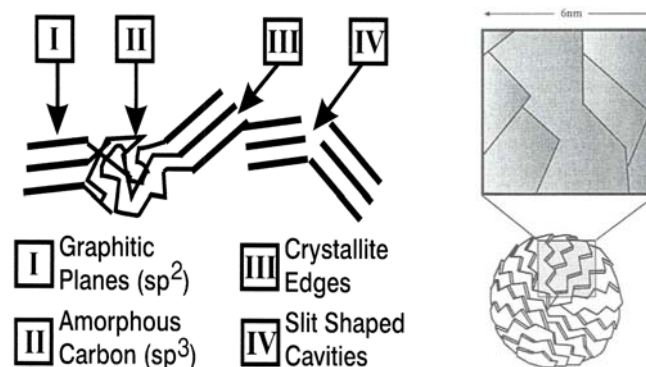


Figure 16: Different energetic sites on the carbon black surface<sup>31</sup> (left) and surface morphology of a single particle (right)<sup>32</sup>

For typical furnace carbon blacks like N220, the concentration of the functional groups on the surface would be 1 - 2 COOH groups per nm<sup>2</sup> or 2 - 4 OH groups per nm<sup>2</sup>, which is much lower than for silica. For most types of precipitated silica's used in the tire industry, the concentration of silanol groups varies from 4 – 7 per nm<sup>2</sup><sup>33</sup>.

Differences between silica and carbon black are not limited only to surface chemistry and energy. The morphology of the particles of these two fillers have a strong impact on the overall vulcanizate properties. Aggregates of carbon black are smaller than aggregates of precipitated silica, probably because of lower interactions between particles. Less aggregation means also a smaller surface to interact with.

Comparing the temperature dependence of  $\tan \delta$  of carbon black and silica (without coupling agent) filled rubber compounds as illustrated in Figure 17, the difference between these two fillers is easily noticeable. The hysteresis of a carbon black reinforced material in the rubbery state is still higher than the hysteresis of silica filled compounds. This is mainly due to energy dissipation during repeated destruction and reconstruction of the filler network. However, along with increasing temperature, the hysteresis becomes lower, just like in the case of polymer in the absence of fillers. This is caused by relatively easy thermal destruction of the carbon black filler network. Conversely, it is interesting to notice that the hysteresis of silica filled rubber increases with increasing temperature. This behavior can be explained by weakening of the filler-filler hydrogen bonding interactions and by increasing part of filler network that can be broken and reformed.

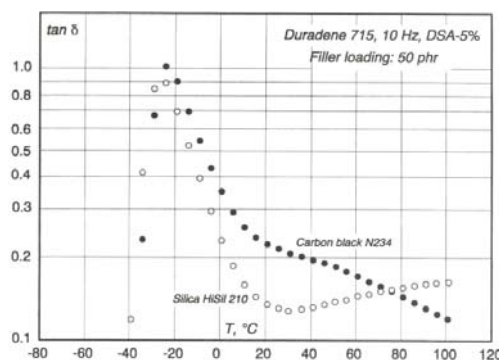


Figure 17: Temperature dependence of  $\tan \delta$  for vulcanizates filled with carbon black and silica without coupling agent<sup>34</sup>

Applying a silane coupling agent that changes the surface properties of silica leads to a drastic change of the dynamic properties. Strong polymer-filler interactions induced by the coupling agent shifts the loss angle – temperature curve of silica filled rubber towards the one of gum rubber.

The surface of carbon black can be also chemically modified. However, this modification does not increase dynamic properties as distinctively as it does in the case of silica.

### *2.3.1.2 Silica production*

Depending on the production method, two types of silica can be distinguished: precipitated and fumed (pyrogenic) silica. Precipitated silica is produced by the controlled neutralization of diluted sodium silicate (waterglass) by sulfuric, hydrochloric or carbonic acid. The starting materials are sand and soda ash or caustic soda. The silicate can be produced in a furnace or digester reactor. Dilution with water provides relatively low silicate concentrations, which together with moderate acidification rates produces precipitated particles rather than gels, but a minor amount of gel is usually present. The reaction temperature is the major determinant factor of the primary particle size.

To obtain reinforcing silica, much care must be taken in formulating the precipitation recipes to guarantee small rigid particles, and also in the drying conditions to avoid agglomeration and maintain high dispersibility. The temperature at which neutralization is conducted correlates with the size of the silica particles; low temperatures for instance produce small particles. A slow rate of neutralization reduces gel formation, while high silicate and acid concentrations produce more gel<sup>29,35</sup>.

#### *2.3.1.2.1 Silica surface characteristics*

The surface of silica is covered with silanol groups which are highly reactive. There are three types of silanol groups as shown in Figure 18.

- Isolated (free) silanol groups, where the surface silicon atom has three bonds into the bulk structure and the fourth to a hydroxyl group.

- Vicinal or bridged silanols, where two isolated silanol groups are bridged by a H-bond.
- Geminal silanols consist of two hydroxyl groups attached to one silicon atom.

The geminal silanols are close enough to form H-bonds, whereas free silanols are too distant. The pioneering work by Ong et al.<sup>36</sup> has shown the presence of two types of pKa values for the silanol groups at 4.9 and 8.5 with a surface population of 19 and 81%. The silanol groups with a lower pKa value (4.9) are believed to be isolated silanol groups with no hydrogen bonding to its neighbor. They are considered as isolated silanols due to the easy dissociation of the hydrogen compared to other silanols, which are coupled through a hydrogen bond<sup>36</sup>.

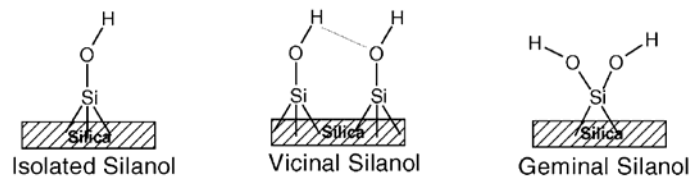


Figure 18: Types of hydroxyl groups on the silica surface<sup>37</sup>

Three fundamental properties of silica determine their influence on the rubber properties:

- specific surface area;
- single particle diameter;
- concentration of silanol groups on the silica surface.

Silica with a larger surface area has simply more surface to physically interact with the rubber. The specific surface area for precipitated silica's ranks from 140 to 250 m<sup>2</sup>/g, compared to 50 – 350 m<sup>2</sup>/g for fumed silica's<sup>38</sup>. The CTAB surface area of these silica's is in the range of 110 – 200 m<sup>2</sup>/g<sup>38</sup>.

In general, a smaller filler particle size results in a higher reinforcing capability. Inter-particle attraction forces (e.g. hydrogen bonding, London or Van der Waals forces) cause strong agglomeration of particles during drying of the precipitated silica. However,

when high shear forces are applied, the agglomerates break to form the reinforcing species: aggregates. It must be stated that single colloidal particles with average dimensions of 10 to 30 nm have no reinforcing capability (aspect ratio  $\sim 1$ ). The aggregate morphology determines the influence of the filler on the properties of rubber. Typical dimensions of aggregates are ranging from 100 to 200 nm<sup>38, 39, 40</sup>.

The concentration of the silanol groups on the silica surface plays an important role during the silanisation process. Silanol groups act as reaction centers for a silane coupling agent which finally results in covalent bonds between filler and polymer. The estimated number of silanol groups accessible on the porous silica surface is between 4 and 8 Si-OH groups per nm<sup>2</sup><sup>37, 41</sup>. Because of the nature of the production process, especially the high temperatures, fumed silica's have a lower number of silanol groups. Additionally, the local density of silanol groups in both cases varies from place to place<sup>36, 39</sup>.

### **2.3.1.3 Surface energy**

The compatibility and interaction of two physico-chemically different materials like polymer and filler can be characterized by the surface energy. The surface energy of a material,  $\gamma_s$ , is defined as the energy necessary to create one unit of new surface. This energy is comprised of different types of cohesive forces, such as dispersive, dipole-dipole, induced dipole-dipole, acid-base and hydrogen bonds<sup>42</sup>. Therefore surface energy can be expressed as the sum of all these components. However, for most substances the surface energy is described as the sum of two components: the dispersive  $\gamma^d$  and specific  $\gamma^{sp}$  energy (Equation 12).

$$\gamma_s = \gamma_s^d + \gamma_s^{sp} \quad \text{Equation 12}$$

The dispersive component  $\gamma_s^d$  indicates the ability of filler adhesion to organic matrices (such as a polymer), while the specific or polar component  $\gamma_s^{sp}$  indicates filler-filler interactions. To obtain a good filler dispersion in a polymer, the specific component should be as low as possible to limit formation of a filler network. Practically this can be realized by two different ways:

- (1) Proper selection of the filler, for example carbon black, silica or dual phase fillers;
- (2) Change of the surface properties of the filler <sup>41</sup>.

For non-silanised silica, the specific component is relatively high compared to carbon black, due to the highly polar nature of the silica surface <sup>37</sup>. The polar and dispersive component of some carbon black types and silica are summarized in Table 1.

Table 1: Comparing dispersive and polar components of silica and carbon black

|              | Specific surface area<br>(m <sup>2</sup> /g) | Dispersive<br>component (mJ/m <sup>2</sup> ) | Polar component<br>(mJ/m <sup>2</sup> ) |
|--------------|--|--|---|
| N550         | 140  | 270  | 120                                     |
| N770         | 76   | 197  | 86                                      |
| Ultrasil VN2 | 134  | 23   | 64                                      |
| Ultrasil VN3 | 181  | 34   | 72                                      |

Reaction of silica with a silane coupling agent decreases the specific component of the surface energy. When interactions between silica particles are inhibited, a better dispersion in the polymer matrix is obtained <sup>43</sup>.

## 2.3.2 Alternative fillers

### 2.3.2.1 Dual phase fillers

Carbon black historically was the first reinforcing filler used in the tire industry. Properties of rubber such as tensile strength, elastic modulus and wear resistance are improved when carbon black is used. However, carbon black and rubber interact mostly in a physical way. This causes high energy losses during a dynamically applied load, and as a consequence the tire is rather energy-inefficient. Increasing fuel prices forced tire companies to search more sophisticated and environmentally friendly technologies which will improve tire properties, especially rolling resistance. A major breakthrough was the silica/silane system in tire tread rubber. The most important parameter of silica filled rubber was a lower loss tangent at higher temperatures (ca. 60°C) and a higher

loss tangent in lower temperatures (ca. 0°C). Such a correlation of the loss tangent with temperature gives both, low rolling resistance and high skid resistance. But wear resistance of silica filled rubber is lower compared to carbon black. This brings up an obvious question: is it possible to combine the advantages of both fillers in one filler material?

Carbon-silica dual phase fillers are a partial answer to this question. Carbon-silica dual phase fillers can be characterized as carbon black having a surface modification of a thin layer of silica. The modification of carbon black particles can be realized by precipitation of silica from solution onto dispersed carbon black <sup>44</sup> or by a co-fuming process <sup>45</sup> which gives better effects than the previous method. Depending on the production process, there are two types of commercialized carbon-silica dual phase fillers which differ in silica content and distribution, as shown in Figure 19. When a silicon containing compound is introduced simultaneously with a carbon containing compound into the precipitation process, the silica phase is distributed throughout the particle. If the silicon containing compound is introduced behind the zone of carbon black formation but before quenching, the silica layer is present mostly on the surface of the carbon black aggregate <sup>45</sup>.

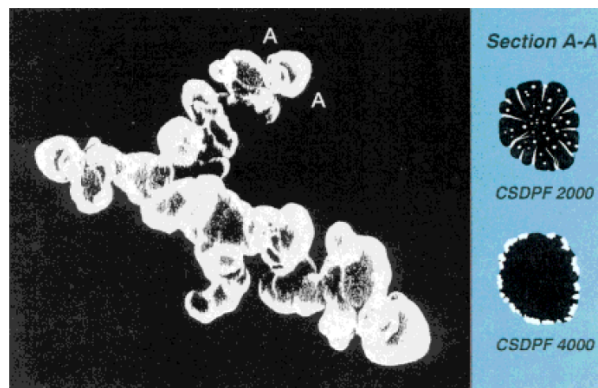


Figure 19: General views of silica-carbon black dual phase fillers with silica throughout the particle (top) and silica on the surface (bottom) <sup>46</sup>.

In carbon silica dual phase fillers, the filler-filler interactions are substantially reduced due to the carbon content in the surface, and the polymer-filler interactions are



improved by preserving the high dispersive component of the surface energy, which originates from carbon domains. Covering the surface of carbon black by a silica layer makes silanization useful. The carbon silica dual phase filler demands less than half of the silane coupling agent loading that is typically used for silica-based passenger tread compounds. Consequently, the tradeoff between rolling resistance and wear resistance is greatly improved, significantly enhancing one without sacrificing another<sup>46</sup>.

The main factor influencing rolling resistance and wet skid resistance is the loss tangent balance at different temperatures, as shown in Figure 20. The dual phase filler is similar to the silica-silane filler; however, it gives a better balance of the loss tangent at different temperatures: significantly lower  $\tan \delta$  at high temperatures and high hysteresis at lower temperatures compared to carbon black. This special behavior can be attributed to increased chemical filler-polymer interactions which was the main drawback of carbon black filled rubber. Taking into account that the dual phase filler contains only 10% of silicon at a silica coverage of 55%, the improvement of the loss tangent balance is significant compared to carbon black at a good abrasion resistance. Based on the well-known correlation between rolling resistance and loss tangent at high temperatures (50 - 70°C), it can be expected that the rolling resistance of the dual phase filler reinforced tires is comparable to that of a silica-filled tire and much lower than that of carbon black filled tires<sup>46, 47, 48</sup>.

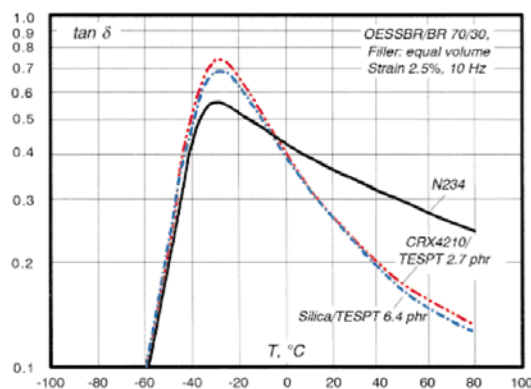


Figure 20: Temperature dependence of  $\tan \delta$  for vulcanizates reinforced with different fillers: carbon black (N234), carbon silica dual phase filler (CRX4210) and silica<sup>46</sup>.

With regard to abrasion resistance, the polymer-filler interaction plays a dominant role. Due to a high polarity difference between silica and hydrocarbon rubber, even with a coupling agent, the abrasion resistance of silica filled rubber is still significantly lower than of carbon black reinforced material. However, in the case of carbon silica dual phase fillers, this deficiency seems to be partially compensated for by the high surface activity of the carbon domains. As can be seen in Figure 21, the abrasion resistance of a new kind of filler does not fully reach the same level as the carbon black compound although it is still significantly better than the silica filled rubber <sup>46, 47, 48</sup>.

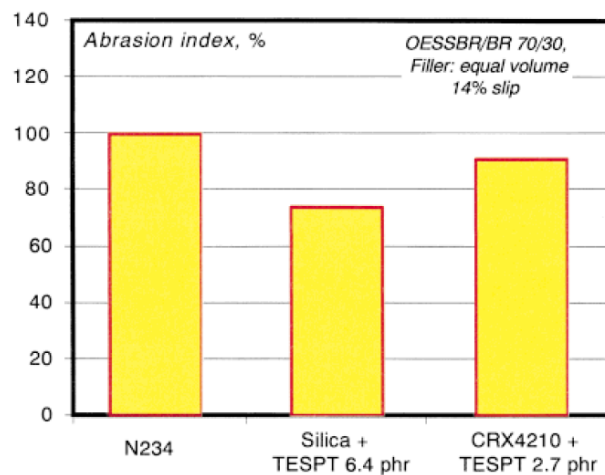


Figure 21: Abrasion resistance of vulcanizates filled with various fillers: carbon black (N234), silica and carbon silica dual phase filler (CRX4210) <sup>46</sup>

Rubber vulcanizates in which dual fillers have been applied are characterized by a very low Payne effect, indicating weak filler-filler interactions. These weak filler-filler interactions is explained as follows: when the carbon black aggregates are partly covered by silica, the probability of facing the same type of surface at a neighboring aggregate is lower for dual phase fillers than for mono phase fillers.

### 2.3.2.2 Layered silicates

Reinforcing capabilities of fillers depend mostly on the specific surface area (particle dimensions), surface chemistry (reactive sites) and aspect ratio. The incorporation of layered silicates into polymer matrices has been known for over 60 years <sup>49</sup>. Layered

silicates are a class of compounds that possesses a unique combination of particle morphology (extraordinary high specific surface area in exfoliated state) and chemistry (surface silanol groups). For instance, the specific surface area of exfoliated montmorillonite is 700 – 760 m<sup>2</sup>/g. This filler is composed of individual clay sheets which are only 1 nm thick, and display a perfect crystalline structure. However, the smaller the reinforcing elements are, the larger is their specific surface and hence their tendency to agglomerate rather than to disperse homogeneously in the polymer matrix. Due to their availability and relatively low price, layered aluminosilicate filled composites became subject of many works in recent years<sup>50, 51</sup>.

There are many types of layered silicates like: montmorillonite, hectorite, saponite, fluoromica, fluorohectorite, vermiculite, kaolinite, and magadiite. Chemical formulas of the three predominantly used layered silicates are depicted in Table 2.

The above-mentioned layered silicates belong to a structural family called 2:1 layered silicates. The crystal lattice of 2:1 layered silicates (or 2:1 phyllosilicates) consists of two-dimensional layers where a central octahedral sheet of alumina is fused to two external silica tetrahedra by the tip, so that the oxygen ions of the octahedral sheet also belong to the tetrahedral sheets, as shown in Figure 22<sup>51</sup>.

Table 2: Chemical composition of some chosen 2:1 phyllosilicates

| 2:1 Phyllosilicate | General formula                     |
|--------------------|-------------------------------------|
| Montmorillonite    | $M_x(Al_{4-x}Mg_x)Si_8O_{20}(OH)_4$ |
| Hectorite          | $M_x(Mg_{6-x}Li_x)Si_8O_{20}(OH)_4$ |
| Saponite           | $M_xMg_6(Si_{8-x}Al_x)O_{20}(OH)_4$ |

M = monovalent cation; x = degree of isomorphous substitution (between 0.5 and 1.3).

The most interesting property of all layered silicates is their special structure which provides a high aspect ratio almost as high as the aspect ratio of carbon nanotubes. Layered silicates are composed from very thin layers that are usually bonded together by counter-ions like sodium, potassium or calcium<sup>[35]</sup>. The layer thickness is around 1 nm and the lateral dimensions may vary from 100 nm to several microns and even larger, depending on the particular silicate, the source of the clay and the method

of preparation. Clays prepared by milling typically have lateral platelet dimensions of approximately 0.1–1.0  $\mu\text{m}$ . Therefore, the aspect ratio of these layers, the ratio of length to thickness, is particularly high with values of 500 – 1000. In case of montmorillonite, the primary particle is composed from five to ten parallel layers with an overall thickness of 7 – 12 nm<sup>51, 52, 53</sup>.

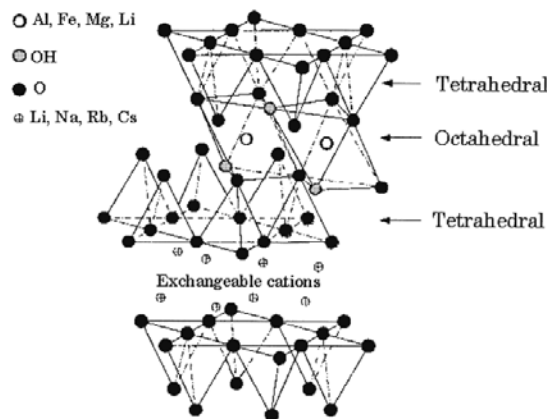


Figure 22: Structure of 2:1 phyllosilicates.

Silicate layers organize themselves to form stacks with regular gaps in-between them called interlayer or gallery. Usually the width of this gap is 0.3 nm. As the forces that hold the stacks together are relatively weak, the intercalation of small molecules between the layers is easy. The ion exchange capability of layered silicates is based on a moderate negative surface charge known as the cation exchange capacity, CEC, and expressed in meq/100 g. Only a small part of the charge balancing cations is located on the external crystallite surface; the majority of these exchangeable cations are located inside the galleries.

Changing clay into a reinforcing filler can be achieved through ion-exchange reactions. The previously mentioned counter-ions that bond galleries together can relatively easy be exchanged for organic ions. For this purpose, long chain alkylammonium ions are mostly used, although other “onium” salts can also be used, such as sulfonium and phosphonium. Using bulky “onium” salts results in a larger interlayer spacing reaching distances of up to 2.9 nm<sup>54</sup>. Figure 23 schematically

presents the cation-exchange reaction between the layered silicate and an alkylammonium salt.

Water swelling is required for an ion exchange reaction. For this reason, alkali cations are preferred in the galleries because 2-valent and higher valent cations prevent swelling by water. Natural clays containing divalent cations such as calcium require exchange procedures with sodium prior to further treatment with “onium” salts [38].

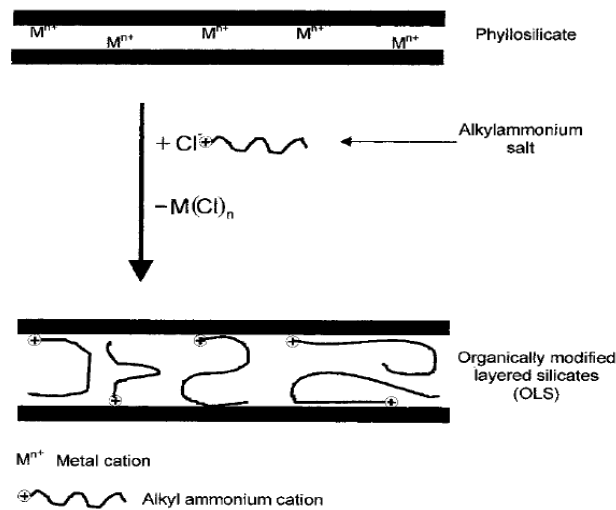


Figure 23: Cation-exchange reaction between the silicate and an alkylammonium salt <sup>55</sup>.

There are three possible ways of interaction between polymer and organo-clay during compounding:

1. The polymer is unable to intercalate between the silicate sheets, a phase separated composite is obtained, whose properties stay in the same range as traditional micro-composites (Figure 24a)
2. An intercalated structure in which a single (and sometimes more than one) extended polymer chain is intercalated between the silicate layer resulting in a well ordered multilayer morphology built up with alternating polymeric and inorganic layers (Figure 24b)
3. An exfoliated or delaminated structure is obtained, when the silicate layers are completely and uniformly dispersed in a continuous polymer matrix (Figure 24c) <sup>54</sup>.

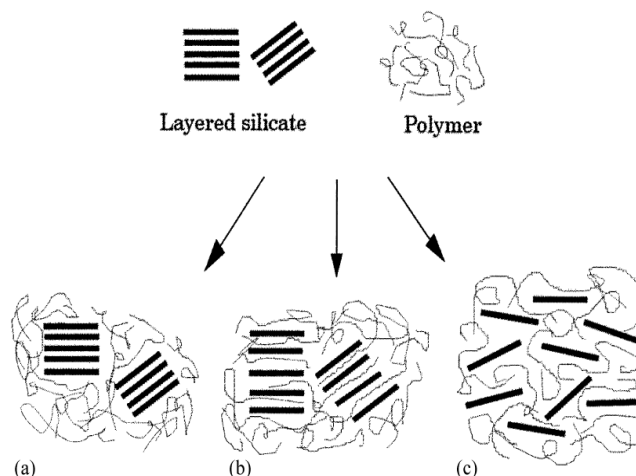


Figure 24: Three possible structures of layered silicate filled composites: (a) conventional, (b) intercalated and (c) exfoliated composite <sup>54</sup>.

Nevertheless, random exfoliation of organo-clays is not easy to obtain. In most of the cases, composites reported in literature were found to have an intercalated or mixed intercalated – exfoliated molecular structure. This is due to the fact that high anisotropic filler layers (primary particles) can not be dispersed randomly in a polymer matrix even when they are separated by large distances. In most cases, the mixed intercalated-exfoliated structure is dominating in polymers <sup>51</sup>. Techniques like solution blending, latex compounding, melt intercalation and in-situ polymerization are used for obtaining a good dispersion of organo-clays in a polymer <sup>56, 57</sup>. Among these, only melt intercalation seems to have some potential for practical application in the rubber industry. This method is very cost effective, as existing compounding lines can be used, direct and also environmentally friendly, as no organic solvent is used <sup>57</sup>.

A lot of work has been done in clay nano-composites for many thermoplastics and thermosetting polymers, but the studies on rubber – based nano-composites are less frequent. Most rubber products containing organoclays are making use of the flame retardancy. A small part of the articles focus on mechanical and dynamic properties of this kind of rubber composites, and often they lack to show evidence of exfoliation or even intercalation.

Direct mixing of organoclay with SBR in an internal mixer without using a compatibilizer, e.g. a coupling agent or a polar polymer, leads to relatively good mechanical properties. Mechanical and dynamic properties of organoclay filled rubber vulcanizates exhibit much stronger dependence on filler fraction comparing to silica filled composites. This means that a lower amount of filler is needed to obtain the same reinforcing effect as with silica. However, in contrast to silica, the loss tangent/temperature curve of organoclay filled SBR shows a small second peak in the temperature range of 20 – 60°C. In this experiment, there was no direct evidence of exfoliation or intercalation.

Recently, the incorporation of ion-exchanged clays (montmorillonite) is achieved by applying the so-called compatibilizing polymers. For transferring organo-clay to SBR, highly polar elastomers like carboxylated acrylonitrile butadiene rubber (XNBR) or epoxidized natural rubber (ENR) are used. Exfoliation or intercalation of organo-clays is carried out in polar rubbers using high temperatures (160°C) during mixing (XNBR) or solution blending (ENR). This masterbatch was used for further compounding with SBR. No silane coupling agent was used in these experiments<sup>58, 59</sup>. The test results indicate that mechanical properties as well as dynamic mechanical properties were improved. Improvement of mechanical properties has been observed for low filler loadings of 5-10 phr, what indicates a very low percolation threshold for the organo-clays. Applying organo-modified clay leads also to an increase of the glass transition temperature compared to pure SBR, as shown in Figure 25. This increase can be attributed to partial immobilization of polymer chains on silicate layers, stronger than in the case of typical fillers<sup>58</sup>.

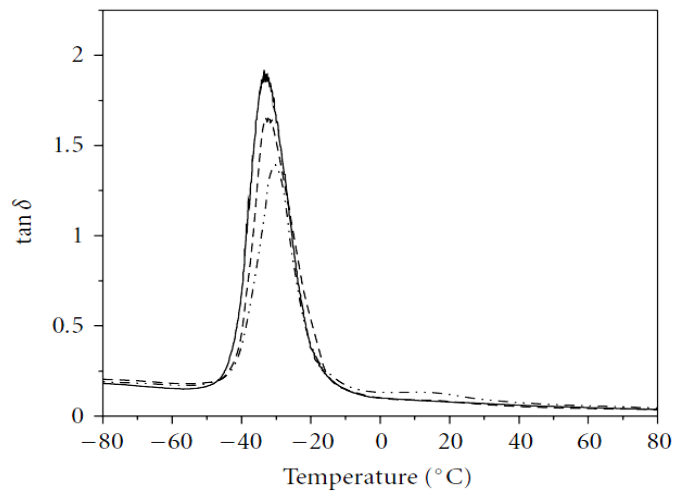


Figure 25: Temperature influence on the loss tangent for SBR/Montmorillonite composites prepared from an ENR/MMT masterbatch, (—) SBR, (--) SBR+1.8 phr MMT, (-·-·-) SBR+3.7 phr MMT <sup>58</sup>

The mechanism proposed by Fisher et al. <sup>60</sup> assumes that high aspect ratio fillers, with at least one dimension in the nanometer range, can form in situ grafts by adsorbing large amounts of polymer, which in turn are very effective in reducing the interfacial tension and inducing compatibilization in highly immiscible blends <sup>60</sup>. However, according to Mousa <sup>61</sup>, the reinforcement capabilities of organo-clay can also be explained by encapsulation of filler particles by a highly crosslinked elastomer layer. Increased crosslink density around filler particles is the effect of an acceleration of crosslinking rate caused by amine functionalities entrapped in the silicate layers <sup>61</sup>.

Noticeable is the second maximum at higher temperatures in most of the rubber composites containing organoclays; this energy dissipation can be caused by sliding and reorientation processes of the silicate platelets <sup>53, 62</sup>. Furthermore, a second maximum on the tangent  $\delta$  curve indicates that intercalation or exfoliation of the layered silicate was not sufficient. The above mentioned 2<sup>nd</sup> maximum appearing on the tangent  $\delta$  curve can be caused by the relaxation of the regular montmorillonite structure which was not sufficiently intercalated.

Dynamic mechanical analysis revealed that ion-exchanged layered silicates may also act as compatibilizers between two chemically different polymers, e.g. unpolar SBR and highly polar XNBR. A vulcanizate containing SBR blended with 9 phr XNBR without



organo-clay (SB-15 in Fig. 27) was compared to a vulcanizate containing additionally 5.6 phr of organo-clay (SB-12 in Fig. 27). The latter shows a smaller storage modulus value at room temperature indicating a low compatibility between these two different elastomers. With increasing organo-clay content, the modulus at 300% is increasing linearly, while the samples containing only SBR with XNBR without a filler have corresponding values of elastic modulus which are very low (Figure 26)<sup>59</sup>. According to the authors of this article<sup>59</sup>, this is a proof that the reinforcement effect indeed comes from the organo-clay and not from XNBR.

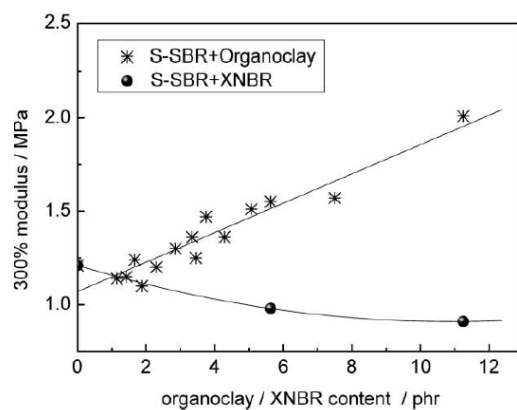


Figure 26: Variation of the 300% modulus values with the organo-clay and XNBR amount<sup>59</sup>

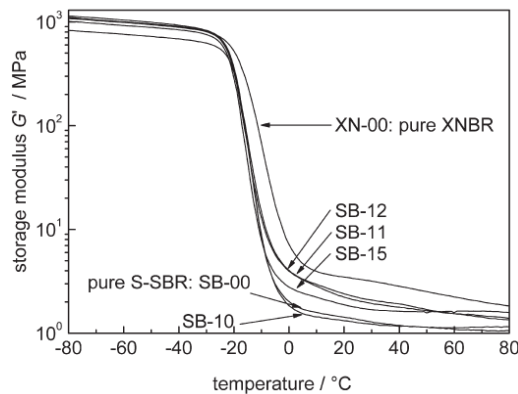


Figure 27: Temperature dependence of  $G'$  of the organo-clay filled rubber composites<sup>59</sup>.

The literature discussed above does not cover wet traction and wear resistance, which are equally important as rolling resistance.

## 2.4 COUPLING AGENTS AND THEIR EFFECT ON RUBBER COMPOUND PROPERTIES

### 2.4.1 The effect of coupling agents

Because of the high concentration of surface hydroxyl groups (high polarity), unmodified silica does not create an appreciable interface connection with the non-polar rubber polymer. The reinforcing capabilities of unmodified silica in a rubber matrix are rather poor, and the viscosity of the rubber blend is high (Table 3) because of strong filler-filler interactions and creation of agglomerates<sup>63</sup>.

Table 3: Viscosity comparison of carbon black (N110) and silica (VN2) filled compounds<sup>64</sup>

|                              | DBP*<br>ml/100 g | BET**<br>m <sup>2</sup> /g | Mooney viscosity ML 4   |    |
|------------------------------|------------------|----------------------------|-------------------------|----|
|                              |                  |                            | SBR 1500 <sup>[i]</sup> | NR |
| Corax N110                   | 113              | 140                        | 104                     | 52 |
| Ultrasil VN2 <sup>[ii]</sup> | 231              | 130                        | 201                     | 93 |

\* dibutyl phthalate adsorption

\*\* specific surface area measured by nitrogen adsorption

i emulsion type of the styrene butadiene rubber

ii silica type with BET surface area 125 g/m<sup>2</sup>

Additionally, unmodified silica interferes with the vulcanization process: some of the amine accelerators and the Zn stearic acid complex, which acts as curing activator, could be trapped by the silanol groups on the silica surface<sup>65</sup>.

These deficiencies exclude silica as reinforcing filler in non-polar polymers, basically in the whole tire industry. For this reason, the application of a coupling agent is necessary and a reasonable way to enhance polymer – filler interactions. Since silane coupling agents have been discovered, new opportunities in the field of interface modification did appear. Silane coupling agents are specific types of chemical compounds that can react with both, a polymer chain and the filler surface. After silanisation, the silica surface

becomes hydrophobic and thus more compatible with the polymer. Strong filler – filler interactions (hydrogen bonding) are partially replaced with strong filler – polymer interactions which results in decreasing Mooney viscosities, which in turn has a large effect on power consumption during mixing.

Applying of a silane coupling agent leads to:

- decreasing rolling resistance
- increasing wear resistance (higher abrasion resistance)
- increasing tensile strength, modulus at 300% and elongation

The improvement of mechanical properties is caused by the strong covalent bond between polymer chain and filler particle, which is not present in the case of carbon black. Decreasing tire rolling resistance leads to lower fuel consumption, the well-known green tire technology.

#### **2.4.2 Silanisation process chemistry**

Silane coupling agents have two types of reactive groups: the alkoxy groups capable to react with silanol groups on the silica surface, and the sulfide groups that can react with the polymer chain. The reaction mechanism between silica and the most widely used silane coupling agent, bis (3-triethoxy silylpropyl) tetrasulphide TESPT, was investigated using  $^{13}\text{C}$  and  $^{29}\text{Si}$  solid state NMR spectroscopy<sup>66</sup> and kinetic studies in decane as an inert solvent<sup>67</sup>. This resulted in a reaction model, which divides the silanization reaction into a primary and a secondary reaction.

During the primary reaction shown in Figure 28, one ethoxy group of each silane reacts with a silanol group on the silica surface and links chemically to the filler. Two possible mechanisms are reported:

1. Direct reaction of silica silanol group with the ethoxy group of the coupling agent.
2. Fast preliminary hydrolysis of the ethoxy group (with formation of ethanol) followed by a condensation reaction of partially hydrolyzed silane with silanol groups on the silica surface releasing a second portion of water needed for the hydrolysis step.

Partial hydrolysis of the silane will probably occur in the outer sphere of the silica surface due to its high concentration of adsorbed water. It must be stated that a clear distinction between the hydrolysis step of the silane and the following condensation step is not possible yet. However, the influence of adsorbed water on the silica surface is very clear. The amount of ethanol generated in the rubber blend increases with increasing moisture content of the silica, but at a moisture content higher than 7% no further acceleration is observed<sup>68</sup>.

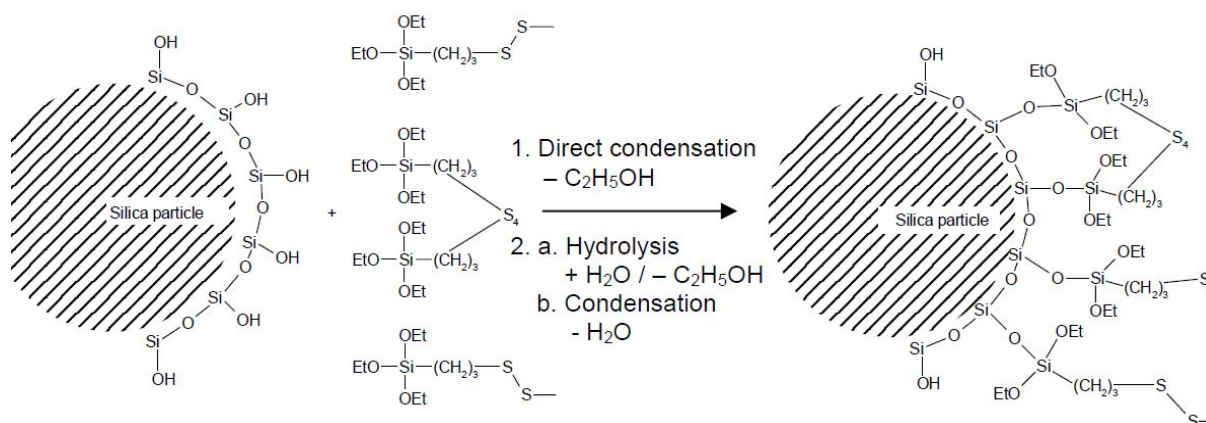


Figure 28: Primary silanisation reactions<sup>27</sup>

The amount of silane used during silanisation influences the reaction rate of the primary reaction as well. With increasing silane dosage in a rubber blend from 4 to 12 phr, the reaction rate decreases (Figure 29) due to a competition of the silane molecules with the accessible silanol groups on the silica surface. In addition, the TESPT reaction with silanol groups reduces their concentration, and the remaining groups become less accessible to the rubber chains because of the TESPT polylayer<sup>68, 69</sup>.

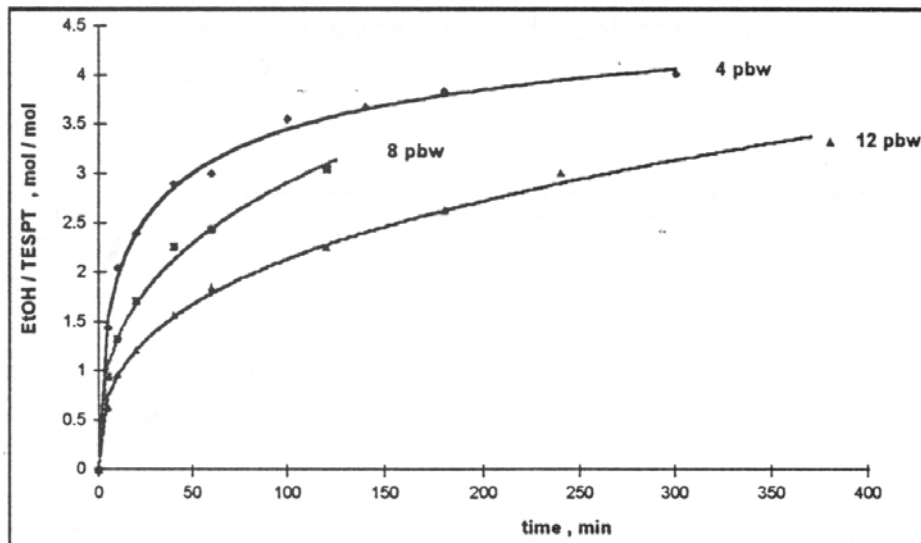
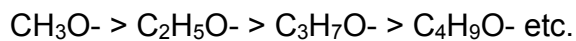


Figure 29: Ethanol evolution in different TESPT concentrations at 140°C <sup>70</sup>

The rate of hydrolysis and also the primary reaction rate is in great part predisposed by the type of the hydrolysable group of the silane. The influence of the hydrolysable group on the silane coupling activity was determined by the comparison of methoxy, ethoxy and propoxy derivatives. The reactivity decreases in the following order:



With the propoxy group, the reaction rate is generally too slow. Although the methoxy group reacts very rapidly, for toxicological reasons it is not used as a silanising agent – at least for the in situ process – because it evolves methanol. This leaves the ethoxy group, which reacts quickly enough and which is toxicologically sufficiently harmless if necessary precautions are taken <sup>71</sup>.

Measuring of the amount of ethanol evolved from a rubber blend during silanisation is the base of the estimation of the silanisation efficiency. Experiments show that the amount of ethanol evolved rises with increased dump temperature. Effective bonding of silane to the silica surface requires evaporation of 2 mol ethanol per 1 mol of TESPT. However, at 150 °C only less than half of the TESPT reacted with silica surface. From the viewpoint of silica/silane reaction time it is necessary to use the highest dump

temperature possible. On the other hand, the temperature of the entire process is limited by two parallel processes: polymer chain degradation and TESPT sulfur donation effect (scorch)<sup>68, 72</sup>. Comparing the kinetic rate constants at different temperatures in this case (Table 4), it can be concluded that mixing times should be within limits of reasonable time starting at temperatures of about 160 °C.

Table 4. Kinetic rates constants for primary ( $k_a$ ) and secondary reaction ( $k_b$ )<sup>73</sup>

| Temp. (°C)                 | 120    | 140   | 160   |
|----------------------------|--------|-------|-------|
| $k_a$ (min <sup>-1</sup> ) | 0.061  | 0.122 | 0.229 |
| $k_b$ (min <sup>-1</sup> ) | 0.0055 | 0.008 | 0.012 |

However, experiments that measure the amount of ethanol evolved during the silica/silane reaction measure not only of the reaction of surface silanol groups with the ethoxy moieties (primary reaction), but also self condensation (polymerization) of TESPT under the influence of moisture.

At low strain amplitudes, filler-filler interactions and by this indirectly silanisation efficiency can be particularly well measured in a rubber process analyzer in uncured state. From Figure 30, it can be noticed that along with increasing dump temperature, filler-filler interactions decrease because (lower  $G'$ ) of the higher degree of silanisation at higher dump temperatures. The minimum on the graph can be recognized as a point in which the suppression of filler-filler interaction turns into filler-polymer interaction due to the surface coverage of the filler. Additionally, the sulfide groups of the silane react with the polymer chains leading to scorch<sup>74</sup>.

At higher temperatures (above 160 °C), the relatively weak sulfide bridges of the coupling agent anchored on the surface of silica are breaking, causing a coupling effect and sulfur donation. Replacing TESPT by bis(triethoxysilyl)hexane (HTES), which is unable to react with the rubber due to the absence of the sulfur group, reduces the scorch problems during mixing. Interactions between with HTES silanised silica and the polymer are limited to physical interactions<sup>74</sup>.

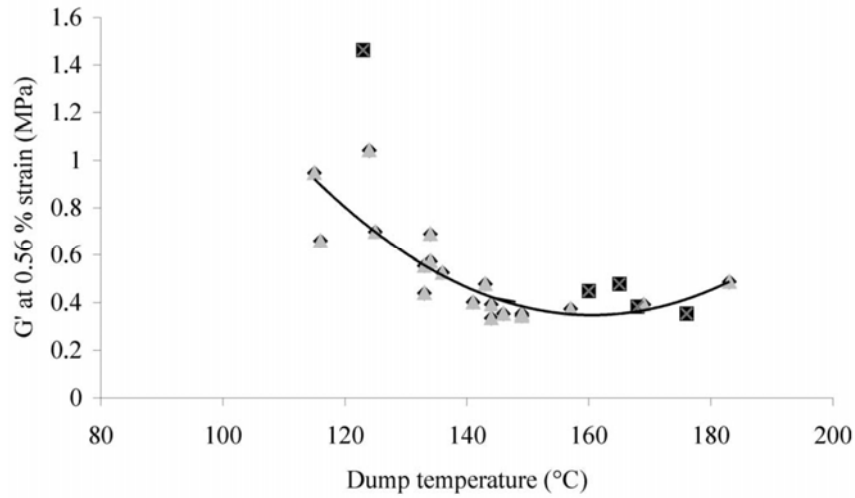


Figure 30: Influence of dump temperature on loss modulus for TESPT (□) and HTES (■)

The secondary reaction (Figure 31) is a condensation reaction with further evolution of ethanol between unreacted, adjacent ethoxy groups of the coupling agent on the filler surface or between ethoxy groups of the coupling agent and the silanol groups of the silica in cases when there is no sterical hindrance. In contrast to the primary reaction, this reaction is approximately 20 times slower at 120 °C and 10 times slower at 160 °C<sup>73</sup>. The rates of both reactions are influenced by the acidity of the matrix, and the reaction is acid as well as alkaline catalyzed<sup>27</sup>. The secondary reaction requires moisture for the hydrolysis before the actual condensation reaction can take place. Two mols of ethanol are released for each siloxane bond formed. The extent to which the secondary reaction takes place has only slight influence on the in-rubber properties<sup>68</sup>.

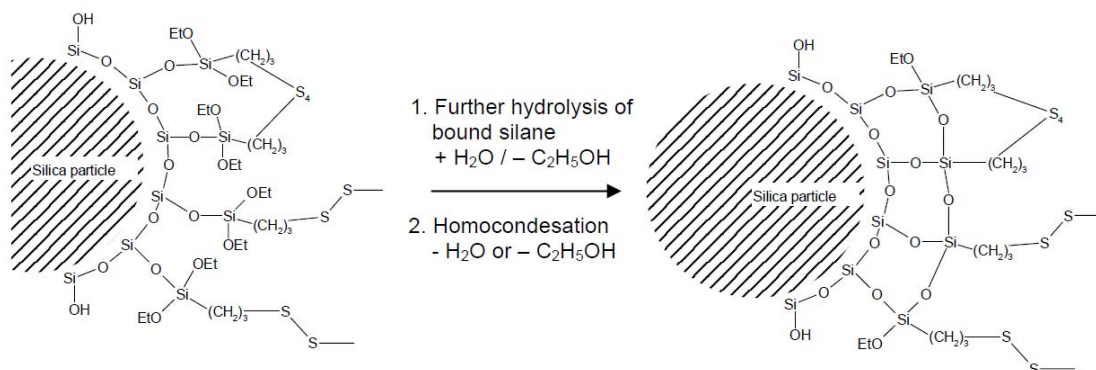


Figure 31: Secondary silanisation reactions.<sup>27</sup>

### 2.4.3 Silica – rubber coupling mechanism

In silica reinforcement systems containing TESPT, Wolff<sup>29</sup> has suggested that the TESPT-silica intermediate reacts with mercaptobenzothiazyl disulfide (MBTS) to form two moles of a polysulfide intermediate, see Figure 32. This polysulfidic pendant group on the silica surface will undergo crosslinking with the polymer chain in much the same way as it occurs in curing intermediates that converts to crosslinks. Wolff suggested that the MBT entity reacts with the allyl position of a double bond of the elastomer, thus releasing MBT (Figure 32). A covalent bond between the rubber and filler was assumed to be formed by this reaction resulting in permanently connecting rubber and filler<sup>29</sup>. This reaction takes place under normal curing conditions.

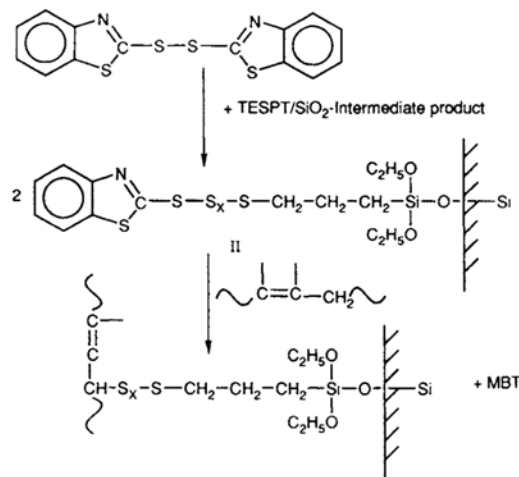


Figure 32: Possible silica-silane intermediate reaction with a rubber chain during accelerated vulcanization.<sup>29</sup>

### 2.4.4 New silanes

For sulfur cured rubber compounds, the three following types of sulfur functional silanes are used:

- di- or polysulfidic bifunctional silanes
- unblocked silanes with a reactive S-moiety
- blocked mercaptosilanes



Bis-(triethoxysilylpropyl)tetrasulfide, TESPT, is shown in Figure 33. It is a widely used coupling agent in the tire industry because it provides a good coupling. TESPT is not a pure tetrasulfide, it is a mix of polysulfides, and the average sulfur rank of the polysulfide is 3.86. In combination with accelerators like tetramethylthiuramdisulphide (TMTD) and N-cyclohexyl-2-benzothiazolesulpheneamide (CBS) but without sulfur, TESPT causes crosslinking.

TESPT requires a minimum temperature to become active during silanisation because of the steric hindrance around the silylpropyl group, but at the same time the temperature must not exceed a maximum above which premature crosslinking occurs which is the main drawback of TESPT <sup>75</sup>.

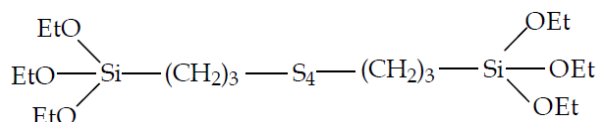


Figure 33: Bis(triethoxysilylpropyl)tetrasulfide (TESPT).

To overcome the problems with sulfur donation during processing, an alternative silane was introduced: bis(triethoxysilylpropyl)disulfide, TESP, Figure 34. TESP is again not a pure disulfide but a mixture of polysulfides. The average sulfur rank is close to 2. The major advantage of TESP is a higher stability under high shear and temperature conditions. However, due to its sulfur deficiency compared to TESPT, additional elemental sulfur is required to achieve a comparable reinforcement effect of TESPT.

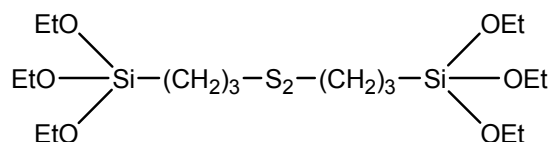


Figure 34: Bis(triethoxysilylpropyl)disulfide (TESPD).

The sulfur donation effect of the silane is one problem, but the high amount of generated ethanol during the silanisation reaction is another. To overcome this particular problem,

silanes with only one ethoxy group, e.g. bis-(dimethylethoxysilylpropyl) tetrasulfide, DMESPT (Figure 35) were developed.

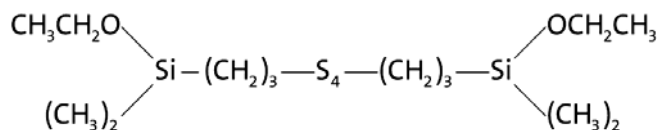


Figure 35: Bis-(dimethylethoxysilylpropyl) tetrasulfide (DMESPT).

Test results indicated that even a better dispersion is achieved compared to TESPT, as shown by the lower storage modulus  $G'$  at 0.56% strain. However, the tensile strength of the DMESPT containing vulcanizates is lower compared to the TESPT-containing material, but all other mechanical properties are similar to the TESPT material. According to Reuvekamp et al.<sup>76</sup>, a minor adjustment of the curatives in the compound recipe should overcome problems with lower tensile strength<sup>77</sup>.

A very simple and effective representative of the second group of silanes is (3-mercaptopropyl) trimethoxysilane, MPTMS, shown in Figure 36. Unfortunately, the unblocked mercapto groups make this compound too reactive during mixing causing premature crosslinking. Besides, mercapto groups carry a strong odor which is highly unpleasant and methoxy groups make it toxic during processing. Mercaptosilanes are mainly used for industrial rubber goods and for shoe soles<sup>75, 78</sup>.

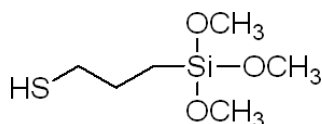


Figure 36: (3-Mercaptopropyl) trimethoxy silane (MPTMS).

Another representative of unblocked silanes is (3-thiocyanatopropyl) triethoxy silane, Figure 37. The thiocyanato group might be able to react readily with the vulcanization system during curing, whereas the tetrasulfide group in the above-mentioned silane

must be cleaved prior to reacting with the polymer. The cyanato-silane imparts better reinforcement than TESPT in conventional vulcanization (CV) and semi-efficient vulcanization (semi-EV) systems, whereas contrary results were found in an efficient vulcanization (EV) system <sup>79</sup>.

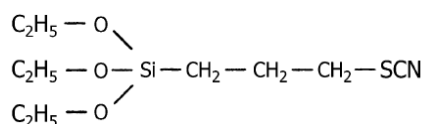


Figure 37: (3-Thiocyanatopropyl) triethoxy silane.

Recently, a reduction of the emission of ethanol during the silanisation process was achieved by the introduction of blocked silanes, Figure 38.

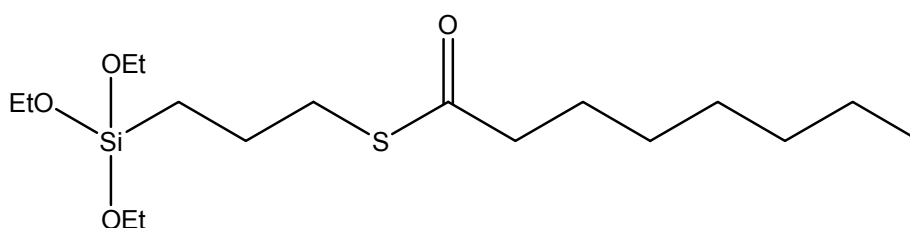


Figure 38: 3-Octanoylthio-1-propyltriethoxysilane.

In this silane, the highly reactive mercapto group is blocked (esterificated) by using octanethionic acid. The blocking of the mercapto group leads to a lower reactivity of the silane with rubber during processing. The long octanoyl group also prevents reagglomeration through steric hindrance. Removing of the octanoyl moiety is taking place during vulcanization, but some proton donor compounds, e.g. amine activators, are needed for this reaction <sup>80, 40</sup>.

The silane in Figure 39 is based on a completely different approach: A long-chain and partially polar substituent replaces two alkoxy-moieties. This side chain has two major tasks: (1) the non polar part acts as a physical shield of the mercapto group during



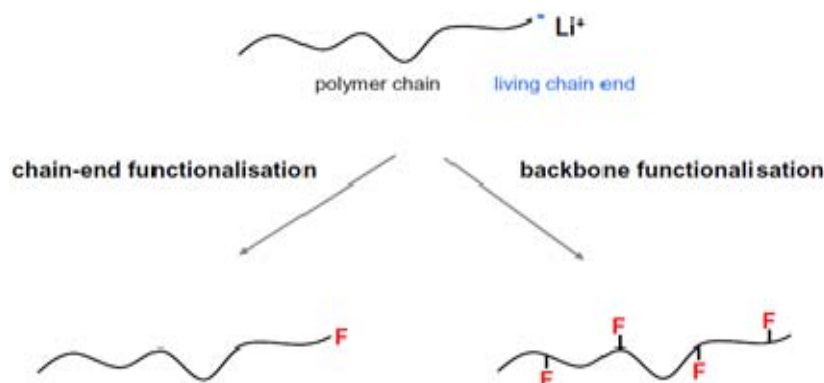


Figure 40: Polymer functionalisation <sup>84</sup>.

### 2.5.1. Chain-end functionalisation

In this mode, the polymer chain is terminated by a silane compound with reactive groups towards silica. Anionic copolymerization of styrene with butadiene is a “living polymerization” process, which means that the polymer chain is still active despite the fact that there is no monomer to react with; implementation of reactive silane compounds or tin compounds at this moment of copolymerization leads to termination of the copolymer by this silane or a tin compound. Polymers, in which a silane was used as a chain terminator or as a backbone modifier are generally used with silica, while tin ended polymers are preferably be used in combination with carbon black. As the coupling with the filler can occur only from the modified polymer chain ends, the density of the silane coupling groups is rather low and so is the bonding efficiency with silica.

Tin polymer modification (Figure 41) is a complex process, in which branching of the polymer chain caused by tin tetrachloride (or alkyl tin chloride) is playing the main role. The living polymerization allows for the termination of polymer chains in two ways: firstly, a small dosage of styrene (ST) is added to the reactor before termination followed by a tin compound; alternatively, butadiene (BD) is added followed by a tin compound in second mode. The difference between these two reaction paths is the insertion of oligomeric styryl or butadienyl molecules between the chain ending tin and the rest of the chain.

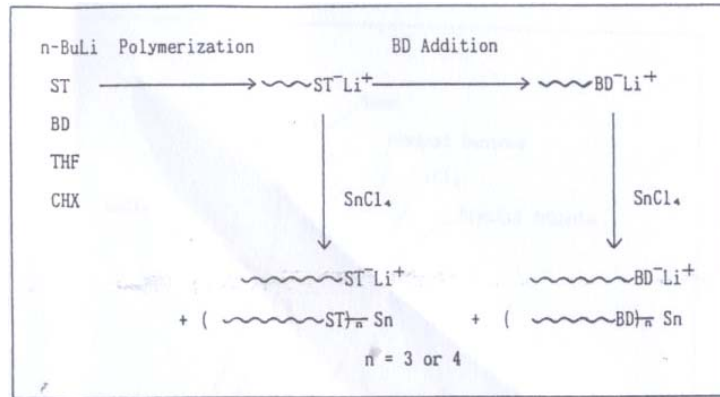


Figure 41: Two types of chain termination by tin tetrachloride  
 THF: tetrahydrofuran, CHX: cyclohexane <sup>85</sup>.

Experiments indicated that butadienyl tin terminated styrene butadiene rubber filled with carbon black have considerably lower tangent  $\delta$  values in comparison to styryl tin ended chains. This fact has been attributed to steric hindrance in the second case <sup>85, 86, 87</sup>.

Styrene butadiene rubber terminated by tin tetrachloride creates a higher fraction of bound rubber with carbon black than the non-functionalized polymer. Generally, the vulcanizates of tin coupled SBRs show lower hysteresis with the increase in bound rubber. However, the vulcanizates of randomly modified SBR with tin compounds and SBR containing low molecular weight tin coupled SBR do not show a lower hysteresis in spite of a large amount of bound rubber. Therefore the reduction of the hysteresis can not be explained by the formation of bound rubber. During tin chain termination, branched polymer structures can be created, which also can have a higher physical interaction with carbon black <sup>85, 86, 88</sup>.

### 2.5.2 Backbone functionalisation

More promising is a functionalization of the backbone of polymer chains. This modification changes the polymer itself in a considerable way, and it must be regarded as a different polymer.

In-chain chemical modification is easily achieved by using chemical compounds containing thiol groups like thioglycolic acid or ethyl mercaptoacetate. Modification is

conducted in a solution of already terminated SBR by using azobisisobutyronitrile (AIBN) as a radical source <sup>89</sup>. The chemical structure of a styrene butadiene copolymer modified by using thioglycolic acid is shown on Figure 42.

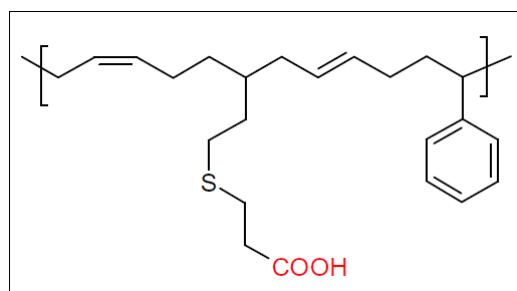


Figure 42: In-chain modified SSBR <sup>84</sup>

Introduction of polar groups in polymer chains increase polymer-filler interactions by hydrogen bonding which can be formed between the carboxylic group and the silanol group on the silica surface (Figure 43). It must clearly be stated that above mentioned modification does not eliminate using the coupling agent which still must be applied. A disadvantage of this system is that carboxylic groups can also react with amine accelerators used during vulcanization, slowing down the vulcanization process. Nevertheless, this drawback can be solved by adjusting the amount of the accelerators.

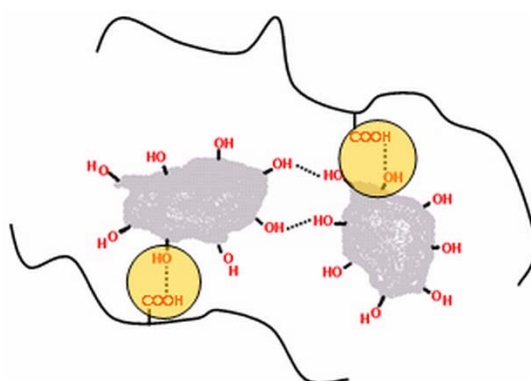


Figure 43: Interactions of in-chain modified polymer and silica

Dynamic mechanical analyses indicate that a compound composed from 70 phr of in-chain modified SBR and 30 phr BR, filled with 90 phr of silica and TESPT, have considerably increased  $\tan \delta$  values at lower temperatures and decreased  $\tan \delta$  values at higher temperatures. Additionally, the DIN abrasion of these modified polymers decreased by 12% for the highest level of functionalisation compared to the non-modified material. The influence of the degree of modification on the  $\tan \delta$  – temperature correlation is shown on Figure 44.

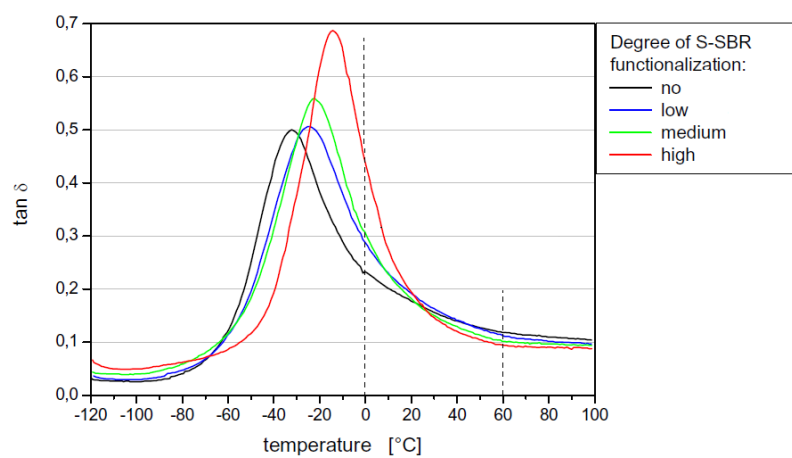


Figure 44: Impact of in-chain functionalization on the tangent  $\delta$  vs. temperature curve <sup>84</sup>

Experiments with in-chain modification of SBR resulting in different microstructures indicate that functionalization of SBR with a high styrene content (38% styrene, 23% vinyl groups) give better results than SBR with a low styrene content (24% styrene, 40% vinyl groups). A comparison of the two types of compounds is shown in Table 5.

Table 5: Influence of the microstructure on compound properties <sup>84</sup>

| S-SBR   |                  | Tan $\delta$ temp. sweep (1K·min <sup>-1</sup> , 10 Hz) |                     |                      | Amplitude sweep: tan $\delta$ max. | Rebound at 60°C [%] | DIN Abrasion [mm <sup>3</sup> ] |
|---|------------------|---|---------------------|----------------------|------------------------------------|---------------------|---------------------------------|
| No.   | Degree of funct. | Temp. at tan $\delta$ max. [°C]                         | tan $\delta$ at 0°C | tan $\delta$ at 60°C |                                    |                     |                                 |
| <b>S-SBR in compound: high-vinyl S-SBR (40% vinyl, 24% styrene, T<sub>g</sub>: -33°C)</b>   |                  |   |                     |                      |                                    |                     |                                 |
| 1   | no               | -32   | 0.232               | 0.119                | 0.211                              | 49.5                | 91                              |
| 3   | medium           | -22   | 0.305               | 0.102                | 0.161                              | 58.5                | 81                              |
| <b>S-SBR in compound: high-styrene S-SBR (23% vinyl, 38% styrene, T<sub>g</sub>: -32°C)</b> |                  |   |                     |                      |                                    |                     |                                 |
| 5   | no               | -21   | 0.308               | 0.128                | 0.213                              | 47                  | 101                             |
| 6   | medium           | -11   | 0.533               | 0.096                | 0.155                              | 58                  | 78                              |



From all above mentioned methods of polymer modification, only backbone modified polymers seem to have the potential of significant improvement of the magic triangle of tire properties. Polymer modification is limited almost only to introduction of groups capable to hydrogen bonding with the silica surface, because introduction of chemically reactive groups into the polymer backbone could induce coupling already during the mixing stage, which can lead to processing problems. Chemical bonds formed between silica and polymer during mixing result in higher transfer of shear forces from the polymer to the filler. This can lead to an increased mixing torque, because the silica agglomerates would be efficiently broken by the polymer which is attached to their surface. Chemical bonding in the mixing stage could also cause scorch during compound mixing, because each silica particle acts as a multiple crosslink nod for polymer chains. Groups capable of hydrogen bonding significantly increase the filler dispersion, despite the fact that there are no covalent bonds.

The scope of this project is to understand which characteristics of fillers, filler-polymer interactions and network characteristics are determining the performance of tread material. **The focus is on improvement of wet grip**, but rolling resistance and wear will also be considered. At the end of the thesis, a filler-polymer system will be defined, which results in a significantly improved wet grip compared to current tread materials, without trading any of the other tire performance properties.

## 2.6 FINAL CONCLUSIONS

The ideal compound for tire treads should meet the following demands:

- During breaking, the tire tread should easily deform, thus increase the contact area between tread and road.
- Applying fillers should not cause any change in the  $\tan \delta = f(T)$  curve of a polymer. In other words: energy dissipated due to rolling should be the energy dissipated by the pure polymer. The dynamic properties of the filled and unfilled polymer should be the same. Silanization is a method which increases the filler –

polymer interactions and reduces the influence of the filler on the dynamic properties. Additionally there is a lack of knowledge about the number of silanol groups that should be bound to the polymer chain, to further decrease the hysteresis of material.

- This problem could be solved by tightened filler – polymer bonding: using more efficient coupling agents, modified polymers or both at the same time.
- Applying low amounts of highly reinforcing fillers which will cause the same effect as high amount of low reinforcing filler. Due to the low filler content in the rubber matrix, its influence on dynamical properties will be low.
- The filler – filler network should break in the temperature region of wet skid, amplifying energy dissipation in this moment. However, it should be strong enough to withstand the higher strain under rolling conditions.
- The polymer network, namely physical and chemical crosslink's, should partially break under wet skid conditions, and being reformed under rolling conditions. Breaking of the bonds will cost energy, and this would help to dissipate some of the energy input when breaking. This should lead to a second maximum of the  $\tan \delta = f(T)$  curve at the temperature region of wet skid. The material should be partially thixotropic, which can be achieved by partially change the crosslink system to other which is not able to withstand higher temperature prevailing during wet skid (leads to thermal softening).
- The tread rubber should be resistant to thermal degradation – high energy dissipation during breaking means that the tread material will be exposed to high temperatures.
- The surface properties of the tire tread material should allow for easy breaking (dissipation) of the water layer between the tire and road surface causing dry friction. In other words, the surface of the tire tread should be more hydrophilic. Conversely, the inner surface of the tire tread profile should be hydrophobic to ease water drainage.
- Using TESPT or TESP as coupling agent is related with emission of large quantities of ethanol during compounding.

- Pre-silanised silica can be solution of this problem. However silanisation in solvent is related with its evaporation, what makes this process more expensive than the in-situ silanization.
- Another solution is to use coupling agents with only one ethoxy group. One reactive group instead of two in case of TESPT leads to using higher amount of this new coupling agent.

The scope of this project is to understand which characteristics of fillers, filler-polymer interaction and network formation are determining the performance of tread material. The focus is on improvement of wet grip, but rolling resistance and wear will also be considered. At the end of the thesis, a filler-polymer system will be defined, which results in significantly improved wet grip compared to current tread materials, without trading other tire performance properties.

## REFERENCES

---

- [1] R. Bond, G. F. Morton, *Polymer* 25 (1984) 132.
- [2] M. J. Wang, *Kautschuk Gummi Kunststoffe* 7 (2007) 438.
- [3] A. Yoshioka, K. Komuro, A. Ueda, H. Watanabe, S. Akita, T. Masuda, A. Nakajima, *Pure and Applied Chemistry* 58 (1986) 1697.
- [4] M.J. Wang, *Rubber Chemistry and Technology* 71 (1998) 520.
- [5] M. J. Wang, *Kautschuk Gummi Kunststoffe* 1 (2008) 33.
- [6] S. Cervenya, A. Ghilarduccib, H. Salvab, A.J. Marzoccaa, *Polymer* 41 (2000) 2227.
- [7] B. J. Allbert, J. C. Walker, *Rubber Chemistry and Technology* 41 (1968) 753.
- [8] V. Hermann W. Niedermeier, American Chemical Society, Rubber Division Meeting, Cleveland Ohio October 16-18 (2007).
- [9] Marion G. Pottinger, Thomas J. Yager "The Tire pavement interface" (1986) 125.
- [10] Adel F. Halasa, J. Prentis, B. Hsu, Ch. Jasiunas, *Polymer* 46 (2005) 4166.
- [11] K.H. Nordsiek, *Kautschuk Gummi Kunststoffe* 38 (1985) 177.
- [12] I. M. Hutchings, D. W. Deuchar, *Journal of Material Science* 22 (1987) 4071.
- [13] Mushack, R., Lüttich, R., Bachmann, W., *European Rubber Journal* 7-8 (1996) 24.
- [14] M. J. Wang, *Kautschuk Gummi Kunststoffe* 4 (2008) 159.
- [15] I. M. Hutchings, "Friction and Wear of Engineering Materials" (1992) 150.
- [16] Schallamach A. "Chemistry and Physics of Rubber-like Substances" (1963) 382.
- [17] R. A. Beck, R. W. Truss, *Wear* 218 (1998) 145.
- [18] N. Tabsana, S. Wirasatea, K. Suchiva, *Wear* 269 (2010) 394.
- [19] A. Hunsche, U. Görl, A. Muller, M. Knaack, Th. Göbel, *Kautschuk Gummi Kunststoffe* 50 (1997) 881.
- [20] Y. Fukahori, H. Yamazaki, *Wear* 178 (1994) 109.
- [21] B. B. Boonstra, *Polymer* 20 (1979) 691.
- [22] A.I. Medalia, *Rubber Chemistry and Technology*, 46 (1973) 877.
- [23] G. Kraus, *Rubber Chemistry and Technology* 44 (1971) 199.
- [24] P.P.A. Smit, *Rubber Chemistry and Technology* 41 (1968) 1194.
- [25] J. B. Donnet, *Rubber Chemistry and Technology* 71 (1998) 323.
- [26] E. Guth, O. Gold, *Physical Review* 53 (1938) 322.
- [27] Dierkes, Wilma Karola, Economic mixing of silica-rubber compounds: interaction between the chemistry of the silica-silane reaction and the physics of mixing. Thesis (2005).
- [28] M. Akiba, A.S. Hashim, *Progress in Polymer Science* 22 (1997) 475.
- [29] S. Wolff, *Rubber Chem. Technol.* 55 (1983) 967.
- [30] A. Schröder, M. Klüppel, R. H. Schuster, J. Heideberg, *Kautschuk Gummi Kunststoffe* 54 (2001) 260.
- [31] A. Schröder M. Klüppel R.H. Schuster J. Heideberg, *Carbon* 40 (2002) 207.
- [32] J. B. Donnet, "Science and Technology of Rubber" (2005) 367.

- 
- [33] M. P. Wagner, *Rubber Chemistry and Technology* 49 (1976) 703.
- [34] M. J. Wang, *Rubber Chemistry and Technology* 71 (1998) 520.
- [35] N. Hewitt, "Compounding Precipitated Silica in Elastomers" (2007) 12.
- [36] P.K. Jal, S. Patel, B.K. Mishra, *Talanta*, 62 (2004) 1005.
- [37] D.R. Bassett, E.A. Boucher, A.C. Zettlemyer, *Journal of Colloid and Interface Science* 27 (1968) 649.
- [38] J. L. Leblanc, *Progress in Polymer Science* 27 (2002) 627.
- [39] O. Klockmann, A.Hasse, *Kautschuk und Gummi Kunststoffe* 7 (2007) 82.
- [40] Satoshi Mihara, *Reactive processing of silica-reinforced tire rubber*, thesis, 2009.
- [41] M. J. Wang, *Kautschuk und Gummi Kunststoffe* 9 (2007) 438.
- [42] M. J. Wang, S. Wolff, J. B. Donnet, *Rubber Chemistry and Technology*, 64 (1991) 559.
- [43] U. Gori, A. Hunsche, A. Mueller, H.G. Koban, *Rubber Chemistry and Technology*, 70 (1997) 608.
- [44] United States Patent No. 6,197,274, (2001).
- [45] United State Patent No. 5,904,762, (1999).
- [46] M. J. Wang, Y. Kutsovsky, P. Zhang, G. Mehos, L. J. Murphy, K. Mahmud, *Kautschuk Gummi Kunststoffe* 55 (2002) 33.
- [47] M. J. Wang, Y. Kutsovsky, P. Zhang, L. J. Murphy, S. Laube, K. Mahmud, *Rubber chemistry an technology* 75 (2002) 247.
- [48] P. Zhang, M. J. Wang, Y. Kutsovsky, S. Laube, K. Mahmud, Rubber Division, American Chemical Society, Cleveland, Ohio October 16 - 19 (2001).
- [49] United States Patent No. 2,531,396, (1950).
- [50] H. Fischer *Material Science and Engineering* 23 (2003) 763.
- [51] S. Pavlidou, C.D. Papaspyrides, *Progress in Polymer Science* 33 (2008) 1119.
- [52] C. Debek, *Elastomers* 5 (2006) 1.
- [53] M. Zanetti, S. Lomakin, G. Camino, *Macromolecular Materials and Engineering* 1-9 (2000) 279.
- [54] M. Alexandre, P. Dubois, *Materials Science and Engineering* 28 (2000) 1.
- [55] F. Schon, W. Gronski, *Kautschuk Gummi Kunststoffe* 56 (2003) 166.
- [56] M. Ganter, W. Gronski, H. Semke, T. Zilg, C. Thomman, R. Muhlhaupt, *Kautschuk und Gummi Kunststoffe* 54 (2001) 166.
- [57] R. Sengupta, S. Chakraborty, S. Bandyopadhyay, R. Mukhopadhyay, S. Dasgupta K. Auddy, A.S. Deuri *Polymer Engineering and Science* 47 (2007) 1956.
- [58] R. Rajasekar, G. Heinrich, A. Das, Ch. K. Das, *Research Letters in Nanotechnology* 2009 (2009) 1.
- [59] A. Das, R. Jurk, K. W. Stockelhuber, T. Engelhardt, J. Fritzsche, M. Kluppel, G. Heinrich, *Journal of Macromolecular Science* 45 (2008) 144.
- [60] H. Essawy, D. El-Nashar, *Polymer Testing* 23 (2004) 803.

- 
- [61] A. Mousa, J. Karger-Kocsis, *Macromolecular Materials and Engineering* 286 (2001) 260.
- [62] M. Ganter, W. Gronski, H. Semke, T. Zilg, C. Thomann, *Kautschuk Gummi Kunststoffe* 54 (2001) 166.
- [63] J. H. Bachmann, J. W. Sellers, M. P. Wagner, R. F. Wolf, *Rubber Chemistry and Technology* 32 (1959) 1286.
- [64] S. Wolff, Wesseling, *Kautschuk und Gummi Kunststoffe* 28 (1975) 379.
- [65] J.T. Byers, *Rubber World* 218 (1998) 38.
- [66] A. Hunsche, U. Gorl, A. Muller, M. Knaack, *Kautschuk und Gummi Kunststoffe* 50 (1997) 881.
- [67] A. Hunsche, U. Gorl, H.G. Koban, T. Lehmann, *Kautschuk und Gummi Kunststoffe* 51 (1997) 525.
- [68] H. D. Luginsland, A. Hasse, American Chemical Society, Rubber Division Meeting, Dallas Texas, April (2000).
- [69] A. Ansarifar, H.P. Lim, R. Nijhawan, *International Journal of Adhesion and Adhesives* 24 (2004) 9.
- [70] U. Gorl, A. Hunsche, *Kautschuk und Gummi Kunststoffe* 51 (1998) 525.
- [71] Annemieke ten Brinke, *Silica Reinforced Tyre Rubbers*. Thesis (2002).
- [72] R. Bond, Chemical Society, Rubber Division Meeting, Chicago, May 3-6 (1977).
- [73] L.A.E.M. Reuvekamp, *Reactive mixing of silica and rubber for tires and engine mounts*. Thesis (2003).
- [74] J.W. ten Brinke, S.C. Debnath, L.A.E.M. Reuvekamp, J.W.M. Noordermeer, *Composites Science and Technology* 63 (2003) 1165.
- [75] B. Rodgers "Rubber compounding: chemistry and applications" (2005) 424.
- [76] L.A.E.M. Reuvekamp, P.J. van Swaaij, J.W.M. Noordermeer, *Kautschuk und Gummi Kunststoffe* 1 (2009) 35.
- [77] M. Zaborski, A. Vidal, G. Ligner, H. Balard, E. Papirer, and A. Burneuf, *Langmuir* 5 (1989) 447.
- [78] F. Thorn, S. Wolff, *Kautschuk und Gummi Kunststoffe* 28 (1975) 733.
- [79] P. Sae-oui, Ch. Sirisinha, U. Thepsuwan, K. Hatthapanit, *Polymer Testing* 23 (2004) 871.
- [80] P.G. Joshi, R.W. Cruse, R.J. Pickwell, K.J. Weller, W.E. Sloan, M. Hofstetter, E.R. Pohl, M.F. Stout and F.D. Osterholtz, *Momentive performance materials*.
- [81] A. Blume, *Kautschuk und Gummi Kunststoffe* 4 (2011) 38.
- [82] O. Klockmann, *Rubber World*, 3 (2010) 21.
- [83] O. Klockmann, A. Hasse, *KGK*, 3 (2007) 82.
- [84] N. Steinhäuser, A. Lucassen, Belgian Plastics and Rubber Institute Conference, Brussels, 25th November (2009).
- [85] F. Tsutsumi, M. Sakakibara, N. Oshima, *Rubber Chemistry and Technology* 63 (1990) 8.

- 
- [86] V. R. S. Quiteria, C. A. Sierra, J. M. G. Fatou, *Die Angewandte Makromolekulare Chemie* 246 (1997) 85.
- [87] C. A. Sierra, C. Galan, V. Ruiz Santa Quiteria, *Rubber Chemistry and Technology* 68 (1995) 259.
- [88] S. Thiele, D. Bellgardt, M. Holzleg, *Kautschuk Gummi Kunststoffe*, 5 (2008) 244.
- [89] F. Romani, E. Passaglia, M. Aglietto, G. Ruggeri, *Macromolecular Chemistry and Physics* 200 (1999) 524.





---

# **Influence of the silica specific surface area and structure on rolling and wet skid resistance of a passenger car tire tread compound**

---

*In this study, five different rubber reinforcing silica types are investigated concerning their influence on properties related to tire performance. The silicas are characterized by different specific surface areas, aggregate sizes and structure, but with otherwise comparable properties. A standard “Green tire” tread recipe is used as base compound, and bis-(triethoxysilylpropyl)tetrasulfide (TESPT) is used as coupling agent. The amount of coupling agent is adjusted to the specific CTAB surface area of the silicas. The silicas are tested in two modes: the silica loading is kept constant and the silica loading is empirically adjusted to reach equal hardness in the vulcanized state. The value of the dynamic loss tangent,  $\tan \delta$  at 60 °C is used to assess the influence on rolling resistance, and the Laboratory Abrasion Tester (LAT 100) is used to evaluate the wet skid resistance of the tested compounds. This equipment was chosen due to the good correlation with on-road tests. Besides these tire performance indicators, also other properties are investigated in this paper. Silica with the smallest aggregate size provides superior wet skid resistance at constant loading mode. The highest wet skid resistance is maintained even when the silica load is decreased to equalize the hardness of its corresponding vulcanizates. A decreased concentration of the high surface area silica provides also low values of  $\tan \delta$  at 60 °C which correspond with better rolling resistance of tires made therewith.*

### 3.1 INTRODUCTION

Despite many studies on the performance of tire tread compounds, thorough knowledge of the influence of the characteristics of silica reinforcing fillers on wet skid and rolling resistance is still limited. It is well-known that by the change from carbon black to a silica-silane filler as reinforcing system, the rolling and wet skid resistances of tire treads are improved. Therefore, the present European passenger car tire industry uses preferably silica as filler in tire tread formulations. Apart from the rolling resistance improvement, the wet skid or traction performance of tire treads is also an important safety and performance criterion. However, it is still somewhat questionable which silica characteristics result in a simultaneous improvement of wet skid resistance as well as rolling resistance. The friction, traction or skid resistance, in dry and wet conditions, of tire treads on various surfaces has been subject of numerous experimental and modeling studies already: Wang [1,2,3], Heinz and Grosch [4,5,6], Derham [7], Heinrich et al. [8,9,10], Klüppel and Heinrich [11], Müller et al. [12], Le Gal and Klüppel [13], Persson et al. [14], Isono et al. [15].

In order to investigate the influence of the specific silica surface area, aggregate size and structure on tire performance indicators, five different highly dispersible silica types are compared in the present study. Commercially available silicas can be divided into two groups: conventional silicas (CV) and highly dispersible silicas (HDS). U.S. Patent No. 6,180,076 discloses HDS defined by the ratio of the peak heights of primary particles in non-degraded state (1-100  $\mu\text{m}$ ) to their size in degraded state ( $< 1 \mu\text{m}$ ), that is after ultrasonic treatment, termed the  $W_k$  coefficient. In HDS this coefficient must not exceed a level of 3.4 and the lower the value, the higher is the silica dispersion level [16,17]. The major difference between conventional silica and HDS lays in their structure and aggregate size distribution. Aggregates of HDS are more branched, with 3-4 branches on average. This results in the fact that HDS has an improved dispersion over the conventional ones due to better transfer of shear forces during mixing [18,19]. The aggregate size distribution for both conventional and HDS is shown in Figure 1.

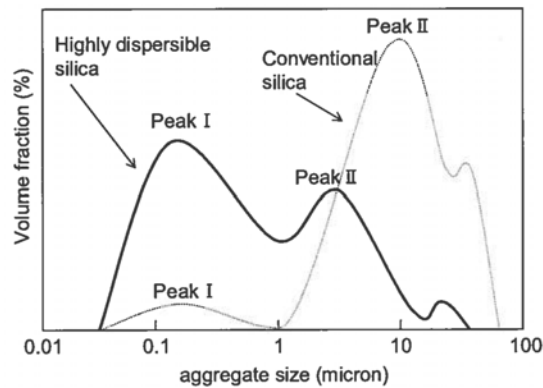


Figure 1: Size distribution of silica aggregates for conventional and highly dispersible silica [18].

The specific surface areas measured in accordance with Brunauer Emmett Teller (BET) and Cetyl Trimethylammonium Bromide (CTAB) describe the accessibility of the silica surface to relatively small molecules like nitrogen in case of the BET measurement, or relatively large molecules like polymers in the case of the CTAB measurements [20,21]. The BET value is a measure of the “total” surface area, while the CTAB value corresponds to the “outer” surface area of the silica. The ratio of BET to CTAB is often used to compare the particular silica types. A large difference between the two specific surface areas is hard to achieve. For the majority of silica types the value of the BET to CTAB ratio ranges somewhere in between 0.8 and 1.2. However higher values of 1.5 to 2.4 are also reported in the literature [22,23,24].

The goal of the present study is to characterize the underlying mechanisms involved in filler-rubber interactions for wet skid and rolling resistance of tire treads, a dynamic-viscoelastic phenomenon. The storage and loss moduli are commonly measured as dynamic properties for the assessment of the tire properties. The ratio of loss to storage modulus is the definition of the loss tangent or tangent delta. The influence of the filler-polymer interaction on wet skid performance is investigated by testing the dynamic properties, the  $\tan \delta$  in the temperature range from 0 – 20 °C at 10 Hz. The values of the loss angle in this temperature range are so far considered to be the most suitable indicators for the wet skid performance of a tire tread [8,25,26]. Assessment of rolling resistance by measuring the tangent delta value at 40 – 60 °C on laboratory scale is

common practice, and a correlation between dynamic properties of the material and on-road tests is widely accepted [27]. Additionally, measurements on a Laboratory Abrasion Tester 100 (LAT 100) are performed to assess the wet skid performance, as this method comes closer to the practical case of a rolling tire [28,29].

## 3.2. EXPERIMENTAL

### 3.2.1 Materials and compound formulations

To assess the influence of the silica specific surface area and morphology on the wet skid, rolling resistance and other related properties, 5 types of silica differing in these two properties but otherwise comparable were used in this study. The silica samples are commercial grades produced by Rhodia Silices, presently member of the Solvay group (Lyon, France). The physical properties of these silica types are described in Table 1. A detailed specification of the other compounding ingredients is shown in Table 2.

Table 1: Physical properties of the different silica types.

| Silica characteristics                               |               |               |               |              |              |
|--|---------------|---------------|---------------|--------------|--------------|
| Silica type  | Zeosil 1085GR | Zeosil 1115MP | Zeosil 1165MP | Zeosil 200MP | Z HRS 1200MP |
| Silica code  | SSA-80        | SSA-110       | SSA-160       | SSA-200      | SSA-195      |
| BET surface area (m <sup>2</sup> /g)                 | 90            | 115           | 165           | 215          | 200          |
| CTAB surface area (m <sup>2</sup> /g)                | 80            | 110           | 160           | 200          | 195          |
| Humidity (%)   | 6.0           | 6.0           | 7.0           | 6.5          | 7.0          |
| Mean diameter of aggregates * (nm)                   | 120           | 90            | 53            | 65           | 40           |
| Diameter of elementary particles ** (nm)             | -             | 25            | 20            | 10           | 15           |
| Structure:<br>Diocetyl adipate adsorption (ml/100 g) | 221           | 220           | 213           | 218          | 220          |

\* Determined by X-ray disc centrifugation in water suspension after desagglomeration in-situ using an ultrasonic probe [30].

\*\* Small-Angle X-ray scattering [31]

Particular attention is drawn to two silica types, namely Zeosil 200MP and Zeosil 1200 MP. Measurements of the BET specific surface area gives evidence of similar primary particle size of these two silicas. However the aggregate size measurements performed after the desagglomeration confirm existence of the larger aggregates for Zeosil 200MP. Considering the dimensions given by these two experiments, a model depicting the

morphology of these two silicas can be drawn, see Figure 2. The model shows also a different aspect ratio of these two silica types.

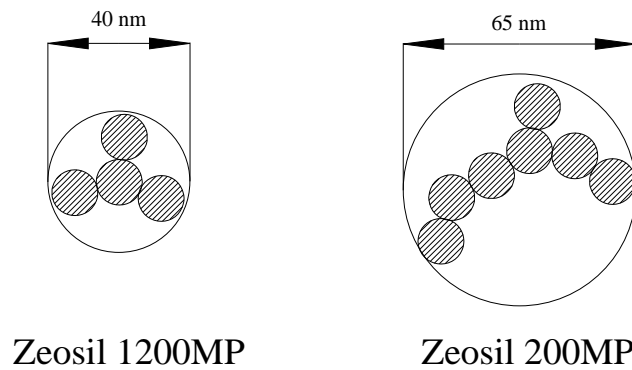


Figure 2: Differences in silica structure for Zeosil 1200MP and 200MP.

Table 2: Ingredients specification.

| Ingredient   | Specification  | Supplier                                   |
|--------------|--|--|
| S-SBR        | Solution Styrene-Butadiene Rubber<br>Buna VSL 5025-2 HM          | Lanxess,<br>Leverkusen, Germany            |
| BR           | High -cis Butadiene Rubber<br>Europrene BR40                     | Eni Polimeri, Ravenna, Italy               |
| TESPT        | Bis-(triethoxysilylpropyl)tetrasulfide                           | Evonik GmbH, Essen,<br>Germany             |
| TDAE         | Treated Distillate Aromatic Extract oil,<br>VivaTec 500          | Hansen & Rosenthal,<br>Hamburg, Germany    |
| Zinc oxide   | Inorganic oxide  | Sigma Aldrich, St. Louis,<br>United States |
| Stearic acid | Organic acid   | Sigma Aldrich, St. Louis,<br>United States |
| 6PPD         | Antiozonant N-phenyl-N'-1,3-dimethylbutyl-p-<br>phenylenediamine | Flexsys, Brussels, Belgium                 |
| TMQ          | Antioxidant 2,2,4-trimethyl-1,2-di-<br>hydroquinoline            | Flexsys, Brussels, Belgium                 |
| Sulfur       | Elemental sulfur, purified by sublimation                        | Sigma Aldrich, St. Louis,<br>United States |
| TBBS         | Accelerator N-tert-butylbenzothiazole-2-<br>sulphenamide         | Flexsys, Brussels, Belgium                 |
| DPG          | Accelerator - diphenyl guanidine                                 | Flexsys Brussels, Belgium                  |

Bis-(triethoxysilylpropyl)tetrasulfide (TESPT) was chosen as coupling agent. The experiments were performed using a typical “Green tire” recipe as given in Table 3 and

[32]. The TESPT content was adjusted to the surface area of the particular silica type by using the empirical equation proposed by L. Guy et al. [31]: Equation 1.

$$TESPT (phr) = 5.3 \times 10^{-4} \times (CTAB)_{silica} \times (phr)_{silica} \quad (\text{Equation 1})$$

Two series of batches were prepared:

1. Series I, in which the silica loading was kept at the same level of 80 phr (Table 3).
2. Series II, in which the silica loading was empirically adjusted to obtain equal hardness for all compounds after vulcanization (**Error! Reference source not found.**). Similar hardness of the samples provides more comparable materials for the LAT 100 tests.

### 3.2.2 Mixing and vulcanization

A 1.6 liter Banbury mixer was used for mixing. This process was done in three steps according to the parameters as given in Table 5. The first two steps of the mixing process were done in the internal mixer with an initial set temperature of 40 °C. The dump temperature of the compound was adjusted to be 155 °C by manually changing the cooling water flow and changing the rotor speed, if necessary. Addition of curatives was done on a two roll mill preheated to 50 °C.

Table 3: Compound formulations – constant silica loading (Series I).

|                       | I-80 | I-110 | I-160 | I-200 | I-195 |
|-----------------------|------|-------|-------|-------|-------|
| SBR Buna VSL 5025-2HM | 103  | 103   | 103   | 103   | 103   |
| Europrene BR40        | 25   | 25    | 25    | 25    | 25    |
| SSA-80                | 80   |       |       |       |       |
| SSA-110               |      | 80    |       |       |       |
| SSA-160               |      |       | 80    |       |       |
| SSA-200               |      |       |       | 80    |       |
| SSA-195               |      |       |       |       | 80    |
| TESPT                 | 3,39 | 4,66  | 6,78  | 8,48  | 8,27  |
| TDAE                  | 5    | 5     | 5     | 5     | 5     |
| Zinc oxide            | 2,5  | 2,5   | 2,5   | 2,5   | 2,5   |
| Stearic acid          | 2,5  | 2,5   | 2,5   | 2,5   | 2,5   |
| 6PPD                  | 2    | 2     | 2     | 2     | 2     |
| TMQ                   | 2    | 2     | 2     | 2     | 2     |
| Sulphur               | 2,22 | 1,91  | 1,4   | 1,00  | 1,05  |
| DPG                   | 2    | 2     | 2     | 2     | 2     |
| TBBS                  | 1,7  | 1,7   | 1,7   | 1,7   | 1,7   |

Table 4: Compound formulations – equal hardness (Series II).

|                       | II-80 | II-110 | II-160 | II-200 | II-195 |
|-----------------------|-------|--------|--------|--------|--------|
| SBR Buna VSL 5025-2HM | 103   | 103    | 103    | 103    | 103    |
| Europrene BR40        | 25    | 25     | 25     | 25     | 25     |
| SSA-80                | 115   |        |        |        |        |
| SSA-110               |       | 95     |        |        |        |
| SSA-160               |       |        | 80     |        |        |
| SSA-200               |       |        |        | 72     |        |
| SSA-195               |       |        |        |        | 65     |
| TESPT                 | 5     | 5,5    | 6,8    | 7,6    | 6,7    |
| TDAE                  | 5     | 5      | 5      | 5      | 5      |
| Zinc oxide RS         | 2,5   | 2,5    | 2,5    | 2,5    | 2,5    |
| Stearic acid          | 2,5   | 2,5    | 2,5    | 2,5    | 2,5    |
| 6PPD                  | 2     | 2      | 2      | 2      | 2      |
| TMQ                   | 2     | 2      | 2      | 2      | 2      |
| Sulphur               | 1,8   | 1,7    | 1,4    | 1,2    | 1,42   |
| DPG                   | 2     | 2      | 2      | 2      | 2      |
| TBBS                  | 1,7   | 1,7    | 1,7    | 1,7    | 1,7    |

Table 5: Mixing procedure.

|  |  |
|--|--|
| Stage I  |  |
| Rotor speed: 75 RPM                                      |  |
| Initial temp.: 40 °C                                     |  |
| Timing   | Ingredient                                 |
| (Min. sec.)  |  |
| 0.0  | Add polymers                               |
| 1.0  | Add ½ silica, ½ silane, ZnO + stearic acid |
| 3.0  | Add ½ silica, ½ silane, oil, TMQ, 6PPD     |
| 4.0  | Sweep                                      |
| 6.30   | Dump @ ~ 155 °C                            |
| Stage II   |  |
| Rotor speed: 90 RPM                                      |  |
| Initial temp.: 40 °C                                     |  |
| Timing   | Ingredient                                 |
| (Min. sec.)  |  |
| 0.0  | Add I stage batch                          |
| 6.30   | Dump @ ~ 155 °C                            |
| Stage III  |  |
| Mixing in the curatives was performed on a two roll mill |  |

Vulcanization of the sheeted samples for tensile tests was performed on a Wickert laboratory press (WLP 1600) at 160 °C and 100 bar for an optimal curing time ( $t_{95}$ ) obtained from Moving Die Rheometer (MDR 2000, Alpha Technologies) measurements according to ISO 6502. The samples for hardness tests were prepared in cylindrical molds and cured for a period of two times the  $t_{90}$ . The samples for the DIN abrasion test

were cured for  $t_{90}$  multiplied by 1.2. The adjustment of the curing time as measured in the rheometer was necessary due to the high thickness of the samples and the low thermal conductivity of the rubber compounds.

### **3.2.3 Characterizations**

The Mooney viscosity ML(1+4) of the compounds was measured at 100 °C on a Mooney viscometer MV2000E (Alpha Technologies) according to ISO 289-1.

Payne effect measurements were done by using a Rubber Process Analyzer, RPA 2000 from Alpha Technologies, after prior vulcanization for  $1.2 \times t_{90}$  at 160 °C in the RPA 2000. In order to assess the Payne effect values, the storage moduli at 1% strain and 90% strain were measured at 100°C and a frequency of 0.5 Hz.

Mechanical properties of the samples were tested using a Zwick Z020 tensile tester according to ISO-37. A crosshead speed of 500 mm/min was used. The measurements were done at ambient temperature.

Filler macrodispersion measurements were done using the visual microscopic inspection method with 100 × magnification according to ISO 11345 method C. Measurements were done by using a Leica microscope.

Shore A hardness of the samples was measured in five different places on the samples, which were cylindrical with a diameter of 10 mm. The median value was given as a representative hardness of the particular sample.

Abrasion resistance was measured by a DIN abrader machine (Abrasion tester 564C from Karl Frank GmbH) according to method A of DIN 53516. The weight loss was measured and recalculated to a volume loss for each sample.

In order to characterize the wet skid resistance, dynamic mechanical analysis was performed on a Gabo Dynamic Mechanical Analyzer in a temperature-sweep mode from



-100 °C to +100 °C with 1 % static and 0,1 % dynamic strain and a frequency of 10 Hz. In order to predict the rolling resistance, single point measurements of  $\tan \delta (= G''/G')$  at 60 °C with 2 % strain and a frequency of 10 Hz were made, where  $G'$  is the storage modulus and  $G''$  the loss modulus.

A Laboratory Abrasion Tester 100 (LAT 100, VMI the Netherlands) was used to estimate the wet skid resistance of the tire treads in conditions which simulate the real conditions on a road: Figure 3 [4]. Wheel samples were made by compression molding in a special mold using the Wickert laboratory vulcanization press for 11 mins. at 170 °C. Testing was performed at five different water temperatures: 2 °C, 8 °C, 15 °C, 22 °C, 30 °C and at constant slip angle of 15°. An electro-corundum disc with relative roughness 180 was used to simulate the tire-road interactions. Tests were performed at constant speed of 1,5 km/h and load of 75 N for a distance of 33 meters. The Side Force Coefficient (SFC) values (Equation 2) for the particular samples are compared with the value obtained for the reference sample and given as relative values. The property with higher rating is always better.

$$SFC = \frac{F_y}{F_z} \quad (\text{Equation 2})$$

Where  $F_y$  = the side force; and  $F_z$  = the normal load on the rubber wheel sample.

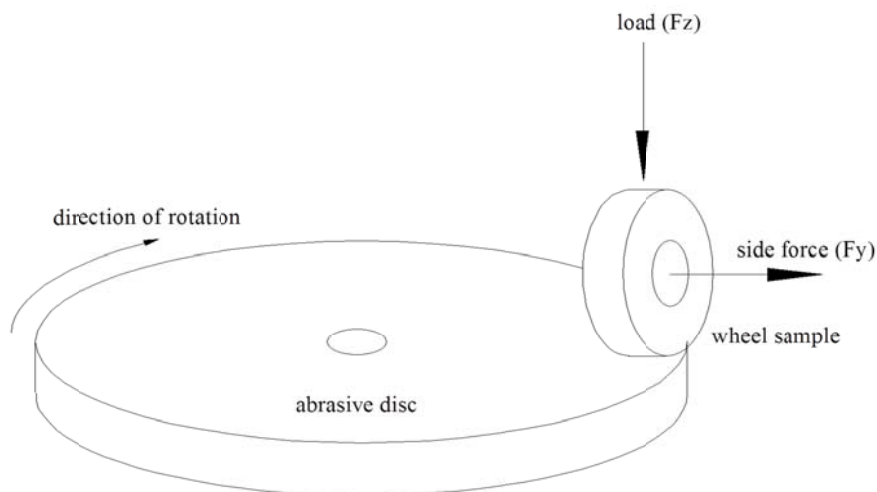


Figure 3: Principle of measurement on the LAT 100.

### 3.3 RESULTS AND DISCUSSION

#### 3.3.1 Mixing fingerprints

The energy consumption during mixing is an important factor from both an economic and environmental point of view. Power profile and mixing chamber temperature were registered and are shown in Figure 4 and Figure 5 for the first mixing stage, as well as Figure 6 and Figure 7 for the second mixing stage. As the silicas are characterized by different specific surface areas, the degree of filler-polymer interaction varied, and thus the shear forces during mixing differed in strength. Hence, to prevent an excessive rise in the discharge temperature the mixing time had to be shortened for some batches.

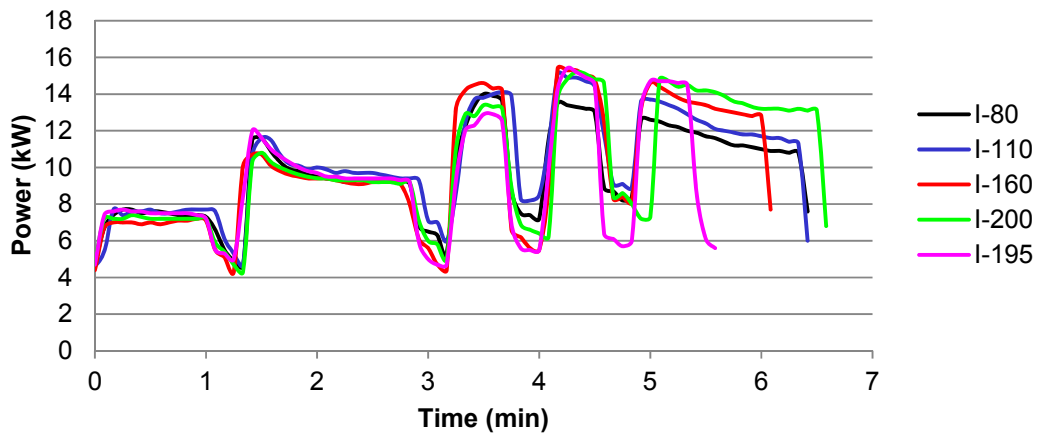


Figure 4: Power profile for the different silica types during the first stage of mixing – Series I.

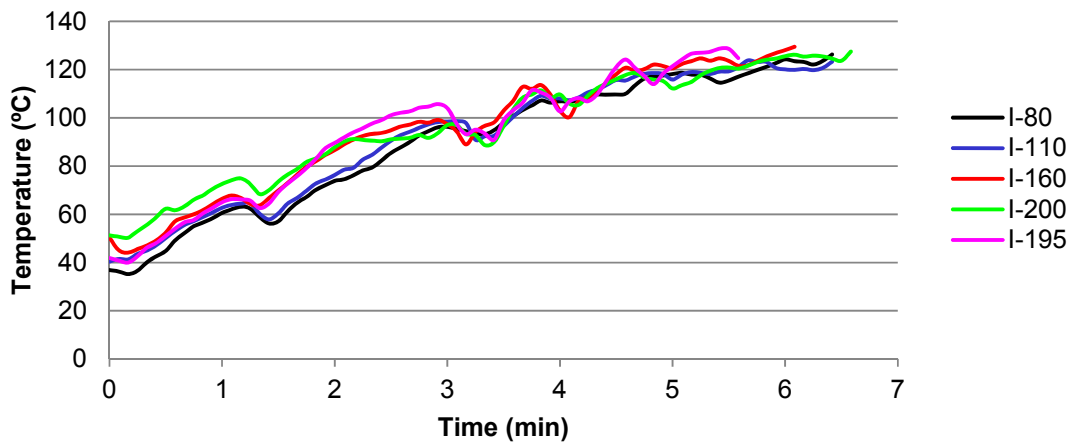


Figure 5: Temperature profile during the first mixing stage – Series I.

The second mixing stage was preceded by 24 hours of batch stabilization. With increasing surface area, the mixing process became more energy consuming, caused by the fact that with the same amount of silica (80 phr), different total surface areas are involved in the mixing process.

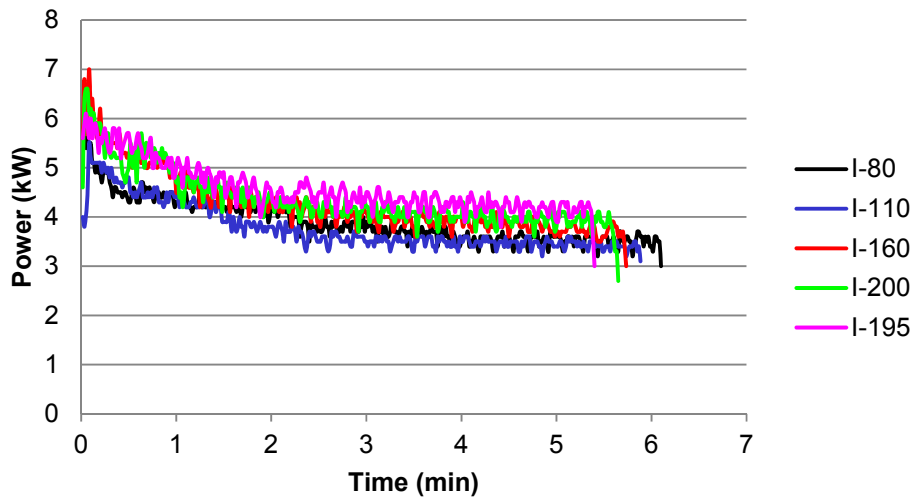


Figure 6: Power profile during the second mixing stage – Series I.

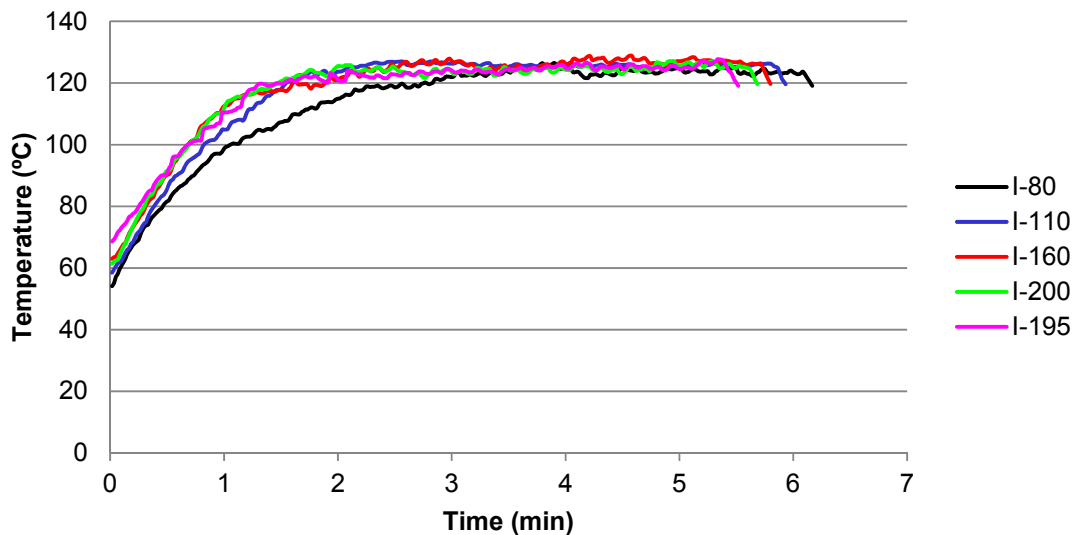


Figure 7: Temperature profile during the second stage of mixing – Series I.

Fingerprints of the first mixing stage for Series II, which contain variable amounts of silica, are shown in Figure 8 and Figure 9. In order to obtain equal hardness, the silica loading was increased for the low reinforcing types, SSA-80 and SSA-110 and decreased for the highly reinforcing types, SSA-195 and SSA-200. The value of hardness obtained for the batch containing 80 phr of silica SSA-160 was used as reference value. Increase of the silica loading with lower reinforcing capabilities, lower specific surface area, still turns out to result in higher shear forces: Figure 8. This points at the benefit of using a relatively small amount of highly reinforcing fillers over larger amounts of low reinforcing fillers. By the strong reinforcing effect caused by silicas with smallest aggregates and highest specific surface area, the loading of the silicas can in fact be decreased resulting in lower energy consumption during mixing.

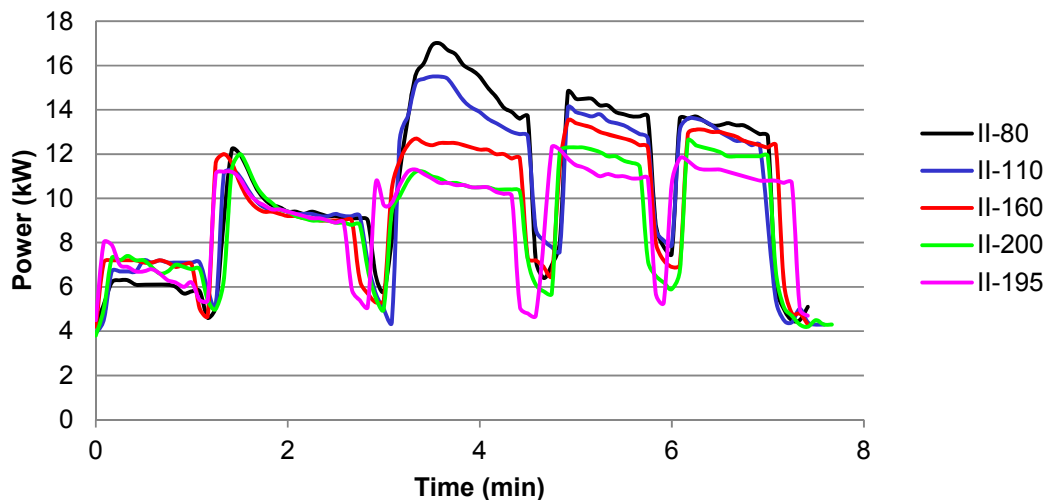


Figure 8: Power profile during first mixing stage – Series II.

The second stage of mixing is shown in Figure 10 and Figure 11. Again, it shows that the batch containing 65 phr of silica SSA-195, the highly reinforcing type, is characterized by the lowest energy consumption.

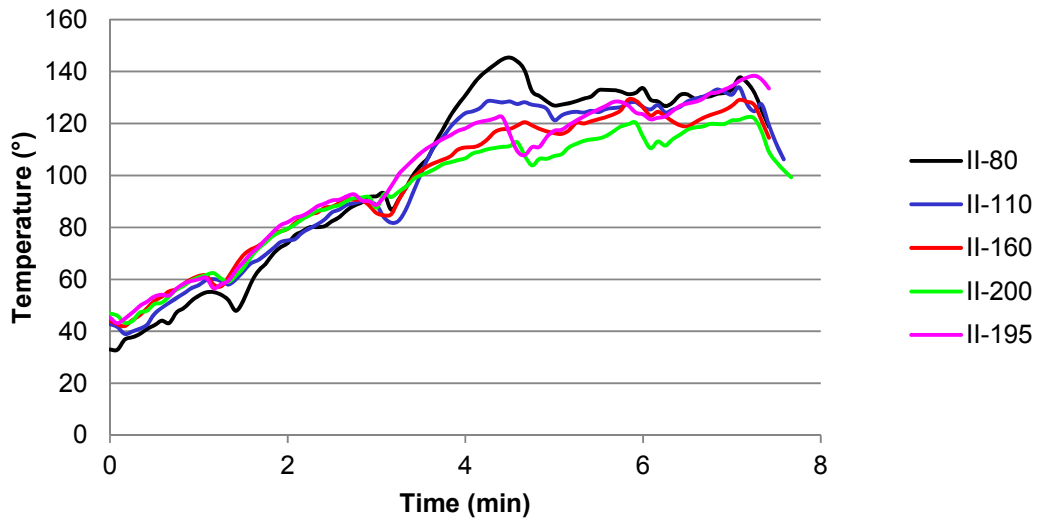


Figure 9: Temperature profile during first mixing stage – Series II.

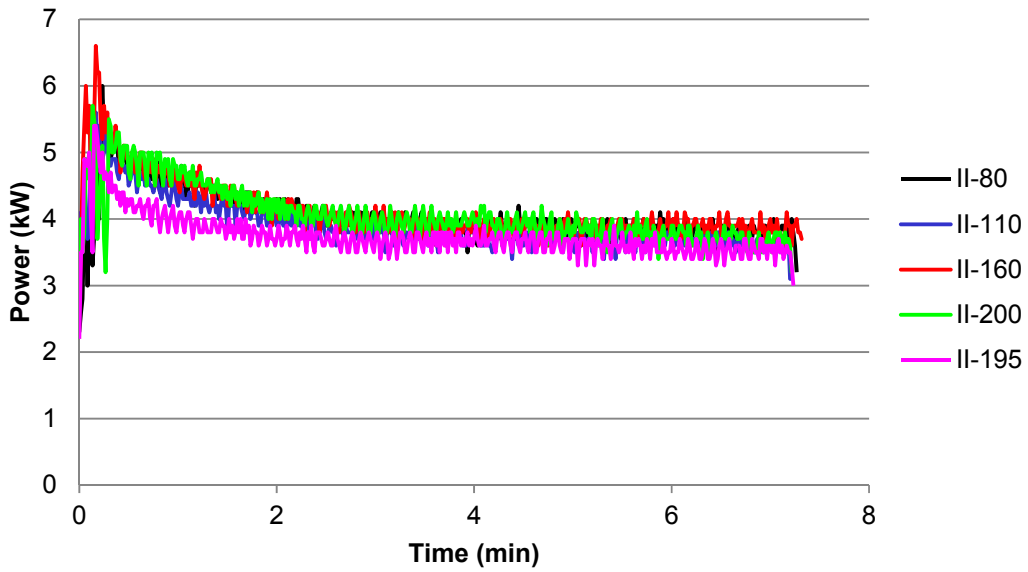


Figure 10: Power profile during second mixing stage – Series II.

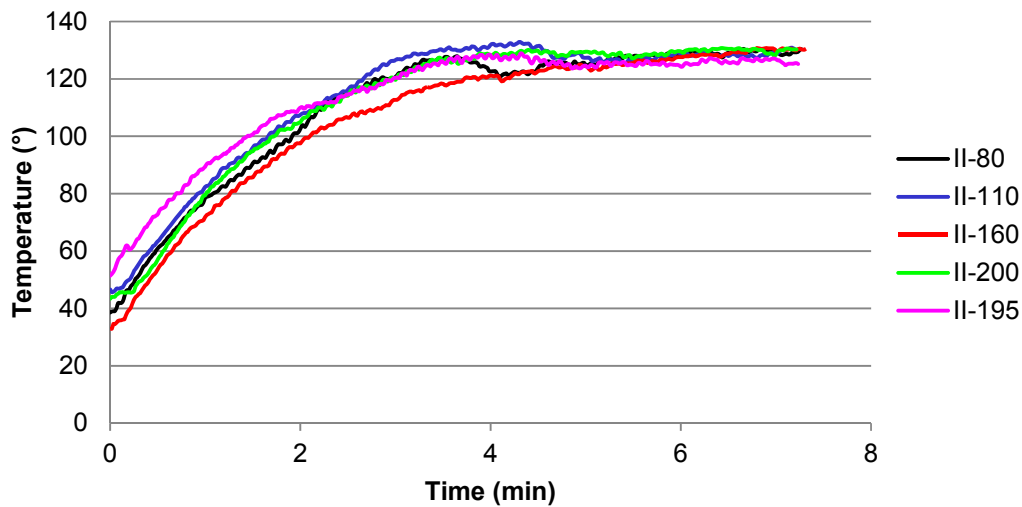


Figure 11: Temperature profile during second mixing stage – Series II.

### 3.3.2 Compound Mooney viscosity

The Mooney viscosity of the compounds increases substantially with increasing CTAB surface area of the silicas as shown in Figure 12. An increased surface area of the silica is the result of a smaller size of the primary particles (Table 1), and both properties tend to increase the viscosity: smaller particles result in lower inter-particle distances for a given degree of dispersion. Thus these particles have a higher mutual interaction and higher forces are needed to displace the particles within the elastomer matrix. Furthermore, a higher surface area increases the filler-polymer interaction, which results in a higher degree of rubber immobilized on the surface of the filler. This increases the effective diameter of the filler, which also results in an increase of the viscosity.

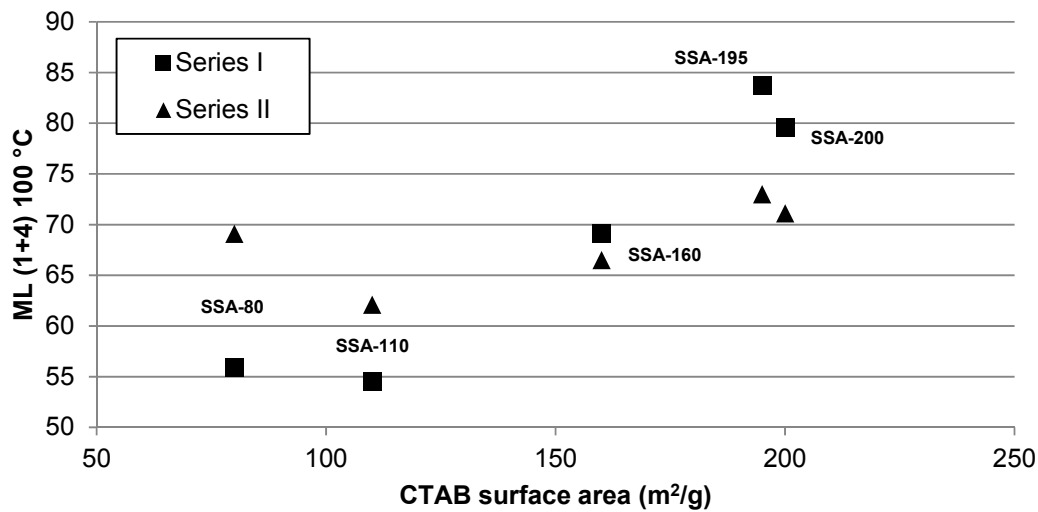


Figure 12: Mooney viscosity versus CTAB specific surface area of different silica types.

The Mooney viscosity for SSA-200 in Series I is 4 MU lower in comparison to the SSA-195. However, considering the specific surface area of SSA-200, the viscosity of the compound containing this filler should be higher or at the same level as for SSA-195. The off-trend viscosity for silica SSA-200 is even more pronounced when the Mooney viscosity is plotted against the aggregate size; see Figure 13. This discrepancy in viscosity can be caused by the different aggregate morphology of silica SSA-200. The aggregates of silica SSA-200 are substantially larger than those of the SSA-195 at comparable specific surface areas.

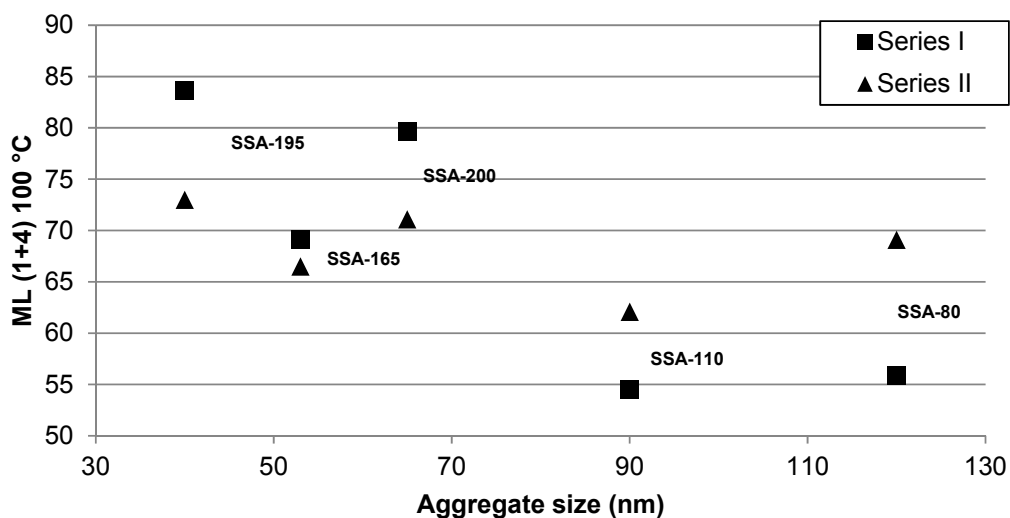


Figure 13: Mooney viscosity versus aggregate size of different silica types.

Filler agglomerates are broken and dispersed in the rubber by mechanical mixing. The more branched structure of silica SSA-200 shown in Figure 2 facilitates transfer of shear forces during mixing. Therefore, a more effective disagglomeration and better dispersion are obtained for the compounds containing SSA-200 in comparison with the silica SSA-195: see Figure 14.

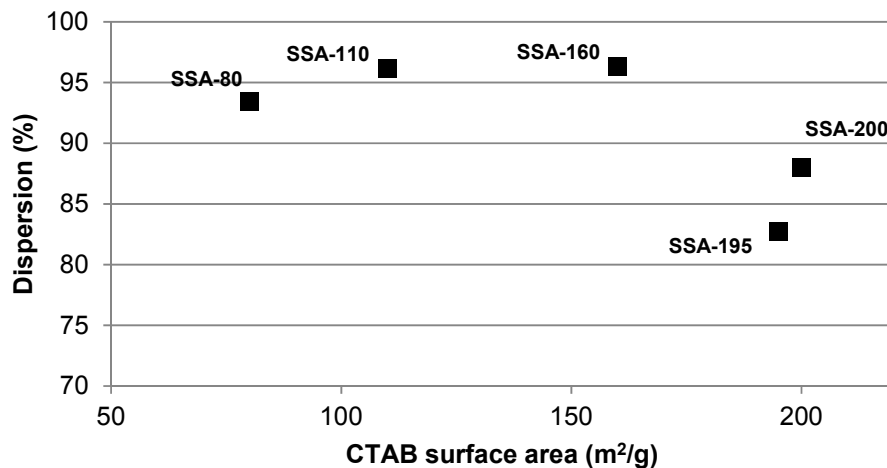


Figure 14: Dispersion of the compounds Series I.

### 3.3.3 Tensile properties

The tensile strength gives information about the strength of interactions between filler particles and polymer chains at high deformation. An extreme example of this effect is when the compound is filled with silica without using a coupling agent. When filler-polymer interaction is low, the polymer chains adsorbed or entangled on the filler surface slide on the filler surface under the influence of the applied load and are desorbed from the filler surface. Molecular slippage of chains on the filler surface is also known for carbon black filled elastomers [33,34]. At medium strain, the load is transferred via polymer entanglements, and finally, when all entanglements are disentangled, the load is transferred via the crosslinked polymer chains [35,36]. In such a case the fillers show a relatively low reinforcing effect: tensile strength is low and elongation at break is high. When the polymer chains are linked to the filler surface via covalent bonds, for instance by a coupling agent, the elongation at break drops but the tensile strength increase, because the molecular slippage phenomena are suppressed.



Along with the increasing CTAB surface area, the tensile strength of the vulcanized compounds rises. The tensile strength value for the SSA-200 is only slightly lower in comparison to the SSA-195, as seen in Figure 15.

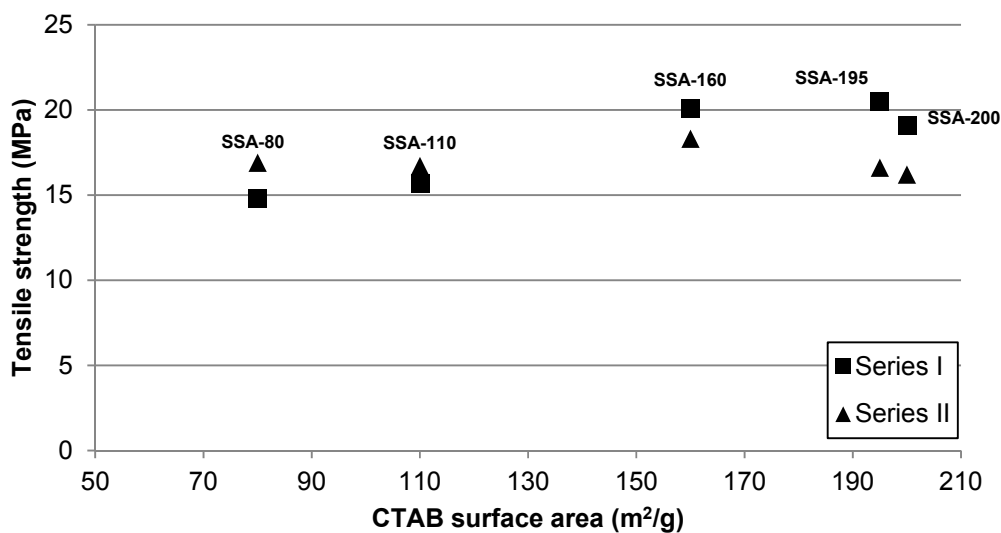


Figure 15: Tensile strength in correlation with CTAB surface area.

When the tensile strength is plotted versus aggregate size: Figure 16, it decreases with increasing aggregate size. Now the tensile strength of the SSA-200 is following the general trend. Apparently the aggregate size is the governing factor to influence the tensile strength. It should be emphasized that the aggregate size does not necessarily correlate with the primary particle size. The aggregates of silica SSA-200 are much larger than the aggregates of SSA-195. However, the minor differences in the specific surface areas of these two silicas suggest that their primary particle sizes must be similar.

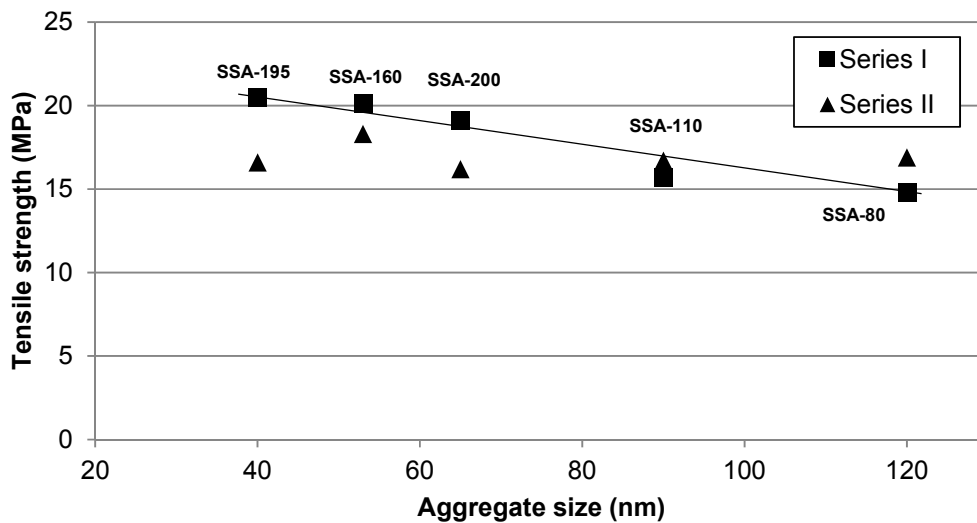


Figure 16: Tensile strength versus aggregate size.

For the series of batches in which the silica loading was adjusted to keep the hardness at constant level, the tensile strength depends only slightly on the aggregate size or specific surface area. Apart from silica loading, the tensile strength of the vulcanizates therefore depends mainly on the aggregate size which determines the reinforcing capabilities of the fillers.

The elongation at break is shown in Figure 17 and Figure 18. The general trend becomes also more clear now: along with increasing surface area of the silica or decreasing aggregate size, elongation at break increases. The value of the elongation at break is more sensitive to the filler structure than the tensile strength.

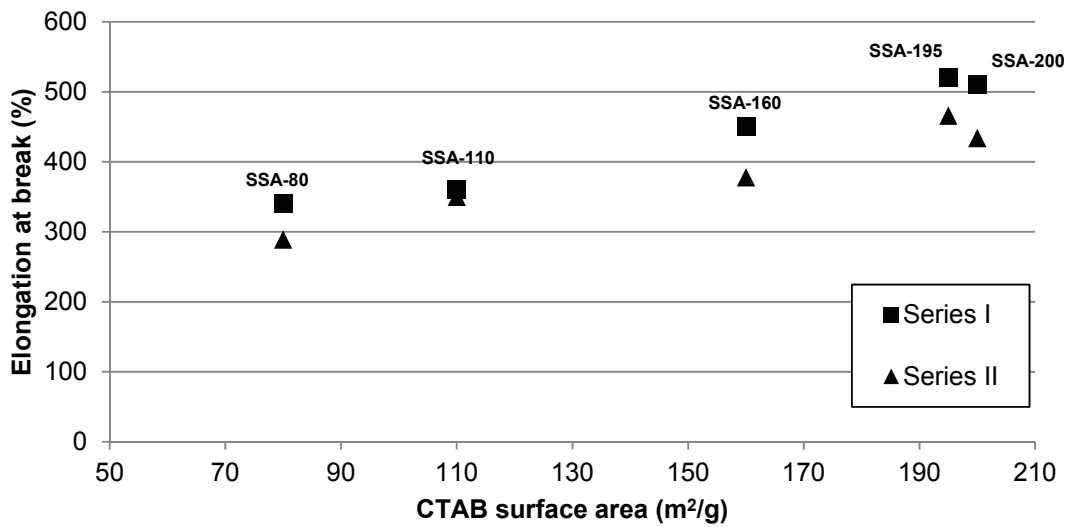


Figure 17: Elongation at break versus CTAB surface area.

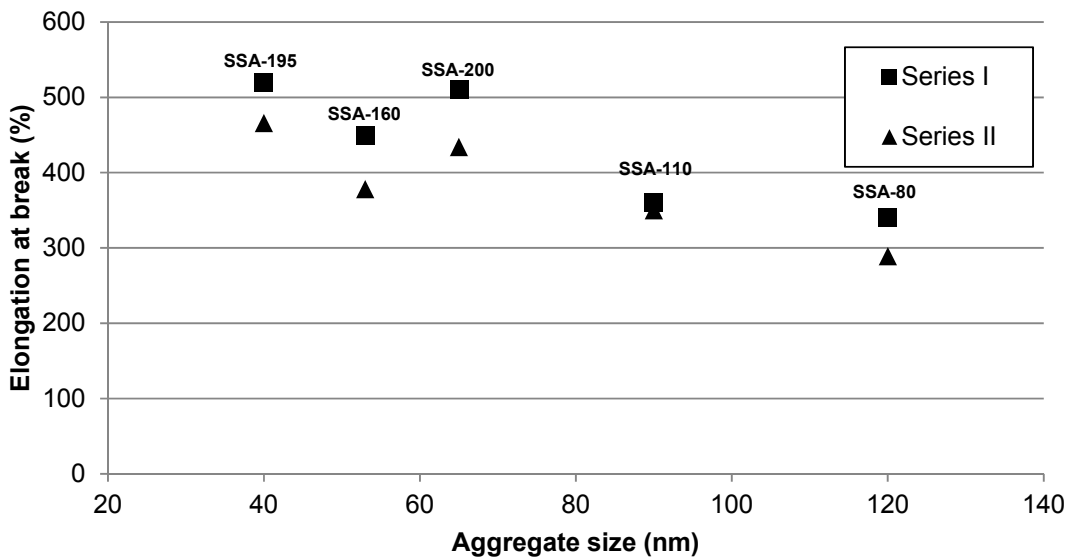


Figure 18: Elongation at break versus aggregate size.

Just like in Series-I, the general trend of increasing elongation at break with decreasing aggregate size is also visible for the series with equal hardness, Series-II. Despite the fact that the silica loading is adjusted, still the aggregate size has a dominating effect on elongation at break. Taking into the consideration that the filler-filler interactions measured with the Payne effect for the Series-II are similar, see below in Figure 19, the

polymer-filler interactions must differ for each silica type. The more polymer is adsorbed at the filler surface by the smaller aggregate size the higher elongation at break can be reached.

The ability of crack dissipation or propagation has also an impact on elongation at break. At the final stages of straining, cracks are formed somewhere in the rubber sample, which lead to sample damage. Samples, in which cracks can propagate easily throughout the body of the sample, have lower values of elongation at break. It seems that highly reinforcing fillers can dissipate cracks more efficiently, resulting in a higher elongation at break.

#### **3.3.4 Filler-Filler interactions – Payne effect**

The Payne effect [37] may be used as an indication for filler-filler interaction; it is an indirect method that allows to assess the interactions, partly also due to the dispersion of the filler in a polymer matrix. It is measured as the difference between the storage modulus measured at low and high strain. Physically, it can be described as the difference between two different states of the filler-rubber composite: one state in which the filler network dominates in the composite, and energy can be transferred through this filler network; and a second state in which the silica network is broken and energy must be absorbed by the matrix.

Decreasing specific surface area of the silica or larger particles lead to a reduced Payne effect: Figure 19, due to a less developed filler-filler network. Where the silicas SSA-80 and SSA-110 are characterized by low Payne effects, their value as reinforcing filler is also lower: Figure 16.

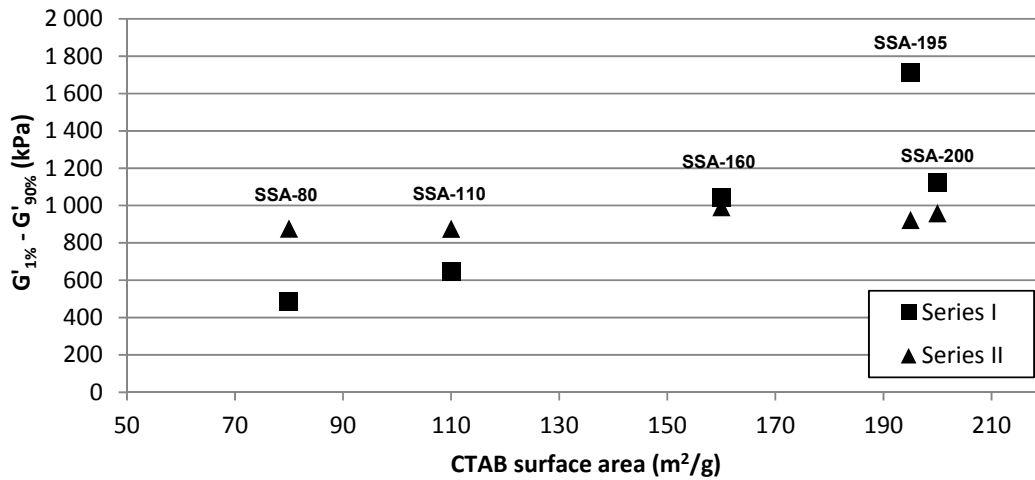


Figure 19: Payne effect versus CTAB surface area Series I and II.

Again, aggregate size is a more appropriate parameter to plot the Payne effect than CTAB specific surface area, as shown in Figure 19 and Figure 20. It is well known that smaller particle fillers are more difficult to disperse because of the higher particle to particle affinity. Adjustment of the silica loading in order to equalize the Shore A hardness: Series II, causes also more or less equal values of the Payne effect for all samples.

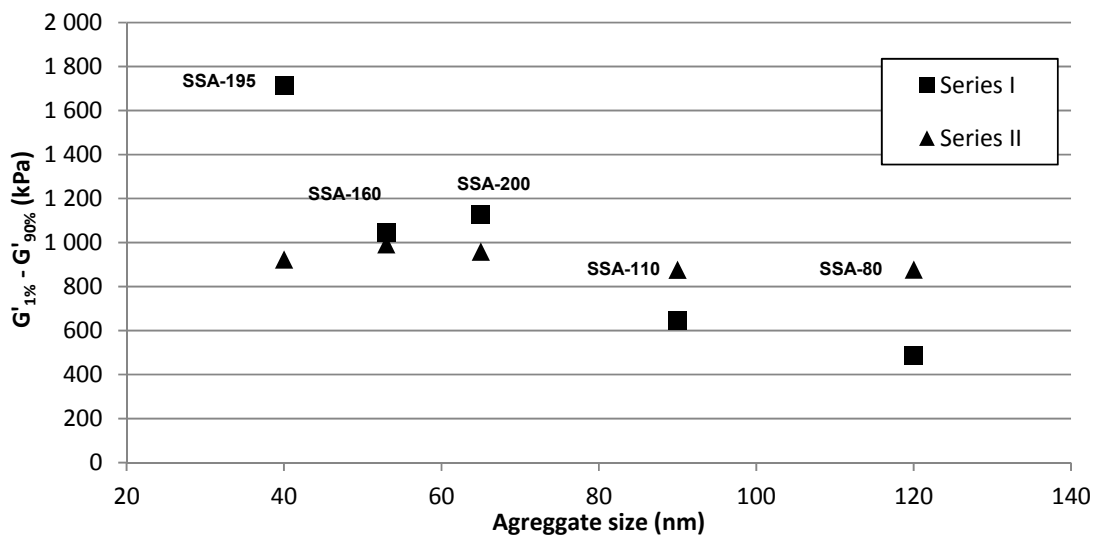


Figure 20: Payne effect versus aggregate size Series I and II.

### 3.3.5. Hardness

In general, hardness of vulcanizates can be correlated with filler-filler interactions and silica loading. For instance, in the extreme case of no coupling agent, thus low filler-polymer and high filler-filler interactions, much higher hardness values are observed. Introduction of coupling agent suppresses the filler-filler interactions and consequently reduces the hardness.

With increasing dimensions of the silica aggregates, the hardness of the vulcanizates decreases: Figure 21, Series-I. Adjustment of the silica loading in Series-II causes equalization of the filler-filler interactions as well, see Figure 20.

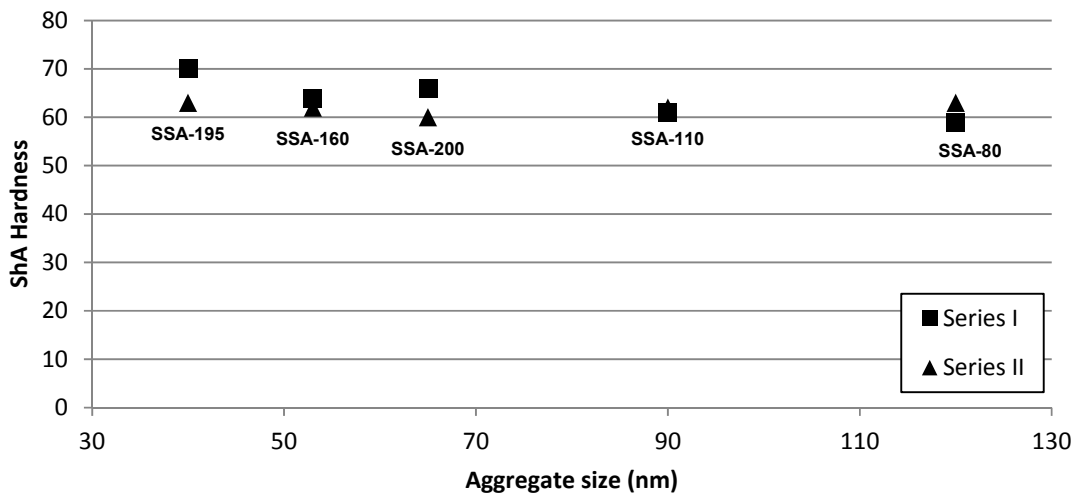


Figure 21: Shore A hardness in relation to aggregate size.

### 3.3.6 Abrasion resistance

It is commonly accepted that there is inverse relation between the glass transition temperature of a polymer matrix and abrasion resistance. DIN abrasion is expressed in volume loss, and describes the ability of the rubber composite to resist tearing-off small pieces of rubber from its surface by the sharp asperities of the counter surface. When the same formulation is used, the abrasion represents the strength of polymer-filler interactions: the stronger the interaction, the more difficult it is to break small particles out of the rubber composite. Abrasion resistance turns out to be worse for larger aggregate size, as shown in Figure 22.

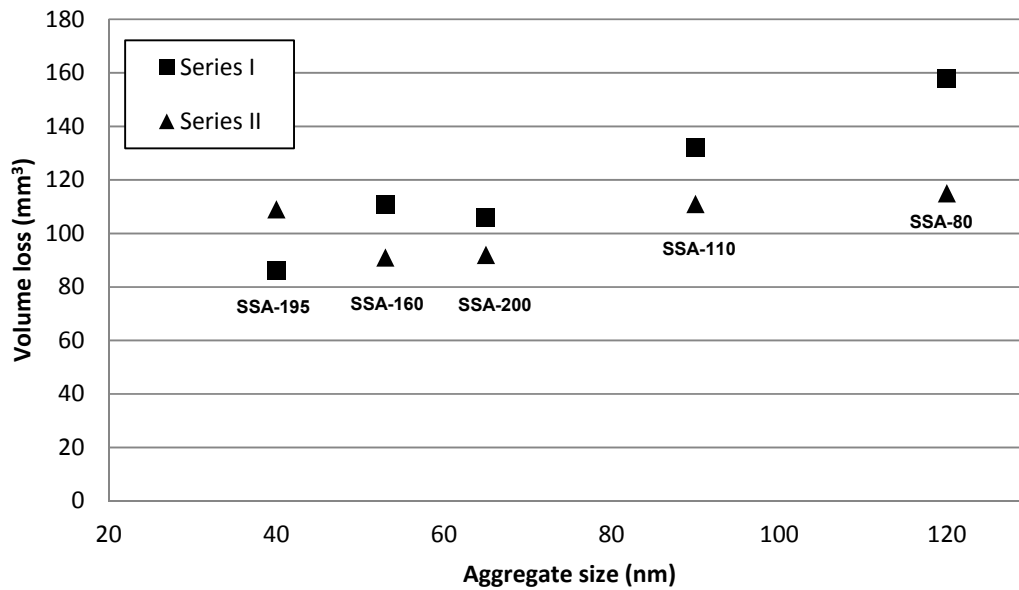


Figure 22: DIN abrasion versus aggregate size.

The fact that smaller aggregate sizes result in higher abrasion resistance may be related again to better interaction with the polymer due to the higher available contact area. The degree of dispersion might be lower for the finer silica types, but this effect is not strong enough to counterbalance the effect of the strong filler-polymer interaction. Silica's with a smaller aggregate size, for example SSA-160, SSA-200 and SSA-195, are therefore the preferred fillers in terms of abrasive wear resistance.

The compounds in which the silica loading was adjusted to equalize the hardness show a more comparable abrasion loss than without adjustment, but the general trend is not changed. Moreover, the abrasion losses obtained for the compounds containing highly reinforcing silicas like SSA-160, SSA-200 and SSA-195 are less affected than for low reinforcing types. In all cases, except for the sample with silica SSA-195, equalizing the hardness improves the abrasion resistance.

### 3.3.7 Dynamic mechanical analysis

Two effects related to the  $\tan \delta$  curve are visible in Figure 23:

1. The  $\tan \delta$  peak becomes broader and shifts towards a higher temperature with decreasing silica aggregate size. This effect is visible just for Series-I;

2. The height of the  $\tan \delta$  peak drops with decreasing aggregate size. This effect occurs for both, Series-I and Series-II.

Decreasing dimensions of the silica aggregates lead to increased filler-filler and filler-polymer interactions, which manifest themselves in a shift of the  $\tan \delta$ -curve towards higher temperature. The  $\tan \delta$ -peak for the compounds with constant silica loading shifts from  $-13\text{ }^{\circ}\text{C}$  to  $-4\text{ }^{\circ}\text{C}$ ; see Table 6. It also shows that in particular the values of the loss modulus ( $G''$ ) are decreasing with decreasing aggregate size, what suggests that the polymer chain movements are more restricted with decreasing aggregate size. At this moment, however, a clear conclusion is difficult to draw about which interactions: filler-filler or filler-polymer, cause this effect because of the differences in the Payne effect for Series-I. The adjustment of the silica loading in Series-II leads to similar Payne effects – similar filler-filler interactions; see Figure 20. And in this case the  $\tan \delta$ -peak position is remaining relatively stable at a value of ca.  $-11\text{ }^{\circ}\text{C}$ . Therefore, the position of the  $\tan \delta$ -peak on the temperature axis or its width is more related to the filler-filler and less to the polymer-filler interactions.

The height of the  $\tan \delta$ -peak decreases when HDS are used both for the Series-I and Series-II, which means less hysteresis of the compounds. For the Series-II, the values of the storage modulus ( $G'$ ) are also relatively constant and independent of the aggregate size; see Table 6. However, the values of the loss modulus ( $G''$ ) measured for Series-II decrease with decreasing aggregate size. Consequently, the variations in the  $\tan \delta$  maximum are here caused by differences in the polymer adsorption. The filler-filler interactions measured for Series-II are similar, and therefore the changes in the  $\tan \delta$  maximum are caused by the filler-polymer interactions which influence the polymer movements at temperatures close to the glass transition of the polymer.

#### *3.3.7.1 Tan $\delta$ at low temperatures: indicator of wet skid resistance*

Values of  $\tan \delta$  in the temperature region from  $0\text{ }^{\circ}\text{C}$  to  $20\text{ }^{\circ}\text{C}$  are generally taken as indicator for the wet skid resistance of a tire tread. For the Series-I in which silica loading was kept constant, it can be seen in Figure 23 that the  $\tan \delta$ -values for smaller aggregate size are higher than the values for the compounds containing larger



aggregates. This effect is associated with filler-filler interaction as indicated before, as monitored in the Payne effect; Figure 20. The higher the filler-filler interactions, the higher the values of the hysteresis, not only in the range of 0 - 20 °C, but also at higher temperatures.

When the silica loading is adjusted to obtain similar Shore A hardness an inverse dependence of the  $\tan \delta$ -values on the aggregate size is visible in the range of 0 - 20 °C. The equalization of the Shore A hardness leads to similar values of the Payne effect for the whole Series II. Therefore, the differences in the  $\tan \delta$ -values in this temperature range are caused entirely by changes in the filler-polymer interactions.

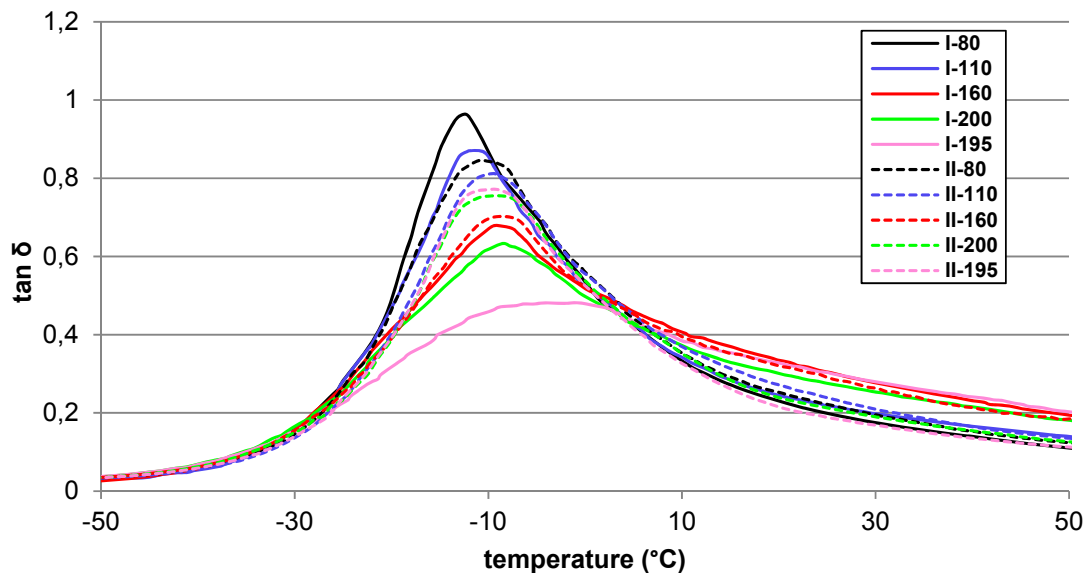


Figure 23:  $\tan \delta$  – temperature dependence.

Polymer-filler interactions determine how well the polymer chains adsorb on the filler surface: physically via the entanglement of the polymer chains on the filler surface, chemically via covalent links between the filler surface and the polymer. Despite the fact that the silicas with the smallest aggregate sizes were used in lower concentration in Series-II, the adsorption of the polymer chains is still higher than for the silicas with larger aggregates used in higher concentrations. Increased adsorption of the polymer chains on the silica surface is demonstrated by a lower loss modulus for the silicas with

smallest aggregates. The more polymer chains are adsorbed on the filler surface, the lower the hysteresis at both high and low temperatures.

As opposed to the case in which the silica loading was kept constant, in Series-II high values of the hysteresis between 0 - 20 °C are observed for the compounds containing silica with the largest aggregates, and are anticipated to correspond with higher values of the side force coefficient: see later.

Table 6: Comparison of the storage and loss moduli for different silica types at the  $\tan \delta$  maximum.

| type   | $\tan \delta$ peak temp. (°C) | G' (MPa) | G'' (MPa) | $\tan \delta$ |
|--------|-------------------------------|----------|-----------|---------------|
| I-80   | -13                           | 32       | 30        | 0,95          |
| I-110  | -12                           | 28       | 24        | 0,87          |
| I-160  | -10                           | 29       | 19        | 0,66          |
| I-200  | -6                            | 27       | 16        | 0,60          |
| I-195  | -4                            | 33       | 16        | 0,49          |
| II-80  | -11                           | 34       | 29        | 0,85          |
| II-110 | -10                           | 34       | 28        | 0,81          |
| II-160 | -10                           | 30       | 21        | 0,68          |
| II-200 | -12                           | 24       | 17        | 0,75          |
| II-195 | -11                           | 23       | 18        | 0,77          |

### 3.3.8 $\tan \delta$ at 60 °C: indicator of rolling resistance

Considering an average speed of a vehicle of 70 km/h and car wheel dimensions: 255/65/16, a typical frequency of deformation of the revolving tire is around 10 Hz. The hysteresis of the rubber compound causes an increase of the tire temperature to approx. 60 °C. The weight of the vehicle exerted on the tire is estimated to result in around 2 – 6 % tire tread deformation. Therefore, measuring  $\tan \delta$  values at 10 Hz, 2 % of dynamic strain and at 60 °C is a good indicator of rolling resistance. The lower the value of the  $\tan \delta$  under these conditions, the lower the predicted rolling resistance.

In Figure 24 and Figure 25, the silica types used in Series-I can be separated into two groups. The first have a low specific surface area and larger primary particles, which provide substantially lower values of  $\tan \delta$  at 60 °C. That is due to the good dispersibility of the larger particles (weaker filler-filler attraction forces) and less tendency to agglomerate. When each silica aggregate is surrounded by a rubber layer, there is less

filler-filler friction and tendency to recombination of the filler network, thus lower hysteresis.

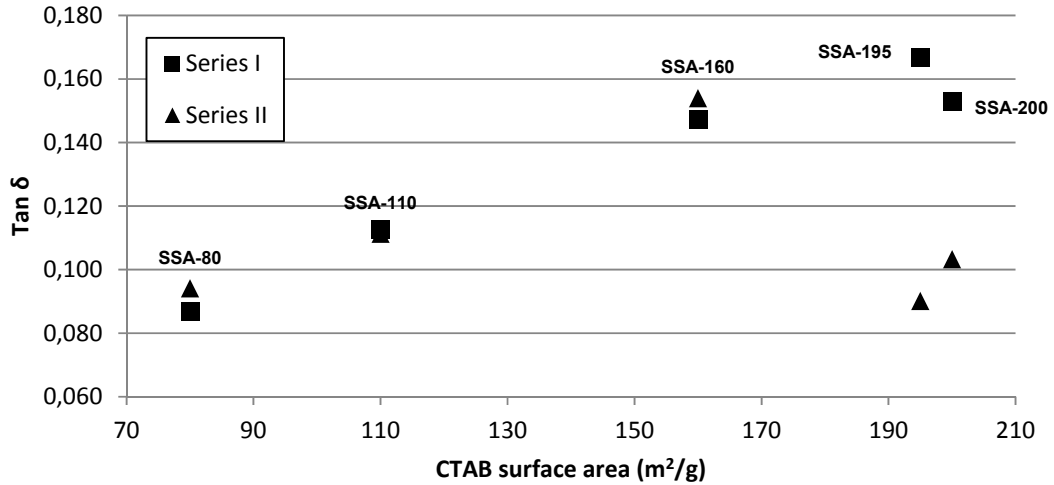


Figure 24: Loss tangent at 60 °C versus CTAB specific surface area.

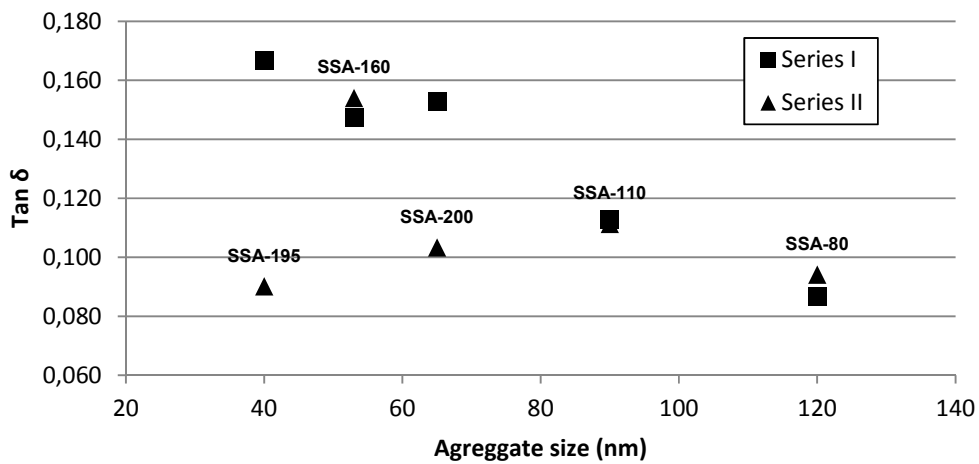


Figure 25: Loss tangent at 60 °C versus aggregate size.

The second group of silicas includes SSA-195, SSA-200 and SSA-160, which give substantially higher values of  $\tan \delta$  at 60 °C caused by the higher specific surface areas and smaller aggregate sizes. This leads to a more agglomerated filler in the polymer matrix manifested in the Payne effect and gives more inter-particle friction during dynamic deformation causing the energy loss.

On the one hand, a decreased loading of the silicas SSA-200 (8 phr reduction) and SSA-195 (15 phr reduction) in order to adjust the hardness causes a substantial drop of the  $\tan \delta$ -values. On the other hand, increased loading of silicas with larger aggregates, SSA-80 (35 phr increase) and SSA-110 (15 phr increase), does not cause significant differences in comparison with constant loading of 80 phr. The dynamic properties of the pure elastomer are the governing factors for the composite material based on this elastomer. Reducing the amount of filler in the polymer matrix decreases the inter-particle friction by increasing the distance between the silica aggregates, which brings the hysteresis of the composite closer to the hysteresis of the pure elastomer.

Silica SSA-200 shows quite a different behavior compared to SSA-160 and SSA-195, as the  $\tan \delta$  value at 60 °C is lower than expected from its specific surface area. However, the reinforcing potential is still in the range of the highly reinforcing types of silica. This difference between SSA-200 and the other highly reinforcing types of silica might be explained by better dispersion of this silica type in comparison with the SSA-195, see Figure 14. The dispersion level of SSA-200 is comparable with SSA-160 what explains similar values of the  $\tan \delta$  value at 60 °C for the two silica types.

### **3.3.9 LAT 100 side force coefficient: wet skid resistance**

Measurements were performed at different water temperatures; the results are shown in Figure 26. Side force coefficient values increase with increasing surface area of silica. Increasing surface area of silica leads to higher values of  $\tan \delta$  between 0 and 20 °C, indicative of higher hysteresis. The ranking of the side force coefficient correlates roughly with the  $\tan \delta$  between 0 and 20 °C. Higher values of  $\tan \delta$  stand for more energy dissipation during wet skidding. Elastic material is sliding over the surface of a relatively rough material: electro-corundum. Roughness of the disc surface causes micro-scale deformations on the wheel sample surface. On the one hand the elastic material which loses more energy during one deformation cycle will be characterized by higher values of the side force coefficient. On the other hand, elastic material with higher storage modulus (stiffer), will be also characterized by higher values of the side

force coefficient, because its lower deformability in one deformation cycle leads to a higher force necessary to deform the rubber surface on micro-scale.

During skidding the surface of the rubber wheel undergoes small deformations trying to fill in the micro-cavities existing at the surface of the LAT-disc on which sliding is taking place. The load applied to the wheel, the average dimensions (depth and width) of the micro-cavities and the water film limit the degrees of micro-deformation. Since the wheel is moving with linear speed with respect to the sliding surface, the deformed compound which fills in the above mentioned cavities must be pushed back to its original position on the wheel.

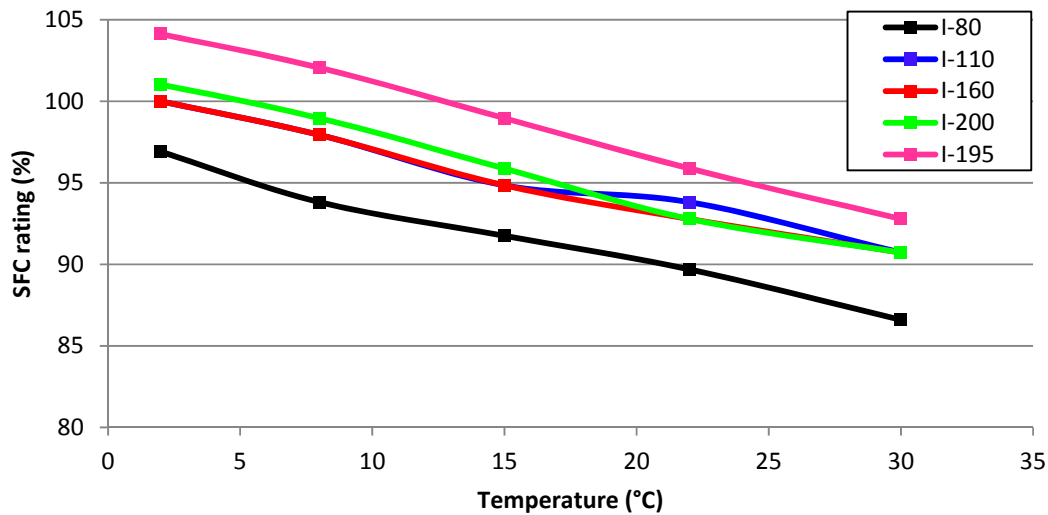


Figure 26: Side force coefficient versus temperature – Series I.

Depending on the compound stiffness different wet skid scenarios can be envisaged. In the first case, the wheel is made out of very stiff compound which is not able to deform under the applied load, leading to extremely low wet skid resistance. In the second case, a wheel made out of soft rubber which deforms relatively easily, filling the micro-cavities until its dimensional limits – the wet skid resistance is much higher. However when less significant differences in the compound stiffness are considered, for instance when the load applied to the wheel exceeds the load needed to completely fill the micro-cavities for both the softer and stiffer compounds, the force necessary to push the stiffer compound back to its original position on the wheel is higher than the force needed to push back a softer compound. Hence, the wheel made out of the stiffer but still

deformable compound will lead to a higher resistance during skidding. In such a case the side force coefficient correlates better with the values of the storage and loss moduli than with the hysteresis.

In Series-I, the SSA-80 provides the lowest values of the  $\tan \delta$  at 0 – 20 °C and its side force coefficient value is also the lowest among the other samples. However, in spite of the highest hysteresis in the range of 0 – 20 °C for the SSA-160, its side force coefficient values rank in the 3<sup>rd</sup> place. Regardless of the substantial differences in the hysteresis among the samples in Series-I, a correlation between the  $\tan \delta$  at 0 – 20 °C and the side force coefficients was not observed. This lack of correlation may be related to a minor contribution of the hysteresis during the measurements on the LAT-100 with the parameters selected.

Adjustment of the silica loading to equalize the hardness causes narrowing of the side force coefficient values range; see Figure 27. The sample containing silica with the smallest aggregate size, SSA-195 is characterized by the highest values of the side force coefficient. Like for the other properties, the aggregate dimensions apparently have a dominant effect on the side force coefficient. Like in the case of Series-I, no apparent correlation between the  $\tan \delta$  at 0 – 20 °C and side force coefficient exists in this case.

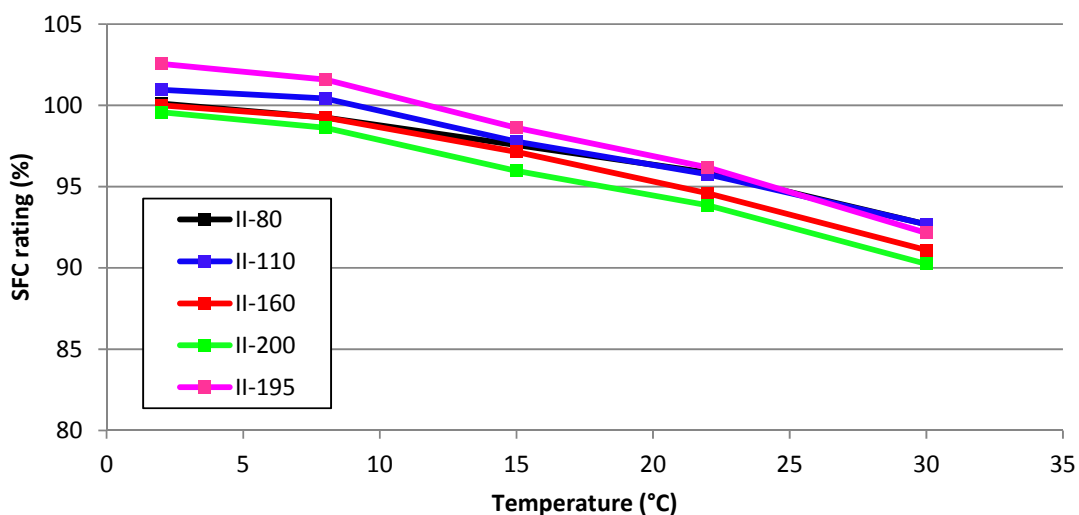


Figure 27: Side force coefficient versus temperature – Series II.

Along with increasing temperature of the measurements, the values of the side force coefficient decrease for all compounds, because the elasticity of rubber increases. More elastic material loses less energy per deformation cycle, hence the side force coefficients decrease.

### 3.4 CONCLUSIONS

Five types of silica, differing in specific CTAB surface area and aggregate size, were tested in a passenger car tire compound. One of the silicas, SSA-200 is also characterized by different structure – its aggregates are larger while the specific surface area is similar to the SSA-195 type.

- The silica types with smaller aggregate dimensions and larger specific surface areas show a higher reinforcing effect, as illustrated by improved tensile properties. However, the dispersibility of these silicas is more difficult compared to the silica types with larger aggregate sizes. Compounds, in which SSA-195 was used, had superior tensile properties and the lowest loss modulus at lower temperatures. This silica type also resulted in the highest values of the side force coefficient, indicating best wet grip.
- Adjustment of the silica loading in order to obtain similar hardness of the cured compounds reverses the order of the dynamic curves. Silica with smallest aggregates is still superior regarding side force coefficient. However, the trend visible for constant silica loading has disappeared. This demonstrates that from the view point of wet skid resistance, smaller aggregate sizes of fillers are better, and that a higher aspect ratio of the fillers like in the case of SSA-200 type does not improve the wet skid resistance.
- Silicas with a larger aggregate sizes, SSA-80 and SSA-110 lead to low hysteresis at high temperatures, but the low reinforcing effect makes them also less appropriate as reinforcing filler for tire tread compounds.
- The dynamic properties of materials containing highly reinforcing silica can be further improved by using less filler, but the tensile properties will suffer in case of SBR/BR used as polymer matrix. Furthermore, good dispersion of the nano-sized

aggregates is the key to obtain rubber composites with superior overall properties.

- With the selected measurement parameters for dynamic analysis and on the LAT-100, no correlation of the hysteresis at 0 – 20 °C with the side force coefficient was found for both series.



## REFERENCES

---

- [1] M. J. Wang, Rubber Chem. Technol., 71 (1998) 520.
- [2] M. J. Wang, Kautsch. Gummi Kunstst., 60 (2007) 438.
- [3] M. J. Wang, Kautsch. Gummi Kunstst., 61 (2008) 33.
- [4] M. Heinz, K.A. Grosch, 167<sup>th</sup> Technical meeting of the Rubber Division ACS, May 16-18 2005, San Antonio, Texas, USA.
- [5] M. Heinz, J. Rubb. Res., 13 (2010) 91.
- [6] K. R. Grosch, Rubber Chem. Technol., 80 (2007) 379.
- [7] C. J. Derham, R. Newell and P. McL. Swift, NR Technology, 19 (1988) 1.
- [8] G. Heinrich, Kautsch. Gummi Kunstst., 45 (1992) 173.
- [9] G. Heinrich, N. Rennar, H. Dumler, Kautsch. Gummi Kunstst., 49 (1996) 32.
- [10] G. Heinrich, Rubber Chem. Technol., 70 (1997) 1.
- [11] M. Klüppel, G. Heinrich, Rubber Chem. Technol., 73 (2000) 578.
- [12] A. Müller, J. Schramm, M. Klüppel, Kautsch. Gummi Kunstst., 55 (2002) 432.
- [13] A. le Gal, M. Klüppel, J. Phys. Condens. Matter, 20 (2008) 1.
- [14] B. N. J. Persson, U. Tartaglino, E. Tosatti, O. Albohr, Kautsch. Gummi Kunstst., 57 (2004) 532.
- [15] Y. Isono, T. Oyama, S. Kawahara, Adv. Tech. Mat. Proc. J. 5 (2003) 84.
- [16] S. Uhrlandt, A. Blume 161<sup>th</sup> Technical meeting of the Rubber Division ACS, April 29 - May 1, 2002, Savannah, Georgia, USA.
- [17] A. Blume, B. Freund, B. Schwaiger, M. Siray, S. Uhrlandt, EP0983966 A1 (2000), to Degussa-Hüls Aktiengesellschaft.
- [18] H.D. Luginsland, 161<sup>th</sup> Technical meeting of the Rubber Division ACS, April 29 - May 1, 2002, Savannah, Georgia, USA.
- [19] D.W. Schaefer, J. Appl. Crystallography 33 (2000) 587.
- [20] S. Brunauer, P.H. Emmet, E. Teller, J. Am. Chem. Soc. 59 (1936) 2682.
- [21] ASTM D 3765-02.
- [22] S. Uhrlandt, A. Blume, Rubber World 4 (2003) 43.
- [23] A. Wehmeier, O. Stenzel, 7<sup>th</sup> Fall Rubber Colloquium DIK, November 8 – 11 2006, Hannover, Germany.
- [24] Leaflet Hi-Sil EZ 200G, PPG Industries.
- [25] S. L. Aggarwal, I. G. Hargis, R. A. Livigni, H. J. Fabris and L. F. Marker, "Advances in elastomers and rubber elasticity". Plenum Press (1986) 17.
- [26] R. R. Rahalkar, Rubber Chem. Technol., 62 (1989) 246.
- [27] M. J. Wang, Kautsch. Gummi Kunstst., 61 (2008) 33.
- [28] M. Heinz, J. Rubb. Res., 13 (2010) 91.
- [29] K.R. Grosch, Rubber Chem. Technol., 80 (2007) 379.
- [30] P. Cochet, S. Daudey, L. Guy, Rhodia, Elastomer reinforced by precipitated silica and their specific viscoelastic behaviour, IRC Mumbai (2010).

- 
- [31] L. Guy, Ph. Cochet, Y. Bomal , S. Daudey, *Kautsch. Gummi Kunstst.*, 63 (2009) 383.
- [32] R. Rauline, European Patent No. EP0501227B1, (1992), to Michelin Co.
- [33] E. M. Dannenberg, *Rubber Chem. Technol.*, 48 (1975) 410.
- [34] E. M. Dannenberg, *Trans. Inst. Rubber Ind.*, 26 (1966) 42.
- [35] M. Kaliske, G. Heinrich, *Rubber Chem. Technol.*, 72 (1999) 602.
- [36] D. F. Jones, L. R. G. Treloar, *J. Phys. D: Appl. Phys.*, 8 (1975) 1285.
- [37] A. R. Payne, *J. Appl. Polym. Sci.*, 6 (1962) 57.



# **Influence of physical and chemical polymer-filler bonds on tire wet-traction performance indicators for passenger car tire tread materials**

---

*The rubber compound used for a tire tread is a composite material of which the dynamic properties can be adjusted over a relatively broad range by modification of the polymer-filler interaction. For silica-reinforced compounds, control over the polymer-filler interaction is realized by chemical coupling of the silica to the rubber by applying different silane coupling agents. Different molecular structures can be obtained which lead to changes in macroscopic material properties including wet skid resistance. The understanding of one of the influencing factors, the polymer-filler interaction, helps to answer the key question: Which type of polymer-silica bonds govern wet skid phenomena: weak (physical) or strong (chemical) bonds?*

## 4.1 INTRODUCTION

The goal of the present study is to characterize the underlying mechanisms involved in rubber-filler interactions for the wet skid resistance of silica-reinforced tire treads, a dynamic viscoelastic phenomenon. The use of silica instead of carbon black has proven to be of great importance for the reinforcement of rubbers designed for tire treads, because of the corresponding much lower rolling resistance of tires made thereof. To characterize the dynamic properties of rubber, storage and loss moduli are commonly measured. The ratio of loss to storage modulus is indicated as the loss tangent ( $\tan \delta$ ), frequently used to characterize tire performance on small, laboratory scale [1,2,3]

Apart from the rolling resistance improvement, the wet skid or traction performance of tire treads is an important safety and performance criterion. The friction, traction or skid resistance, in dry and wet conditions, of tire treads on various surfaces has already been subject of numerous experimental and modeling studies: Wang [3,4,5], Heinz and Grosch [6,7,8], Derham [9], Heinrich et al. [10,11,12], Klüppel and Heinrich [13], Müller et al. [14], Le Gal and Klüppel [15], Persson et al. [16], Isono et al. [17]. The focus of the present study is on the effect of the silane coupling agent used for the rubber-silica interfacial bonding on wet skid resistance. A first approach towards influencing the rubber-filler interaction could be based on inducing chemical interactions between the silica and polymer, that might lead to improvement of wet skid resistance by raising the  $\tan \delta$  values in the low temperature region (0 – 20 °C) and decreasing the same in the higher temperature region. Based on the time-temperature superposition, increased hysteresis at lower temperatures and frequencies should increase energy dissipation at higher frequencies and temperatures, occurring during wet and dry skidding. An opposite approach would be that the filler-polymer interaction should be limited, ultimately to physical interactions. Physical interactions mean that under the influence of energy resulting from skidding, polymer molecules can easily be displaced on the filler surface, which should increase energy dissipation. These two approaches are clearly each others opposite and it is not a priori obvious which of the two approaches is the best.

The influence of the silica-polymer interaction on wet skid performance is investigated by testing the dynamic properties, the  $\tan \delta$  in the temperature range from 0 – 20 °C at 10

Hz. The values of the loss angle in this temperature range are so far considered to be the most suitable indicators for the wet skid performance of a tire tread [10,18,19]. To assess the influence of silica-polymer interactions on the wet skid and other physical properties of the tire tread compounds, two cases are investigated. In the first case, silica-polymer interactions are aimed for to be mostly chemical of nature, inducing a strong and rigid interface. In the second case the interactions aimed for shall be limited to mostly physical – weak interactions. In order to check a more practical value of the wet skid resistance, additional measurements on a Laboratory Abrasion Tester 100 (LAT 100) are performed in the final stage of this investigation.

## **4.2 EXPERIMENTAL**

### **4.2.1 Materials and compound formulations**

Two silane coupling agents are applied to achieve the two opposite effects in rubber-filler interaction. Bis(3-triethoxysilylpropyl)tetrasulfane (TESPT, Evonik, Germany) was chosen as a silane which can react directly with silica and unsaturated polymers for a strong silica-polymer interaction, and 1,6-bis-(triethoxysilyl)hexane (TESH) which possesses a similar molecular structure as TESPT, however it does not have sulfur atoms which makes it inert towards reaction with the polymers. The TESH was synthesized according to the procedure described by Reuvekamp et al. [20]. The products structure and purity was determined with an LC-MS analyzer (Agilent-1100/Bruker-Esquire 3000 Plus). A product with purity of 96 % was obtained. The mass calculated for  $C_{18}H_{42}O_6Si_2H^+$  was 411.25; found 411.26. The refractive index of the product at 25 °C was 1.4184. The chemical structures of both silanes are shown in Figure 1. The experiments were performed using a formulation based on the well-known Green Tire concept [21] as given in Table 1. A blend of styrene-butadiene rubber 37,5 phr oil-extended (Buna VSL 5025-2 HM, Lanxess, Germany), with high-cis butadiene rubber (Kumho KBR 01, S-Korea) was used as elastomer base. Silica Zeosil 1165 MP (Rhodia Silices, France) was chosen as filler. Four compounds containing TESPT in varying amounts and a same number of compounds containing corresponding equimolar amounts of TESH were prepared.

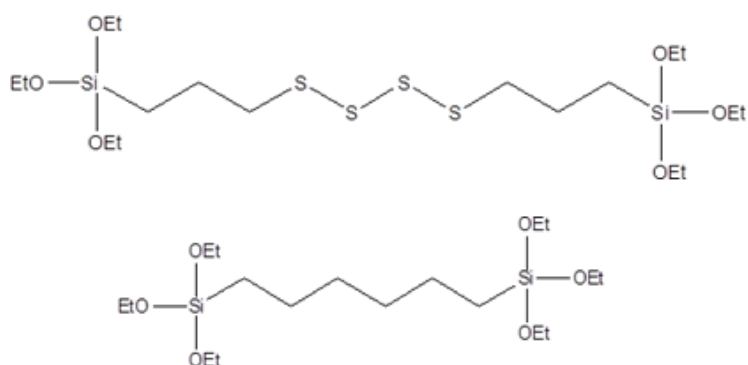


Figure 1: Bis-(3-triethoxysilylpropyl)tetrasulfane, MW = 532 g/mol (upper) and 1,6-bis-(triethoxysilyl)hexane MW = 410 g/mol (lower).

The TESPT content was adjusted for the first compound according to the cetyltrimethylammonium bromide (CTAB) surface area of the silica type by using the empirical equation proposed by L. Guy et al. [22]: Equation 1. The amount of free sulfur added with the curatives was adjusted to keep the total molar amount including the sulfur contained in the coupling agent at a constant level in all batches.

$$TESPT (phr) = 5.3 \times 10^{-4} \times (CTAB)_{silica} \times (phr)_{silica} \quad (\text{Equation 1})$$

Table 1. Compounds formulations.

| Compound name  | TESPT<br>7 | TESPT<br>9.5 | TESPT<br>12.0 | TESPT<br>14.4 | TESH<br>5.3 | TESH<br>7.3 | TESH<br>9.3 | TESH<br>11.3 |       |
|----------------|------------|--------------|---------------|---------------|-------------|-------------|-------------|--------------|-------|
| SSBR           | 103        | 103          | 103           | 103           | 103         | 103         | 103         | 103          |       |
| BR             | 25         | 25           | 25            | 25            | 25          | 25          | 25          | 25           |       |
| Silica         | 80         | 80           | 80            | 80            | 80          | 80          | 80          | 80           |       |
| Coupling agent | phr        | 7            | 9,5           | 12            | 14,4        | 5,3         | 7,3         | 9,3          | 11,3  |
|                | mol        | 0,013        | 0,018         | 0,023         | 0,028       | 0,013       | 0,018       | 0,023        | 0,028 |
| Processing oil | 5          | 5            | 5             | 5             | 5           | 5           | 5           | 5            |       |
| ZnO            | 2,5        | 2,5          | 2,5           | 2,5           | 2,5         | 2,5         | 2,5         | 2,5          |       |
| Stearic acid   | 2,5        | 2,5          | 2,5           | 2,5           | 2,5         | 2,5         | 2,5         | 2,5          |       |
| Sulphur        | 1,4        | 0,8          | 0,24          | 0             | 3,1         | 3,1         | 3,1         | 3,1          |       |
| TBBS           | 1,7        | 1,7          | 1,7           | 1,7           | 1,7         | 1,7         | 1,7         | 1,7          |       |
| DPG            | 2          | 2            | 2             | 2             | 2           | 2           | 2           | 2            |       |

#### 4.2.2 Mixing and curing

To prepare the compounds, an internal laboratory mixer Brabender 350 S with mixing volume of 390 cm<sup>3</sup> was used. The mixing procedure is specified in Table 2. The total volume of the batches was adjusted to a fill factor of 70 %. Preparation of sheets for testing was done on a Schwabentan Polymix 80T 300 ml two roll mill.

Table 2. Mixing procedure.

| Stage I  |  |
|--|--|
| Rotor speed: 110 RPM<br>Initial temp.:50 °C              |  |
| Timing<br>(Min. sec.)                                    | Ingredient                                 |
| 0.00   | Add polymers                               |
| 1.00   | Add ½ silica, ½ silane, ZnO + Stearic acid |
| 2.30   | Add ½ silica, ½ silane, Oil, TMQ, 6PPD     |
| 3.00   | Sweep                                      |
| 4.00   | Dump @ ~ 155 °C                            |
| Stage II   |  |
| Rotor speed: 130 RPM<br>Initial temp.:50 °C              |  |
| Timing<br>(Min. sec.)                                    | Ingredient                                 |
| 0.00   | Add I stage batch                          |
| 3.00   | Dump @ ~ 155 °C                            |
| III stage  |  |
| Mixing of the curatives was performed on a two roll mill |  |

Vulcanization of the sheeted samples for tensile tests was performed on a Wickert laboratory press WLP 1600/5\*4/3 at 160 °C and 100 bars pressure for a curing time 1.2 x t<sub>90</sub> obtained from a Rubber Process Analyzer (RPA 2000, Alpha Technologies, USA) rheometer measurements according to ISO 6502. The samples for hardness tests were prepared in cylindrical moulds and cured for a period of twice the t<sub>90</sub> - time. The samples for DIN abrasion tests were also cured for 1.2 x t<sub>90</sub>. The adjustment of the curing times was necessary due to the large thickness of the samples and the generally well known low thermal conductivity of the rubber compounds.



### **4.2.3 Characterizations**

The Mooney viscosities ML(1+4) of the compounds were measured at 100 °C on a Mooney viscometer MV 2000E (Alpha Technologies) according to ISO 289-1.

In order to estimate the chemical and physical polymer – filler interactions, bound rubber tests were performed. These tests were done by immersing approximately 0.2 g of the uncured compound in 60 ml of toluene for 7 days to obtain equilibrium swelling. Additionally, to separate physically from chemically bound rubber, the immersion was done in an ammonia atmosphere. The mass of the samples before and after the test was used to calculate the bound rubber [23,24,25].

Payne effect measurements were done by using the RPA 2000 after prior vulcanization for  $1.2 \times t_{90}$  at 160 °C in the RPA. In order to estimate the Payne effect, the values of the storage modulus at 0,56 % strain and 100 % strain were measured at 100 °C and a frequency of 0.5 Hz.

The apparent crosslink density and distribution were measured by the swelling experiments done in toluene according to Schotman and Datta, Ellis and Moore [26,27,28]. The test sheets were cut to obtain appropriate test pieces. Propanethiol in combination with piperidine was used to characterize polysulphidic crosslinks, hexanethiol in combination with piperidine was used to characterize the poly- and di-sulphidic crosslinks. In order to reduce the measurement error the determinations were done in twofold.

Mechanical properties of the samples were tested using a Zwick Z020 tensile tester according to ISO-37 at crosshead speed of 500 mm/min.

Abrasion resistance was measured with a DIN – abrader according to method A of DIN 53516. The weight loss was measured and recalculated to a volume loss for each sample.

Tear resistance was measured using a Zwick Z020 tensile tester on Delft type samples at a crosshead speed of 500 mm/min.

In order to characterize the wet skid resistance, dynamic mechanical analysis was performed on a Metravib DMA 2000 in the temperature-sweep mode from -50 °C to +50 °C with 1 % static and 0,1 % dynamic strain at a frequency of 10 Hz. In order to predict the rolling resistance, single point measurements of  $\tan\delta$  at 60 °C and 6 % strain were performed on the RPA 2000, after prior vulcanization for  $1.2 \times t_{90}$  at 160 °C in the RPA.

A Laboratory Abrasion Tester 100 (LAT 100, VMI the Netherlands) was used to estimate the wet skid resistance of the tire treads in conditions which simulate the real conditions on the road: Figure 2 [6]. Wheel samples were made by compression molding in a special mold using the Wickert laboratory vulcanization press for 11 mins. at 170 °C. Testing was performed at five different water temperatures: 2 °C, 8 °C, 15 °C, 22 °C, 30 °C and at constant slip angle of 15°. An electro-corundum disc with relative roughness: 180 was used to simulate the tire-road interactions. Tests were performed at constant speed of 1,5 km/h and load of 75 N for a distance of 33 meters. The Side Force Coefficient (SFC) values (Equation 2) for the particular samples are compared with the value obtained for the reference sample TESPT 7 and given as relative values. The given property with higher rating is always better.

$$SFC = \frac{F_y}{F_z} \quad (\text{Equation 2})$$

Where  $F_y$  = the side force; and  $F_z$  = the normal load on the rubber wheel sample.

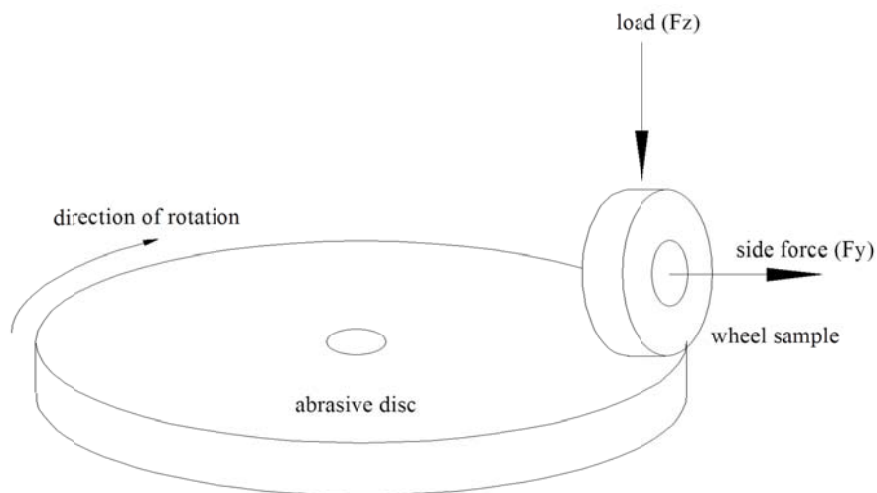


Figure 2: Measuring principle of the LAT 100.

## 4.3 RESULTS AND DISCUSSION

### 4.3.1 Mooney viscosities

The Mooney viscosities of the batches containing equimolar amounts of TESH and TESPT silanes are shown in Figure 3. Higher concentrations of both TESH and TESPT cause a decrease in Mooney viscosity. The effect is more evident in the case of TESH than for TESPT. The increase in Mooney viscosity of the batch containing 14.4 phr of TESPT is most probably caused by a slight scorch during mixing. Both silanes are reactive towards the silica surface and after silanization their distribution between polymer and filler phase is not homogenous. The largest amount of coupling agent molecules is concentrated on the surface of the silica. Condensation of silane as a side reaction due to increased concentrations of the silanes can cause formation of a thicker layer of partially polymerized silane on the surface of the silica [29]. This thicker layer could act as an interface lubricant which facilitates movement of filler particles in the polymer matrix and consequently decreases the viscosity.

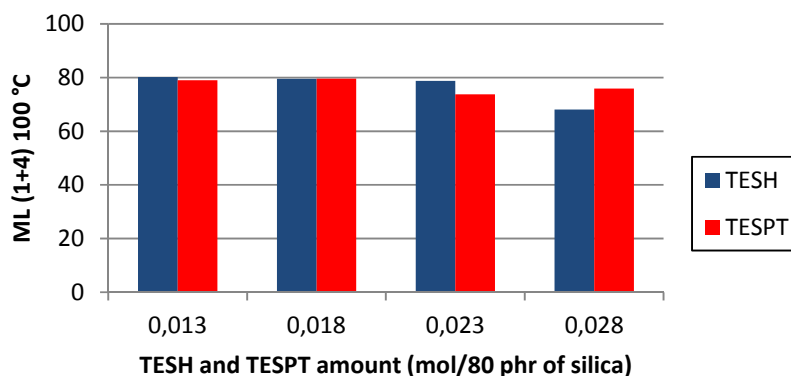


Figure 3: Mooney viscosities of the batches.

### 4.3.2 Bound rubber

These test results shown in Figure 4 clearly show the differences in polymer-filler interactions before vulcanization for the compounds containing TESH and TESPT. The compounds containing TESH silane dissolve completely in the presence of the ammonia atmosphere, indicating that all rubber-filler interactions in this still unvulcanized state are

physical of nature. Consequently the values of the chemically bound rubber are equal to zero. This confirms that silica covered by TESH is not able to form chemical bonds with the rubber in the unvulcanized state, and that the interactions are limited to just physical, regardless of the silane concentration. In case of TESPT, an increased concentration entails changes in physically bound rubber. However a substantial increase in chemically bound rubber is also visible at concentrations ranging from 7 phr (0,013 mol) to 9,5 phr (0,028 mol) of TESPT. The latter suggests that 7 phr of TESPT per 80 phr of silica is still below a threshold concentration above which the chemically bound rubber reaches a plateau. In the plateau the silica surface is saturated with bulky molecules of TESPT, and a further increase of the concentration does not lead to formation of new chemical bonds between silica and the polymer.

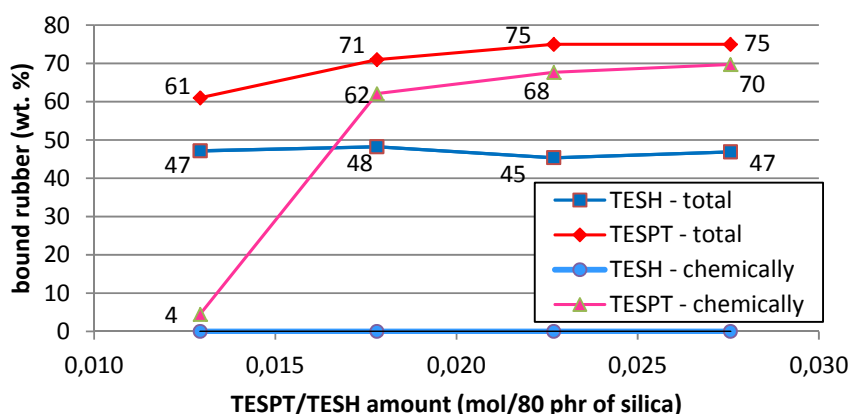


Figure 4: Bound rubber of the TESPT and TESH containing compounds.

The results obtained from the bound rubber experiments are inherently related to the tensile strengths of the vulcanizates, as shown in Figure 5. The threshold concentration of TESPT is also visible in the values of tensile strength, however to a lesser extent than in the bound rubber. Replacing strong, chemical bonds with relatively weak physical interactions lowers the values of the tensile strength. The lower values obtained for the vulcanizates with TESH are caused by the fact that the filler is not strongly connected with the polymer and consequently cannot actively participate in transfer of the load

applied to the sample. An explanation in a mechanistic sense could be that the polymer chains under high deformations are simply sliding on the surface of the silica.

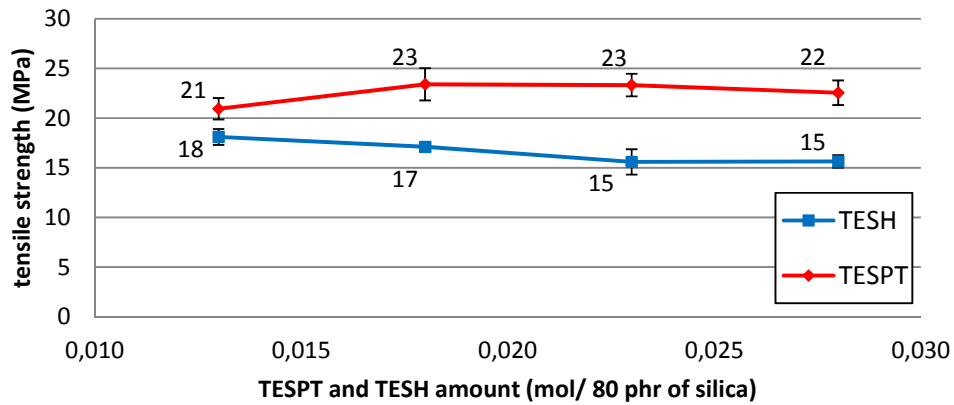


Figure 5: Tensile strength of the vulcanizates containing TESPT and TESH.

#### 4.3.3 Abrasion resistance

The abrasion resistance of rubber is commonly associated with the glass transition of the polymer. The higher the glass transition temperature of the polymer, or the closer the  $\tan\delta$  maximum to the temperature at which abrasion is taking place, the less elastic the rubber is, resulting in increased abrasion [2]. Rubber which is less elastic is less able to withstand the concentrated loads coming from the asperities existing on the abrasive surface. Nevertheless, as the same polymer blend is used (SBR/BR) for all compounds in the present study, the abrasion resistance must depend on different factors than only the glass transition temperature of the polymer blend. The DIN abrasion of the samples in Figure 6 depends on the amounts of silanes used, and therefore on the polymer-filler interactions. With increasing concentration of TESPT the abraded volume of rubber decreases, resp. the abrasion resistance increases. This behavior could be explained by the fact that, by the increasing amount of TESPT more elemental sulfur from the TESPT molecules is released into the silica-polymer interphase. A higher sulfur concentration at the silica surface causes a gradient of crosslink density from high at the silica surface towards low at the polymer phase. Consequently, the silica particles are more immobilized in the polymer matrix and their extraction by sharp asperities is impeded. In case of TESPT, the DIN abrasion correlates in opposite manner with the bound rubber values.

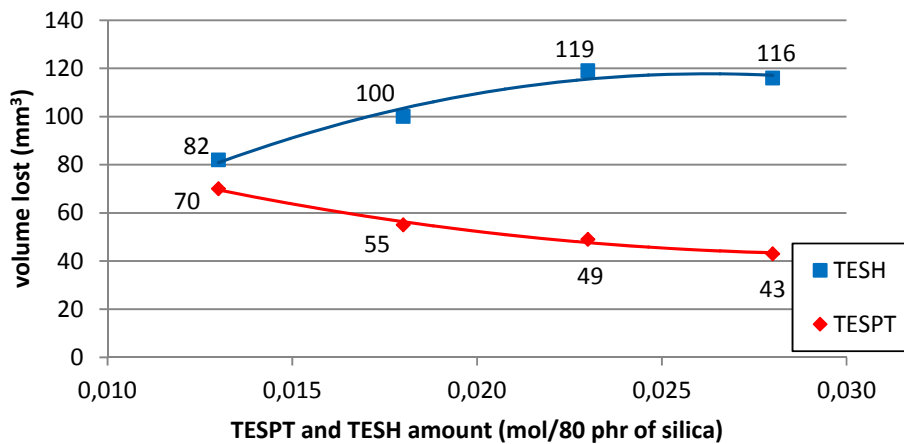


Figure 6: DIN abrasion of the samples containing TESPT and TESH silanes.

With increasing concentration of TESH-silane, the volume of rubber lost during abrasion increases substantially. This cannot be related to the bound rubber content, because the values for total bound rubber for TESH-containing compounds are constant, regardless of the TESH-loading. On the other hand, the chemically bound rubber content measured for this coupling agent is zero, irrespective of the loading, contrary to the TESPT-case. Consequently, an explanation may be based on the interface lubrication effect which was already discussed in the case of the Mooney viscosity. The changes in Mooney viscosity caused by the increased amount of TESH seem to have an impact on the DIN abrasion as well. The TESH acts as a silica-polymer interface-lubricant and facilitates polymer chain-sliding on the silica-surface. That in turn causes easier extraction of small particles by sharp asperities of the abrasive disc and increases wear.

#### 4.3.4 Tear resistance

The tear resistance of the samples as shown in Figure 7, gives information about the crack-growth throughout the material. Physical interactions also affect the tear resistance. Contrary to what was expected from the tensile tests, the tear resistance values show a diametrically different relation. The tear resistance values for the TESH containing samples are actually higher than those obtained for the TESPT samples.

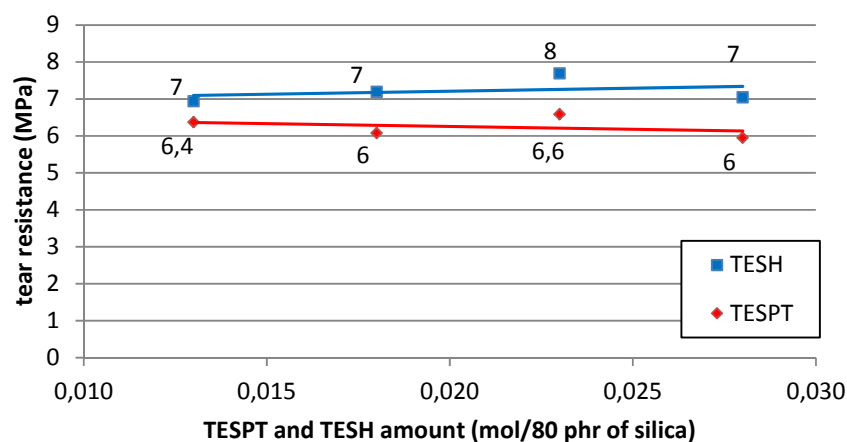


Figure 7: Tear resistance of the TESH and TESPT containing samples.

Hysteretic losses of the compounds play an important role in the tear mechanism. The closer the glass transition temperature to the temperature where tearing is taking place, the higher the tear strength. The glass transition temperature of the samples containing TESH is higher in comparison with the TESPT-containing samples: see Figure 8. Vulcanizates containing TESH are characterized by higher hysteresis during the tearing process, therefore they have a higher possibility towards crack dissipation – higher tear resistance.

#### 4.3.5 *Tan $\delta$ @ at low temperatures: indicator of wet skid resistance*

The practical laboratory assessment methods for wet skid resistance for carbon black filled compounds indicate that higher values of  $\tan \delta$  at lower temperatures, preferably 0 °C to 20 °C, correspond to better wet skid resistance of the tire treads [10,18,19]. When the tire stops its rotation and is skidding, the frequency rises up to the megahertz region. This high frequency is on the one hand caused by roughness of the surface on which the rubber is sliding [30,15]. However, this high frequency is also the result of stick-slip phenomena during skidding [31]. The service temperature of the tire during rolling is relatively high: around 40 °C to 80 °C. Because of the frequency-temperature superposition principle, under the influence of the high frequency during skidding the  $\tan \delta$  peak of the elastomer shifts toward higher temperatures [11,32]. The values of  $\tan \delta$  at

0 – 20 °C at 10 Hz are therefore representative for the  $\tan \delta$  at service temperature and high frequency [2,33,34]. Hence, rubbers which dissipate more energy in the low temperatures range of 0 – 20 °C should provide a higher wet skid resistance.

The dependence of the  $\tan \delta$  on temperature for the various compounds is shown in Figure 8. In general, compounds in which TESH is used are characterized by a lower peak at the glass transition temperature in comparison with the TESPT-samples.

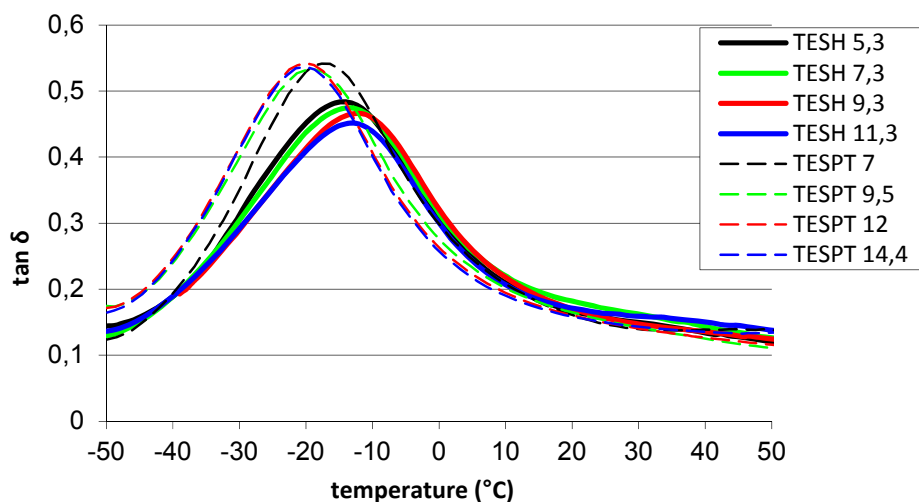


Figure 8:  $\tan \delta$  – temperature dependence.

Apparently, this is due to lower loss moduli  $G''$  at the glass transition, rather than differences in the storage modulus  $G'$ , as seen in Table 3. The different loss moduli point at more restricted polymer segmental motion for the TESH-containing samples in comparison with TESPT. It suggests that silica treated with TESH as silane adsorbs more polymer on its surface than in the case of TESPT, leaving less free polymer to participate in the glass transition process.

Table 3. Comparison of the storage and loss moduli at  $\tan \delta$  peak.

|            | Tg (°C) | G' MPa | G'' MPa |
|------------|---------|--------|---------|
| TESH 5.3   | -13     | 185    | 85      |
| TESH 7.3   | -15     | 206    | 95      |
| TESH 9.3   | -14     | 221    | 95      |
| TESH 11.3  | -14     | 226    | 98      |
| TESPT 7    | -18     | 180    | 100     |
| TESPT 9.5  | -19     | 215    | 115     |
| TESPT 12   | -20     | 236    | 128     |
| TESPT 14.4 | -20     | 234    | 126     |



Further, the TESH containing compounds have higher values of  $\tan \delta$  in the temperature range of 0 to 20 °C compared with the TESPT-containing compounds. In fact, replacing TESPT with TESH shifts the curves towards higher temperature and that is why the values of  $\tan \delta$  at 0 – 20 °C are higher. The shift of the  $\tan \delta$  peak could be caused by differences in the rubber crosslink density. However, the values of the apparent crosslink densities measured for the samples containing TESH are actually lower than for the TESPT containing samples; see Table 4.

Table 4. Crosslink density, distribution and hardness of the samples containing TESPT and TESH

|            | Overall |       | Polysulphidic |      | Disulphidic |      | Monosulphidic |      | ShA hardness |
|------------|---------|-------|---------------|------|-------------|------|---------------|------|--------------|
| TESPT 7    | 1.71    | -100% | 1.05          | -61% | 0.08        | -5%  | 0.58          | -34% | 58           |
| TESPT 9.5  | 2.00    | -100% | 1.23          | -62% | 0.13        | -7%  | 0.64          | -32% | 61           |
| TESPT 12   | 2.11    | -100% | 1.30          | -62% | 0.13        | -6%  | 0.68          | -32% | 60           |
| TESPT 14.3 | 2.28    | -100% | 1.35          | -59% | 0.17        | -7%  | 0.76          | -33% | 63           |
| TESH 5.3   | 1.40    | -100% | 0.78          | -56% | 0.15        | -11% | 0.47          | -34% | 58           |
| TESH 7.3   | 1.64    | -100% | 0.95          | -58% | 0.24        | -15% | 0.45          | -27% | 59           |
| TESH 9.3   | 1.62    | -100% | 1.00          | -62% | 0.18        | -11% | 0.44          | -27% | 61           |
| TESH 11.3  | 1.80    | -100% | 1.10          | -61% | 0.24        | -13% | 0.46          | -26% | 63           |

The shift of the glass transition temperature is also visible in the compounds as they differ in filler-filler interactions measured by the Payne effect. At sufficient loading the filler particles in the elastomer matrix form a secondary filler-network yielding reinforcement well beyond the hydrodynamic effect. This filler-network is progressively broken with increasing strain amplitude. The consequent reduction in modulus with strain amplitude is commonly referred to as the Payne effect [35]. A good example of the glass transition peak shift towards higher temperatures are vulcanizates in which highly-reinforcing silica is compared with low reinforcing grades [36]. The data shown in Figure 9 indicate higher values of the Payne effect for the samples containing TESH, so higher filler-filler interactions, which could be the cause of the above mentioned shift. Nevertheless, the higher values of  $\tan \delta$  at the temperatures range of 0 - 20 °C are related to increased hysteresis, as observed for the TESH-compounds and are anticipated to correspond with higher side force coefficient values compared to the TESPT-containing samples: see below.

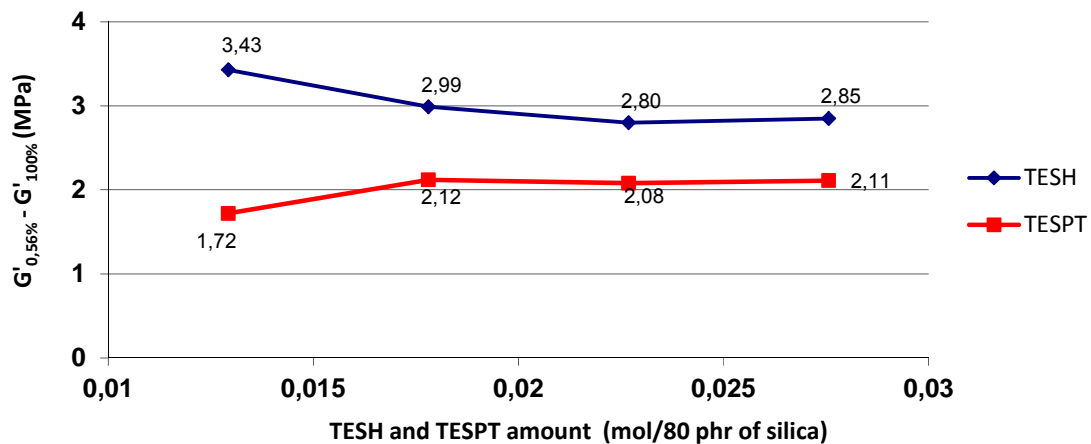


Figure 9: Payne effect dependence on silane concentration

#### 4.3.6 $\tan \delta$ @ 60 °C: indicator of rolling resistance

Considering an average speed of a vehicle of 70 km/h and car wheel dimensions: 255/65/16, the typical frequency of deformation of the revolving tire is around 10 Hz. The hysteresis of the rubber compound causes an increase of the tire temperature to approx. 60 °C. The weight of the vehicle exerted on the tire results in around 6% tire tread deformation. Therefore, measuring the  $\tan \delta$  values at 10 Hz, 6% of dynamic strain and at 60 °C: Figure 10, is a good indicator of rolling resistance. The lower the value of the  $\tan \delta$ , under these conditions, the lower the predicted rolling resistance.

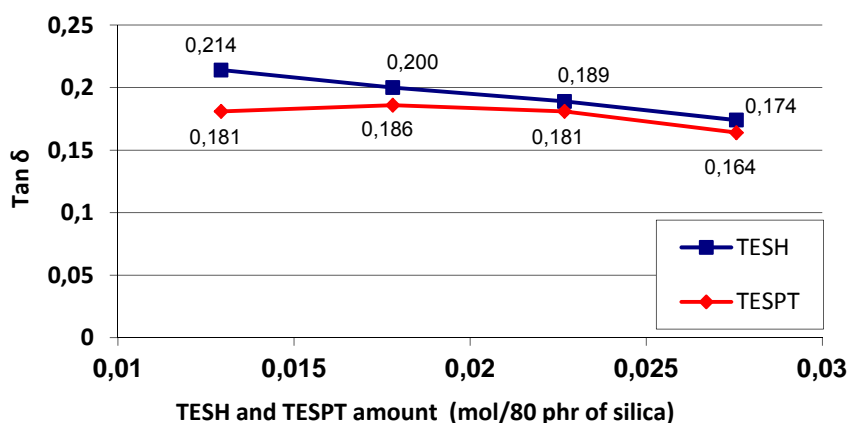


Figure 10: Values of  $\tan \delta$  at 60 °C

In general, the TESH-silane containing compounds show higher values of  $\tan \delta$  than those with TESPT. This indicates that chemical bonds between silica and rubber via coupling agents are needed for lower rolling resistance. Less adherent particles means less reinforcement and higher energy lost at the interphase: the polymer chains can slide with respect to the silica surface. As stated before, with increasing TESH-concentration the bound rubber content did not change: the total bound rubber values were constant, chemically bound rubber was zero. Increasing the TESH-concentration caused a decrease in  $\tan \delta$ -values, because of the suppressed filler-filler interaction. In the case of TESPT the  $\tan \delta$ -values are relatively constant until the highest silane concentration, where a drop is visible. It shows that compound hysteresis at higher temperatures and relatively high strains is almost independent of the concentration of TESPT.

#### 4.3.7 LAT 100 side force coefficient: wet skid resistance

To further simulate the tires wet skid resistance, the Laboratory Abrasion Tester (LAT 100) was used. This test better resembles the real conditions occurring on a wet road. Values of the side force coefficient are shown in Figure 11.

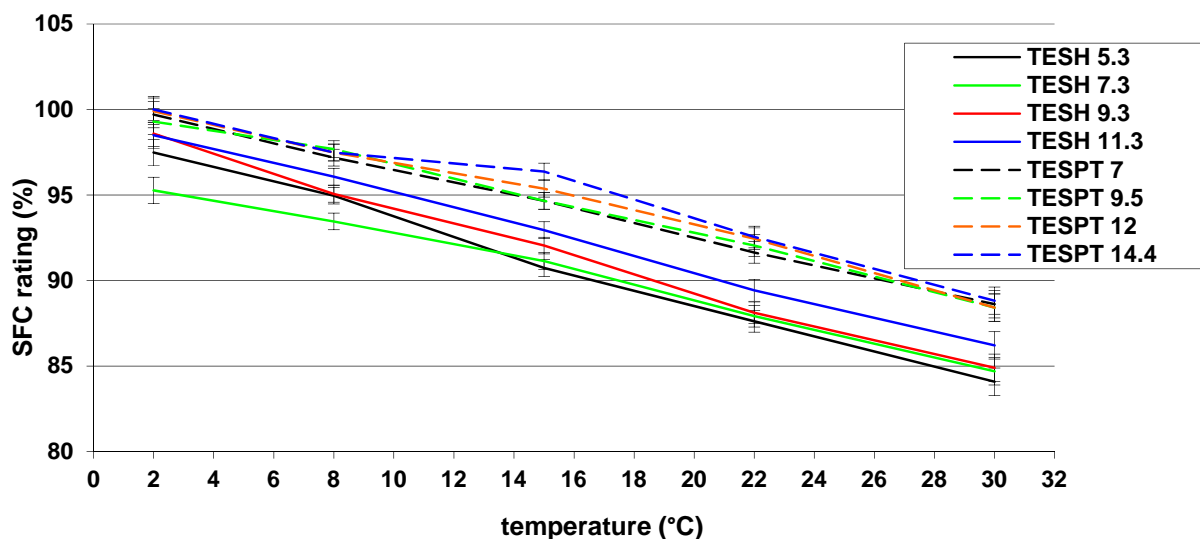


Figure 11: LAT 100 side force coefficient rating values in different water temperatures

Despite the fact that the samples containing TESH have higher hysteresis at temperatures of 0 – 20 °C in the  $\tan \delta$ -values than TESPT, the side force coefficient values are lower for the samples containing TESH. In order to find an explanation for this apparently contradicting phenomenon, mechanical properties could also be considered. Apart from differences in tensile strength between the TESPT-and TESH-containing vulcanizates, also the moduli of the compounds can be taken into consideration. The shapes of the stress-strain curves obtained for the compounds containing TESPT and TESH show that the samples containing TESH are characterized by lower values of the secant moduli: see Figure 12. Micro-asperities existing on the surface of the abrasive disc or surface of the road can therefore cause higher strain deformations on a micro scale, in which fragments of the rubber compounds are detached from the surface of the wheel or just displaced. Further, the higher the tensile strength of the rubbers, the higher the force needed to remove the micro-fragments. The higher the modulus of the compound the higher the force that is used to displace the micro-fragments on the surface of the wheel sample. Both mechanisms contribute to the larger opposing force during sliding which results in higher wet skid resistance of the TESPT-containing samples.

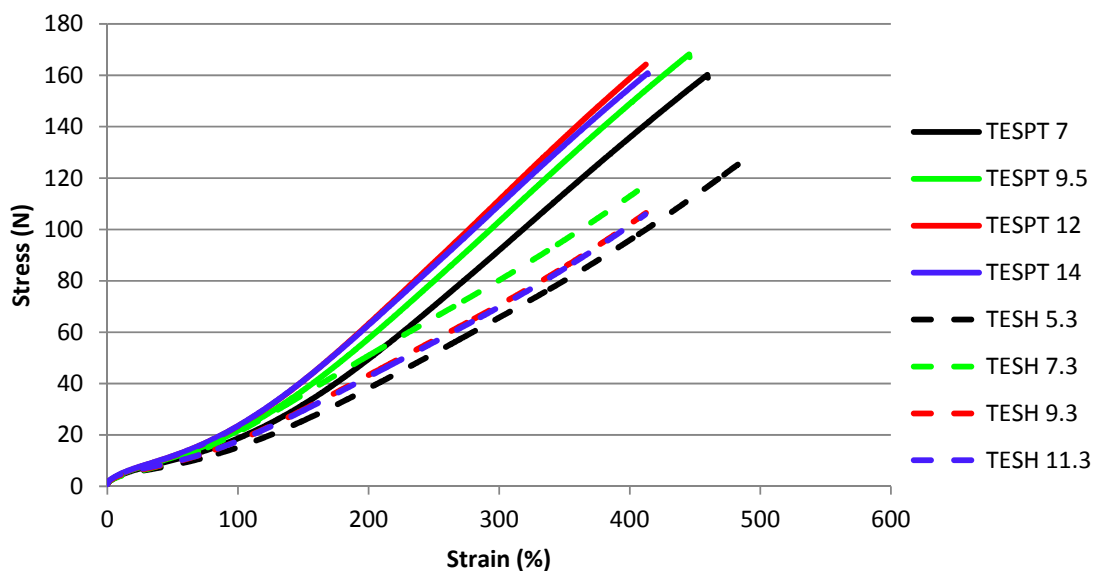


Figure 12: Stress-strain curves of the TESH and TESPT containing samples

#### 4.3.7.1 Final remarks

Experiments performed by Heinz [7] show strong correlation between the values of the side force coefficient measured on the LAT 100 and (wet) skid values obtained during road tests. At the same time he points out that no correlation exists between dynamic measurements and road tests. As a consequence, a correlation between LAT 100 and dynamic measurements do not exist. The contradiction between the higher hysteresis of the compounds at 0 – 20 °C but yet lower values of the side force coefficient measured with the LAT 100 found in the present study concur with the tests done by Heinz. The authors of the present article incline towards the use the LAT 100 as a decisive tool during assessment of the wet skid potential of a rubber compound. As a consequence, chemical polymer-filler interactions by appropriate coupling agent (TESPT) are to be preferred for good wet skid resistance.

## 4.4 CONCLUSIONS

- Silica can be treated with TESH, to obtain interactions similar to those which exist between carbon black and rubber. The bound rubber content confirms this.
- Introduction of physical interactions instead of chemical bonds radically decreases the values of the tensile strength because of inertness of the silica surface.
- The dynamic properties of the samples measured at low temperatures do not correspond with the wet skid resistance as measured by the LAT 100.
- Replacement of physical bonds (TESH) by chemical interactions (TESPT) between rubber and fillers increases the values of side force coefficient measured with the LAT 100. Consequently chemical bonds are preferred for good wet skid resistance of the tire treads.
- The assumption that under the influence of energy resulting from skidding, polymer molecules physically bonded to the filler surface can easily be displaced, what should increase the energy dissipation and as a consequence increase the wet skid resistance, is not correct.

## References

---

- [1] A. A. Ward, A. A. Yehia, A. M. Bishai, *Kautsch. Gummi Kunstst.*, 61 (2008) 569.
- [2] K.H. Nordsiek, *Kautsch. Gummi Kunstst.*, 38 (1985) 177.
- [3] M. J. Wang, *Rubber Chem. Technol.*, 71 (1998) 520.
- [4] M. J. Wang, *Kautsch. Gummi Kunstst.*, 60 (2007) 438.
- [5] M. J. Wang, *Kautsch. Gummi Kunstst.*, 61 (2008) 33.
- [6] M. Heinz, K.A. Grosch, 167<sup>th</sup> Technical meeting of the Rubber Division ACS, 16-18 May 2005, San Antonio, Texas, USA.
- [7] M. Heinz, *J. Rubb. Res.*, 13 (2010) 91.
- [8] K. R. Grosch, *Rubber Chem. Technol.*, 80 (2007) 379.
- [9] C. J. Derham, R. Newell and P. McL. Swift, *NR Technology*, 19 (1988) 1.
- [10] G. Heinrich, *Kautsch. Gummi Kunstst.*, 45 (1992) 173.
- [11] G. Heinrich, N. Rennar, H. Dumler, *Kautsch. Gummi Kunstst.*, 49 (1996) 32.
- [12] G. Heinrich, *Rubber Chem. Technol.*, 70 (1997) 1.
- [13] M. Klüppel, G. Heinrich, *Rubber Chem. Technol.*, 73 (2000) 578.
- [14] A. Müller, J. Schramm, M. Klüppel, *Kautsch. Gummi Kunstst.*, 55 (2002) 432.
- [15] A. le Gal, M. Klüppel, *J. Phys. Condens. Matter*, 20 (2008) 1.
- [16] B. N. J. Persson, Julich U. Tartaglino, E. Tosatti, O. Albohr, *Kautsch. Gummi Kunstst.*, 57 (2004) 532.
- [17] Y. Isono, T. Oyama, S. Kawahara, *Adv. In Tech. Of Mat. And Mat. Proc. J.* 5 (2003) 84.
- [18] S. L. Aggarwal, I. G. Hargis, R. A. Livigni, H. J. Fabris and L. F. Marker, "Advances in elastomers and rubber elasticity". Plenum Press (1986) 17.
- [19] R. R. Rahalkar, *Rubber Chem. Technol.*, 62 (1989) 246.
- [20] L.E.A.M. Reuvekamp, P.J. van Swaaij, J.W.M. Noordermeer, *Kautsch. Gummi Kunstst.*, 63 (2009) 35.
- [21] R. Rauline, European Patent No. EP0501227B1, (1992), to Michelin Co.
- [22] L. Guy, Ph. Cochet, Y. Bomal, S. Daudey, *Kautsch. Gummi Kunstst.*, 63 (2009) 383.
- [23] J. H. Fielding, *Industr. Eng. Chem.*, 29 (1937) 880.
- [24] E. M. Dannenberg, *Industr. Eng. Chem.*, 40 (1948) 2199.
- [25] C. M. Blow, *Polymer*, 14 (1973) 309.
- [26] A. H. M Schotman, R.N. Datta, *Rubber Chem. Technol.*, 69 (1996) 727.
- [27] B. Ellis, G. N. Welding, *Rubber Chem. Technol.*, 37 (1964) 571.
- [28] C. G. Moore, *J. Polym. Sci.* 32 (1958) 503.
- [29] U. Görl, A. Hunsche, A. Mueller, H.G. Koban, 150<sup>th</sup> Technical meeting of the Rubber Division ACS, 8-10 October 1996, Louisville, Kentucky, USA.
- [30] A. le Gal, M. Klüppel, *Kautsch. Gummi Kunstst.*, 59 (2006) 308.
- [31] A. Schallamach, "Chemistry and Physics of Rubber-like Substances" ed. L.

---

Bateman. McLaren and Sons, London (1963) 382.

[32] S. Cervenya, A. Ghilarduccib, H. Salvab, A.J. Marzoccaa, *Polymer*, 41 (2000) 2227.

[33] A. Yoshioka, K. Komuro, A. Ueda, H. Watanabe, S. Akita, T. Masuda, A. Nakajima, *Pure Appl. Chem.*, 58 (1986) 1697.

[34] P. Roch, *Kautsch. Gummi Kunstst.*, 48 (1995) 430.

[35] A. R. Payne, *J. Appl. Polym. Sci.*, 6 (1962) 57.

[36] E. Cichomski, T.V. Tolpekina, S. Schultz, W.K. Dierkes, J.W.M. Noordermeer, 184<sup>th</sup> Technical Meeting of the Rubber Division ACS, 8-10 October 2013, Cleveland, Ohio, USA.





### ***Influence of modification of the silane coupling agent on wet-traction and rolling resistance performance indicators for passenger car tire tread materials: Influence of number of ethoxy groups***

---

*The elastomer compound used for tire treads is a composite material of which the dynamic properties can be adjusted over a relatively broad range by modification of the polymer-filler interaction. The replacement of carbon black by a silica-silane coupling agent system for instance, allows reducing the hysteresis of the rubber, which results in a reduction of the rolling resistance when applied for tire treads.*

*Selective changes in the structure of the coupling agent, in this chapter the number of ethoxy groups reactive towards silanol groups on the surface of the filler, lead to changes in the microstructure of the silica-polymer interface and determine both, mechanical and dynamic properties of the rubber compound, thus wet grip and rolling resistance when used in a tire tread.*

*In this chapter the effect of the number of ethoxy groups in the silane on the macroscopic dynamic properties as indicators for tire performance is discussed. Silanes with just one ethoxy group instead of three as commonly used, are expected to decrease rolling resistance and to improve wet skid resistance, based on the changes in hysteresis caused by the structural changes of the silane.*

## 5.1 INTRODUCTION

The key element of silica technology is the coupling agent, a silane which chemically couples the silica to the rubber polymer. The chemical structure of the silane determines the polymer-filler interactions, which on their turn influence wet skid and rolling resistance. The goal of the present study is to characterize the underlying mechanisms involved in rubber-filler interactions for wet skid resistance of tires, a dynamic viscoelastic phenomenon. To characterize the dynamic properties of rubber, storage and loss moduli are commonly measured. The ratio of the loss to storage modulus is indicated as the  $\tan \delta$ .

The surface of precipitated silica's is covered with different types of hydroxyl groups, the silanol groups. The concentration of the silanol groups on the silica surface is in the range of 6 to 7 groups per square nanometer of surface <sup>1,2</sup>. High concentrations of silanol groups make the silica surface rather hydrophilic, which in turn causes strong agglomeration of the fine silica particles during mixing with nonpolar rubber such as styrene-butadiene rubber (SBR). Apart from agglomeration, the highly hydrophilic character of silica causes adsorption of amines used as accelerators for the vulcanization process, leading to a substantial increase in curing time and decrease in crosslink efficiency.

Using a silane reduces the hydrophilicity of silica during mixing and at the same time provides chemical bonding <sup>3</sup>. Due to the good dynamic and mechanical properties of compounds, bis-(triethoxysilylpropyl)tetrasulfide (TESPT) is most frequently used as coupling agent in the tire industry. When TESPT is used in an optimal concentration, not more than one out of seven available silanol groups per square nanometer on the silica surface are utilized to form the actual connection to the polymer chains <sup>4</sup>. Studies by Blume et al. <sup>5</sup> show that only 25 % of all available silanol groups on the silica surface can react with a silane coupling agent containing triethoxysilyl moieties. At a reaction temperature of 110 °C, the geminal and isolated silanol groups form bonds with the silane. However, vicinal groups are not utilized which is caused by their lower molecular accessibility.

In order to reduce the number of remaining silanol groups on the silica surface after silanization, a coupling agent with only one silica-silane bonding unit, bis-(dimethylethoxysilylpropyl)tetrasulfide (DMESPT) is applied <sup>6</sup>. In this case, replacing

the two lateral ethoxy groups by methyl moieties leads to less bulky silane molecules, hence it is anticipated that more of them could attach to the silica surface and lead finally to a higher bond density to the polymer matrix. Mechanical properties shouldn't be influenced as, in fact, just only one ethoxy group is necessary to attach the polymer chains to the silica surface. However, it will influence the dynamic properties of the elastomeric material, and is expected to result in improvements in tire properties.

This chapter will try to answer the question if and how a less bulky silane with just one ethoxy group will affect wet traction, rolling resistance and other properties of the compound, and if the changes can be correlated to a higher bond density.

## 5.2 EXPERIMENTAL

In the silane used in this study, two ethoxy groups out of three were replaced by methyl groups: bis-(dimethylethoxysilylpropyl)tetrasulfide (DMESPT). Apart from being inert, these methyl groups result in less steric hindrance in comparison to the more bulky ethoxy groups in the TESPT molecule. This modification leads to a situation in which only one group on each side of the silane molecule can bind to the silica surface. Besides, the reaction of the adjacent ethoxy groups, the so called secondary silanization reaction, is eliminated in the experimental silane. The structures of this coupling agent and TESPT are shown in Figure 1.

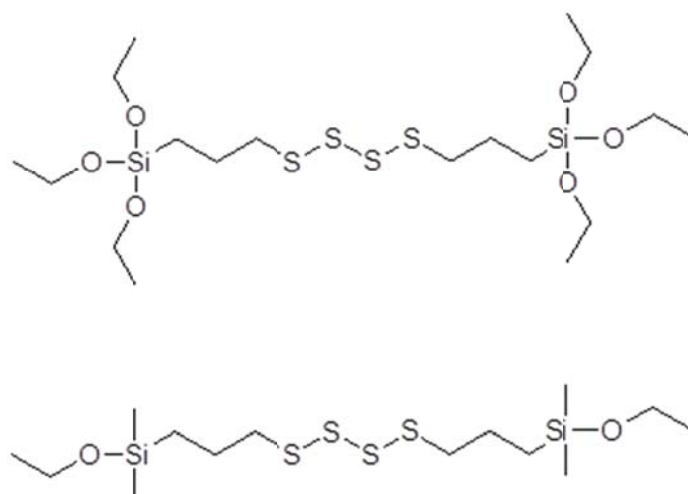


Figure 1: Structure of bis-(triethoxysilylpropyl)tetrasulfide, TESPT (top) and bis-(dimethylethoxysilylpropyl)tetrasulfide, DMESPT (bottom)

The reference silane, TESPT, was obtained from Evonik GmbH, and DMESPT was synthesized.

### 5.2.1 Synthesis of bis-(dimethylethoxysilylpropyl) tetrasulfide (DMESPT)

This silane was synthesized according to the method described by Reuvekamp<sup>7</sup>. The synthesis was performed in absolute ethanol under nitrogen atmosphere by refluxing 3-chloropropyl dimethylethoxysilane (ABCR GmbH, Karlsruhe, Germany) and sodium tetrasulfide (Sigma Aldrich, Zwijndrecht, The Netherlands), as shown in Figure 2. After 2 hours of refluxing, the color of the suspension changed from dark red to yellow. This suspension was filtered and ethanol was removed from the filtrate in a rotary evaporator, which lead to a dark red suspension. The red suspension was diluted with diethyl ether, and the ether layer was extracted with water. After this extraction, the water was colored red, and the extraction was continued until no further coloration of the water phase was visible. The ether extract was dried with anhydrous MgSO<sub>4</sub>, filtered, and remaining ether was removed in the rotary evaporator.

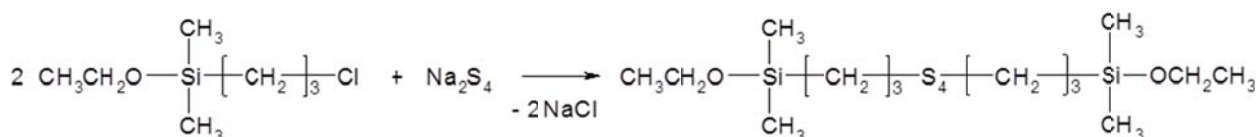


Figure 2: Formation of bis-(dimethylethoxysilylpropyl)tetrasulfide

The yield of the reaction was 82 % of a gold yellow clear liquid, which was identified by liquid chromatography-mass spectroscopy (LC-MS, Agilent-1100/Bruker-Esquire 3000 Plus) as bis-(dimethylethoxysilylpropyl)polysulfide with 95 % purity according to the procedure specified in Table I and Table II. The product structure as determined by LC-MS is given in Figure 3. Each individual peak was characterized by its own molar mass with MS. An average sulfur rank of 2.7 and molar mass of 386 g/mol was

calculated based on the MS-data. The index of refraction of the product at 22 °C was 1.5150.

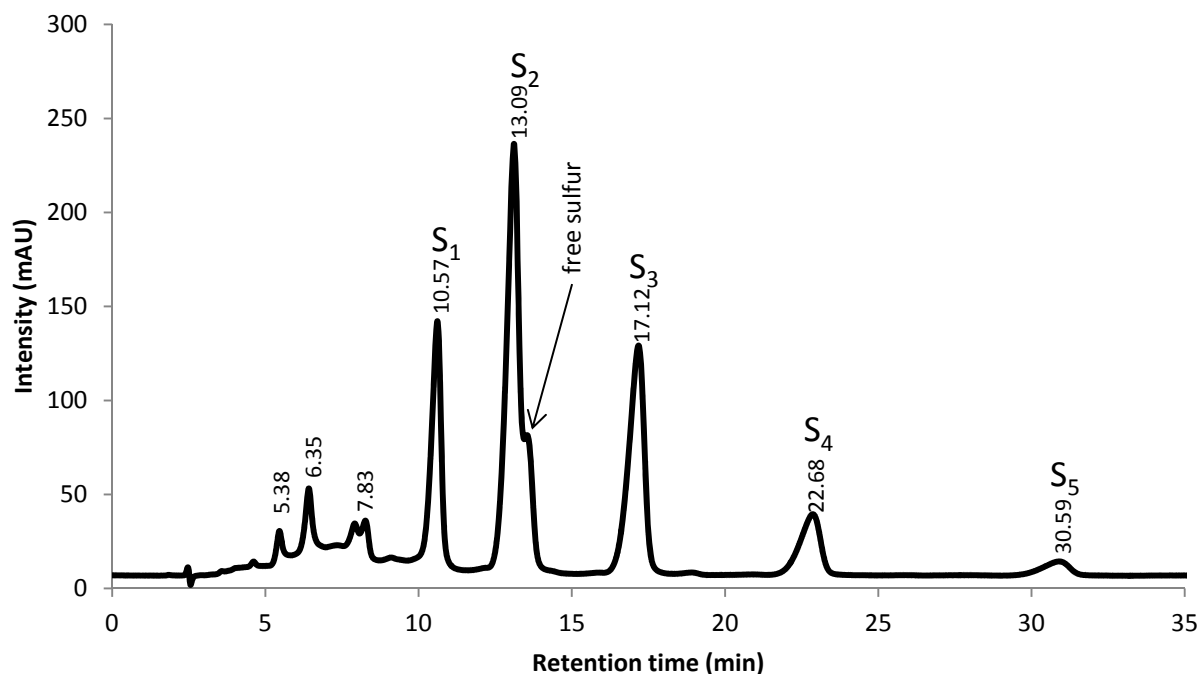


Figure 3: LC-MS chromatogram of DMESPT; the different sulfur ranks and the free sulfur peak are indicated.

Table I: LC-MS parameters to characterize the silane structures

|                 |  |
|-----------------|--|
| Column          | Nucleosil 100-5 C18 HD (reverse phase) |
| Mobile phase    | 97 acetonitrile : 3 water (vol%)       |
| Flow rate       | 0.3 ml/min                             |
| Temperature     | 23 °C                                  |
| Detector        | UV (DAD)                               |
| Wavelength      | 254 nm                                 |
| Injected volume | 5 µl                                   |

Table II: MS ionization conditions in the ESI interface

|                        |             |
|------------------------|-------------|
| Flow rate              | 0.20 ml/min |
| Nebuliser gas pressure | 0.2 MPa     |
| Dry gas flow           | 3 l/min     |
| Dry gas temperature    | 325 °C      |

### 5.2.2 Mixing and curing

A test compound according to the green tire recipe from Michelin was used <sup>8</sup>, containing a highly dispersible silica grade with a cetyltrimethylammonium bromide (CTAB) specific surface area of 160 m<sup>2</sup>/g. Additionally, batches containing two silica grades differing in specific surface area, CTAB 80 and 195 m<sup>2</sup>/g, were tested. The complete comparison of the different silica types is reported in Chapter 3. The compound formulations are shown in Table III, and a detailed specification of all ingredients is shown in Table IV.

Table III: Rubber compound formulations

| Ingredient      | Sample code |           |          |            |          |          |            |             |       |        |         |          |
|-----------------|-------------|-----------|----------|------------|----------|----------|------------|-------------|-------|--------|---------|----------|
|                 | TESPT 7     | TESPT 9.5 | TESPT 12 | TESPT 14.4 | DMESPT 5 | DMESPT 7 | DMESPT 8.5 | DMESPT 10.4 | I-80* | I-195* | II-80** | II-195** |
| S-SBR           | 103         | 103       | 103      | 103        | 103      | 103      | 103        | 103         | 103   | 103    | 103     | 103      |
| BR              | 25          | 25        | 25       | 25         | 25       | 25       | 25         | 25          | 25    | 25     | 25      | 25       |
| Silica CTAB 160 | 80          | 80        | 80       | 80         | 80       | 80       | 80         | 80          |       |        |         |          |
| Silica CTAB 80  |             |           |          |            |          |          |            |             | 80    |        | 115     |          |
| Silica CTAB 195 |             |           |          |            |          |          |            |             |       | 80     |         | 65       |
| TESPT           | 7           | 9.5       | 12       | 14.4       |          |          |            |             | 3,4   | 8,3    | 5       | 7        |
| DMESPT          |             |           |          |            | 5        | 7        | 8.5        | 10,4        |       |        |         |          |
| TDAE            | 5           | 5         | 5        | 5          | 5        | 5        | 5          | 5           | 5     | 5      | 5       | 5        |
| Zinc oxide      | 2,5         | 2,5       | 2,5      | 2,5        | 2,5      | 2,5      | 2,5        | 2,5         | 2,5   | 2,5    | 2,5     | 2,5      |
| Stearic acid    | 2,5         | 2,5       | 2,5      | 2,5        | 2,5      | 2,5      | 2,5        | 2,5         | 2,5   | 2,5    | 2,5     | 2,5      |
| 6PPD            | 2           | 2         | 2        | 2          | 2        | 2        | 2          | 2           | 2     | 2      | 2       | 2        |
| TMQ             | 2           | 2         | 2        | 2          | 2        | 2        | 2          | 2           | 2     | 2      | 2       | 2        |
| Sulfur          | 1,4         | 0,8       | 0,24     | 0          | 1,8      | 1,2      | 0,8        | 0,4         | 1,8   | 1,4    | 2,2     | 1,0      |
| TBBS            | 1,7         | 1,7       | 1,7      | 1,7        | 1,7      | 1,7      | 1,7        | 1,7         | 1,7   | 1,7    | 1,7     | 1,7      |
| DPG             | 2           | 2         | 2        | 2          | 2        | 2        | 2          | 2           | 2     | 2      | 2       | 2        |

\* batches with constant silica loading

\*\* batches in which the silica loading was empirically adjusted to equalize the hardness

Table IV: Ingredient specifications

| Ingredient       | Specification   | Supplier  |
|------------------|---|---|
| S-SBR            | Solution Styrene-Butadiene Rubber                             | Buna VSL 5025-2 HM Lanxess, Leverkusen, Germany |
| BR               | Butadiene Rubber  | Kumho KBR Seoul, S-Korea                        |
| Silica (1165MP)  | Precipitated silica with CTAB SSA* = 160 m <sup>2</sup> /g    | Rhodia Silices, Lyon, France                    |
| Silica (1085 GR) | Precipitated silica with CTAB SSA* = 80 m <sup>2</sup> /g     | Rhodia Silices, Lyon, France                    |
| Silica (1200 MP) | Precipitated silica with CTAB SSA* = 195 m <sup>2</sup> /g    | Rhodia Silices, Lyon, France                    |
| TESPT            | Bis-(triethoxysilylpropyl)tetrasulfide                        | Evonik GmbH, Essen, Germany                     |
| TDAE             | Treated Distillate Aromatic Extract oil, ENERTHENE 1849 F     | Hansen & Rosenthal, Hamburg, Germany            |
| Zinc oxide       |   | Sigma Aldrich, St. Louis, United States         |
| Stearic acid     |   | Sigma Aldrich, St. Louis, United States         |
| 6PPD             | Antiozonant, N-phenyl-N'-1,3-dimethylbutyl-p-phenylenediamine | Flexsys, Brussels, Belgium                      |
| TMQ              | Antioxidant, 2,2,4- trimethyl-1,2-di-hydroquinoline           | Flexsys, Brussels, Belgium                      |
| Sulfur           | Elemental sulfur, purified by sublimation                     | Sigma Aldrich, St. Louis, United States         |
| TBBS             | Accelerator, N-tert-butylbenzothiazole-2-sulphenamide         | Flexsys, Brussels, Belgium                      |
| DPG              | Accelerator, diphenyl guanidine                               | Flexsys Brussels, Belgium                       |

\* Specific Surface Area measured by using cetyltrimethylammonium bromide

DMESPT was applied at four different concentrations equimolar to the concentrations of the reference silane, TESPT, and with sulfur adjustment. The reference compound contained 7 phr TESPT, calculated according to the empirical equation proposed by L. Guy: Equation 1<sup>9</sup>. The amount of free sulfur added together with the curatives was adjusted to keep the total molar amount including the sulfur contained in the coupling agent at a constant level in all batches.

$$TESPT (phr) = 5.3 \times 10^{-4} \times (CTAB)_{silica} \times (phr)_{silica} \quad (\text{Equation 1})$$

To prepare the compounds, an internal laboratory mixer, Brabender 350 S with mixing chamber volume of 390 cm<sup>3</sup> was used. The mixing procedure is specified in Table V. The total volume of each batch was adjusted to a fill factor of 70 %. Preparation of sheets for testing was done on a Schwabenthan Polymix 80T 300 ml two roll mill.

Table V: Mixing procedure for internal mixer

| Stage I                                    |  |
|--|--|
| Rotor speed: 110 RPM, initial temp.: 50 °C |  |
| Timing<br>(min. sec.)                      | Ingredient                                 |
| 0.00                                       | Add polymers                               |
| 1.00                                       | Add ½ silica, ½ silane, ZnO + stearic acid |
| 2.30                                       | Add ½ silica, ½ silane, oil, TMQ, 6PPD     |
| 3.00                                       | Sweep                                      |
| 4.00                                       | Dump at ~ 155 °C                           |
| Stage II                                   |  |
| Rotor speed: 130 RPM, initial temp.: 50 °C |  |
| Timing<br>(min. sec.)                      | Ingredient                                 |
| 0.00                                       | Add stage I batch                          |
| 3.00                                       | Dump at ~ 155 °C                           |
| Curative addition                          |  |
| Rotor speed: 75 RPM, initial temp.: 50 °C  |  |
| Timing<br>(min. sec.)                      | Ingredient                                 |
| 0.00                                       | Add stage II batch                         |
| 1.00                                       | Add curatives                              |
| 3.00                                       | Dump at ~ 100 °C                           |

The samples were vulcanized in a Wickert press WLP 1600 at 160 °C to sheets with a thickness of 2 mm, according to their  $t_{90}$  optimum vulcanization times multiplied by 1.2 as determined in a Rubber Process Analyzer, RPA 2000, from Alpha Technologies.

### 5.2.3 Characterization methods

Additional to the tests described in Chapter 3, bound rubber tests were performed. These tests were done by immersing approximately 0.2 g of the uncured compound in 60 ml of toluene for 7 days to obtain equilibrium swelling. After swelling, the samples were dried in a vacuum oven at 80 °C for 24 hours. The weight of the sample before ( $m_0$ ) and after equilibrium swelling ( $m_1$ ) was used to calculate the bound rubber value according to Equation 2. Additionally, to distinguish physically and chemically bound rubber, the immersion of the sample in toluene was performed



in an ammonia atmosphere. According to Wolff and Polmanteer et al., ammonia treatment cleaves physically bound rubber<sup>10,11,12</sup>.

$$BR = \left(1 - \frac{m_0 - m_1}{m_0}\right) \times 100 \% \quad (\text{Equation 2})$$

The Mooney viscosity ML(1+4) of the compounds was measured at 100 °C on a Mooney viscometer MV 2000E (Alpha Technologies) according to ISO 289-1.

Payne effect measurements were done using the RPA 2000 before and after vulcanization for  $1.2 \times t_{90}$  at 160 °C, also in the RPA. For determination of the Payne effect, the values of the storage modulus at 1 % strain and 90 % strain were measured at 100 °C and at a frequency of 0.5 Hz.

In order to predict the rolling resistance, single point measurements of  $\tan \delta$  at 60 °C and 6 % strain were performed on the RPA 2000, after vulcanization for  $1.2 \times t_{90}$  at 160 °C also in the RPA<sup>7</sup>.

Filler macrodispersion measurements were done using the visual microscopic inspection method with 100 x magnification according to ISO 11345, method C.

Dynamic mechanical analysis was performed in tension mode on a Metravib DMA 2000 dynamic spectrometer. The samples were cut from cured sheets of the rubber compounds. Temperature sweeps were performed in a range between -50 °C and 60 °C at a dynamic strain of 0.1 %, pre-strain of 2 % and a frequency of 10 Hz.

A Laboratory Abrasion Tester 100 (LAT 100, VMI Group) was used to estimate the wet skid resistance of the tire treads under conditions which better reflect the real conditions on the road; see Figure 4<sup>13</sup>. Wheel samples with a diameter of 80 mm were made by compression molding in a special mold using the Wickert laboratory vulcanization press for 11 minutes at 170 °C. Testing was performed at five different water temperatures: 2 °C, 8 °C, 15 °C, 22 °C, 30 °C, and at a constant slip angle of 15°. An electro-corundum disc with a diameter of 350 mm and relative roughness of 180 was used to simulate road contact. Tests were performed at a constant speed of 1.5 km/h and a load of 75 N for a distance of 33 meters. The Side Force Coefficient (SFC) values for the particular samples were calculated according to Equation 3 and compared to the reference value obtained for the sample TESPT 7, expressed as relative values. The given property with a higher rating is better.

$$SFC = \frac{F_y}{F_z}$$

(Equation 3)

In Equation 3,  $F_z$  and  $F_y$  are the applied load and side force respectively: see Figure 4.

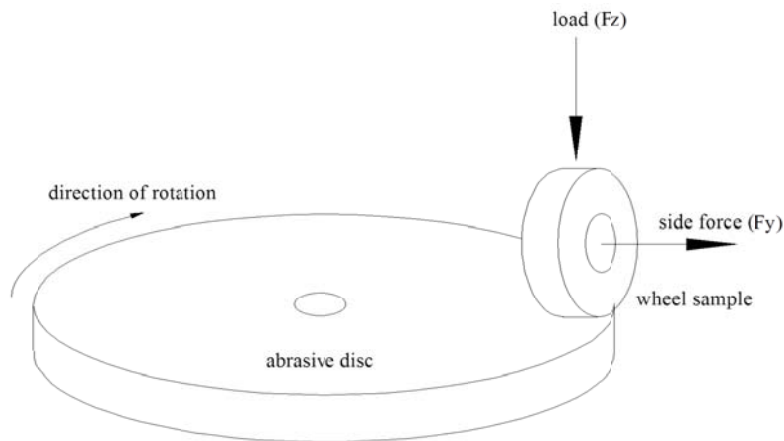


Figure 4: Measuring principle of the LAT100.

## 5.3 RESULTS AND DISCUSSION

### 5.3.1 Bound rubber

Results of the bound rubber test are shown in Figure 5. Batches containing TESPT are characterized by higher values of both, total as well as chemically bound rubber, in comparison to DMESPT containing samples. For a specific type of filler, the chemically bound rubber value can be used to describe the reactivity and sulfur donor ability of a silane coupling agent. At elevated temperatures, which occur during the second mixing stage, a sulfur containing silane can donate sulfur which can lead to scorch<sup>14</sup>, or establish already a bond to the polymer.

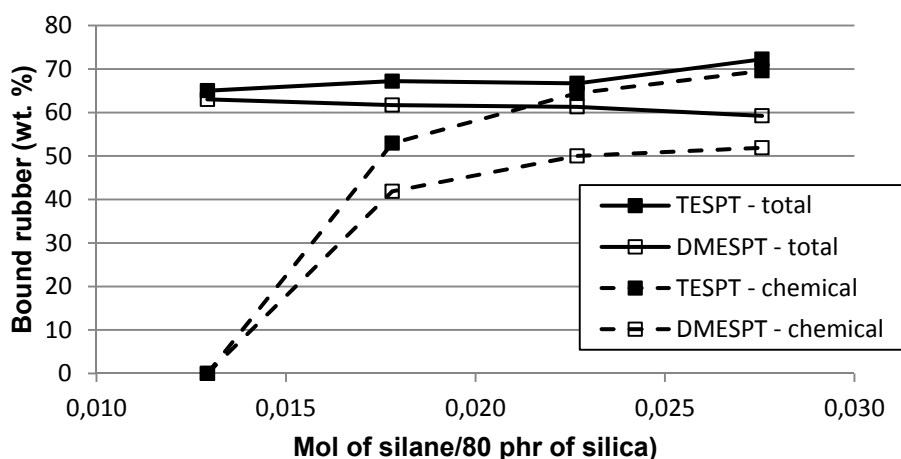


Figure 5: Bound rubber contents of TESPT and DMESPT containing compounds.

The sulfur donation ability of a coupling agent increases with the average sulfur rank of a silane for ranks higher than 1: the higher the sulfur rank, the less stable is the silane during compound preparation, resulting in a higher scorch risk<sup>15</sup>. Differences in bound rubber values between the coupling agents can be explained by the difference in average sulfur rank. The average sulfur rank for TESPT is 3.7, which is higher than for DMESPT with an average sulfur rank of 2.7. Therefore compounds with TESPT are more prone to a scorch reaction during the mixing process than the DMESPT containing compounds, what can also be seen in the Mooney viscosity values; see Figure 6. The sample containing 14.4 phr TESPT shows an extraordinarily high viscosity, caused by a scorch reaction due to the high sulfur-content of this compound from the high silane-dosage.

### 5.3.2 Mooney viscosity

Silica compounds present considerable disadvantages in processing in comparison to carbon black. These difficulties include short scorch times, environmental problems related to alcohol evolution, and higher compound Mooney viscosities. The high viscosity and poor processability of the silica filled rubber compounds are associated with silica reagglomeration after compound preparation<sup>1,16</sup>. Although both silanes use one ethoxy group to form bonds with the surface silanol groups of silica, the missing lateral, polar ethoxy groups in the DMESPT molecule reduces the hydrophilic character of the silica surface to a higher extent compared to TESPT. The

lower polarity of the silica surface leads to suppressed filler reagglomeration followed by lower Mooney viscosity of the compounds containing DMESPT.

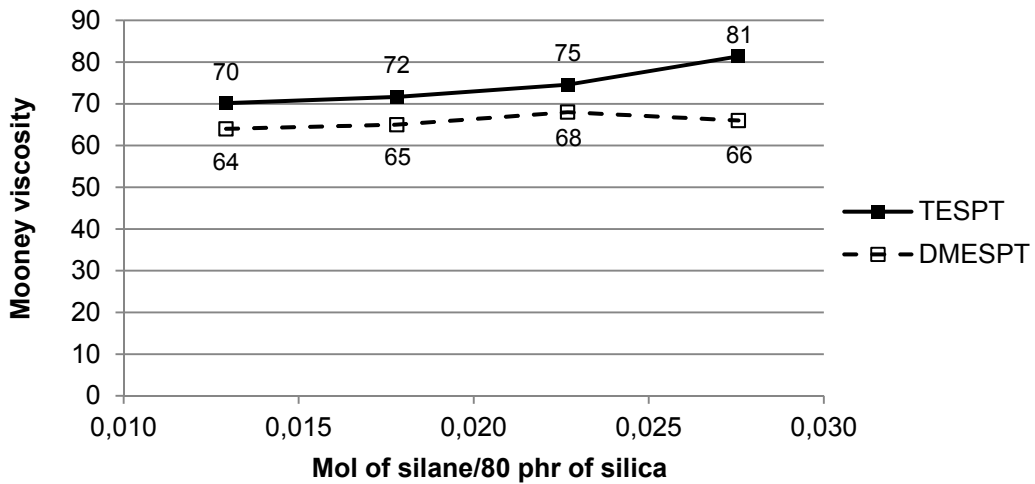


Figure 6: Mooney viscosity of the batches.

### 5.3.3 Payne effect

At a sufficiently high loading, the filler particles in the elastomer matrix form a secondary filler-filler network yielding reinforcement well beyond the hydrodynamic effect. This filler-filler network is progressively broken with increasing strain amplitude, and the consequent reduction in modulus is commonly referred to as the Payne effect <sup>17</sup>. Apart from the filler-filler network, the polymer-filler interaction also has its contribution to the Payne effect value in the vulcanized state. At equilibrium, elastomer chains are adsorbed onto the filler surface. When strain increases, it induces a progressive extension of elastomer chain segments which bridge filler particles as depicted in Figure 7. This extension is much larger than macroscopic deformation because of strain amplification. At very low strain values, the macroscopic deformation energy is stored in elongated chains as elastic energy and can therefore be fully recovered when the strain is released.

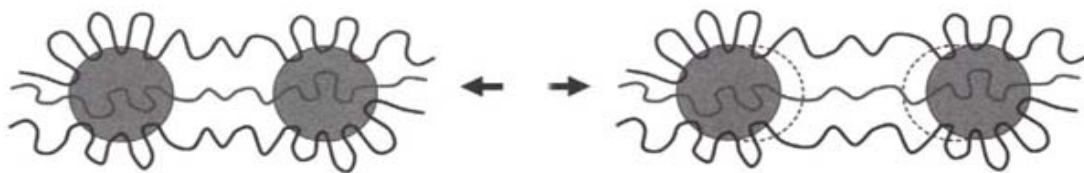


Figure 7: Filler particles and elastic polymer extension at low strain amplitude <sup>18</sup>.

Along with progressing strain amplitudes, the stored elastic energy overcomes the adsorption energy and causes gradual desorption of the elastomer chains. The storage modulus decreases because part of the initially elastic energy stored in deformed chains is converted into molecular mobility and mechanically lost as depicted in Figure 8 <sup>18</sup>.

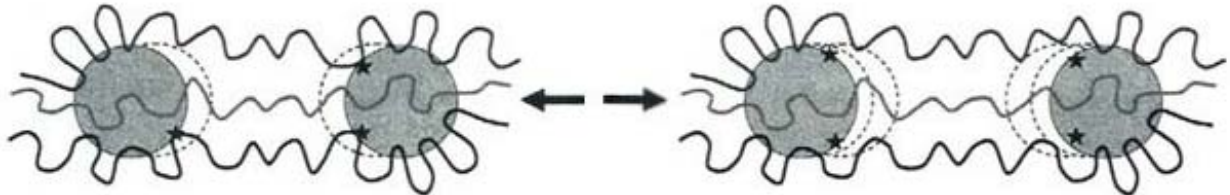


Figure 8: Filler particles at high strain amplitude <sup>18</sup>.

The higher the bond density of the elastomer chains on the silica surface, the higher the storage modulus at high strains. The influence of the polymer-silica bonds is obvious when the Payne effect values before and after curing are compared; see Figure 9 and Figure 10. Two phenomena occurring during the vulcanization lead to an increase of the Payne effect: Firstly, formation of the polymer-crosslinks increases the low strain storage modulus. Secondly, the curing process also binds the polymer chains to the filler surface via the coupling agent. Strong filler-polymer bonds are able to withstand higher deformations, what contributes to increased values of the storage modulus at highest strain amplitudes <sup>19</sup>.

In the unvulcanized state, there is no clear trend in the Payne effect values; see Figure 9. The filler-filler interaction is not significantly influenced neither by the silane concentration nor by the type of silane. At this stage, polymer-crosslinks and linkages between filler surface and polymer chains are not yet formed, resulting in low values compared to the Payne effect in the cured state as seen in Figure 10. This also suggests that DMESPT, despite its lower steric hindrance, does not lead to increased use of the silanol groups on the silica surface: similar Payne effect values, thus comparable filler-filler interaction is an indication of equal silanol group density.

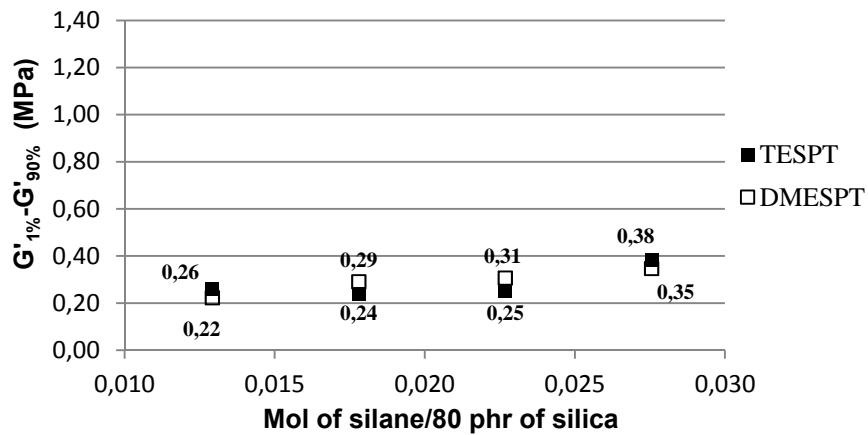


Figure 9: Payne effect for the TESPT and DMESPT containing compounds – before vulcanization.

After vulcanization, differences between the two coupling agents become more pronounced, see Figure 10: the Payne effect of the material containing DMESPT is higher than the Payne effect of the rubber containing the reference silane TESPT. Due to the sulfur adjustment, the differences in crosslink densities can be ruled out as a potential cause of the higher Payne effect values of the compounds with DMESPT silane.

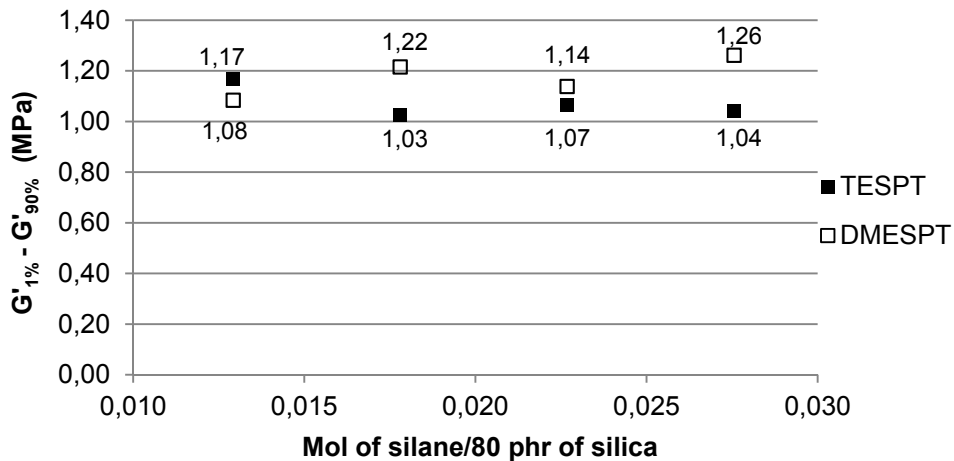


Figure 10: Payne effect for the TESPT and DMESPT containing compounds – after vulcanization

Diminishing differences in the values of the storage modulus at highest strain amplitudes, see Figure 11, suggest that bonds formed by DMESPT do not differ in strength from bonds formed by TESPT, so again this cannot explain the differences

between the two materials. A possible explanation of the lower values of the Payne effect for the TESPT containing compounds may be in the ability of this silane to form bonds in a secondary silanization reaction. Before the reaction with silane, the silica surface is covered with silanol groups; dependent on the analysis technique there may be up to 7 SiOH-groups per square nanometer of the silica surface <sup>1,2</sup>. In the case of TESPT, there is still a substantial number of unreacted lateral ethoxy groups after the primary silanization reaction, which occurs during mixing. During the vulcanization stage under the influence of high temperatures, these lateral ethoxy groups can further condensate and generate ethanol, which acts as an interface plasticizer, see Figure 12 on the right hand side. Rearrangement or desorption of the polymer chains at such a “soft” filler-polymer interface leads to a lower storage modulus in the case of TESPT. Lack of the lateral ethoxy groups in the case of DMESPT blocks this silane to undergo a secondary silanization reaction, which leads to a stiffer polymer-filler interphase and thus a higher storage modulus at low strains, see Figure 12 on the left hand side.

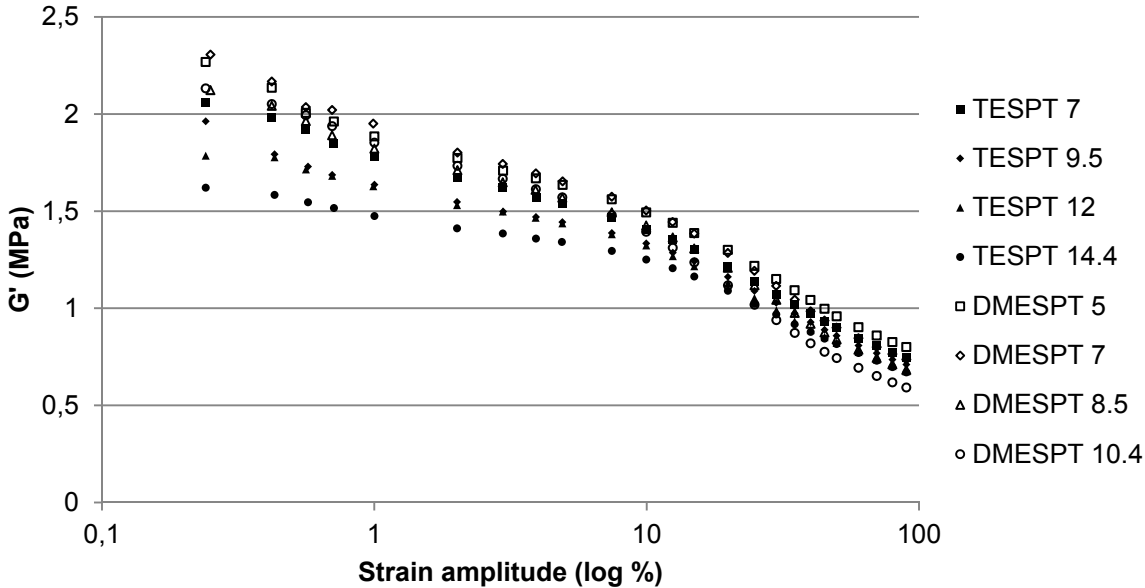


Figure 11: Storage modulus versus strain for TESPT and DMESPT containing compounds.

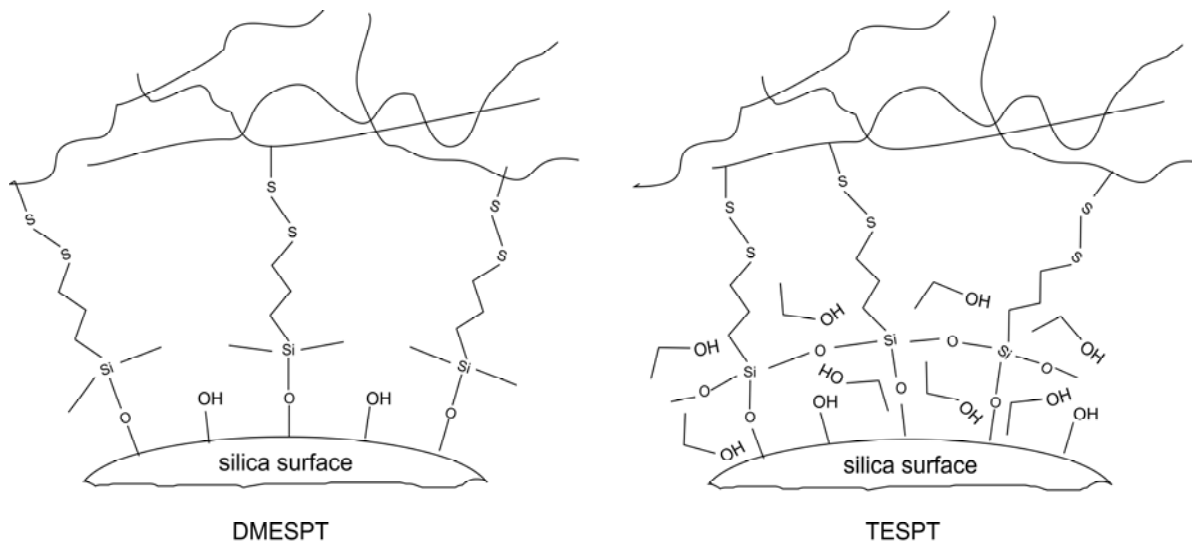


Figure 12: Pictorial view of the silica surface after treatment with TESPT and DMESPT.

#### 5.3.4 $\tan \delta$ values at 60 °C: indication of rolling resistance

The  $\tan \delta$  values at 60 °C as indication of rolling resistance are shown in Figure 13. A lower value of  $\tan \delta$  corresponds to lower rolling resistance, when this material is used in the tread of a tire. Concentrations of TESPT higher than the commonly used loading of 7 phr do not result in changes in the hysteresis, as saturation of the silica surface occurs at 7 phr, and further increase of the silane loading does not lead to changes in the filler-polymer interaction. However, due to the scorchiness of the sample with the highest TESPT loading of 14.4 phr, a decrease of the  $\tan \delta$  value is observed: polymer network formation occurs, increasing the elasticity of the material.

The difference in  $\tan \delta$  values between the TESPT and DMESPT containing material is based on the same phenomenon as the difference in storage modulus. As explained above, the main difference is the occurrence of the secondary reaction in the case of TESPT, resulting in generation of ethanol which is accumulated at the interface and results in an increased energy loss due to rearrangements on the filler surface.



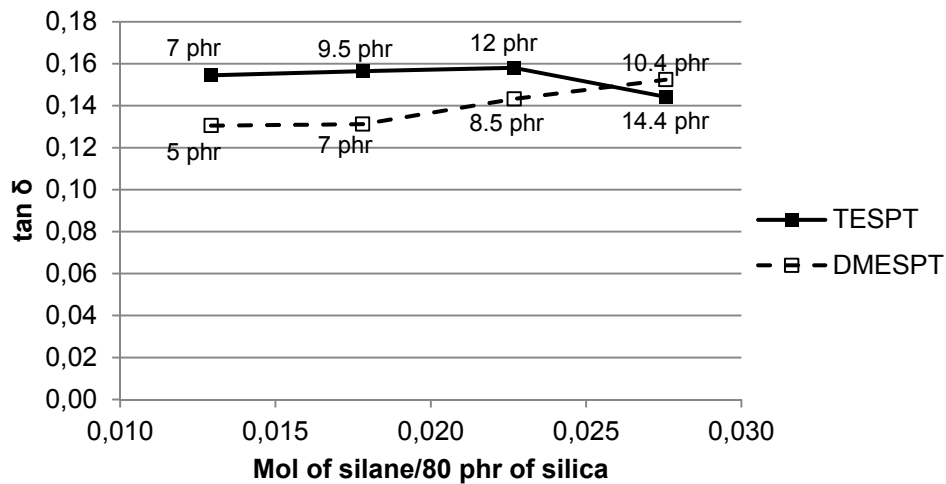


Figure 13: Differences in  $\tan \delta$  values at 60 °C as indication of rolling resistance for the triethoxysilane (TESPT) and monoethoxysilane (DMESPT) containing compounds.

Apart from the higher stiffness of the polymer-filler interface, filler macrodispersion is another contributing factor to the hysteresis at higher temperatures. Reduced polarity of the silica surface in the case of DMESPT containing compounds causes a higher degree of filler macrodispersion, see Figure 14. Better dispersed silica particles lead to less interparticle friction, hence less energy is lost during dynamic deformation of the compound.

The  $\tan \delta$  values are more discriminating for the DMESPT concentration than the storage modulus values. With a rising amount of DMESPT, the values of  $\tan \delta$  at 60 °C increase: With an increasing loading of DMESPT, a higher concentration of unreacted silane is expected. This unreacted silane condenses further what finally leads to more ethanol at the silica surface like in the case of TESPT.

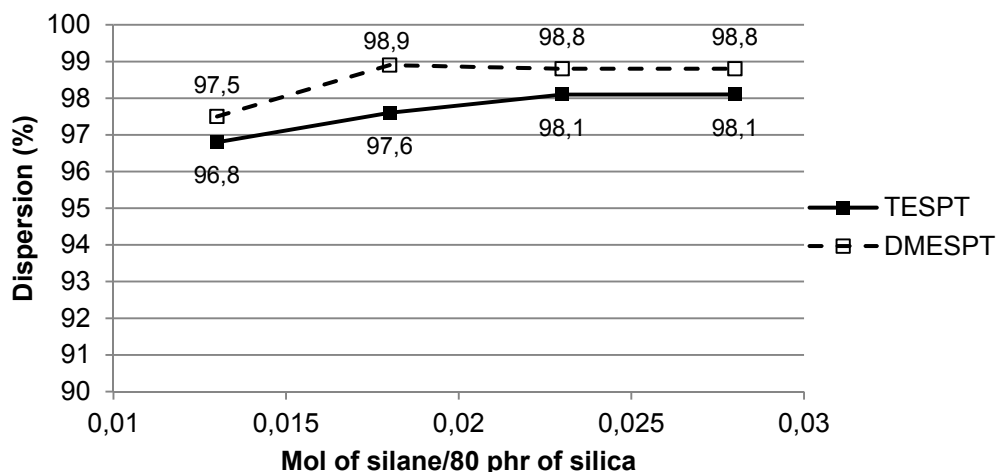


Figure 14: Macrodispersion of the TESPT and DMESPT containing vulcanizates.

### 5.3.5 *Tan δ at low temperatures: indicator of wet skid resistance*

When equimolar concentrations of both silanes are compared, the hysteresis of the compounds containing the monoethoxy silane is lower compared to the hysteresis of the TESPT containing compounds in the lower temperature range, as can be seen in Figure 15. This behavior is similar to what is observed when silica's with different specific surface areas are compared; see Chapter 3. Silica's with a higher specific surface area reduce the height of the  $\tan \delta$  peak, but are also characterized by higher values of the side force coefficient, as illustrated in Figure 16 and Figure 17. In this series of experiments, the silica concentration was also adjusted for equal hardness; samples II-80 and II-195. Additionally, equal Payne effect values were measured indicating similar filler-filler interactions<sup>20</sup>.

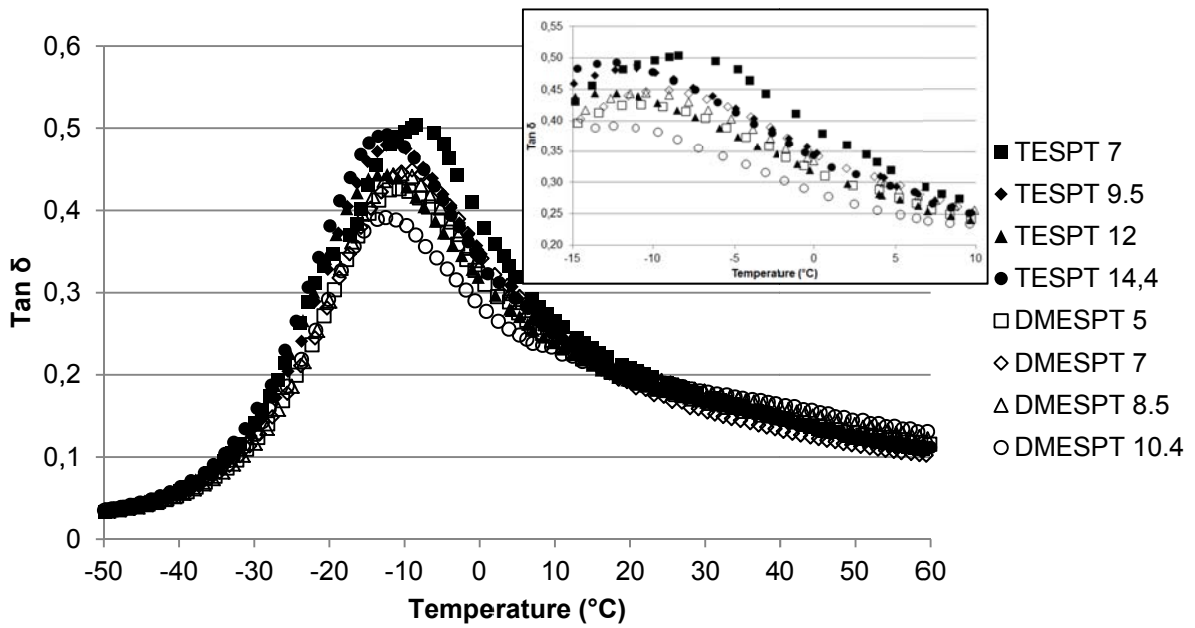


Figure 15:  $\tan \delta$  versus temperature measured at 1% static and 0.1% dynamic strain for the compounds containing different concentrations of TESPT and DMESPT.

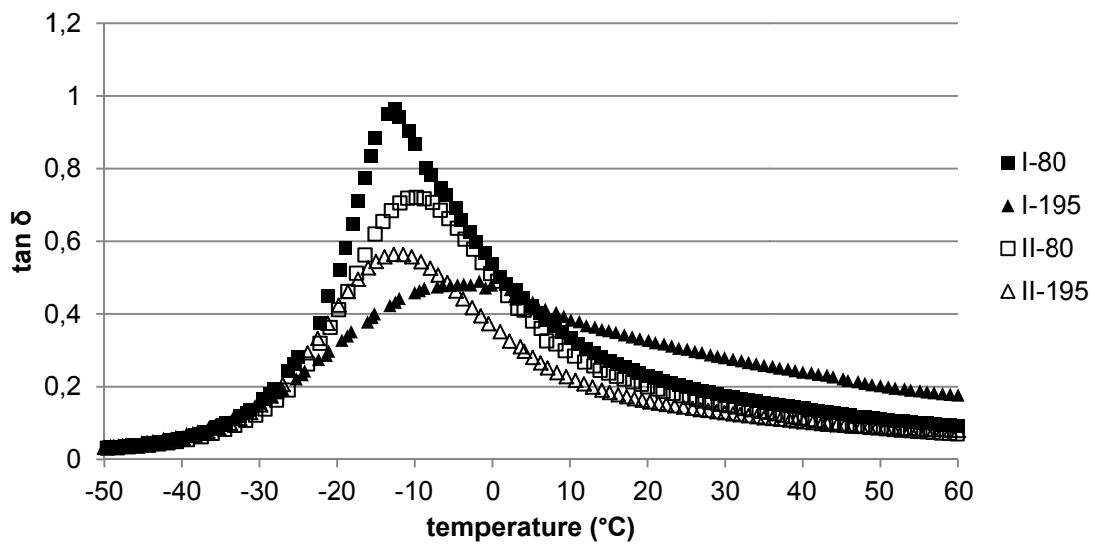


Figure 16:  $\tan \delta$  versus temperature measured at 1% static and 0.1% dynamic strain for the compounds containing two silica types differing in CTAB surface area.

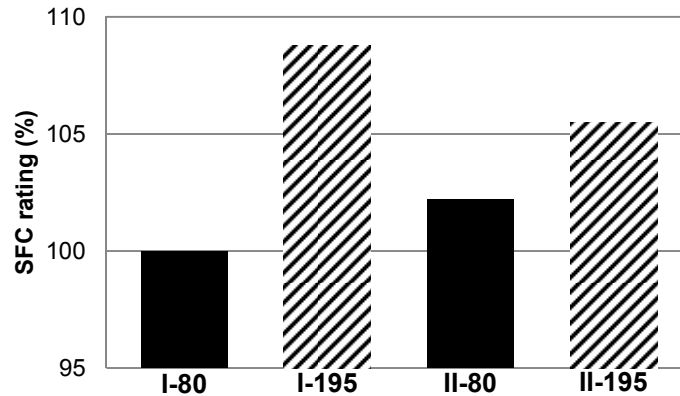


Figure 17: Side force coefficient for the silica's with different CTAB surface area.

The effect of reduced height of the  $\tan \delta$  peak is caused by more restricted movements of the polymer chains on the surface of silica types with a higher specific surface area - formation of a glassy layer. The same effect of decreasing height of the  $\tan \delta$  peak is also observed when silica or carbon black filled rubber is compared with unfilled compounds<sup>21,22</sup>. Based on these different studies, it can be generally concluded that the maximum of the  $\tan \delta$  curve is decreasing in height with increasing stiffness of the glassy layer. As this decrease in the  $\tan \delta$  peak value is observed here as well when replacing TESPT by DMESPT, this supports the assumption of more restricted polymer chain movements caused by a decreased amount of ethanol in the interface between polymer and filler in the case of DMESPT.

### **5.3.6 LAT 100 side force coefficient: indicator for wet skid resistance**

Unlike for TESPT, for DMESPT the SFC as indicator for wet skid resistance is dependent on the silane concentration within the range of this study, as seen in Figure 18. More restricted polymer movements in the glassy layer, as explained above, cause lower values of  $\tan \delta$  for the compounds with DMESPT, as seen in Figure 15. This indicates a higher degree of immobilization in the lower temperature range and stiffening of the interface in the case of DMESPT. However the results as presented in Figure 18 indicate that the SFC increases with rising concentration of DMESPT, contrary to TESPT. Micro-asperities existing on the surface of the road, or equally on the abrasive disk in the LAT 100 test, cause high strain deformations on

micro scale. The stiffer the interface between filler surface and elastomer, the higher the force required for this deformation. Hence, a higher local stiffness around the filler particles with high DMESPT concentrations results in higher wet skid resistance. Compounds containing TESPT are characterized by equal stiffness at lower temperatures, therefore the side force coefficient values do not undergo substantial changes.

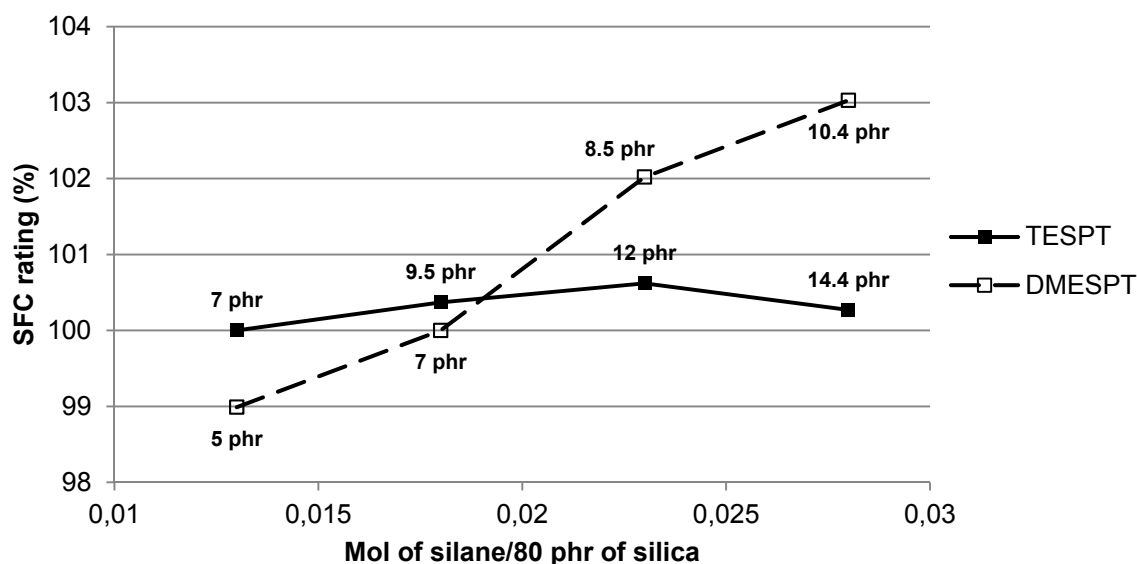


Figure 18: Correlation between side force coefficient and silane concentration as an indication for wet skid resistance for DMESPT and TESPT containing compounds.

## 5.4 CONCLUSIONS

- Using just one ethoxy group instead of three in the silane coupling agent, improves both, wet skid and rolling resistance. An explanation of these effects is a more rigid filler-polymer interface in the case of DMESPT, compared to TESPT with three ethoxy groups, which generate ethanol. The alcohol remains adsorbed on the interface between filler and polymer and thus influences the properties of the material.
- Both silanes, TESPT and DMESPT, bind the same number of silanol groups available on the silica surface as measured by the Payne effect of the green compounds. Therefore, low steric hindrance caused by absence of lateral ethoxy groups in the DMESPT molecule is not followed by a higher number of bonded silanol groups than in the case of TESPT.

- The filler-polymer interactions determine the peak height of the  $\tan \delta = f(T)$  curve: the more restricted the polymer movements on the filler surface, the lower the height of the peak, as the immobilized polymer acts more filler-like than polymer-like. In the case of DMESPT, the polymer-filler interface is more rigid in comparison to TESPT: The latter possesses secondary ethoxy groups, which react when the material is heated up during further processing, and splits off ethanol which is accumulated in the interface, softening the interface and thus increasing the energy loss (indicated by  $\tan \delta$ ) by desorption and sliding of polymer chains at lower temperatures.
- Contrary to TESPT, for DMESPT the SFC of the samples increases with rising loading of this silane. More restricted movements of the polymer chains in the glassy layer cause increased stiffness of the compounds containing DMESPT. A higher local stiffness around the filler particles with high DMESPT concentrations results in higher wet skid resistance as indicated by the SFC.

## REFERENCES

---

- [1] M. J. Wang, *Rubber Chem. Technol.* 71 (1998) 520.
- [2] A. P. Legrand, H. Hommel, A. Tuel, A. Vidal, *Adv. Coll. Interf. Sci.* 33 (1990) 91.
- [3] S. Wolff, 1<sup>st</sup> Franco-German Rubber Symposium, November 14-16<sup>th</sup> 1985, Obernai, France.
- [4] H. D. Luginsland, A. Hasse, 157<sup>th</sup> Technical meeting of the Rubber Division ACS, April 4-6<sup>th</sup> 2000, Dallas, Texas.
- [5] A. Blume, J. P. Gallas, M. Janik, F. Thibault-Starzyk, A. Vimont, *Kautsch. Gummi Kunstst.* 7-8 (2008) 359.
- [6] L. A. E. M. Reuvekamp, P. J. van Swaaij, J. W. M. Noordermeer, *Kautsch. Gummi Kunstst.* 63 (2009) 35.
- [7] L. A. E. M. Reuvekamp, "Reactive mixing of silica and rubber for tires and engine mounts", PhD Thesis: 2003, Dept. of Rubber Technology, Univ. of Twente, Enschede, the Netherlands ISBN 90 365 1856 3.
- [8] R. Rauline, European Union Patent No. EP0501227B1, (1992), to Michelin Co.
- [9] L. Guy, Ph. Cochet, Y. Bomal, S. Daudey, *Kautsch. Gummi Kunstst.* 63 (2009) 383.
- [10] S. Wolff, M.-J. Wang, E.-H. Tan, *Rubber Chem. Technol.* 66 (1993) 163.
- [11] S. Wolff, *Rubber Chem. Technol.* 69 (1996) 325.
- [12] K. E. Polmanteer, C. W. Lentz, *Rubber Chem. Technol.* 48 (1975) 795.
- [13] M. Heinz, *J. Rubb. Res.* 13 (2010) 91.
- [14] L. A. E. M. Reuvekamp, J. W. ten Brinke, P. J. van Swaaij, J. W. M. Noordermeer, *Rubber Chem. Technol.* 75 (2002) 187.
- [15] H. D. Luginsland, *Kautsch. Gummi Kunstst.* 53 (2000) 10.
- [16] J. Mewis, *Adv. Colloid Interface Sci.* 37 (1976) 132.
- [17] A. R. Payne, *J. Appl. Polym. Sci.* 6 (1962) 57.
- [18] J. B. Donnet, E. Custodero, *Reinforcement of Elastomers by Particulate Fillers., Science and Technology of Rubber (Third Edition), 2005, Pages 367-400*
- [19] J. Fröhlich, H.D. Luginsland, *Rubber World* 4 (2001) 28.
- [20] A. R. Payne, R. E. Whittaker, *Rubber Chem. Technol.* 44 (1971) 440.
- [21] M. M. Jacobi, M. V. Braum, T. L. A. C. Rocha, R. H. Schuster, *Kautsch. Gummi Kunstst.* 60 (2007) 460.
- [22] M. J. Wang, *Kautsch. Gummi Kunstst.* 60 (2007) 438.





---

### ***Modification of the silane coupling agent for improvement of wet traction and rolling resistance: Influence of the length of the aliphatic linker***

---

*The European tire manufacturers for the passenger car market have changed to the almost exclusive use of silica-silane technology for the treads. Next to the silica and polymer types, the chemical configuration of the silane coupling agent plays an important role in the final properties of the tire tread materials. The silane coupling agent comprises three building blocks: commonly a trialkoxysilyl moiety which reacts with the silica surface, a polysulfide moiety which reacts with the double bonds of a polymer, and a hydrocarbon chain connecting the two moieties. The influence of the alkoxy-silyl- and sulfide-moieties on the wet skid- and rolling resistance-related properties were discussed in Chapters 4 and 5; this chapter deals with the hydrocarbon chain or simply the linker within the silane coupling agent.*

*In order to investigate the influence of the linker length on the wet skid and rolling resistance indicators, a silane with a decyl-linker, bis-(triethoxysilyldecyl)-tetrasulfide (TESDeT), was compared with bis-(triethoxysilylpropyl) tetrasulfide (TESPT) on equimolar basis. The study shows that a longer linker lowers the hysteresis at elevated temperatures, corresponding to a lower energy loss at the service temperature of a running tire. Simultaneously, the silane with a longer linker increases the hysteresis in the temperature range close to the glass transition of the elastomer blend. However, no substantial difference in the wet skid performance indicator could be recorded between the two investigated silanes, using the Side Force Coefficient on a LAT 100 apparatus.*

## 6.1 INTRODUCTION

Because of their reduced rolling resistance (RR) and improved wet skid resistance (WSR), tire treads of passenger cars in Europe are nowadays almost exclusively produced with the use of silica instead of carbon black as filler. The key element in this technology is the coupling agent, a silane, which chemically couples silica to the polymer. The chemical structure of the silane determines the polymer-filler interactions, which on their turn influence wet skid and rolling resistance. The goal of the present study is to elaborate the underlying mechanisms of rubber-filler interaction determining the wet skid and rolling resistance of tires, a dynamic viscoelastic phenomenon. Dynamic properties of the rubber vulcanizates are directly related to wet skid and rolling resistance of the tire tread <sup>1,2,3,4</sup>. The structure of the coupling agent has a strong influence on the dynamic properties and therefore is the main subject of this chapter.

The effect of a progressively decreasing storage modulus with increasing amplitude of applied strain, a phenomenon related to filler-filler interactions, was investigated by Payne <sup>5,6</sup>. According to investigations described by Fröhlich, Luginsland <sup>7,8</sup> and Stelandre <sup>9</sup>, the magnitude of the Payne effect decreased with increasing length of the alkyl pending group of silane shielding/covering agents – a silane without sulfur moiety, which therefore cannot couple to a rubber molecule, see Figure 1. Ten Brinke et al. <sup>10</sup> studied silane covering agents, which are similar in structure to bis-(triethoxysilylpropyl)tetrasulfide (TESPT), but without sulfur and differing in the length of the aliphatic linker. In their investigation, the decrease of the of storage modulus values with increasing linker length was less significant than in the case of silanes with long pending groups. The observed effects in both cases were related to a higher degree of hydrophobation of the silica surface by the covering agent with a longer pending group or linker.

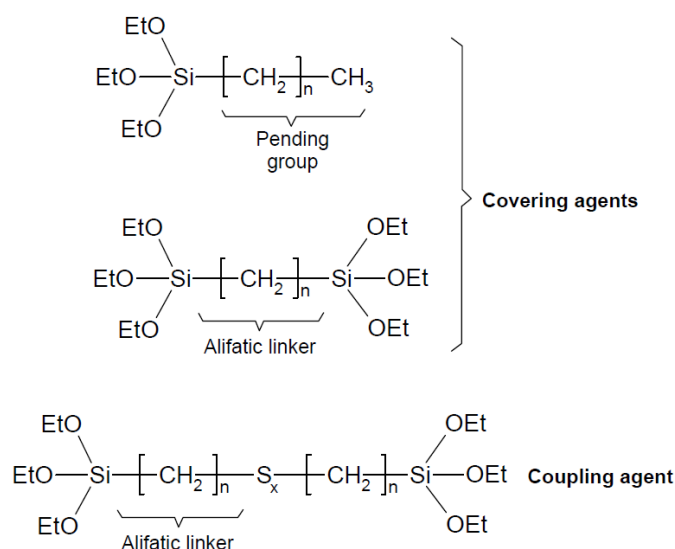


Figure 1: Differences between pending group and linker of the covering and coupling agent.

The silica surface covered by a more complete and thicker shell of silane results in a less developed filler network, hence suppressed filler-filler interactions to a higher degree. A covering agent however, cannot form chemical bonds between the filler and the polymer, reflected in inferior mechanical properties of the vulcanizates in comparison with a coupling agent. Klockmann<sup>11,12</sup> described coupling agents with long adjacent pending groups, nevertheless the bonding to the polymer chain was realized by a propylene group like in the commonly used organosilane coupling agents such as TESPT. In-depth knowledge about the influence of the linker which bonds filler and polymer on the compound properties is still lacking.

The investigation of the above mentioned phenomena and their effect on the dynamic properties requires a silane with a longer linker between the silyl-group and the sulfur-moiety. Bis-(triethoxysilyldecyl)tetrasulfide (TESDeT) with a C<sub>10</sub>-group is applied, and it is expected to make the silica-rubber interphase more flexible, easier deformable, but still with chemical coupling to the polymer chains.

The influence of the silica-polymer interface structure on wet skid performance is investigated by testing the dynamic properties of compounds, in particular the  $\tan \delta$  in the temperature range from 0 – 20 °C at 10 Hz. The values of the loss tangent in this temperature range are a commonly accepted indication of wet skid performance of a tire tread<sup>13</sup>. Additionally, a WSR indicator simulating real road conditions much better than mere dynamic analysis, is also used: the Laboratory Abrasion Tester 100 (LAT 100) (see Chapter 3)<sup>14</sup>. Other tire related properties such as:  $\tan \delta$  at 60 °C,

mechanical properties, abrasion resistance, Payne effect are also investigated in this study.

## 6.2 EXPERIMENTAL

The structures of the two silanes used in this part of the study, TESPT and TESDeT, are shown in Figure 2.

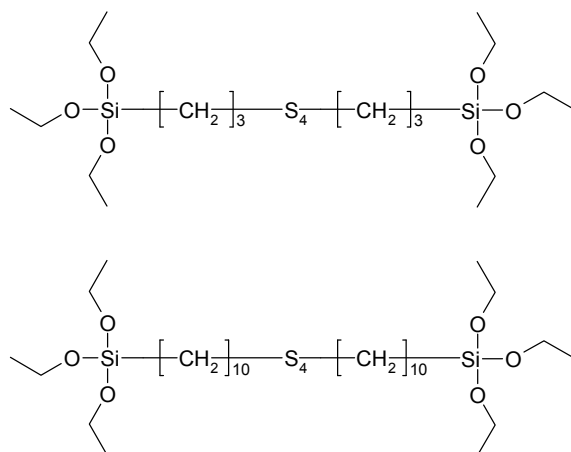


Figure 2: Structure of bis-(triethoxysilylpropyl) tetrasulfide (TESPT) and bis-(triethoxysilyldecyl) tetrasulfide (TESDeT).

In the modified silane, TESDeT in Figure 2, the length of the aliphatic linker between the silicon and the sulfur atoms is increased from propyl to decyl. This modification should result in a better hydrophobation of the silica surface due to the longer apolar hydrocarbon chain in the molecule and a more flexible polymer-filler interphase, but with the chemical bonding to the polymer remaining unchanged. The reference silane, TESPT, was commercially obtained from Evonik GmbH; and TESDeT was synthesized as described below.

### 6.2.1 Preparation of bis-(triethoxysilyldecyl) tetrasulfide

*Bis-(triethoxysilyldecyl) tetrasulfide (TESDeT)* was synthesized in a two-step reaction. During the first step, 10-bromodecyl triethoxysilane was synthesized: A mixture of 10-bromo-1-decene (Synthon Chemicals GmbH & Co. KG, Wolfen, Germany) triethoxysilane (TCI Europe, Zwijndrecht, Belgium) and a chloroplatinic acid (Sigma Aldrich, Zwijndrecht, The Netherlands) catalyst in absolute ethanol were stirred under a dry nitrogen flow for 24 hours at room temperature. Under these circumstances, the

reaction as shown in Figure 3 takes place. The unreacted triethoxysilane was removed in a rotary evaporator. The remaining liquid was a colorless product, 10-bromodecyl triethoxysilane, in a yield of 84 % and a purity of 98 % as determined by Liquid Chromatography - Mass Spectroscopy (LC-MS, Agilent-1100/Bruker-Esquire 3000 Plus). The product structure was also determined with the aid of LC-MS. The mass calculated for  $C_{16}H_{35}O_3SiBrH^+$  is 384,08 g/mol; the mass found by LC-MS was 384,82 g/mol.

During the second step of the reaction, as shown in Figure 3, 10-bromodecyl triethoxysilane was refluxed in anhydrous ethanol with sodium tetrasulfide (Sigma Aldrich, Zwijndrecht, The Netherlands). After 5 hours of refluxing, the color of the suspension changed from dark red to yellow. This suspension was filtered and ethanol was removed from the filtrate in a rotary evaporator leading to a dark red suspension, which was then diluted with diethyl ether. The ether phase was extracted with water until no coloration of the water phase was noticed any more. The ether extract was dried with anhydrous  $MgSO_4$ , filtered, and ether was removed in a rotary evaporator.

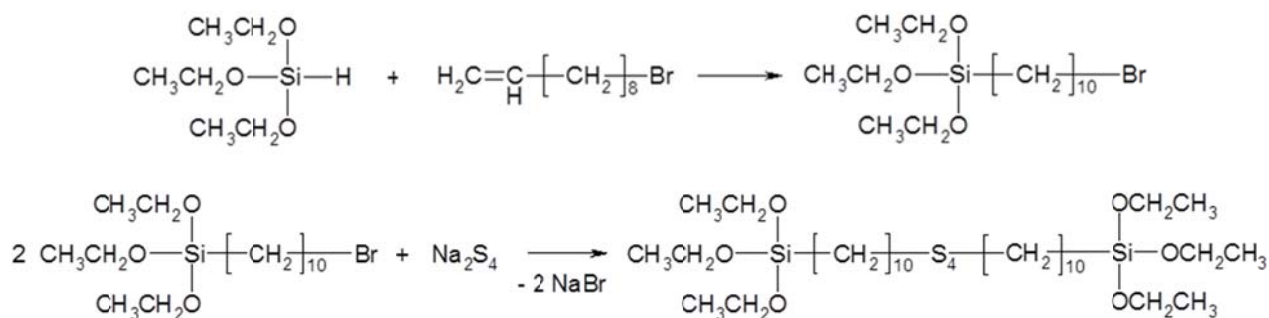


Figure 3: Preparation of bis-(triethoxysilyldecyl) tetrasulfide.

Top: stage one, formation of 10-bromodecyl triethoxysilane.

Bottom: stage two, synthesis of bis-(triethoxysilyldecyl) tetrasulfide.

The yield was 81 % of a gold yellow clear liquid, bis-(triethoxysilyldecyl)-tetrasulfide. Structure and purity of this silane were determined by LC-MS according to the procedure specified in Tables II and III in Chapter 5. The purity was 96 % and the structure is given in Figure 4. An average sulfur rank of 3.5 and molar mass of 721 g/mol was calculated based on the MS-data. The index of refraction of the product at 22 °C was 1.5150.

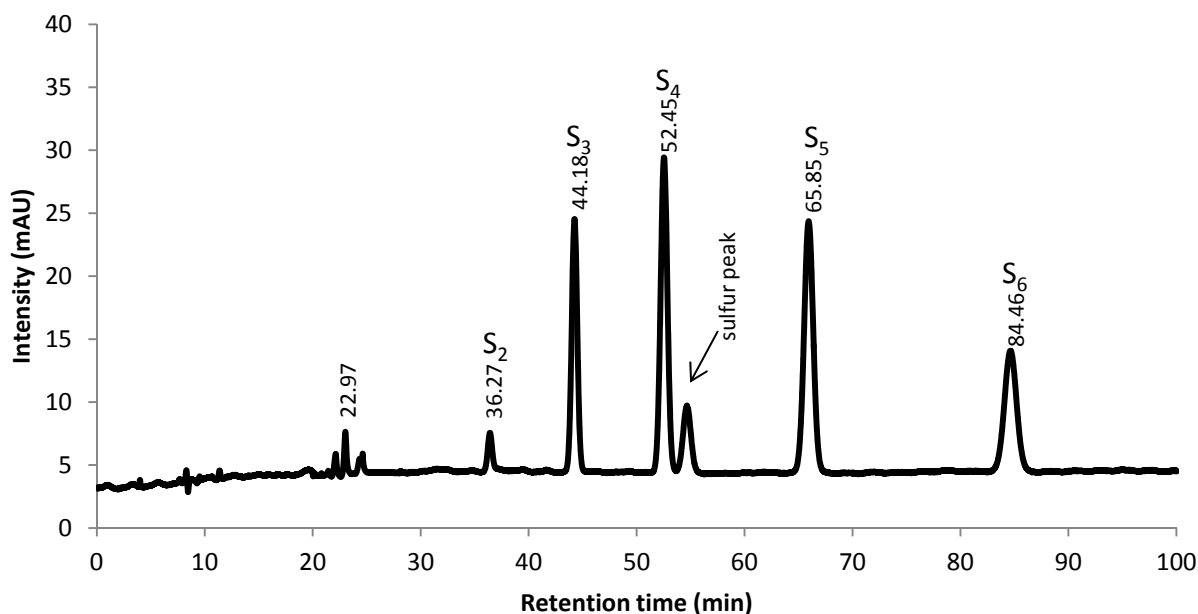


Figure 4: LC-MS chromatogram of TESDeT, the different sulfur ranks and free sulfur peak are indicated.

### 6.2.2 Mixing and curing

A test compound according to the ‘green tire’ recipe containing a highly-dispersible silica grade, Zeosil 1165 MP, which is commonly used in the tire industry, was used. The compound formulations are shown in Table I. A detailed specification of all ingredients was shown in Table IV in Chapter 5.

Table I: Rubber compound formulations

| Ingredient      | Sample code |           |          |            |             |            |              |              |
|-----------------|-------------|-----------|----------|------------|-------------|------------|--------------|--------------|
|                 | TESPT 7     | TESPT 9.5 | TESPT 12 | TESPT 14.4 | TESPDeT 9.5 | TESPDeT 13 | TESPDeT 16.8 | TESPDeT 20.5 |
| S-SBR           | 103         | 103       | 103      | 103        | 103         | 103        | 103          | 103          |
| BR              | 25          | 25        | 25       | 25         | 25          | 25         | 25           | 25           |
| Silica (1165MP) | 80          | 80        | 80       | 80         | 80          | 80         | 80           | 80           |
| TESPT           | 7           | 9,5       | 12       | 14,4       |             |            |              |              |
| TESDeT          |             |           |          |            | 9,5         | 13         | 16,8         | 20,5         |
| TDAE            | 5           | 5         | 5        | 5          | 5           | 5          | 5            | 5            |
| Zinc oxide      | 2,5         | 2,5       | 2,5      | 2,5        | 2,5         | 2,5        | 2,5          | 2,5          |
| Stearic acid    | 2,5         | 2,5       | 2,5      | 2,5        | 2,5         | 2,5        | 2,5          | 2,5          |
| 6PPD            | 2           | 2         | 2        | 2          | 2           | 2          | 2            | 2            |
| TMQ             | 2           | 2         | 2        | 2          | 2           | 2          | 2            | 2            |
| Sulfur          | 1,4         | 0,8       | 0,24     | 0          | 1,5         | 1          | 0,4          | 0            |
| TBBS            | 1,7         | 1,7       | 1,7      | 1,7        | 1,7         | 1,7        | 1,7          | 1,7          |
| DPG             | 2           | 2         | 2        | 2          | 2           | 2          | 2            | 2            |

The two silanes were applied at four different concentrations equimolar to the concentration of the reference silane, TESPT, and with sulfur adjustment. The TESPT content was adjusted for the first - the reference compound - according to the CTAB specific surface area of the silica type by using the empirical equation proposed by L. Guy: Equation 1<sup>15</sup>. The amount of free sulfur added together with the curatives for all compounds was adjusted to keep the total molar amount including the sulfur contained in the coupling agent at a constant level in all batches.

$$TESPT (phr) = 5.3 \times 10^{-4} \times (CTAB)_{silica} \times (phr)_{silica}$$

(Equation 1)

To prepare the compounds, an internal laboratory mixer, Brabender 350 S with mixing volume of 390 cm<sup>3</sup>, was used. The mixing procedure was specified in Chapter 4, Table V. The total volume of each batch was adjusted to a fill factor of 70 %. Preparation of sheets for testing was done on a Schwabenthan Polymix 80T 300 ml two roll mill. The samples were cured in a Wickert press WLP 1600 at 160 °C to sheets with a thickness of 2 mm according to their t<sub>90</sub> optimum vulcanization times as determined in a Rubber Process Analyzer, RPA 2000, from Alpha Technologies.

### 6.2.3 Characterization methods

The Mooney viscosities ML(1+4) of the compounds were measured at 100 °C on a Mooney viscometer MV 2000E (Alpha Technologies) according to ISO 289-1.

Mechanical properties of the samples were tested using a Zwick Z020 tensile tester according to ISO-37 at a crosshead speed of 500 mm/min.

Abrasion resistance was measured with a DIN-abrader according to method A of DIN 53516. The weight loss was measured and recalculated to a volume loss for each sample.

Payne effect measurements were done by using the Rubber Process Analyzer (RPA 2000) after prior vulcanization for 1.2 x t<sub>90</sub> at 160 °C in the RPA. In order to estimate the Payne effect, the values of the storage modulus at 0,56 % strain and 100 % strain were measured at 100 °C and a frequency of 0.5 Hz.

The rolling resistance was assessed by measurement of the  $\tan \delta$  value at 60 °C and 6 % strain, measured on the Rubber Process Analyzer <sup>16</sup>.

Dynamic mechanical analysis was performed in tension mode on a Metravib DMA 2000 dynamic spectrometer. The samples were cut from cured sheets of the rubber compounds. For producing dynamic curves, measurements were performed at temperatures between -50 °C and +80 °C at a dynamic strain of 0.1% and a frequency of 10 Hz.

A Laboratory Abrasion Tester 100 (LAT 100, VMI Group) was used to estimate the wet skid resistance of the tire treads under conditions which better reflect the real conditions on the road; see Figure 10, Chapter 3 <sup>17</sup>. The Side Force Coefficient (SFC) values for the particular samples are calculated according to Equation 2 and compared to the reference value obtained for the sample TESPT 7, and given as relative values. The given property with higher rating is always better.

$$SFC = \frac{F_y}{F_z} \quad \text{Equation 2}$$

In Equation 2,  $F_y$  and  $F_z$  are the applied load and side force respectively: see Figure 10, Chapter 3.

## 6.3 RESULTS AND DISCUSSION

### 6.3.1 Mechanical properties

A pictorial view of the silica surface modified with TESDeT is shown in Figure 5. Since the decyl linker is much longer, it is also more flexible than the propyl linker of TESPT, and it can actually fold on the surface of silica forming more shell-like structures around the silica particles.



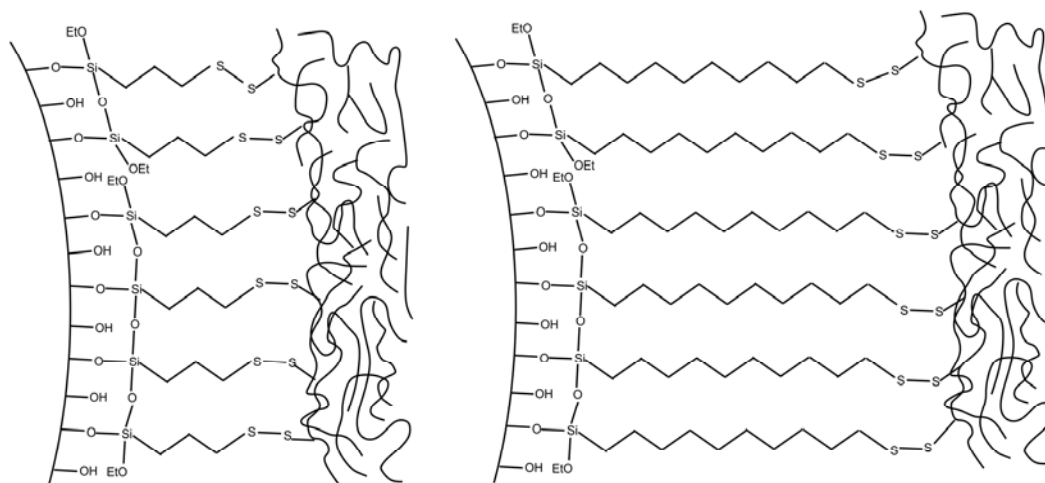


Figure 5: Pictorial structure of the silica surface covered with TESPT (left) and TESDeT (right).

A more flexible bonding between the silica surface and the polymer chains provided by the TESDeT silane does not have a major influence on the tensile strength of the vulcanizates, nor has the concentration of the coupling agent, except for the 20,5 phr of the TESDeT silane; see Figure 6. However, values of the elongation at break, Figure 7, show a small dependence on the silane concentration: With increasing concentration of both silanes, elongation at break decreases somewhat. The values of elongation at break of the compounds containing TESDeT are higher than the values of the TESPT-material. If at all relevant because of the relative accuracy in determining the elongation at break, this effect might be caused by the shorter linker in the TESPT molecule, thus the shorter filler-polymer bond. The load is transferred almost directly to the silica aggregate, leading to high stresses in the interface between polymer and filler and, as a consequence, crack formation and finally breakage of the sample. A longer and more flexible linker as in the case of TESDeT can accommodate higher strains without cracking, which results in a slightly higher value of elongation at break in comparison with the TESPT containing compounds.

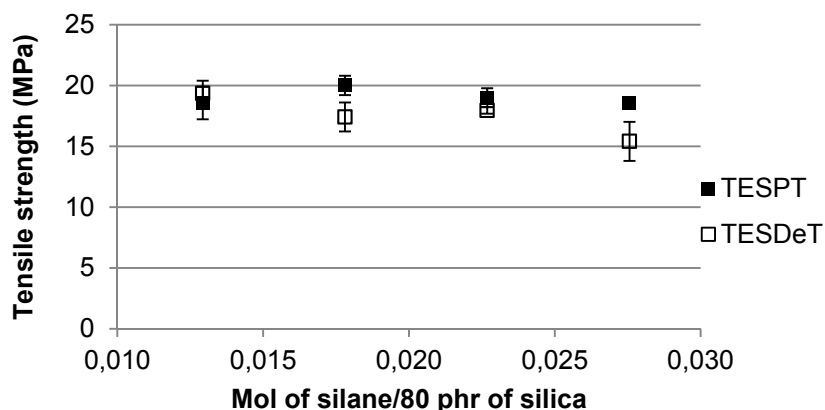


Figure 6: Tensile strength of TESPT and TESDeT containing materials.

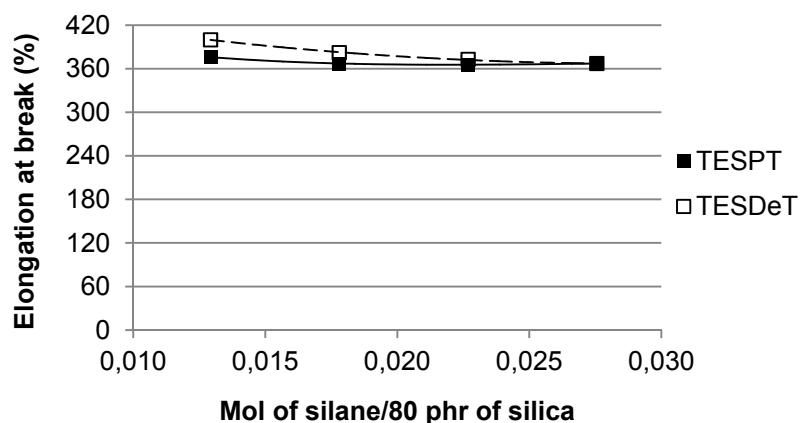


Figure 7: Elongation at break of TESPT and TESDeT containing materials.

### 6.3.2 Abrasion resistance

Abrasion resistance is an important property for tires, because it is directly related to service life. The abrasion properties of vulcanizates essentially depend on the glass transition temperature of the polymer. When the same polymer is used, the abrasion resistance depends on the filler, thus the silica-silane system. Interaction between rubber and filler or the adhesion characteristics of an elastomer are an important issue. When silica and a coupling agents are used, adhesion between the elastomer and the filler is better for a silica type with smaller aggregate sizes. Surface interaction between filler and rubber molecules or network segments comprises a range of bond energies from relatively weak van der Waals forces to very strong chemical bonds. It is generally accepted that more elastic vulcanizates are also characterized by higher abrasion resistance<sup>18</sup>. In this study, the values of abrasion

loss of the materials containing the different silanes are similar within the accuracy of the measurements, see Figure 8. An exception is the sample containing 20.5 phr of TESDeT, for which the abrasion loss is considerably higher than that of the TESPT counterpart - even when the general value of error of approximately 10 % for DIN abrasion is considered.

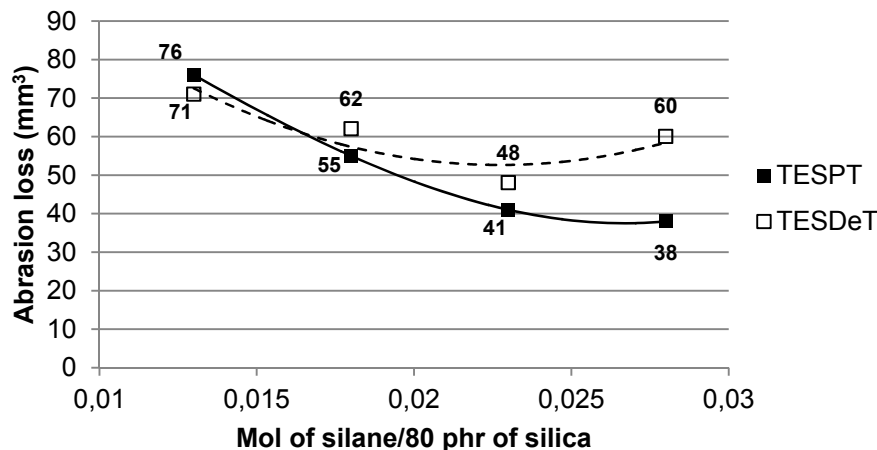


Figure 8: DIN abrasion of the samples containing TESPT and TESDeT silanes

The increased abrasion loss of the sample containing 20.5 phr of TESDeT might be the result of formation of a thick or multi-layer silane-shell around silica particles caused by the high molecular weight of the silane with the longer linker. As a consequence, weak physical silica-polymer interactions become dominant. This effect is similar to the case in which TESH was used, see Figure 6 in Chapter 4. In this extreme case it can lead to loosely bound polymer chains on the surface of the silica particles which deteriorates the integrity of the composite. A lower integrity is also visible in the lower value of tensile strength for the sample containing 20.5 phr of the TESDeT silane; compare with Figure 6.

### 6.3.3 Payne effect – filler-filler interactions

The reduction in storage modulus with increasing strain amplitude in a dynamic mechanical test is commonly referred to as the Payne effect <sup>19</sup>. Values of the Payne effect for both silanes are similar; see Figure 9. Like before, an exception is the sample containing 20.5 phr of TESDeT. An increased Payne effect can be the result of an increased crosslink density around the silica particles as explained in Chapter 5, or simply of higher filler-filler interactions. In case of the silane with the longer

linker, the explanation of increased filler-filler interactions is applicable, as there is no influence from the silane on the crosslink density.

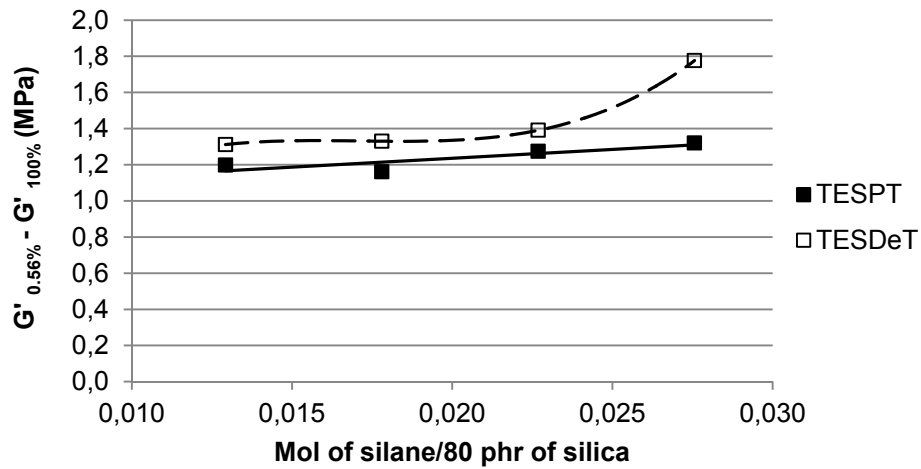


Figure 9: Payne effect of the TESPT and TESDeT containing cured compounds.

Because of its reactivity towards the silanol groups of the silica, both silanes are adsorbed onto the silica surface leading to the formation of a silane layer. In the unvulcanized state, the silane with decyl linker used at the highest loading of 20.5 phr, simply acts as a diluent or plasticizer what decreases the Mooney viscosity of this sample; see Figure 10. Low viscosity of the compound means lower restrictions of the silica particles in the polymer matrix and facilitation of flocculation which in turn leads to higher filler-filler interactions in the vulcanized state.

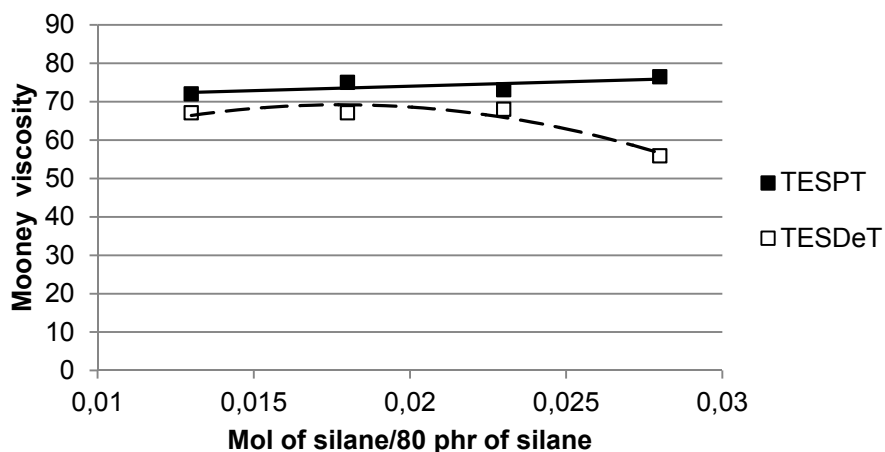


Figure 10: Mooney viscosity of the TESPT and TESDeT containing compounds.

### 6.3.4 $\tan \delta @ 60\text{ }^{\circ}\text{C}$ : indicator of rolling resistance

Increasing the length of the aliphatic linker from 3 to 10 carbon atoms causes a substantial drop in the  $\tan \delta$  value at  $60\text{ }^{\circ}\text{C}$  as shown in Figure 11. During the

dynamic deformation at elevated temperature and strain amplitudes, the energy losses are mainly the result of adsorption-desorption processes of the polymer chains on the filler surface. Due to the flexibility of the TESDeT linker, it can accommodate higher strain amplitudes within the filler-polymer interphase occurring during rolling, instead of transferring them directly onto the filler surface. A thicker layer of silane on the silica surface acts as a soft isolation between the filler surfaces. This in turn leads to less pronounced friction between the filler particles. The contribution of the polymer network in the energy transfer at higher temperatures and strain amplitudes is higher when TESDeT is used, as short, more rigid filler-polymer bonds like in the case of TESPT lead to a thinner silane shell around silica particles in which the polymer movements are more restricted.

Values of  $\tan \delta$  at 60 °C plotted against the molar concentration of TESPT and TESDeT are characterized by the same decreasing trends. That again can be explained by the increasing thickness of the above mentioned silane layer on the silica surface with rising concentration of both silanes.

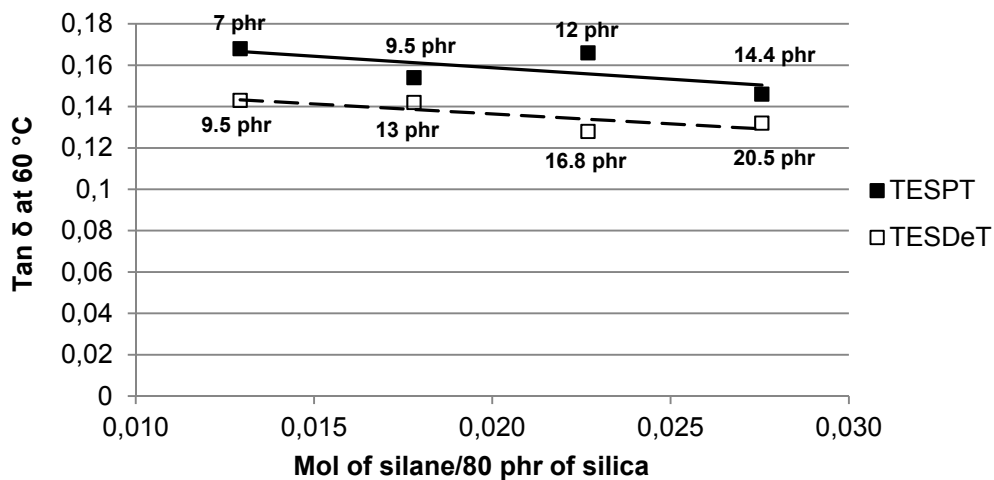


Figure 11:  $\tan \delta$  at 60 °C as indication of rolling resistance of the samples containing TESDeT and TESPT.

Both silanes can be also treated as plasticizers which increase the separation between the polymer chains. Separation of the polymer chains is associated with the formation of swollen compound which basically can temporarily store the energy during a dynamic deformation more efficiently in comparison with the non-swollen state.

### 6.3.5 $\tan \delta$ @ at low temperatures: indicator of wet skid resistance

At lower temperatures, preferably near the glass transition, the replacement of TESPT by TESDeT leads to increased energy dissipation, see Figure 12. The same trend is also perceived when the filler content is reduced<sup>20,21,22</sup>. It again indicates that a longer linker leads to less restricted polymer movements at the silica surface. Less restricted movements of the polymer chains means that a higher number of polymer chains can contribute to energy dissipation at lower temperatures. This consumes extra energy leading to the increase in the hysteresis peak at the glass transition temperature.

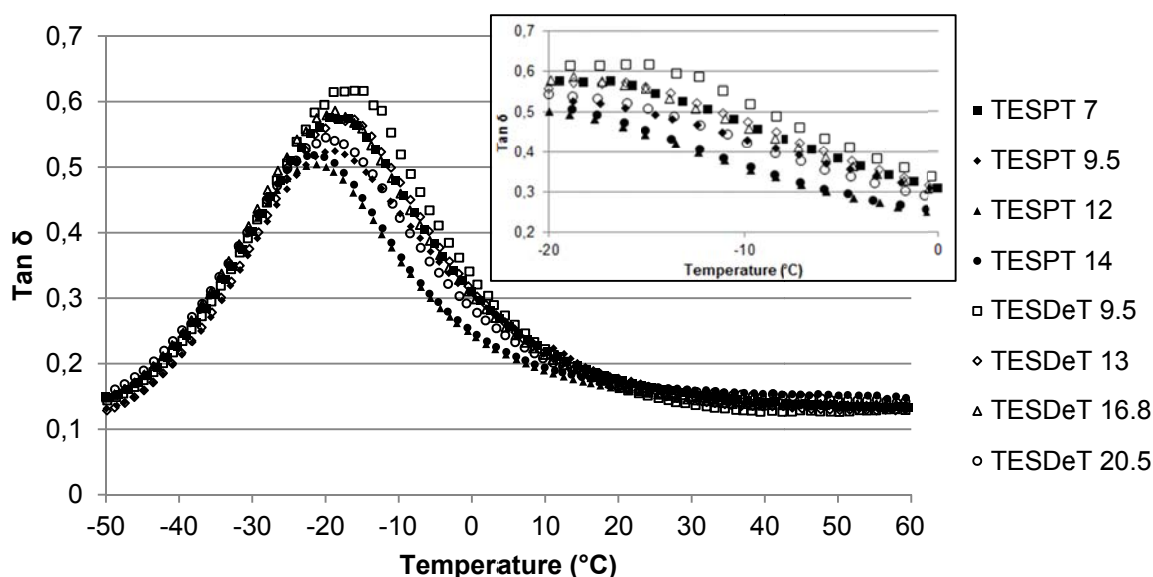


Figure 12:  $\tan \delta$  versus temperature dependence measured at 1% of static and 0.1% of dynamic strain for the compounds containing TESPT and DMESPT.

In order to further explore the nature of the differences in hysteresis between the compounds containing TESPT and TESDeT, the values of the storage ( $G'$ ) and loss moduli ( $G''$ ) need to be considered; see Table II. When the values of  $G'$  and  $G''$  at the  $\tan \delta$  peak are plotted against the molar concentration of the silane, more significant differences in storage modulus than in loss modulus are evident for the samples containing the two investigated silanes; see Figure 13. This suggests that the contribution of the storage modulus in the differences of the  $\tan \delta$  peak height visible in Figure 12 is much higher than the contribution of the loss modulus.

Table II: Comparison of the storage and loss moduli at  $\tan \delta$  peak.

| Sample code | $\tan \delta$ peak temperature | G' (MPa) | G'' (MPa) | $\tan \delta$ |
|-------------|--------------------------------|----------|-----------|---------------|
| TESPT 7     | -19                            | 158      | 91        | 0,58          |
| TESPT 9.5   | -19                            | 177      | 93        | 0,52          |
| TESPT 12    | -21                            | 223      | 113       | 0,50          |
| TESPT 14.4  | -21                            | 205      | 106       | 0,52          |
| TESDeT 9.5  | -16                            | 106      | 65        | 0,62          |
| TESDeT 13   | -19                            | 158      | 90        | 0,57          |
| TESDeT 16.8 | -19                            | 142      | 83        | 0,59          |
| TESDeT 20.5 | -19                            | 154      | 83        | 0,54          |

Compounds containing the TESDeT have a lower ability to store energy at lower temperatures: they have a lower storage modulus in comparison to TESPT containing compounds. Lower values of the storage modulus also correspond with a lower stiffness of the compounds containing TESDeT what causes the increase in energy dissipation at lower temperatures.

The rising silane loading changes the ratio of the polymer to other ingredients. With an increasing concentration of the silane, which stiffness is infinitely low, the stiffness and storage modulus of the compound should decrease. This is indeed the case at temperatures above the glass transition of the polymer.

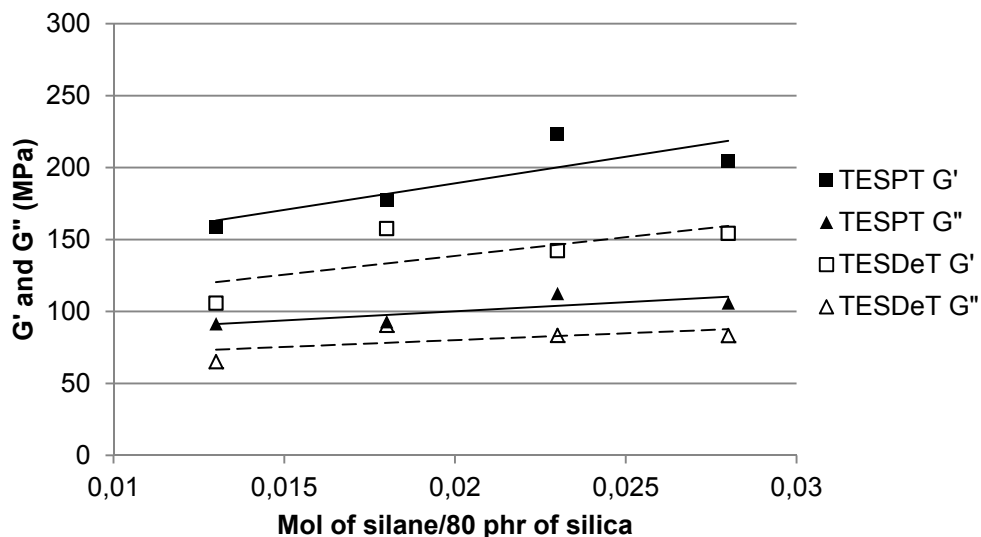


Figure 13: Storage and loss moduli at the  $\tan \delta$  peak temperature of TESPT and TESDeT containing compounds.

At temperatures close to the glass transition of the polymer, the compound with a low ratio of polymer to other ingredients is characterized by a higher stiffness and storage modulus: the result of a decreased amount of polymer in the compound, see Table

III. Furthermore, with increasing loading of the silane, the stiffness and storage modulus further increases and hysteresis decreases.

Table III: Weight ratio of polymer to remaining ingredients of the compound.

| Compound name                         | TESPT 7 | TESPT 9.5 | TESPT 12 | TESPT 14.5 | TESDeT 9.5 | TESDeT 13 | TESDeT 16.8 | TESDeT 20.5 |
|---------------------------------------|---------|-----------|----------|------------|------------|-----------|-------------|-------------|
| Ratio of polymer to other ingredients | 1,27    | 1,24      | 1,21     | 1,19       | 1,24       | 1,2       | 1,16        | 1,13        |

Compounds can also be compared at equalized concentration of silane. When the same concentration of 9.5 phr of both silanes is compared, the storage modulus is lower and the hysteresis is higher for the compound containing TESDeT silane. Apparently, the molecular weight of the silane has a contribution to the compound stiffness: The higher the molecular weight of the silane, the lower the stiffness and storage modulus of the compound, and as a consequence the higher the hysteresis at low temperatures. Because of the long linker of TESDeT, its molar mass is also higher than that of TESPT. At lower temperatures, the molecule of TESDeT itself would be characterized by a higher flexibility than the molecule of TESPT. That in turn contributes to lower values of the storage moduli for the TESDeT containing compounds. Therefore the introduction of a coupling agent with a molecular weight higher than that of the TESPT to the compound will lead to increased hysteresis at lower temperatures.

Summarizing the two last subsections: At higher temperatures, approximately 60 °C, an increasing concentration of both silanes leads to a less stiff compound with less internal filler-filler interactions, and therefore decreasing hysteresis. When the silanes are compared at lower temperature, close to the glass transition, the TESDeT results in a higher hysteresis than TESPT. At lower temperature, a higher concentration of silanes corresponds to a lower amount of polymer, thus the hysteresis is decreasing with increasing concentration of both silanes. The increased hysteresis of the compounds containing the TESDeT in comparison with equimolar concentrations of TESPT is related to the higher molecular weight of the former, which results in a higher mobility of the polymer chains at the silica surface. The higher molecular weight of the TESDeT can be considered as a negative aspect, because higher



amounts of TESDeT need to be applied to obtain concentrations equimolar to the TESPT silane.

### 6.3.6 LAT 100 side force coefficient: wet skid resistance

Increasing the length of the aliphatic linker from 3 to 10 carbon atoms does not show a clear trend for the side force coefficient as seen in Figure 14. The higher hysteresis in the lower temperature range of the compound containing 9.5 phr TESDeT in comparison to the sample containing 14.4 phr TESPT as seen in Figure 12 does not contribute to a higher value of the side force coefficient for the former one.

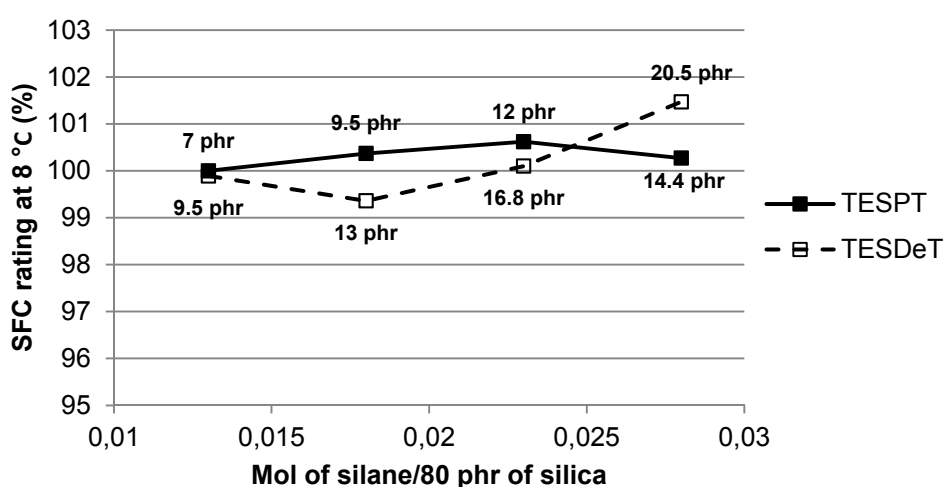


Figure 14: Side force coefficient as measurement of wet skid resistance versus concentration of TESDeT and TESPT.

In the two previous chapters, the silica-polymer interphase was weakened in the case of TESH or toughened like in the case of DMESPT in comparison to the interphase obtained by use of TESPT. However, in the present case it need to be concluded that the changes of the silica-polymer interphase caused by the silane linker length is not radical enough to significantly influence the side force coefficient values.

## 6.4 CONCLUSIONS

- Compounds containing a silane with a longer linker are characterized by a slightly higher elongation at break but similar tensile strength compared to the TESPT containing compounds. A longer and more flexible linker as in the case of TESDeT can accommodate higher strains without cracking.

- An increased linker length of the coupling agent reduces rolling resistance significantly, but does not change wet skid resistance. The longer linker of TESDeT can accommodate higher strain amplitudes within the filler-polymer interphase occurring during rolling, instead of transferring them directly onto the filler surface.
- An increased linked length increases hysteretic losses of the material in the glass transition temperature range of the elastomer. A more flexible linker in the case of TESDeT leads to less restricted polymer movements at the filler-polymer interphase in comparison with the reference silane. Hence more polymer can contribute to the energy dissipation phenomena at the glass transition temperature.
- By replacing TESPT by a silane with a longer linker, the rolling resistance of this material in a tire tread can be improved. However, the major drawback of TESDeT is its high molecular weight: in order to obtain equimolar concentrations, higher amounts of TESDeT need to be applied compared to TESPT.

## REFERENCES

---

- [1] H. G. Monneypenny, J. Harris, S. Laube, 148<sup>th</sup> Technical meeting of the Rubber Division ACS, 17-29<sup>th</sup> October 1995, Cleveland, Ohio.
- [2] S. Futamura, *Rubber Chem. Technol.* 64 (1991) 57.
- [3] K. A. Grosh, *Rubber Chem. Technol.* 27 (1964) 386.
- [4] N. Yoshimura, M. Okuyama, K. Yanagawa, 122<sup>th</sup> Technical meeting of the Rubber Division ACS, 5-7<sup>th</sup> October 1982, Chicago, Illinois.
- [5] A. R. Payne, *Rubb. Plast. Age.* 42 (1961) 963.
- [6] A. R. Payne, R. F. Whittaker, *Rubber Chem. Technol.* 44 (1971) 440.
- [7] J. Fröhlich, H.D. Luginsland, *Rubber World* 4 (2001) 28.
- [8] H. D. Luginsland, J. Fröhlich, A. Wehmeier, *Rubber Chem. Technol.* 75 (2002) 563.
- [9] L. L. Stelandre, Y. Bomal, L. Flandin, D. Labarre, *Rubber Chem. Technol.* 76 (2003) 145.
- [10] J. W. ten Brinke, P. J. van Swaaij, L. A. E. M. Reuvekamp, J. W. M. Noordermeer, *Rubber Chem. Technol.* 76 (2003) 12.
- [11] O. Klockmann, P. Albert, A. Hasse, K. Korth, *Rubber World* 234 (2006) 36.
- [12] O. Klockmann, *Kautsch. Gummi Kunstst.* 60 (2007) 428.
- [13] M. J. Wang, *Kautsch. Gummi Kunstst.* 61 (2008) 33.
- [14] M. Heinz, K. A. Grosch, 167<sup>th</sup> Technical meeting of the Rubber Division ACS, 16-18<sup>th</sup> May 2005, San Antonio, Texas.
- [15] L. Guy, Ph. Cochet, Y. Bomal, S. Daudey, *Kautsch. Gummi Kunstst.* 63 (2009) 383.
- [16] L. A. E. M. Reuvekamp, "Reactive mixing of silica and rubber for tires and engine mounts", PhD Thesis: 2003, Dept. of Rubber Technology, Univ. of Twente, Enschede, the Netherlands ISBN 90 365 1856 3.
- [17] M. Heinz, *J. Rubb. Res.* 13 (2010) 91.
- [18] K.H. Nordsiek, *Kautsch. Gummi Kunstst.* 38 (1985) 177.
- [19] A. R. Payne, *J. Appl. Polym. Sci.* 6 (1962) 57.
- [20] L. Guy, Ph. Cochet, Y. Bomal, S. Daudey, *Kautsch. Gummi Kunstst.* 62 (2009) 383.
- [21] M. M. Jacobi, M. V. Braum, T. L. A. C. Rocha, R. H. Schuster, *Kautsch. Gummi Kunstst.* 60 (2007) 460.
- [22] M. J. Wang, *Kautsch. Gummi Kunstst.* 60 (2007) 438.



---

### **Modification of the silane coupling agent for improvement of wet traction and rolling resistance: Influence of the type of alkoxy group**

---

*The type of alkoxy groups on the silane coupling agent determines the silanization rate and the kind of alcohol evolved during the silanization reaction. Therefore, independent of the reactivity of the silane towards the silica surface and of the reactivity towards the polymer chain, the physical and chemical properties of byproducts of the silanization reaction are of great importance for the material performance. To investigate the influence of the alkoxy group on wet skid and rolling resistance related properties, two silanes differing in the alkoxy group but with otherwise comparable structures were synthesized. One silane with methoxy-groups, bis-(dimethylmethoxysilylpropyl)tetrasulfide (MMeOS), was chosen due to its high silanization rate, and bis-(dimethylmethoxyethoxysilylpropyl) tetrasulfide (MMeOEtOS) for its increased affinity of the hydrolysable group towards the silica surface. Both silanes were compared with the reference silane - bis-(triethoxysilylpropyl) tetrasulfide (TESPT).*

*Silica reinforced compounds containing the novel silanes are characterized by improved wet skid and rolling resistance indicators in comparison with TESPT containing samples. Improvement of both properties is the result of the absence of lateral alkoxy groups in the synthesized silanes, with increased stiffness of the polymer-filler interface as a consequence. The additional effect of extra filler network in the samples containing MMeOEtOS, at lower temperatures induced by hydrogen bonding, causes a higher stiffness followed by the highest rating of the wet skid resistance.*

## 7.1 INTRODUCTION

Silica as a reinforcing filler results in several advantages over carbon black. Used in tire treads, silica reduces rolling resistance (RR) and improves wet skid resistance (WSR) and wear resistance <sup>1</sup>. Therefore, tire treads of passenger cars are nowadays almost exclusively produced in Europe with the use of silica technology instead of carbon black as filler. The key element in this technology is the coupling agent, a silane, which chemically couples silica to the rubber polymer. The molecular structure of the silane determines the polymer-filler interactions, which on their turn influence wet skid, rolling resistance and other physical properties of the tire tread. The most widely used bifunctional silane coupling agent for tire applications is bis-(triethoxysilylpropyl) tetrasulfide or (TESPT) <sup>2,3,4</sup>.

The silica surface contains different types of reactive silanol groups: isolated, vicinal and geminal <sup>5,6</sup>. Apart from the reactive groups, the silica surface contains approximately 6 - 8 % of bound water <sup>7,8</sup>. The reaction of a silane coupling agent with the silanol groups on the silica surface is referred to as silanization. The actual bonding of the polymer chains to the silica surface via the coupling agent occurs during the curing process, and in case of TESPT the mechanism and kinetics were investigated by Görl et al. <sup>9</sup>, Luginsland <sup>10</sup> and Reuvekamp <sup>11,12</sup>. At elevated temperatures during mixing, the alkoxy groups of the silane coupling agent undergo hydrolysis and transform into highly reactive hydroxyl groups. The rate of hydrolysis and silanization depends on the type of alkoxy group: methoxy > ethoxy > propoxy.

The silanization reaction is an equilibrium reaction. To achieve a high yield of silanization, the byproducts of the reaction, an alcohol, needs to be removed from the reaction medium <sup>13,14</sup>. Hence the longer the alkyl chain of the alkoxy group, the more difficult it becomes to evaporate the alcohol and to achieve a high degree of conversion.

Other ingredients of the rubber compound can have a catalytic effect on the silanization. For instance compounds based on styrene-butadiene rubber, in which zinc oxide is used as co-agent for sulfur vulcanization, show a decrease in compound viscosity in comparison with compounds without this oxide <sup>15</sup>. Nevertheless, the type of alkoxy groups of the silane coupling agent remains the most important factor during the silanization process.

The objective of the present chapter is to show the effects of two different alkoxy moieties, methoxy- and methoxyethoxy-, on wet skid and rolling resistance tire performance indicators in comparison with triethoxy- in TESPT.

As a first approach, a silane with the methoxy group was chosen because of its rapid hydrolysis capabilities resulting in a high silanization rate. A coupling agent with a high silanization rate could possibly cover more of the silica surface in comparison with a slower reacting silane in the same period of time, and this should result in improved wet skid and rolling resistance performance. The second approach towards increasing the reactivity of the silane towards the silica is based on an increased polarity of the hydrolysable group of the silane coupling agent. In order to react with silica during the mixing step, the coupling agent must migrate towards the silica surface. Additional oxygen atoms present in a methoxyethoxy-moiety makes it more polar in comparison with the single methoxy group. This could provide better adsorption of the silane molecules on the silica surface and lead to increased efficiency of the silanization reaction.

The influence of the silica-polymer interphase structure on the wet skid performance is investigated by testing the dynamic properties, in particular the  $\tan \delta$  in the temperature range from 0 – 20 °C at 10 Hz. The values of the loss tangent in this temperature range are so far the most suitable indicators for the wet skid performance of a tire tread <sup>16</sup>. However, a WSR indicator closer to actual practice are measurements on a Laboratory Abrasion Tester 100 (LAT 100), on which additional measurements are performed <sup>17</sup>.

## 7.2 EXPERIMENTAL

In order to investigate the influence of modifications in the hydrolysable group of the silane on wet skid as well as rolling resistance, two different silanes were selected for the experiments and synthesized. Both silanes are compared to the reference silane TESPT.

In the first modification, two ethoxy-groups out of three per silicon atom are replaced by inert methyl-groups, and the ethoxy hydrolysable group was replaced by a methoxy-group: bis-(dimethylmethoxysilylpropyl) tetrasulfide or monomethoxysilane (MMeOS). This modification leads to a silane with an alkoxy-group which is more

susceptible to hydrolysis than an ethoxy-group. In the second silane, again two ethoxy-groups out of three per silicon atom are replaced by inert methyl-groups, and the ethoxy hydrolysable group was replaced by a methoxyethoxy-group: bis-(dimethylmethoxyethoxysilylpropyl) tetrasulfide or monomethoxyethoxysilane (MMeOEtOS). This modification should result in a better adsorption of the silane onto the silica surface due to the increased polarity of the hydrolysable group. In order to avoid sterical hindrance influencing the silanization kinetics and efficiency, only one reactive moiety was used; two ethoxy-groups of the reference silane were replaced by non-reactive methyl groups. The structure of the two experimental coupling agents and the reference silane, TESPT, are shown in Figure 1. The silane coupling agent TESPT was commercially obtained from Evonik GmbH with an average sulfur rank of 3,7; the MMeOS and MMeOEtOS were synthesized in our laboratory.

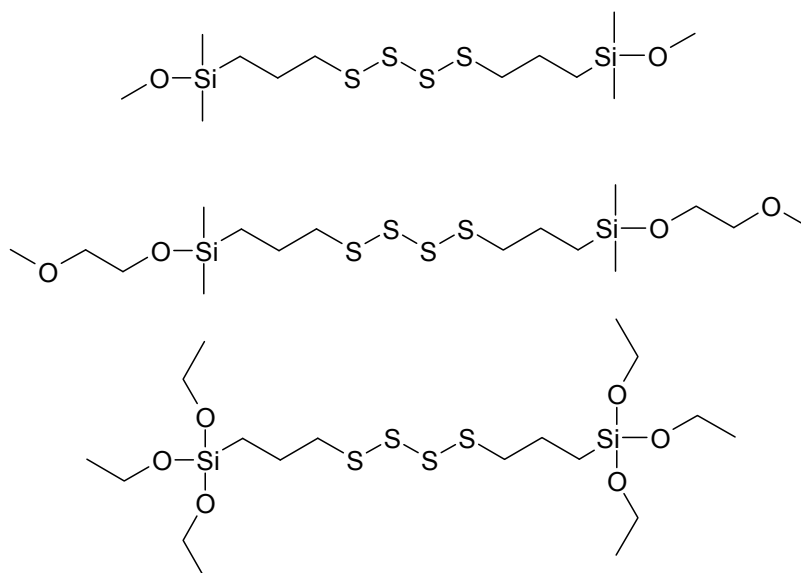


Figure 1: Structure of bis-(dimethylmethoxysilylpropyl) tetrasulfide, MMeOS (top) bis-(dimethylmethoxyethoxysilylpropyl) tetrasulfide, MMeOEtOS (middle), and bis-(triethoxysilylpropyl) tetrasulfide, TESPT (bottom).

### 7.2.1 Preparation of the silanes

*Bis-(dimethylmethoxysilylpropyl) polysulfide (MMeOS)* – This silane was synthesized in absolute methanol in a nitrogen atmosphere by refluxing 3-chloropropyl dimethylmethoxysilane (ABCR GmbH, Karlsruhe, Germany) and sodium



tetrasulfide (Sigma Aldrich, Zwijndrecht, The Netherlands), see Figure 2. After 2 hours of refluxing, the color of the suspension changed from dark red to yellow. This suspension was filtered and methanol was removed from the filtrate in a rotary evaporator, which lead to a dark red suspension. The red suspension was diluted with diethyl ether, and the ether layer was extracted with water to remove the inorganic byproducts. After this extraction, the water was colored red, and the extraction was continued until no further coloration of the water phase was visible. The ether extract was dried with anhydrous  $\text{MgSO}_4$ , filtered, and remaining ether was removed in the rotary evaporator. The yield was 88 % of a gold yellow clear liquid. The structure and purity of the silanes were determined by Liquid Chromatography - Mass Spectroscopy (LC-MS, Agilent-1100/Bruker-Esquire 3000 Plus) according to the procedure specified in Tables I and II in Chapter 3. It was identified as bis-(dimethylmethoxysilylpropyl) polysulfide with 96 % purity base on the absorbance ratio. Each individual peak was characterized by its own molar mass with MS. The average sulfur rank of the product was 3,3, and the calculated molecular weight was 367 g/mol. The product structure as determined by LC-MS is given in Figure 3.

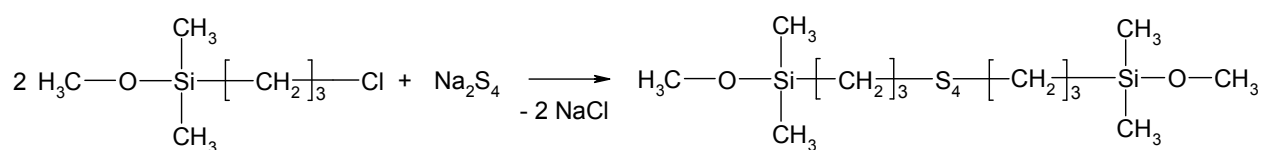


Figure 2: Formation of bis-(dimethylmethoxysilylpropyl) polysulfide.

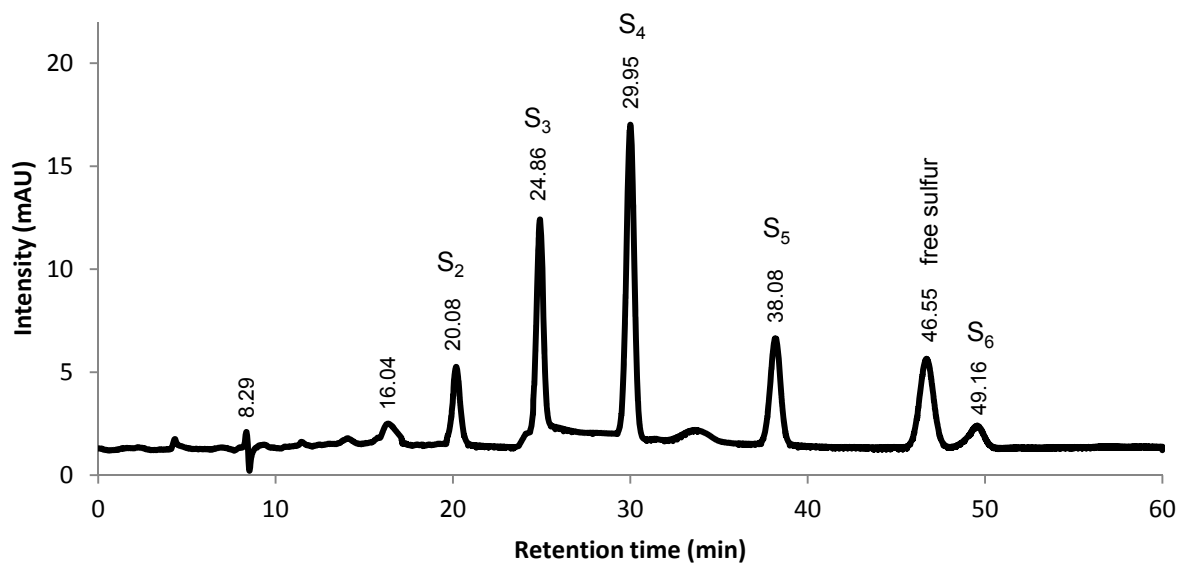


Figure 3: LC-MS chromatogram of MMeOS; the different sulfur ranks are indicated.

*Bis-(dimethylmethoxyethoxysilylpropyl) polysulfide (MMeOEtOS)* – was prepared in a two-step synthesis. During the first step, 3-chloropropyl-dimethylmethoxyethoxysilane was synthesized<sup>18</sup>. 2-Methoxyethanol, dried under anhydrous magnesium sulfate, was placed in a three-neck round bottom flask immersed in an oil bath with a temperature controller. The flask was equipped with a reflux condenser, addition funnel and nitrogen feed. The 3-chloropropyldimethylchlorosilane was added drop wise to methoxyethanol. In order to facilitate the reaction by the evacuation of hydrogen chloride from the reaction medium, a gentle flow of nitrogen was implemented. The reaction was carried out for 7 hours at a temperature of 100 °C. Under these circumstances, the reaction as shown in Figure 4 takes place. Unreacted 2-methoxyethanol and 3-chloropropyldimethylchlorosilane were removed in a rotary evaporator. The remaining liquid was a colorless product, 3-chloropropyldimethylmethoxyethoxysilane, in a yield of 78 % and a purity of 98 % as determined by LC-MS. The product structure was also determined with the aid of LC-MS. The mass calculated for  $C_8H_{19}O_2SiClH^+$  is 211,62 g/mol; the mass found by LC-MS was 212,70 g/mol.

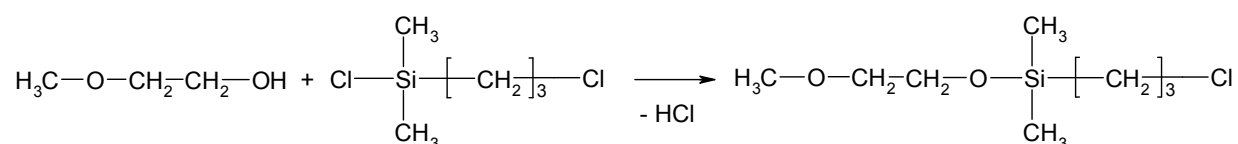


Figure 4: Formation of 3-chloropropyldimethylmethoxyethoxysilane

During the second step of the reaction, 3-chloropropyldimethylmethoxyethoxysilane was refluxed in anhydrous ethanol with sodium tetrasulfide; see Figure 5. After 5 hours of refluxing, the color of the suspension changed from dark red to yellow. This suspension was filtered and ethanol was removed from the filtrate in a rotary evaporator leading to a dark red suspension, which was then diluted with diethyl ether. The ether phase was extracted with water until no coloration of the water phase was noticed any more. The ether extract was dried with anhydrous  $MgSO_4$ , filtered, and ether was removed in the rotary evaporator. The yield was 87 % of a gold yellow clear liquid, bis-(dimethylmethoxyethoxysilylpropyl) tetrasulfide, with 95 % purity measured by LC-MS. The average sulfur rank of the product was 3.7 and the calculated molecular weight was 478 g/mol. The product structure was determined with the aid of LC-MS and given in Figure 6.

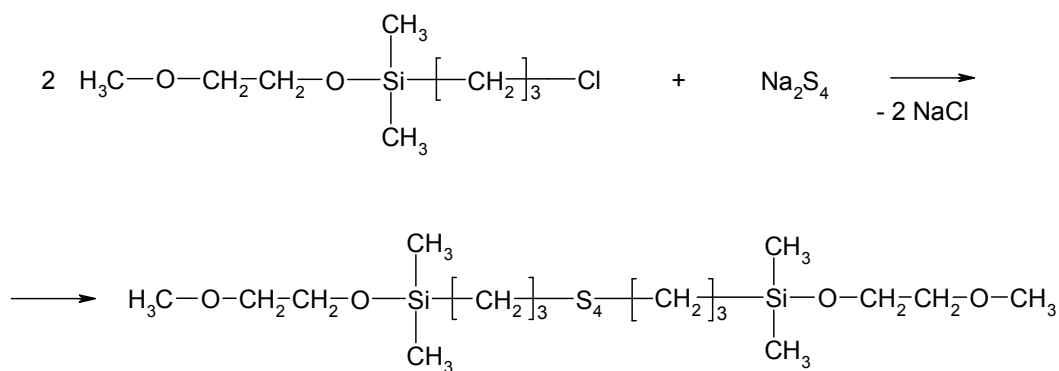


Figure 5: Formation of bis-(dimethylmethoxyethoxysilylpropyl) tetrasulfide

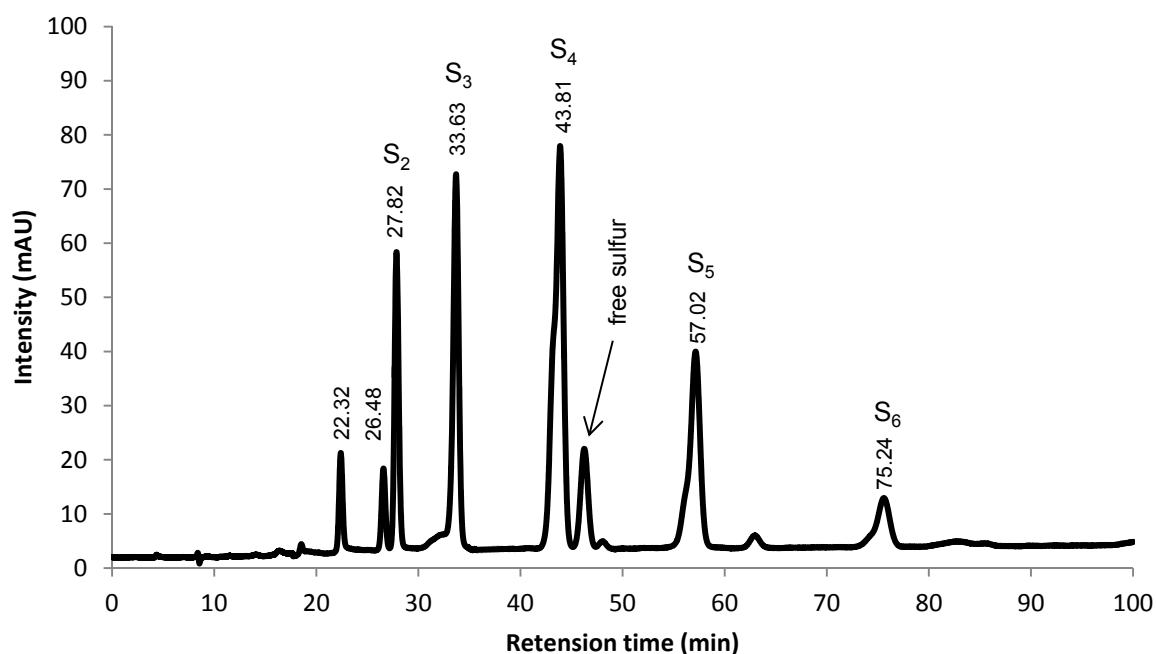


Figure 6: LC-MS chromatogram of MMeOEtOS; the different sulfur ranks and the free sulfur peak are indicated.

### 7.2.2 Mixing and curing

A test compound according to the green tire recipe was used<sup>19</sup>, containing a highly dispersible silica grade with a cetyltrimethylammonium bromide (CTAB) specific surface area of 160 m<sup>2</sup>/g. The compound formulations are shown in Table I. A detailed specification of all ingredients is given in Chapter 4, Table IV.

MMeOS and MMeOEtOS were applied at four different concentrations equimolar to the concentration of the reference silane TESPT, and with sulfur adjustment. The TESPT content was adjusted for the reference compound, the first compound in Table I, according to the CTAB specific surface area of this silica type by using the empirical equation proposed by L. Guy: Equation 1<sup>20</sup>. The amount of free sulfur added together with the curatives for all compounds was adjusted to keep the total molar amount of sulfur including the sulfur contained in the coupling agent at a constant level in all batches. In all cases, the total sulfur content was kept constant; the reactivity difference between polysulfidic groups in the coupling agents containing 3.3 or 3.7 sulfur atoms was not taken into consideration.

$$TESPT (phr) = 5.3 \times 10^{-4} \times (CTAB)_{silica} \times (phr)_{silica} \quad (\text{Equation 1})$$

To prepare the compounds, an internal laboratory mixer, Brabender 350 S with a mixing volume of 390 cm<sup>3</sup>, was used. The mixing procedure was specified in Chapter 4, Table V. The total volume of each batch was adjusted to a fill factor of 70 %. Preparation of sheets for testing was done on a Schwabenthan Polymix 80T 300 ml two roll mill. The samples were cured in a Wickert press WLP 1600 at 160 °C and 10 MPa to sheets with a thickness of 2 mm according to their t<sub>90</sub> optimum vulcanization time as determined in a Rubber Process Analyzer, RPA 2000, from Alpha Technologies.

Table I: Rubber compound formulations

| Ingredient      | Sample code |           |          |            |           |           |           |           |              |              |             |               |
|-----------------|-------------|-----------|----------|------------|-----------|-----------|-----------|-----------|--------------|--------------|-------------|---------------|
|                 | TESPT 7     | TESPT 9,5 | TESPT 12 | TESPT 14,4 | MMeOS-4,9 | MMeOS-6,6 | MMeOS-8,4 | MMeOS-9,7 | MMeOEtOS 6,3 | MMeOEtOS 8,6 | MMeOEtOS 11 | MMeOEtOS 12,7 |
| S-SBR           | 103         | 103       | 103      | 103        | 103       | 103       | 103       | 103       | 103          | 103          | 103         | 103           |
| BR              | 25          | 25        | 25       | 25         | 25        | 25        | 25        | 25        | 25           | 25           | 25          | 25            |
| Silica (1165MP) | 80          | 80        | 80       | 80         | 80        | 80        | 80        | 80        | 80           | 80           | 80          | 80            |
| TESPT           | 7,0         | 9,5       | 12,0     | 14,4       |           |           |           |           |              |              |             |               |
| MMeOS           |             |           |          |            | 5,0       | 6,6       | 8,3       | 9,6       |              |              |             |               |
| MMeOEtOS        |             |           |          |            |           |           |           |           | 6,3          | 8,6          | 11,0        | 12,7          |
| TDAE            | 5           | 5         | 5        | 5          | 5         | 5         | 5         | 5         | 5            | 5            | 5           | 5             |
| Zinc oxide      | 2,5         | 2,5       | 2,5      | 2,5        | 2,5       | 2,5       | 2,5       | 2,5       | 2,5          | 2,5          | 2,5         | 2,5           |
| Stearic acid    | 2,5         | 2,5       | 2,5      | 2,5        | 2,5       | 2,5       | 2,5       | 2,5       | 2,5          | 2,5          | 2,5         | 2,5           |
| 6PPD            | 2           | 2         | 2        | 2          | 2         | 2         | 2         | 2         | 2            | 2            | 2           | 2             |
| TMQ             | 2           | 2         | 2        | 2          | 2         | 2         | 2         | 2         | 2            | 2            | 2           | 2             |
| Sulfur          | 1,4         | 0,8       | 0,2      | 0,0        | 1,5       | 1,1       | 0,5       | 0,2       | 1,4          | 0,8          | 0,2         | 0,0           |
| TBBS            | 1,7         | 1,7       | 1,7      | 1,7        | 1,7       | 1,7       | 1,7       | 1,7       | 1,7          | 1,7          | 1,7         | 1,7           |
| DPG             | 2,0         | 2,0       | 2,0      | 2,0        | 2,0       | 2,0       | 2,0       | 2,0       | 2,0          | 2,0          | 2,0         | 2,0           |

### **7.2.3 Characterization methods**

The Mooney viscosity ML(1+4) of the compounds was measured at 100 °C on a Mooney viscometer MV 2000E (Alpha Technologies) according to ISO 289-1.

Payne effect measurements were done using the RPA 2000 before and after vulcanization for  $1.2 \times t_{90}$  at 160 °C in the RPA. The differences in values of the storage modulus at 1 % strain and 90 % strain were measured at 100 °C and at a frequency of 0.5 Hz.

In order to predict the rolling resistance, single point measurements of  $\tan \delta$  at 60 °C and 6 % strain were performed on the RPA 2000, after vulcanization for  $1.2 \times t_{90}$  at 160 °C in the same RPA<sup>21</sup>.

Dynamic mechanical analysis was performed in the tensile mode on a Metravib DMA 2000 dynamic spectrometer. The samples were cut with a 40 x 5 mm die from the cured sheets of the rubber compounds. For dynamic curves, measurements were performed at temperatures between -50 °C and 80 °C at a dynamic strain of 0.1% and a frequency of 10 Hz.

A Laboratory Abrasion Tester 100 (LAT 100, VMI Group) was used to estimate the wet skid resistance of the tire treads in conditions which better reflect the real conditions on the road; see Figure 3, Chapter 3<sup>22</sup>.

## **7.3 RESULTS AND DISCUSSION**

### **7.3.1 Mooney viscosity**

Despite an expected increase in reactivity of the monomethoxy-moiety towards the silanol groups on the silica surface in comparison with a tri-ethoxy group, the replacement of the tri-ethoxy by the monomethoxy-group does not lead to noticeable changes in the values of Mooney viscosity, see Figure 7. In general, the sulfur rank determines the stability of the sulfidic silane during the mixing: Silanes with a lower sulfur rank are more stable and less prone to scorch during mixing, which would favor a lower Mooney viscosity. The three investigated silanes are characterized by only

slight differences in sulfur rank; the difference of about 0.4 sulfur atoms is not expected to result in large viscosity changes, as actually seen in the experiments. Implementation of the silane with the monomethoxyethoxy-moiety causes a slight drop in viscosity in comparison with the other two silanes. Methoxyethanol with its relatively high boiling point of 125 °C is the byproduct of the silanization reaction in the case of MMeOEtOS. Considering the high boiling point and the additional oxygen atom, methoxyethanol is also characterized by an increased polarity in comparison with ethanol or methanol and may be adsorbed more onto the silica surface acting like an interphase lubricant, thus decreasing the viscosity.

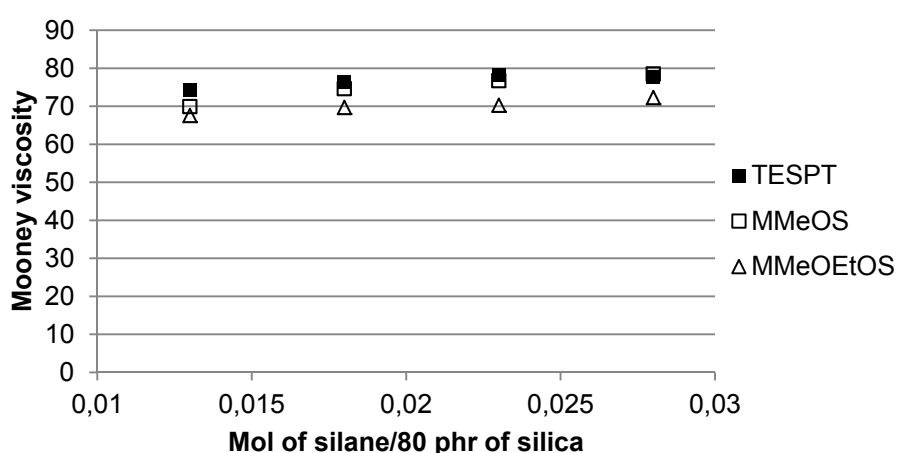


Figure 7: Mooney viscosity of TESPT, MMeOS and MMeOEtOS containing batches

### 7.3.2 Payne effect

Because of the van der Waals forces and hydrogen bonding between silanol groups, the silica aggregates form a rigid network in the polymer matrix. At low strain amplitude, the energy can be stored efficiently in this rigid filler-filler network resulting in high values of the storage modulus. However, when higher strain amplitudes are applied, this network gradually breaks causing a decrease of the storage modulus. Due to slippage of the polymer chains over the filler surface at higher strains energy loss is high, thus the storage moduli are relatively low and depend only on the polymer type and filler loading. The difference between the storage moduli at low and at high strain amplitude is called the Payne effect, and in a silica compound it can be used to describe the magnitude of the filler-filler interaction. In general, a silane coupling agent reacts with the silanol groups and suppresses the filler-filler

interaction, and thus decreases the Payne effect. In this study, the batches with MMeOS as coupling agent are characterized by the lowest values of the Payne effect, see Figure 8.

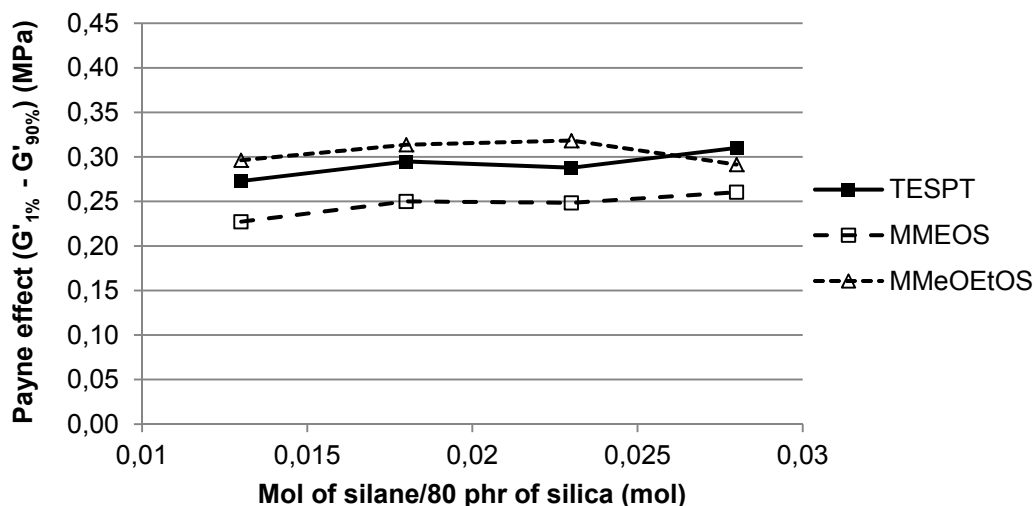


Figure 8: Payne effect of uncured compounds containing TESPT, MMeOS and MMeOEtOS.

The lowest values of the Payne effect in the uncured state indicate that MMeOS reacts with more silanol groups on the silica surface in comparison with the other two silanes. Because of the fast hydrolysis of the methoxy group, more of the MMeOS molecules can hydrolyze at the silica surface during mixing, therefore a higher silanization efficiency is reached than in the case of MMeOEtOS or TESPT. Besides, the generated methanol evaporates fast due to its low boiling temperature and shifts the balance of the silanization reaction towards a higher yield of the silica-silane reaction. In the case of MMeOEtOS, the increased polarity of the alkoxy group apparently does not cause an increase in the silanization efficiency like was expected; on the contrary, the higher polarity of methoxyethanol apparently decreases the silica hydrophobicity to a lesser extent than methanol or ethanol do, what results in somewhat increased filler-filler interactions.

Payne effect measurements performed after vulcanization are shown in Figure 9. The differences between the silanes become smaller after the vulcanization process, but the order of the different silanes remains unchanged: MMeOS still shows the lowest Payne effect. In order to assess if a more efficient use of the silanol groups leads to a higher density of polymer-filler bonds, the values of the storage modulus at high

strains were compared, as they may correspond with the filler-polymer bond strength: The stronger or more numerous the filler-polymer bonds, the more difficult they are to break, and the less molecular slippage is occurring. The energy can better be stored without losses which results in higher values of the storage modulus at both, low and high strains. In this case, the values of the storage modulus at highest strains do not show a clear trend for the different coupling agents, see Figure 10. Opposed to what was expected, an increased degree of reaction of the silanol groups does not automatically result in the buildup of a more dense filler-polymer network.

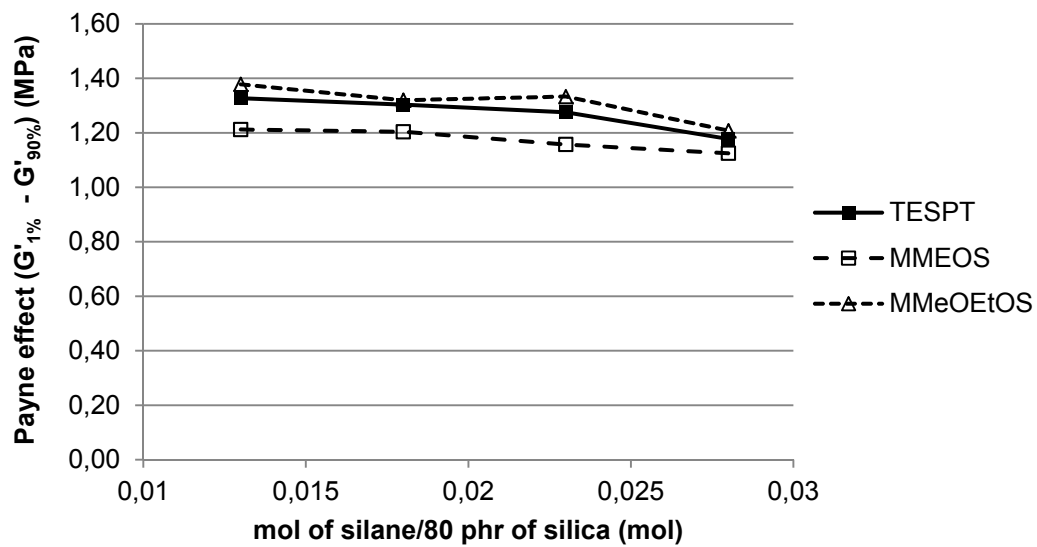


Figure 9: Payne effect after cure of compounds containing TESPT, MMEOS and MMeOEtOS.

There are only minor differences between the values of the storage modulus at highest strain, what suggests that the amount of filler-polymer bonds is similar for all the samples. Therefore, the differences in the Payne effect between the compounds shown in Figure 9 are caused by different filler-filler interactions.



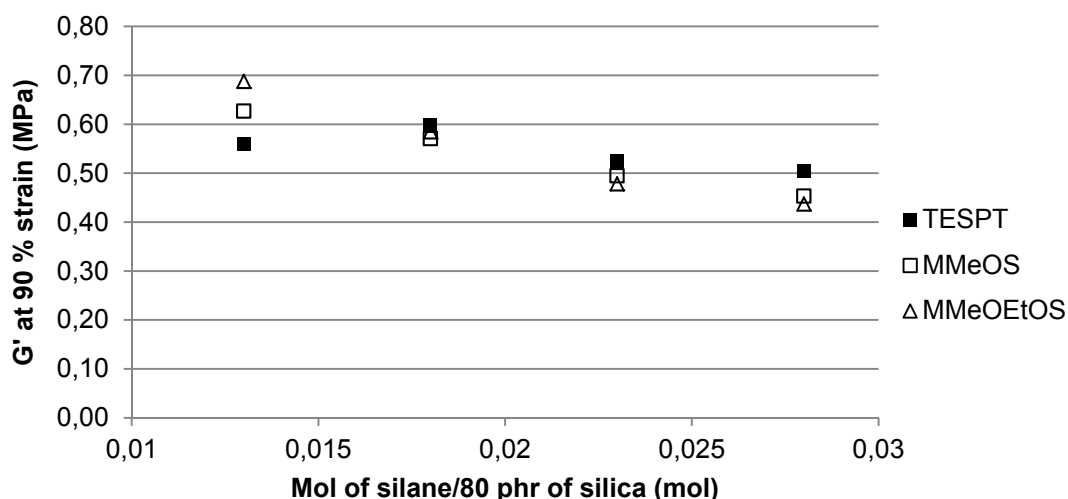


Figure 10: Storage modulus at 90 % strain, after cure.

### 7.3.3 *Tan $\delta$ values at 60 °C: indicator of rolling resistance*

The compounds with the newly synthesized silanes are characterized by lower values of the  $\tan \delta$  at 60 °C in comparison with the TESPT compounds; see Figure 11. Both of the experimental silanes contain one alkoxy group instead of three, like in the case of TESPT, and this leads to the effect described in Chapter 5: in the case of TESPT, unreacted ethoxy-groups hydrolyze during vulcanization and form ethanol which remains bound at the polymer-filler interphase acting as a softener. Consequently, the softer polymer-filler interphase, more energy is lost due to a higher probability of polymer movements. However, during vulcanization of the compounds containing MMeOEtOS and MMeOS, there are no lateral alkoxy groups present which could further hydrolyze and form byproducts, methoxyethanol or methanol, respectively. The interphase remains more or less unaffected, and this leads to lower probability of polymer chain movements on the filler surface in comparison with TESPT. Furthermore, in the case of MMeOS, apart from a lower amount of methanol at the interphase, also lower filler-filler interactions are observed, which will contribute to lower values of  $\tan \delta$  at 60 °C

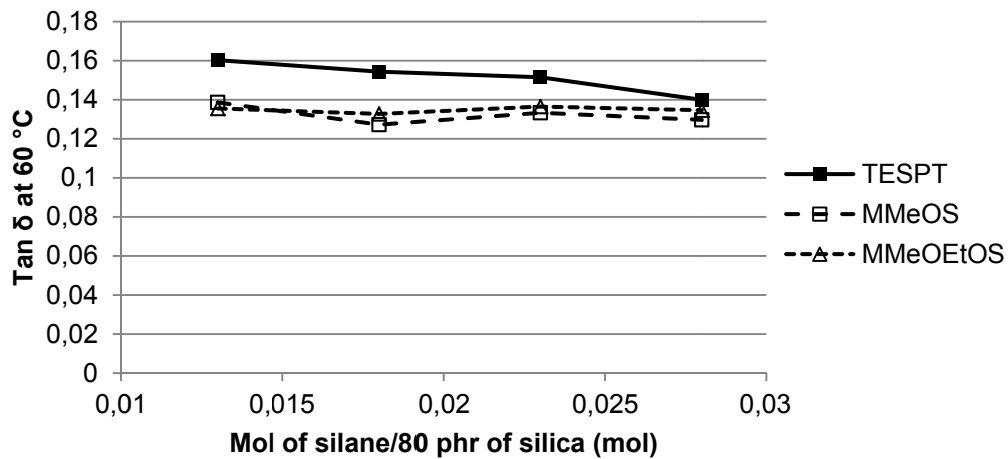


Figure 11: Tan  $\delta$  at 60 °C values versus molar concentration of silanes.

### 7.3.4 Hysteresis and tan $\delta$ at low temperatures

Values of the tan  $\delta$  at temperatures close to the glass transition of the polymer are lower for the MMeOS containing samples than those obtained for the corresponding TESPT samples, see Figure 12. The effect of lowered tan  $\delta$  values at the glass transition temperature is similar to the one obtained for DMESPT in Chapter 5. Apparently, all the investigated monoalkoxy-silanes influence the dynamic curve at lower temperatures in the same manner.

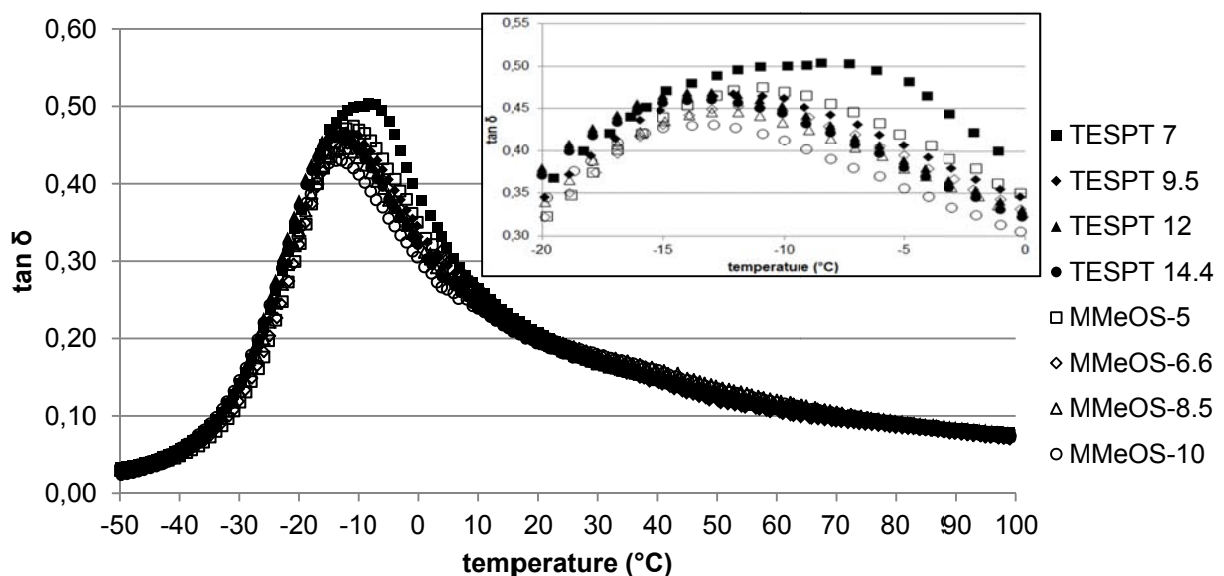


Figure 12: Tan  $\delta$  versus temperature measured at 1% static and 0.1% dynamic strain for the compounds containing different concentrations of TESPT and MMeOS.

The effect of decreased  $\tan \delta$  values near the glass transition temperature is even more evident for the samples with MMeOEtOS, see Figure 13. Additionally a small bump in the range of 20 °C to 70 °C is visible on the curves corresponding to the samples containing MMeOEtOS.

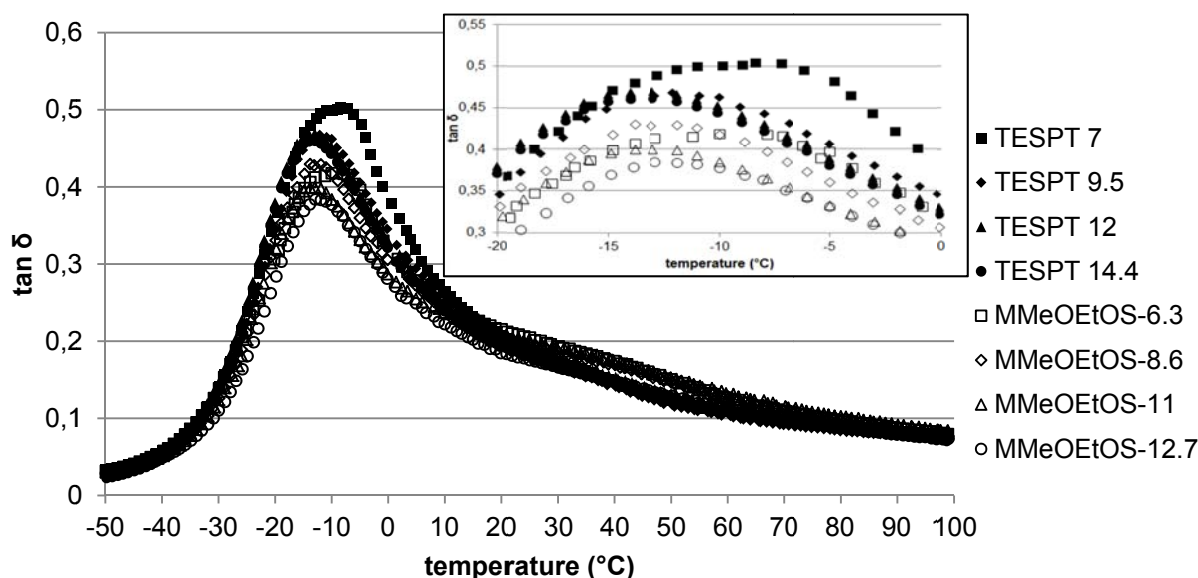


Figure 13:  $\tan \delta$  versus temperature measured at 1% static and 0.1% dynamic strain for the compounds containing different concentrations of TESPT and MMeOEtOS.

As  $\tan \delta$  is the ratio of two different entities: the loss vs. storage modulus, it is worthwhile to consider which of the two causes the changes in  $\tan \delta$  value. The samples containing the three investigated silanes are characterized by similar values of the loss moduli but different values of the storage moduli; see Figure 14. The compounds with MMeOEtOS are characterized by the highest values of the storage modulus, what causes the decrease of the  $\tan \delta$  values at the temperature range close to the glass transition of the polymers.

2-Methoxyethanol is slightly more polar than ethanol or methanol, therefore it can be adsorbed on the silica surface more strongly than the latter two alcohols. Additionally, oxygen in the 2-methoxyethanol makes this molecule more susceptible to intra- and intermolecular hydrogen bonding than methanol or ethanol, which have just one single hydroxyl group. Dependent on temperature, these hydrogen bonds can strengthen or weaken the polymer-filler interphase. At the glass transition

temperature these hydrogen bonds strengthen the polymer-filler interphase what is reflected in the higher storage modulus of the compounds containing MMeOEtOS, see Table II. The hydrogen bonds are strongly affected by temperature: Apparently the weak hydrogen-bond filler network is starting to break and thus increasing the  $\tan \delta$  values at temperatures exceeding 20 °C. At temperatures higher than 70 °C, the weak filler network is completely broken, and the more energy-efficient polymer network plays a dominant role in the hysteretic losses.

The presence of hydrogen bonds may also explain the small differences in the Payne effect values between TESPT and MMeOEtOS containing compounds. The filler network based on hydrogen bonds is broken at temperatures of 100 °C, at which the Payne effect values are measured. Therefore only small differences between TESPT and MMeOEtOS containing samples are visible for the Payne effects measured.

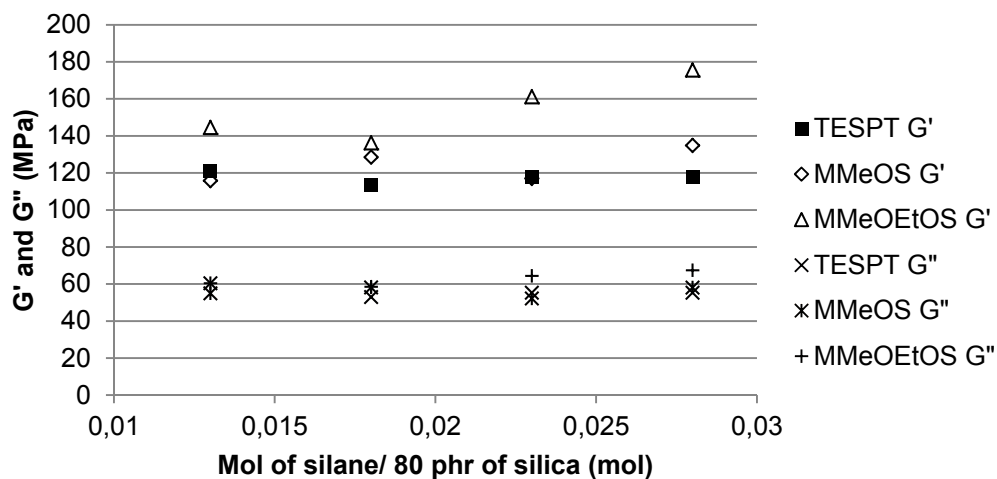


Figure 14: Loss and storage moduli at the glass transition temperature for the samples containing TESPT, MMeOEtOS and MMeOS.

Table II: Comparison of loss and storage modulus at the glass transition temperature

| MMeOEtOS      |                     |          |           |       |
|---------------|---------------------|----------|-----------|-------|
| Mol of silane | T <sub>g</sub> (°C) | G' (MPa) | G'' (MPa) | tan δ |
| 0,013         | -9                  | 145      | 60        | 0,42  |
| 0,018         | -12                 | 136      | 58        | 0,43  |
| 0,023         | -13                 | 161      | 64        | 0,40  |
| 0,028         | -13                 | 176      | 67        | 0,38  |
| MMeOS         |                     |          |           |       |
| Mol of silane | T <sub>g</sub> (°C) | G' (MPa) | G'' (MPa) | tan δ |
| 0,013         | -11                 | 116      | 55        | 0,47  |
| 0,018         | -12                 | 129      | 58        | 0,45  |
| 0,023         | -12                 | 117      | 52        | 0,45  |
| 0,028         | -13                 | 135      | 58        | 0,43  |
| TESPT         |                     |          |           |       |
| Mol of silane | T <sub>g</sub> (°C) | G' (MPa) | G'' (MPa) | tan δ |
| 0,013         | -9                  | 121      | 60        | 0,50  |
| 0,018         | -12                 | 113      | 53        | 0,47  |
| 0,023         | -13                 | 118      | 55        | 0,47  |
| 0,028         | -13                 | 118      | 55        | 0,47  |

**7.3.5 LAT 100 side force coefficient: indicator for wet skid resistance**

Samples containing MMeOEtOS are characterized by the highest values of the side force coefficient compared to the samples with TESPT; see Figure 15. The compound with MMeOS as coupling agent lies in-between and shows an increase with increasing concentration, while the other compounds are rather indifferent to the silane concentration. However, the differences in side force coefficient are not as significant as in the case of DMESPT; see Chapter 5.

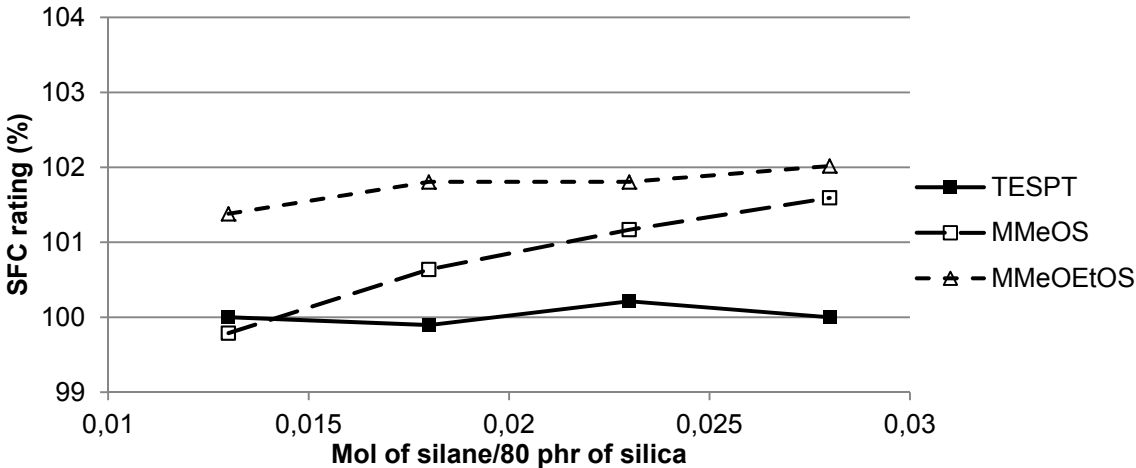


Figure 15: Correlation between side force coefficient as an indication for wet skid resistance and silane concentration for TESPT, MMeOEtOS and MMeOS containing compounds.

The wet skid mechanism described in Chapter 3 applies here as well. In order to elaborate on the earlier explanation some axioms are necessary to be mentioned.

- Car possess certain inertia which is the results of its mass and velocity.
- During skidding, when the wheel is not rotating anymore, the surface of the tire undergoes small deformations trying to penetrate into the micro-cavities existing in the road surface on which sliding is taking place.
- The load applied to the wheel, the average dimensions (depth and width) of the micro-cavities and the water film, limits the extension of micro-deformation.
- Taking into account the quasi triangular shape of the micro-cavities and as result of the sliding movement net force arise. Net force works against the inertia what in the final stage cause the car to stop. This net force can be separated on its components: vertical and horizontal, see Figure 16.
- In the sliding regime a vertical force coming from the micro-cavity surpasses the initial force causing the micro-deformation (deforming force). The forces related with inertia of a car are incomparably higher in comparison with the forces causing the micro-deformation. Hence the tire is sliding relative to the road surface and deformed compound which initially fills the cavities is pushed back to its original position on the tire by a vertical force.
- The horizontal force drags the compound in the direction opposite to the sliding direction what may result in tearing. Water lubricates the tire-road interface what diminishes the contribution of the horizontal force in the wet friction phenomena. Hence the compound stiffness must have the largest contribution during friction when the water film is present.

Depending on the compound stiffness, different wet skid scenarios are possible. In the first case the tire may be considered to be made out of very stiff material which is not able to deform under the applied load and penetrate into the mentioned micro-cavities, what leads to a low wet skid resistance. In the second case, the tire is made out of very soft rubber which deforms relatively easily and thus completely fills the micro-cavity: The wet skid resistance is higher than in the case of a very stiff compound.

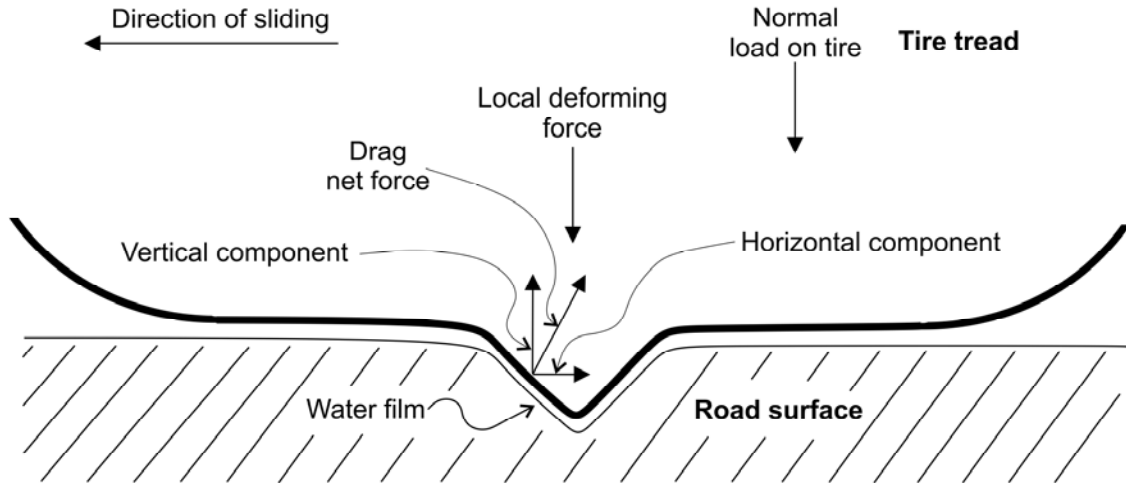


Figure 16: Deformation of a tire tread at a single micro-cavity.

In the third case, when smaller differences in compound stiffness are considered and the normal load applied to the wheel exceeds the load which is needed to completely fill the micro-cavities, both softer and stiffer compounds fill the micro-cavity to its dimensional limits. However, the vertical force necessary to push the stiffer compound back to its original position on the tire is higher than the force which is needed to push back a softer compound. Hence the tire made out of stiffer but still deformable compound will lead to higher resistance during skidding.

Samples containing MMeOEtOS are characterized by higher values of the storage modulus at lower temperatures in comparison to compounds containing MMeOS and TESPT; see Table II. The storage modulus is a measure of the stiffness of the samples, which undergo dynamic deformation at certain temperatures. Therefore the samples in which MMeOEtOS is used are characterized by the highest side force coefficient values. The storage moduli of the samples containing MMeOS are in between the values for the TESPT- and MMeOEtOS-containing materials, hence the side force coefficient values of MMeOS containing compounds are higher than for TESPT, but lower than for MMeOEtOS containing materials. This indicates that the storage and loss moduli should both be considered as separate values and not so much as the combined ratio  $\tan \delta$  in terms of wet skid resistance.

## 7.4 CONCLUSIONS

Two tailored silanes without lateral alkoxy groups were synthesized and compared in a tire tread compound with TESPT as reference. The clear advantage of these silanes compared to TESPT is a substantially lower alcohol generation during the mixing process, what is not only a positive environmental aspect of the monoethoxy silanes, but also gives an improvement in processing of the rubber compounds. The type of alkoxy-group of the silane coupling agents determines the type of alcohol-byproduct of the silanization reaction, and thus the kinetics of the silanization reaction, as well as the influence on compound processing and properties.

- The low boiling point of methanol leads to a relatively fast reaction with the silanol groups on the silica surface, and presumably a higher degree of utilization of silanol groups; this can be derived from the low Payne effect values of the corresponding uncured compounds.
- Apart from the boiling point, another important parameter describing the alcohol evolved during silanization needs to be considered: the ability to form hydrogen bonds. The higher tendency of 2-methoxyethanol to form intra- and intermolecular hydrogen bonds in comparison to methanol or ethanol causes increased stiffness of the polymer-filler interface at lower temperatures, and as a result higher side force coefficient values in comparison to the materials containing MMeOS and TESPT.
- Due to the lack of lateral alkoxy groups, both monomethoxy and monomethoxyethoxy silanes are also characterized by lower values of  $\tan \delta$  at 60 °C in comparison with TESPT. As a result of the lower amount of alcohol provided in the silane, less alcohol remains adsorbed onto the polymer-filler interphase. This decreases the probability of polymer segmental movements, what reduces energy losses.
- The more “rigid” polymer-filler interphase in the case of MMeOS and MMeOEtOS at lower temperatures increases the stiffness of the compound as measured with the storage modulus. The force necessary to deform the tread of the tire into micro-cavities is higher for the stiffer compounds and results in an improved, higher side force coefficient in comparison with TESPT.



## REFERENCES

---

- [1] M. P. Wagner, *Rubber Chem. Technol.* 49 (1976) 703.
- [2] B. T. Poh, *Eur. Polym. J.* 34 (1998) 975.
- [3] R. H. Hess, H. H. Hoekje, J. R. Creasey, F. Strain, US Pat. 3,768,537, (30-10-1973) to PPG Industries.
- [4] P. E. Cassidy, B. J. Yager, *J. Macromol. Sci. -Revs. Polym. Technol.* 1 (1971) 1.
- [5] A. P. Legrand, H. Hommel, A. Tuel, A. Vidal, *Adv. Coll. Interf. Sci.* 33 (1990) 91.
- [6] M. J. Wang, *Rubber Chem. Technol.* 71 (1998) 520.
- [7] H. D. Luginsland, A. Hasse, 158<sup>th</sup> Technical meeting of the Rubber Division ACS, 17-19<sup>th</sup> October 2000, Cincinnati, Ohio, USA.
- [8] L.T. Zhuravlev, *Colloids and Surfaces A: Physicochemical and Engineering Aspects* 173 (2000) 1.
- [9] U. Görl, J. Munzenberg, H. D. Luginsland, A. Müller, *Kautsch. Gummi Kunstst.* 52 (1999) 588.
- [10] H. D. Luginsland, 155<sup>th</sup> Technical meeting of the Rubber Division ACS, 13-16<sup>th</sup> of April 1999, Chicago, Illinois, USA.
- [11] L. A. E. M. Reuvekamp, J. W. ten Brinke, P. J. van Swaaij, J. W. M. Noordermeer, *Kautsch. Gummi Kunstst.* 55 (2002) 41.
- [12] L. A. E. M. Reuvekamp, J. W. ten Brinke, P. J. van Swaaij, J. W. M. Noordermeer, *Rubber Chem. Technol.* 75 (2002) 187.
- [13] W. Dierkes, J. W. M. Noordermeer, M. Rinker, K. U. Kelting, C. Van de Pol, *Kautschuk Gummi Kunststoffe* 56 (2003) 340.
- [14] Wilma K. Dierkes, "Economic mixing of silica-rubber compounds", PhD Thesis: 2005, Dept. of Rubber Technology, Univ. of Twente, Enschede, the Netherlands.
- [15] F. Thurn, S. Wolff, *Kautsch. Gummi Kunstst.* 28 (1975) 733.
- [16] M. J. Wang, *Kautsch. Gummi Kunstst.* 61 (2008) 33.
- [17] M. Heinz, K.A. Grosch, 167<sup>th</sup> Technical meeting of the Rubber Division ACS, 16 18<sup>th</sup> of May 2005, San Antonio, Texas, USA.
- [18] C. D. Seiler, H. J. Vahlensieck, H. J. Kötzsch, United States Patent No. 4173576, (06-11-1979), to Dynamit Nobel Aktiengesellschaft.
- [19] R. Rauline, European Union Patent No. EP0501227B1, (02-09-1992), to Michelin Co.
- [20] L. Guy, Ph. Cochet, Y. Bomal, S. Daudey, *Kautsch. Gummi Kunstst.* 63 (2009) 383.
- [21] L. A. E. M. Reuvekamp, "Reactive mixing of silica and rubber for tires and engine mounts", PhD Thesis: 2003, Dept. of Rubber Technology, Univ. of Twente, Enschede, the Netherlands.
- [22] M. Heinz, *J. Rubb. Res.* 13 (2010) 91.



---

### ***Effect of the crosslink density and sulfur-length on wet-traction and rolling resistance performance indicators for passenger car tire tread materials***

---

*The scope of this chapter is to study the influence of different sulfur vulcanization systems for silica reinforced SBR/BR blends on the performance indicators of tire treads made thereof. Three series of compounds were prepared: with conventional, semi-efficient and efficient vulcanization systems. Each vulcanization system results in a specific overall crosslink density and different sulfur rank distribution: mono-, di- and polysulfidic of nature. The experimental results indicate that the influence of the overall crosslink density on the value of  $\tan \delta$  at 60 °C, an indication of rolling resistance, is higher than the type of crosslinks: A higher density of crosslinks reduces energy losses by limiting the segmental mobility of the polymer chains. Differences between the vulcanization systems manifest themselves only at relatively high strain levels, exceeding those used during measurements of the  $\tan \delta$  values at 60 °C. The dynamic mechanical analysis shows an increase in the glass transition temperature with rising overall crosslink densities. Differences in the crosslink densities turn out to be too small to have a significant influence of the LAT100 side force coefficient values, which are an indication of wet skid resistance of tire treads. This might be caused by the similar values of the storage modulus measured in the low temperature region, particularly close to the glass transition of the polymer blend.*

## 8.1 INTRODUCTION

Next to the elastomer type and silica-silane system, the crosslink density and distribution are important parameters which affect the physical, mechanical and viscoelastic properties of a vulcanizate<sup>1,2,3</sup>. Sulfur and organic peroxides are the two most commonly used vulcanizing agents. Unlike in a peroxide-cured system, in accelerated sulfur-curing systems various complex reactions occur during the curing process that form either mono-, di-, or polysulfidic crosslinks, and sulfidic ring structures within the polymer chains<sup>4,5</sup>. The ratio of accelerator to crosslinking agent determines the type and density of the crosslinks<sup>6,7</sup>. An accelerator increases the rate of cure and the efficiency with which sulfur is used in crosslinking compared to side reactions. The concentration of sulfidic linkages between carbon atoms of the polymer chains can be adjusted by varying the amounts of sulfur and accelerator<sup>8</sup>. High sulfur levels, e.g. 2 to 3.5 phr, and low levels of accelerator, 0.5 to 1 phr, generally described as conventional vulcanizing systems (CV), result in mostly highly flexible polysulfidic networks ( $[-C-S_x-C-]$  where  $x \geq 2$ ) with good mechanical properties<sup>9,10,11</sup>. However, the aging resistance is poor due to the temperature susceptibility of polysulfidic linkages. In conventional vulcanizations, part of the sulfur modifies the polymer chains instead of crosslink formation. Low sulfur levels, 0.25 to 0.7 phr, with high accelerator levels, 2.5 to 5 phr, commonly known as efficient vulcanizing systems (EV), introduce mono- or disulfidic networks ( $[-C-S_x-C-]$  where  $x = 1$  to 2), which exhibit low set characteristics, low stress relaxation and good resistance to aging. The third system called semi-efficient vulcanization (SE) with intermediate sulfur and accelerator loadings was introduced to eliminate poor cut growth of the compounds based on natural rubber in which efficient vulcanization was used. It is important to mention the early work of Scheele<sup>12</sup> and Saville and Watson<sup>13</sup>, who discussed network characterization; as well as the work of several authors from the Tun Abdul Razak Research Centre (TARRC)<sup>14,15</sup>. Ferry et al.<sup>16</sup> described the influence of the crosslink density on the dynamic properties of Natural Rubber (NR). They found that the influence of the crosslinking density on the  $\tan \delta$  values in the rubbery zone is significant, whereas in the transition zone it is minor. Hamed and Rattanasom<sup>17,18</sup> highlighted that a higher crosslink density increases the crack propagation and worsens

cut growth. Bielinski and Stępkowska<sup>19,20</sup> discuss the tribological properties of carbon black reinforced Emulsion-Styrene-Butadiene Rubber (E-SBR) and show that an increasing fraction of polysulfidic crosslinks has minor influence on the friction coefficient. Ramier et al.<sup>21</sup> investigated the adsorption of accelerators onto the surface of silica as reinforcing filler by the use of different grafting and coupling agents. They concluded that without the grafting agents, the vulcanization is likely to be more heterogeneous due to the adsorption of accelerators on the silica surface: crosslinks are more numerous and the polysulfidic bonds shorter in the filler neighborhood. Greensmith et al.<sup>22</sup> relate tensile strength with the crosslink density, and observed that the tensile strength passes through a maximum value with increasing crosslink density. They also reported that the tensile strength of a NR gum decreased in the sequence accelerated sulfur > sulfurless > peroxide > high energy radiation. This observation permitted Mullins<sup>23</sup> to conclude that the tensile strength depends on the type of crosslinks, decreasing in the order polysulphidic > di- and monosulfidic > carbon-carbon, in inverse order of the bond strength. The general dependence of different mechanical properties on the crosslink density is shown in Figure 1. Despite numerous publications in the field of curing systems, the knowledge concerning the influence of the vulcanization system on tire performance indicators in silica filled synthetic rubber is still limited.

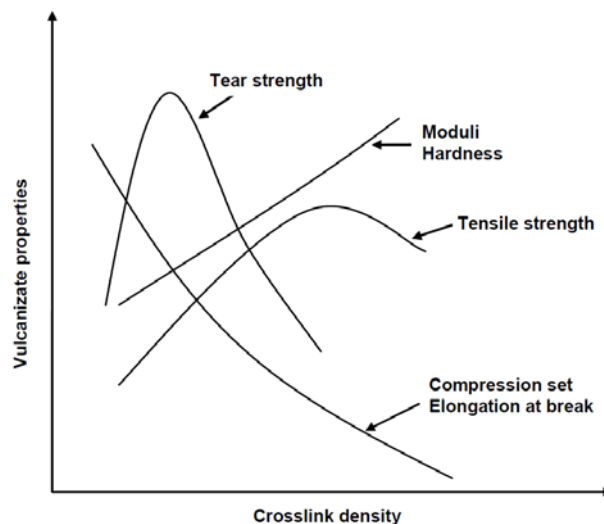


Figure 1: Vulcanizate properties versus crosslink density<sup>24</sup>.

## 8.2 EXPERIMENTAL

### 8.2.1 Compound formulations

In order to assess the influence of crosslink density and distribution on tire performance indicators, a series of batches corresponding to conventional, semi-efficient and efficient vulcanization systems were prepared. The ratio of elemental sulfur to N-tert-butyl-2-benzothiazolesulfenamide (TBBS) and diphenylguanidine (DPG) was adjusted to obtain different curing systems, but in order to limit the number of variables the ratio of TBBS to DPG was kept constant. To guarantee the same silica coverage in all the batches, the amount of silane coupling agent was also kept constant. A typical “Green tire” recipe as indicated in Table 1 was modified with the desired curing system. Additionally, a reference compound identical to the one used in the previous chapters was prepared. Detailed specifications of the ingredients are given in Table 2, Chapter 3.

Table 1: Rubber compound formulations.

| Ingredient     | Sample code |        |      |        |        |        |        |      |        |        |        |        |      |
|----------------|-------------|--------|------|--------|--------|--------|--------|------|--------|--------|--------|--------|------|
|                | CV-2        | CV-2.5 | CV-3 | CV-3.5 | SE-0.7 | SE-1.1 | SE-1.6 | SE-2 | EV-0.3 | EV-0.4 | EV-0.6 | EV-0.7 | Ref. |
| SSBR*          | 103         | 103    | 103  | 103    | 103    | 103    | 103    | 103  | 103    | 103    | 103    | 103    | 103  |
| BR             | 25          | 25     | 25   | 25     | 25     | 25     | 25     | 25   | 25     | 25     | 25     | 25     | 25   |
| Zeosil 1165 MP | 80          | 80     | 80   | 80     | 80     | 80     | 80     | 80   | 80     | 80     | 80     | 80     | 80   |
| TESPT          | 7           | 7      | 7    | 7      | 7      | 7      | 7      | 7    | 7      | 7      | 7      | 7      | 7    |
| TDAE           | 5           | 5      | 5    | 5      | 5      | 5      | 5      | 5    | 5      | 5      | 5      | 5      | 5    |
| Zinc oxide     | 2,5         | 2,5    | 2,5  | 2,5    | 2,5    | 2,5    | 2,5    | 2,5  | 2,5    | 2,5    | 2,5    | 2,5    | 2,5  |
| Stearic acid   | 2,5         | 2,5    | 2,5  | 2,5    | 2,5    | 2,5    | 2,5    | 2,5  | 2,5    | 2,5    | 2,5    | 2,5    | 2,5  |
| 6PPD           | 2           | 2      | 2    | 2      | 2      | 2      | 2      | 2    | 2      | 2      | 2      | 2      | 2    |
| TMQ            | 2           | 2      | 2    | 2      | 2      | 2      | 2      | 2    | 2      | 2      | 2      | 2      | 2    |
| Sulfur         | 2           | 2,5    | 3    | 3,5    | 0,7    | 1,13   | 1,56   | 2    | 0,25   | 0,4    | 0,55   | 0,7    | 1,4  |
| TBBS           | 0,23        | 0,3    | 0,38 | 0,46   | 0,46   | 0,69   | 0,92   | 1,15 | 1,15   | 1,53   | 1,91   | 2,3    | 1,7  |
| DPG            | 0,27        | 0,36   | 0,44 | 0,54   | 0,54   | 0,81   | 1,08   | 1,35 | 1,35   | 1,8    | 2,25   | 2,7    | 2    |

\* including 37,5 phr of extender oil

### **8.2.2 Mixing and curing**

A 1.6 liter Banbury mixer was used for mixing. This process was done in three steps according to the parameters as given in Table 5, Chapter 3. The first two steps of the mixing process were done in the internal mixer with an initial set temperature of 40 °C. The dump temperature of the compound was adjusted to be 155 °C by manually changing the cooling water flow and changing the rotor speed, if necessary. Data acquisition was done automatically. Addition of curatives was done on a two roll mill preheated to 50 °C.

Vulcanization of the sheeted samples for tensile tests was performed on a Wickert laboratory press (WLP 1600) at 160 °C and 100 bar for an optimal curing time ( $t_{95}$ ) obtained from Moving Die Rheometer (MDR 2000, Alpha Technologies) measurements according to ISO 6502. The samples for hardness tests were prepared in cylindrical molds and cured for a period of two times  $t_{90}$ . The samples for the DIN abrasion test were cured for  $t_{90}$  multiplied by 1.2. The adjustment of the curing time as measured in the rheometer was necessary due to the high thickness of the samples and the low thermal conductivity of the rubber compounds.

### **8.2.3 Characterization methods**

The overall apparent crosslink densities and distributions were measured by swelling experiments done in toluene according to Schotman and Datta, Ellis and Moore<sup>25,26,27</sup>. The test sheets were cut to obtain appropriate test pieces. Propanethiol in combination with piperidine was used to characterize the polysulfidic crosslinks according to the so-called chemical probe method as developed for NR. The further chemical probe method with hexanethiol and piperidine to characterize the poly- plus di- sulfidic crosslinks did not work properly, either because the methods pertain to NR and were never re-worked for SSBR or, secondly have never been tuned to silica-reinforced compounds. The determinations were done in twofold, and the average was taken as final value. For the purpose of this study only the overall apparent crosslink densities and polysulfidic fraction thereof are taken into account.

Mechanical properties of the samples were tested using a Zwick Z020 tensile tester according to ISO-37. A crosshead speed of 500 mm/min was used. The measurements were done at ambient temperature.

Payne effect measurements were done by using a Moving Die Rheometer, MDR 2000 from Alpha Technologies, after prior vulcanization for  $1.2 \times t_{90}$  at 160 °C in the MDR 2000. In order to assess the Payne effect values, the storage modulus at 1% strain and 90% strain were measured at 100°C and a frequency of 0.5 Hz.

Shore A hardness of the samples was measured at five different places on the samples, which were cylindrical with a diameter of 10 mm. The median value is given as a representative hardness of a particular sample.

Abrasion resistance was measured by a DIN abrader machine (Abrasion tester 564C from Karl Frank GmbH) according to method A of DIN 53516. The weight loss was measured and recalculated to a volume loss for each sample.

In order to characterize the wet skid resistance, dynamic mechanical analysis was performed on a Gabo Dynamic Mechanical Analyzer in a temperature-sweep mode from -100 °C to +100 °C with 1 % static and 0,1 % dynamic strain and a frequency of 10 Hz. In order to predict rolling resistance, single point measurements of  $\tan \delta = G''/G'$ , where  $G'$  is the storage modulus and  $G''$  is the loss modulus, at 60 °C with 2 % strain and a frequency of 10 Hz were performed.

A Laboratory Abrasion Tester 100 (LAT 100, VMI, the Netherlands) was used to estimate the wet skid resistance of the tire treads in conditions which simulate the real conditions on a road. The method used to measure wet friction has been described in Chapter 3.



## 8.3 RESULTS AND DISCUSSION

### 8.3.1 Crosslink density and sulfur length distribution

The variable ratio of elemental sulfur to accelerators results in different overall crosslink densities and ratios of polysulfidic crosslinks, see Table 2. When lowering the content of elemental sulfur and increasing the amount of accelerators in the compound, the overall crosslink density values decrease and there is a trend away from polysulfidic crosslinks to relatively higher di- and mono- sulfidic ranks.

Table 2: Crosslink densities.

| Crosslink density ( $10^{-4}$ mol/g) |         |              |
|--------------------------------------|---------|--------------|
| Sample code                          | Overall | Polysulfidic |
| CV-2                                 | 1,50    | 0,80 50%     |
| CV-2.5                               | 1,78    | 1,08 61%     |
| CV-3                                 | 1,97    | 1,11 56%     |
| CV-3.5                               | 2,40    | 1,54 64%     |
| SE-0.7                               | 0,74    | 0,29 29%     |
| SE-1.1                               | 1,12    | 0,57 51%     |
| SE-1.6                               | 1,51    | 0,81 54%     |
| SE-2                                 | 2,04    | 1,14 56%     |
| EV-0.3                               | 0,74    | 0,30 41%     |
| EV-0.4                               | 0,97    | 0,35 36%     |
| EV-0.6                               | 1,31    | 0,65 50%     |
| EV-0.7                               | 1,63    | 0,66 40%     |
| Ref.                                 | 1,64    | 0,95 58%     |

It must be clearly stated that unlike for carbon black reinforced and crosslinked elastomers, each silica particle can be treated as a poly-functional crosslink or nod: The silica surface is chemically bound to polymer chains via the coupling agents. The present measurement of the crosslink density and distribution does not differentiate between the polymer-polymer crosslinks and silica-polymer bonds. Considering that the same loading of TESPT was used in all batches, it is assumed that the amount of silica-polymer bonds also remains relatively unaffected. Hence, the effects described in this chapter may be considered as caused by changes in the density or distribution of the sulfidic crosslinks between the polymer chains.

### 8.3.2 Mechanical properties

Depending on the overall crosslink density, the highest values of tensile strength are observed for the efficient and semi-efficient crosslinking systems, see Figure 2. For the conventional system, an optimum in tensile strength is barely visible. Additionally, the efficient vulcanization system is also characterized by the highest values of tensile strength in comparison with the two other systems. This behavior is not a commonly observed feature. Two factors need to be considered in the case of tensile strength: the bond energy of the sulfidic crosslinks and the tendency to crack propagation. A higher bond energy of the mono- and disulfidic crosslinks is responsible for the highest values of the tensile strength for the samples with the efficient curing system. Next to bond energy, the tendency to crack propagation is the main cause of low tensile strength values samples with the conventional system: Crack propagation is easier in compounds with a higher overall crosslink density<sup>17,18</sup>. Hence the samples with conventional vulcanization have the lowest values of the tensile strength.

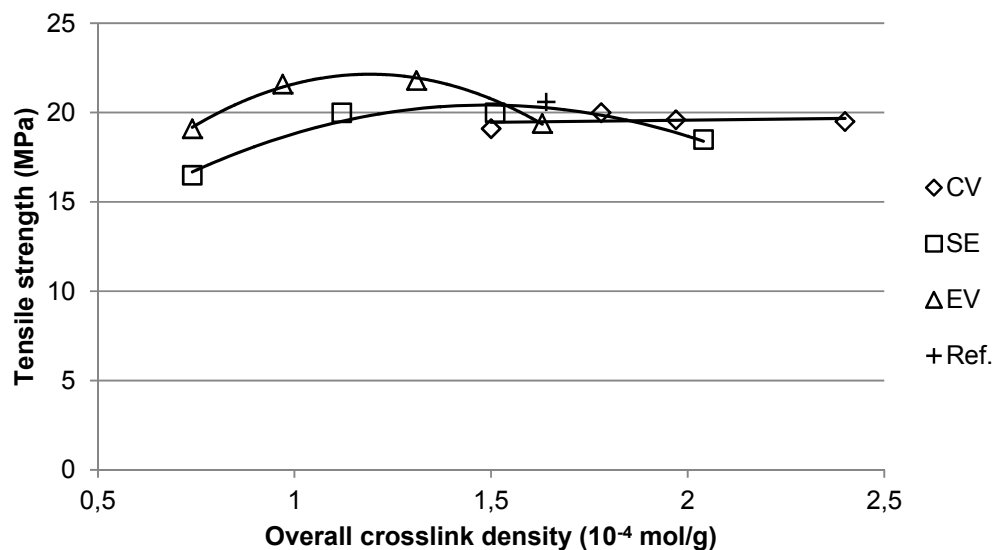


Figure 2: Tensile strength of the compounds with different curing systems.

The higher overall crosslink density is the dominating factor for strength properties, stronger than the well-known ability of the long, poly-sulfidic crosslinks to reformation followed by stress dissipation and increased tensile strength. The semi-efficient system

with moderate values of the overall crosslink density ranks somewhere in between the other two curing systems concerning tensile strength.

The initial increase in tensile strength observed for each vulcanization system can be caused by a primary gain in toughness caused by rising crosslink density. Further increase in crosslink density only increases the stiffness. Compounds with a higher stiffness are more prone to crack propagation what reduces the tensile strength. Furthermore, the appearance of the maximum in tensile strength is not necessarily related to the filler-polymer interaction as other authors reported the appearance of the optimum in the tensile strength also in unreinforced compounds <sup>28</sup>.

With increasing overall crosslink density, the values of elongation at break are decreasing for all the crosslinking systems, see Figure 3: The vulcanizates become less elastic what contributes to easier crack formation and sooner breakage of the sample. When a special case is considered in which the elongation at break is compared for samples with similar overall-crosslink densities, the conventional system is characterized with a highest values of the elongation at break. This shows the ability of the polysulfidic crosslinks to breaking and partial reformation and consequent energy dissipation at very high strains.

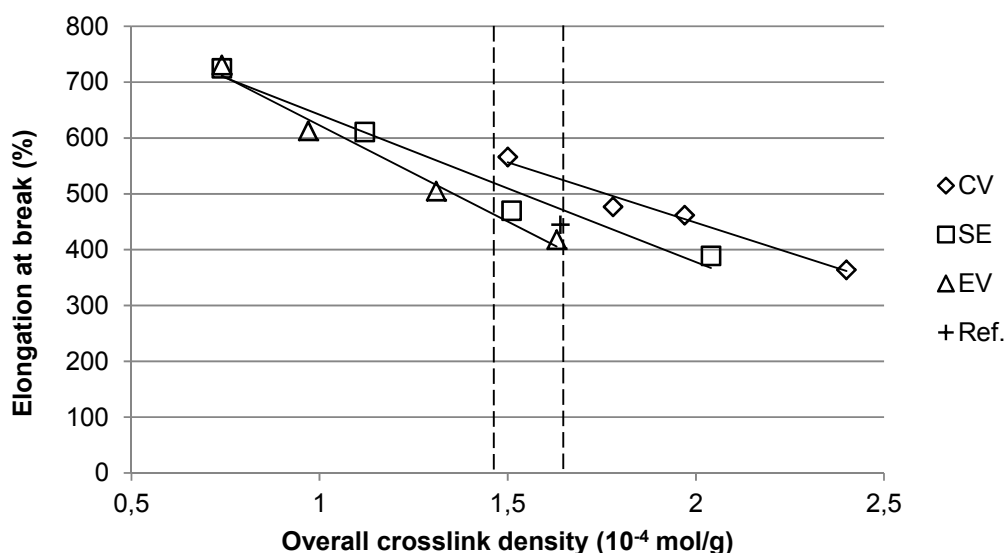


Figure 3: Elongation at break of the compounds with different curing systems.

### 8.3.3 Abrasion resistance

The EV-vulcanizate with the highest crosslink density is also characterized by the lowest value of abrasion loss in comparison with the semi-efficient and conventional vulcanization systems, see Figure 4. This trend is also seen for the SE-material: Increasing the ratio of mono- and disulfidic crosslinks to polysulfidic ones creates a stronger and more durable rubber compound. As a result a higher force is necessary to cut micro-particles out-of the compound by the abrasive micro-asperities.

Additionally, for each curing system the abrasion loss reaches a minimal value with respect to the overall crosslink density. The efficient curing system is characterized by the highest dependence of abrasion loss on the overall crosslink density, while for the conventional vulcanization the abrasion loss does not depend on the crosslink density.

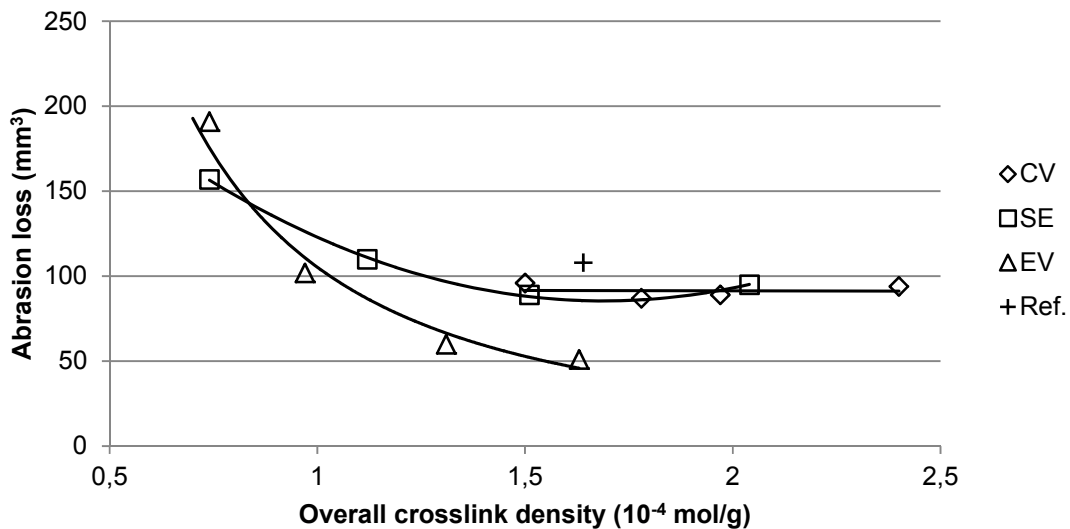


Figure 4: DIN abrasion of the compounds with different curing systems.

### 8.3.4 Payne effect

In the unvulcanized state, compounds with different curing systems are characterized by mutually comparable values of the storage modulus over the entire range of strains, see Figure 5. As expected, in the unvulcanized state, the polymer crosslinks and filler-polymer bonds are not formed yet, therefore they do not contribute to the Payne effect value. Moreover, the comparable values of the storage modulus shown in Figure 5 indicate that in all the cases the silica surface was covered to a similar degree by the

TESPT and accelerators. Even in the case in which 2,3 phr of TBBS and 2,7 phr of DPG were used, the difference in storage modulus is not more than 0,05 MPa.

The vulcanization process creates clear differences in the storage moduli, see Figure 6. The values of the storage modulus at both, very high and very low strain levels, increase with the curative concentrations for each curing system.

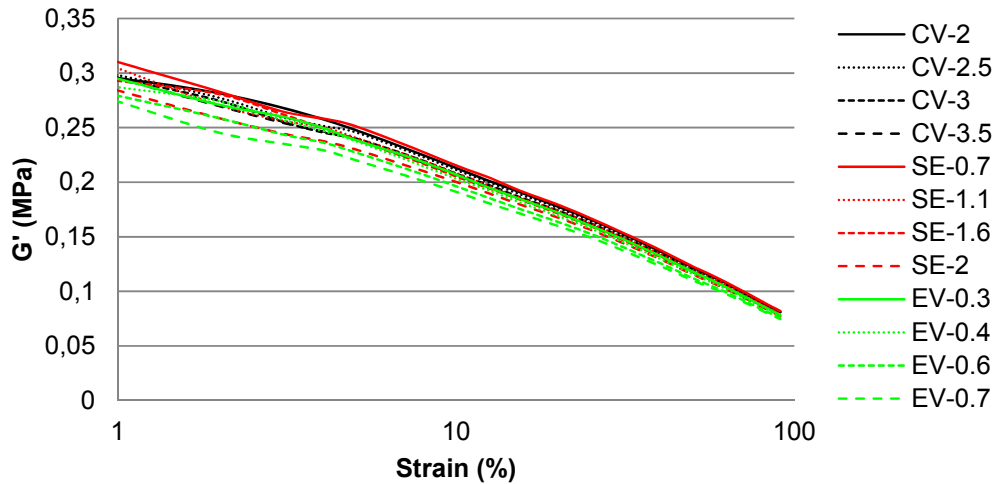


Figure 5: Payne effect versus strain of green compounds.

The polymer network, resp. the filler-filler and filler-polymer interactions contribute to the final values of the Payne effect. At low strain level, the deformation energy is mainly stored in the filler network. This network is unstable and gradually disintegrates with increasing strain levels. At the highest strain levels the polymer-filler and what is left of the polymer network are responsible for the energy storage. When the same types and amounts of filler and coupling agent are used, the differences in the filler-filler interaction can be considered as invariable. In general, the energy can be stored more efficiently in a compound with a higher overall crosslink density, because this increases the storage modulus values at both the low and high range of the strain scale.

Comparison between the values of the storage moduli of a compound before and after vulcanization is an example of how the energy storage increases by introduction of the sulfur crosslinks without changes in the filler-filler interactions. The Payne effect can be used to assess the filler-filler interactions only when the crosslink densities and the polymer-filler interactions are similar.

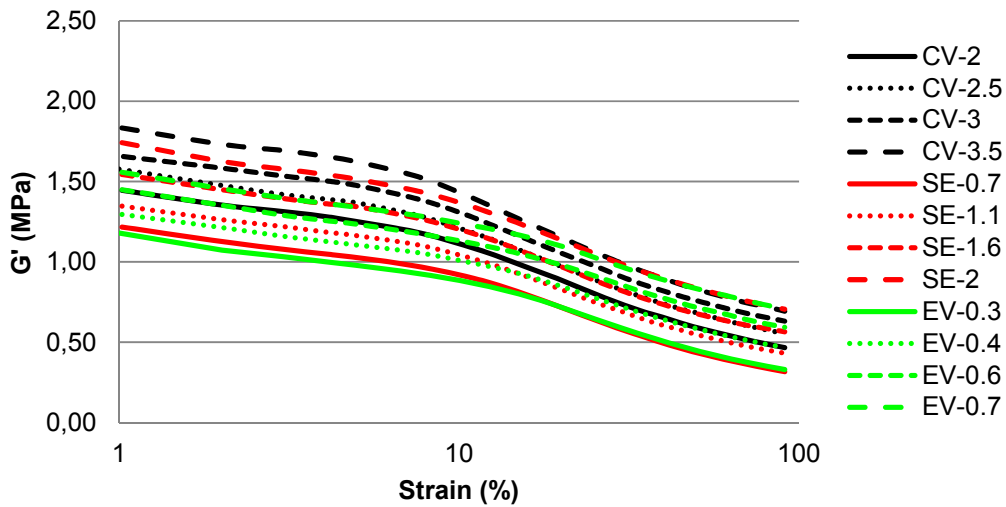


Figure 6: Storage modulus versus strain of cured compounds.

The dependence of the Payne effect on the overall crosslinking density varies for each curing system, see Figure 7. This dependence is stronger for the conventional and semi-efficient systems and fades away for the efficient curing. With increasing content of the polysulfidic crosslinks the Payne effect becomes higher.

The conventional curing system is characterized by the highest Payne effect because of its high storage modulus at low strains which is the result of the highest overall crosslink density. The efficient curing system is characterized by the lowest values of the Payne effect because lower overall crosslink density leads to low values of the storage modulus at low strains. Furthermore, probably the higher percentage of mono- and di-sulfidic crosslinks can last unbroken, preventing the drop in the value of the storage modulus at high strains. This effect is particularly clear when the samples with the highest concentration of curatives are compared, see Figure 6.

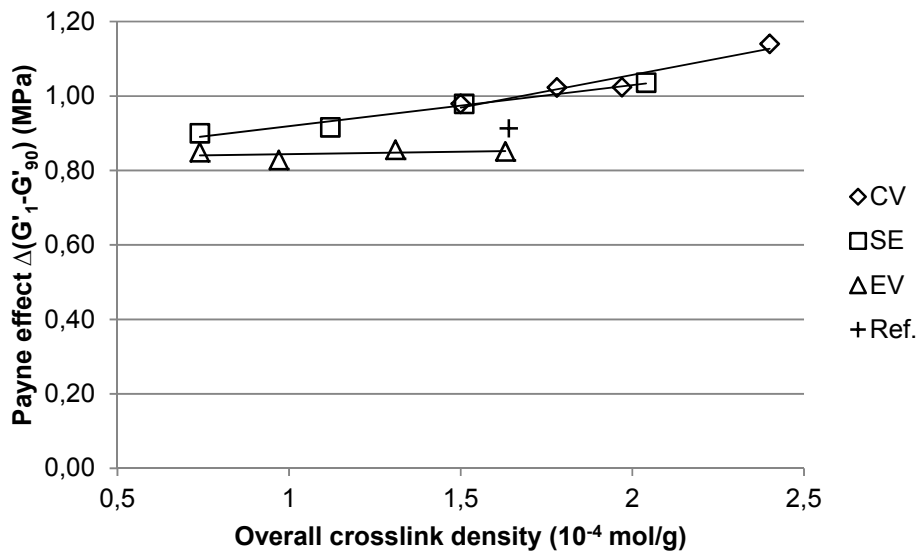


Figure 7. Payne effect of cured samples versus overall crosslink density.

The compounds with the efficient vulcanization system reach higher storage moduli at 90 % strain in comparison with the semi efficient and conventional systems at similar overall crosslink densities, see Figure 8. The higher values of the storage modulus might be the result of differences in the ratios of mono- and disulfidic crosslinks to polysulfidic ones. Apparently, at similar overall crosslink density, a higher percentage of the rigid mono- and disulfidic crosslinks increases the efficiency of energy storage of the compound, which is evident in the higher storage modulus. A higher percentage of polysulfidic crosslinks which are prone to breaking and recombination during deformation may be the cause of the lower energy storage capabilities of the compounds in which the conventional curing system is used.

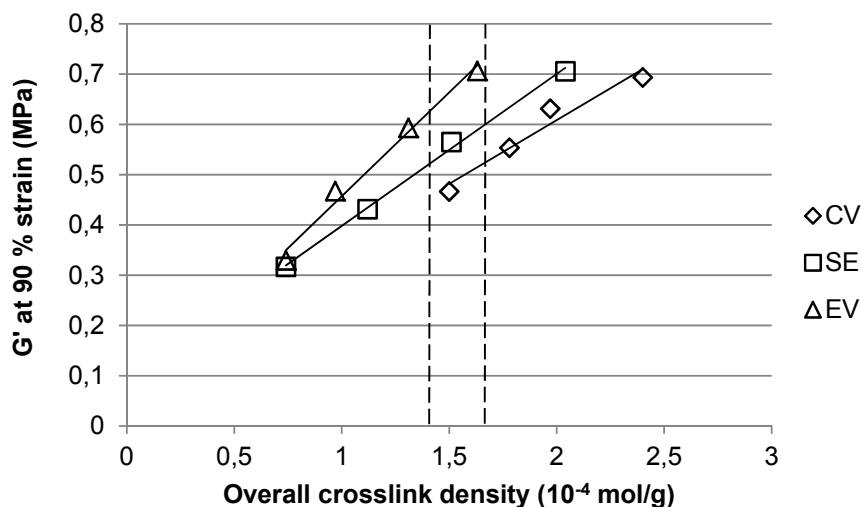


Figure 8: Storage modulus at 90 % strain versus overall crosslink density.

### 8.3.5 $\tan \delta$ at 60 °C: indicator of rolling resistance

Three factors contribute to energy dissipation at higher temperatures: polymer crosslinks, filler-filler and filler-polymer interactions. In this study, the two last factors may be considered as constant because all compounds contain the same amount of coupling agent. With this assumption, the influence of polymer crosslinks on the value of  $\tan \delta$  at 60 °C can be observed. The hysteresis of the compounds at higher temperatures depends mainly on the overall crosslink density: Figure 9 shows a single correlation. Therefore, the compounds in which the conventional vulcanization was used are characterized by the lowest values of  $\tan \delta$  at 60 °C amongst the investigated vulcanization systems. The distribution and type of crosslinks can be considered as negligible for the  $\tan \delta$  values at 60 °C. Patterns as visible in Figure 8, characteristic for each vulcanization system, do not appear in Figure 9.



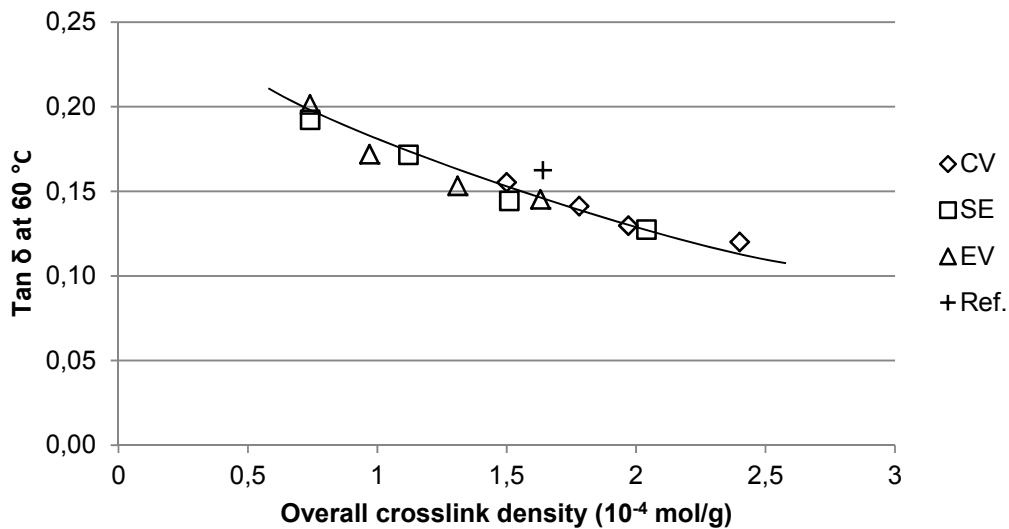


Figure 9: Tan  $\delta$  at 60 °C values versus overall crosslink density.

Since the strain level at which the tan  $\delta$  was measured is 6 %, it may be assumed that none of the existing crosslink types undergoes breaking or recombination like in the case of the measurements of the tensile strength and the storage modulus at 90 % strain. Therefore, the overall crosslink density is the only factor that differentiates the various compounds. The energy can be stored and released more efficiently and without a loss in a compound characterized by a high overall crosslink density: an increased number of chemical nodes connecting the polymer chains decreases the possibility of their rearrangements, what reduces the energy dissipation.

### 8.3.6 Tan $\delta$ at low temperatures: indicator of wet skid resistance

As shown in Figure 10, a rising amount of curatives in the compounds has an influence on the glass transition temperature (as is well known), but only minor changes in the height of the tan  $\delta$  peak are visible. Starting from approximately 10 °C onwards, the differences between the individual curves gradually rise. For each vulcanization system, the compounds with the highest loadings of curatives are characterized by the lowest hysteresis at higher temperatures, as already seen in Figure 9.

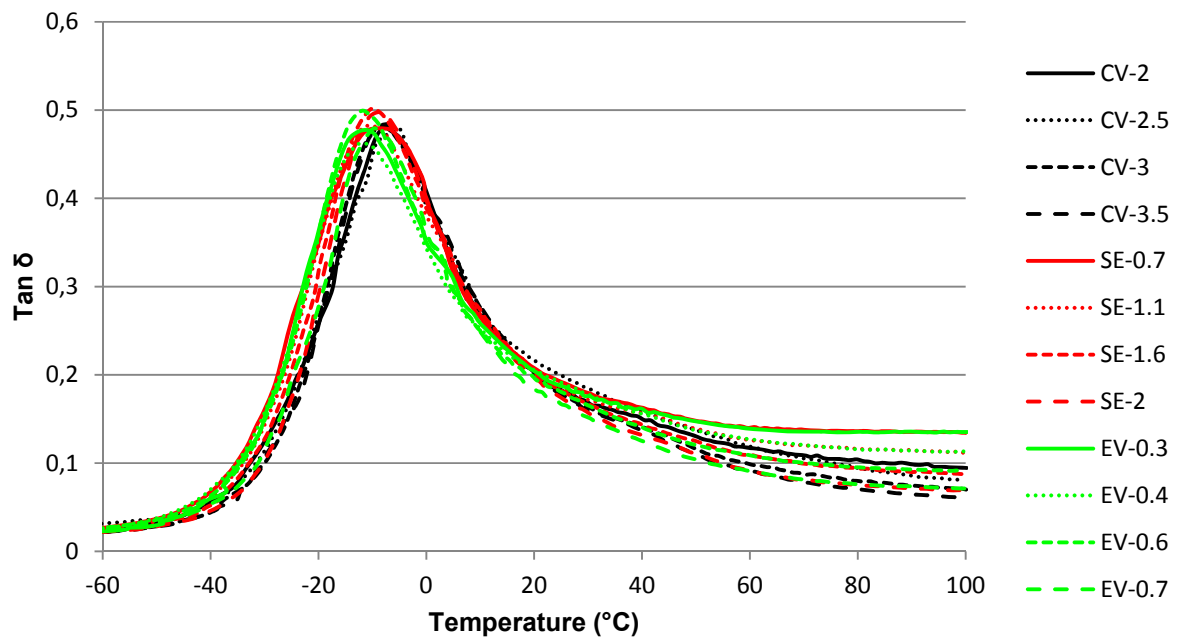


Figure 10: Tan  $\delta$  values in temperature sweep mode for compounds with different vulcanization systems.

The increase in the overall crosslink density is large enough to cause significant changes in the segmental mobility of the elastomer chains which is visible in the increasing glass transition temperature, see Table 3. For the compound with the efficient vulcanization system, the average  $T_g$  is around  $-12\text{ }^\circ\text{C}$ , followed by the compounds with the semi-efficient system, for which the  $T_g$  is equal to  $-9\text{ }^\circ\text{C}$ , and the conventional system with the highest  $T_g$  of around  $-7\text{ }^\circ\text{C}$ . Furthermore, a similar height of the  $\tan \delta$  maximum demonstrates that even substantial changes in the crosslink density cannot significantly change the hysteresis in the glass transition temperature range, hence the amount of polymer chains which contribute to the intermolecular friction remains unaffected. Only a variation in the adsorption of the polymer chains at the filler surface which virtually lowers the fraction of the polymer which undergoes the glass transition can cause changes in the peak height. Change in the crosslinking system does not increase nor decrease the total amount of chains undergoing segmental, intermolecular friction. Hence the peak height remains unaffected.

Table 3: Comparison of dynamic properties at the glass transition temperature.

| Sample code   | x-link density<br>10 <sup>-4</sup> mol/g | T <sub>g</sub><br>(°C) | G'<br>(MPa) | G''<br>(MPa) |
|---------------|--|------------------------|-------------|--------------|
| <b>CV-2</b>   | 1,50                                     | -6,0                   | 115         | 53           |
| <b>CV-2.5</b> | 1,78                                     | -5,5                   | 97          | 39           |
| <b>CV-3</b>   | 1,97                                     | -7,0                   | 100         | 48           |
| <b>CV-3.5</b> | 2,40                                     | -7,0                   | 89          | 43           |
| <b>SE-0.7</b> | 0,74                                     | -9,0                   | 101         | 48           |
| <b>SE-1.1</b> | 1,12                                     | -9,5                   | 95          | 46           |
| <b>SE-1.6</b> | 1,51                                     | -10,0                  | 94          | 47           |
| <b>SE-2</b>   | 2,04                                     | -9,0                   | 100         | 50           |
| <b>EV-0.3</b> | 0,74                                     | -11,0                  | 88          | 42           |
| <b>EV-0.4</b> | 0,97                                     | -11,5                  | 88          | 41           |
| <b>EV-0.6</b> | 1,31                                     | -12,0                  | 99          | 49           |
| <b>EV-0.7</b> | 1,63                                     | -12,0                  | 87          | 43           |

At higher temperatures, above 10 °C, the decreasing hysteresis of compounds with an increasing loading of curatives is the result of the rising overall crosslink density. At temperatures above the glass transition, the polymer chains are more mobile and can perform quasi-liquid cooperative rearrangements, which is the cause of the energy dissipation. A higher overall crosslink density of the compounds reduces the possibility of these quasi-liquid cooperative rearrangements, what is visible in the lower hysteresis.

### **8.3.7 Side force coefficient: wet skid resistance**

The side force coefficient values increase for each crosslinking system with increasing loading of curatives and overall crosslink density, see Figure 11. However, the differences in side force coefficient between the samples are small. The minimum and maximum values of the side force coefficient are very similar for all three curing systems.

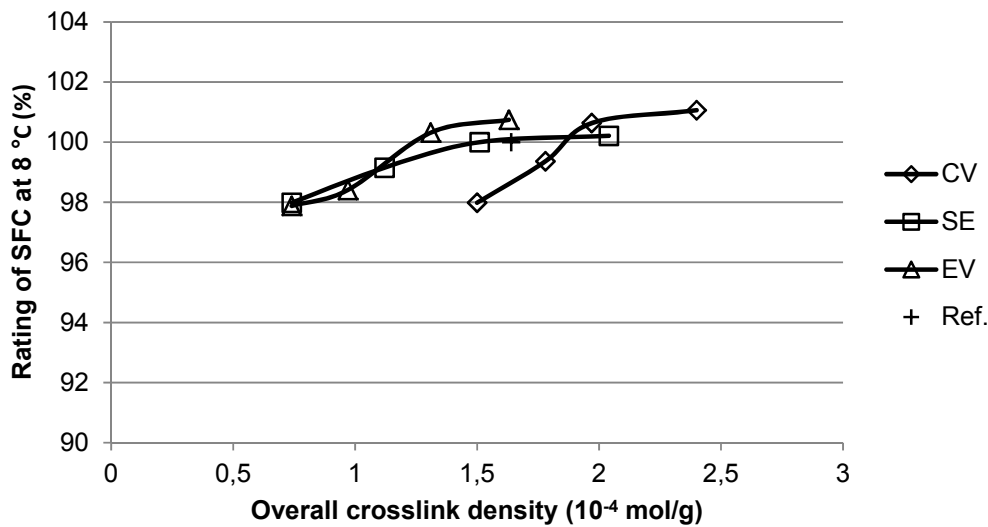


Figure 11: Side force coefficient rating at 8 °C versus overall crosslink density.

These minor differences in the side force coefficient of the samples can be explained when the dynamic properties at lower temperatures, from 0 to 20 °C are considered, see Figure 10. The different vulcanization systems all show similar values of the hysteresis at lower temperatures. The value of the storage modulus for all samples measured at the  $\tan \delta$  peak is in the range of 90 to 100 MPa. The differences in the measured stiffness are therefore too small to show an effect on the side force coefficient.

Another factor which could cause these small differences in SFC-ratings is the rising hardness of the compounds with increasing loading of the curatives. A comparison of the side force coefficient and Shore A hardness values is shown in Figure 12. The side force coefficient correlates with hardness for each vulcanization system separately. However, when for example the minimal values of the side force coefficient for the efficient and conventional systems are compared, it is clear that in spite of a substantial hardness difference of 8 °ShA between the samples, the same value of the side force coefficient is registered. Therefore, a clear correlation between hardness and the side force coefficient does not exist as this study has shown: a correlation only exist within a series with the same type of curing system.

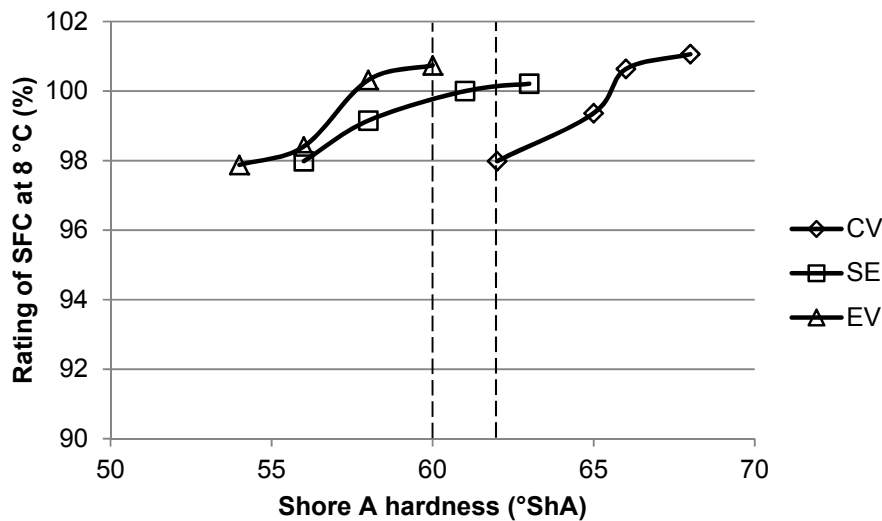


Figure 12: Rating of the side force coefficient versus Shore A hardness.

The data shown in Figure 12 also allow to compare the individual systems with a similar hardness. When the hardness in the range of 60 to 62 °ShA is considered, the efficient curing system is characterized by the highest value of the side force coefficient followed by the efficient and conventional systems.

#### 8.4 CONCLUSIONS

- A maximum in tensile strength is pronounced for the efficient curing system, and the least visible for the conventional vulcanization system. The samples with the efficient vulcanization are also characterized by the highest values of the tensile strength, which can be caused by the lower crack propagation ability of the material with lower overall crosslink density together with a higher bond energy of the mono- and disulfidic crosslinks.
- Increasing the overall crosslink density of the compounds causes a rise in the glass transition temperature by about 5 °C between the compounds with the efficient curing system and the conventional system. However, no major changes in the height of the  $\tan \delta$  peak are registered. Apparently, only variations in the polymer immobilization on the filler surface can lead to changes in the peak

height, for instance in the case of silicas differing in the specific surface area or different coupling agents.

- The values of  $\tan \delta$  at 60 °C are decreasing with increasing overall crosslink density of the compounds. This trend is independent of the crosslink types, as at the strain level applied during the measurement the ability towards recombination of longer poly-sulfidic crosslinks is not yet playing a role.
- The compounds with the different curing systems are characterized by only a small changes in the LAT-100 side force coefficient. This could be caused by minor differences in the storage and loss moduli of the compounds at low temperatures. For a similar value of hardness the efficient and semi-efficient curing systems give slightly higher values of the SFC in comparison with a conventional system.

## REFERENCES

---

- [1] J. Lal, *Rubber Chem. Technol.* 43 (1970) 664.
- [2] C.G. Moore, B.R. Trego, *J. Appl. Polym. Sci.* 5 (1961) 299.
- [3] C.M. Kok, V.H. Yee, *Eur. Polym. J.* 22 (1986) 341.
- [4] M. Nasir, G.K. Teh, *Eur. Polym. J.* 24 (1988) 733.
- [5] W. Salgueiro, A. Marzocca, A. Somoza, G. Consolati, S. Cerveny, F. Quasso, S. Goyanes, *Polymer* 45 (2004) 6037.
- [6] A.J. Marzocca, S. Goyanes, *J. Appl. Polym. Sci.* 91 (2004) 2601.
- [7] R. Joseph, K.E. George, D.J. Francis, *J. Appl. Polym. Sci.* 35 (1988) 1003.
- [8] J.A. Brydson, "Rubber Chemistry", Applied Science Publishers Ltd, London (1978) Ch. 8.
- [9] L. Bateman, J.I. Cunneen, C.G. Moore, L. Mullins, "The chemistry and physics of rubber-like substances", John Wiley & Sons, New York (1963) 715.
- [10] B.A. Dogadkin, Z.N. Tarasova, *Rubber Chem. Technol.* 27 (1954) 883.
- [11] K.J. Saunders, "Organic Polymer Chemistry", 2nd ed. Chapman & Hall, London, (1988) Ch. 20.
- [12] W. Scheele, *Rubber Chem. Technol.* 34 (1961) 1306.
- [13] B. Saville, A.A. Watson, *Rubber Chem. Technol.* 40 (1967) 100.
- [14] M. Porter, "The Chemistry of Sulfides," A.V. Tobolsky, Ed., John Wiley & Sons, Inc., New York (1968).
- [15] M. Porter, "Organic Chemistry of Sulfur," S. Oae, Ed., Plenum Press, New York (1977).
- [16] J.D. Ferry, R.G. Mancke, E. Maekawa, Y. Oyanagi, R.A. Dickie, *Rubber Chem. Technol.* 39 (1966) 897.
- [17] G.R. Hamed, N. Rattanasom, *Rubber Chem. Technol.* 75 (2002) 323.
- [18] G.R. Hamed, N. Rattanasom, *Rubber Chem. Technol.* 75 (2002) 935.
- [19] D.M. Bieliński, *Archives of Civil and Mechanical Engineering*, 7 (2007) 15.
- [20] D.M. Bieliński, A. Stępkowska, *Archives of Civil and Mechanical Engineering*, 13 (2013) 192.
- [21] J. Ramier, L. Chazeau, C. Gauthier, L. Guy, M.N. Bouchereau, *Rubber Chem. Technol.* 80 (2007) 183.
- [22] H.W. Greensmith, L. Mullins, A.G. Thomas, "The Chemistry and Physics of Rubber-like substances", Applied Science Publishers Ltd, London (1963) Ch. 10.
- [23] L. Mullins, "Relation between structure and properties", Proc. NRPRA Jubilee Conf. Cambridge (1964).
- [24] Coran, A. Y. In *Science and Technology of Rubber*, 2<sup>nd</sup> ed.; Mark, J. E.; Erman, B.; Eirich, F. R., Eds.; Academic Press: New York, (1994).
- [25] A.H.M Schotman, R.N. Datta, *Rubber Chem. Technol.* 69 (1996) 727.

- 
- [26] B. Ellis, G.N. Welding, *Rubber Chem. Technol.* 37 (1964) 571.
- [27] C.G. Moore, *J. Polym. Sci.* 32 (1958) 503.
- [28] L. Gonzalez, A. Rodriguez, J.L. Valentin, A. Marcos-Fernandez, P. Posadas, *Kautschuk Gummi Kunststoffe*, 58 (2005) 638.





### Summary

---

Since the introduction of the “Green Tire”, silica has become one of the most important fillers used in tire tread rubber compounds due to its contribution to a better environment. Silica reinforced tire treads are characterized not only by reduced rolling resistance but also improved wet skid resistance, compared to carbon black as a filler. However, processing of silica-filled compounds is accompanied with many difficulties caused by the polarity difference between silica and polymer. To overcome these polarity differences a bi-functional silane coupling agent is generally used. A typical silane coupling agent is bis-(triethoxysilylpropyl) tetrasulfide (TESPT). The silane chemistry during rubber processing is very complicated. Basically, from a processing point of view, two coupling reactions take place when TESPT is utilized. The first reaction is a coupling reaction between the TESPT molecule and the silica surface, the so-called silanization reaction. For this reaction hydrolysis of TESPT is required and water necessary for this step is available on the silica surface. Silanization of the silica surface improves processing by a substantial decrease of torque during mixing. The second reaction is silane-rubber coupling, taking place preferably only during the vulcanization stage. However, it is well known that TESPT can act as a sulfur donor during rubber processing. Therefore, premature crosslinking or scorch may take place at excess temperatures in the mixing stage already. Great care needs to be taken during silica compounding to fit in the temperature range in which optimal silanization can proceed and the scorch reaction is minimized. All these reactions can take place simultaneously during silica rubber processing, and therefore the reinforcing mechanism of silica is much more complicated than that of the carbon black.

The thesis starts with a brief history of synthetic rubber in **Chapter 1** where the advantages of silica over carbon black as reinforcing fillers for rubber and the effect of coupling agents are also reviewed. In **Chapter 2** the influence of various reinforcing

fillers as well as of different coupling agents and rubber-polymer modification on tire performance is reviewed.

In **Chapter 3** five types of silica, differing in specific CTAB surface area and aggregate size, are tested in a passenger car tire compound. One of the silicas, SSA-200 (the number indicates the specific CTAB surface area given in  $\text{m}^2/\text{g}$ ) is also characterized by a different structure – its aggregates are larger while the specific surface is similar to the SSA-195 type. The silica types with smaller aggregate dimensions and larger specific surface areas show a higher reinforcing effect, as illustrated by improved tensile properties. However, the dispersibility of these silicas is more difficult compared to the silica types with larger aggregate sizes. Compounds, in which SSA-195 is used, have superior tensile properties and the lowest loss modulus at lower temperatures. This silica type results in the highest values of the side force coefficient (SFC) in LAT-100 testing, indicating best wet grip. Adjustment of the silica loading in order to obtain similar hardnesses of the cured compounds reverses the order of the dynamic curves. Silica with the smallest aggregates is still superior regarding the side force coefficient. However, the trend visible for constant silica loading has disappeared. This demonstrates that from the view point of wet skid resistance, smaller aggregate sizes of fillers are better, and that a higher aspect ratio of the fillers like in the case of the SSA-200 type does not improve the wet skid resistance. Silicas with larger aggregate sizes, SSA-80 and SSA-110 lead to low hysteresis at high temperatures, but their low reinforcing effect makes them also less appropriate as reinforcing fillers for tire tread compounds. The dynamic properties of materials containing highly reinforcing silica can be further improved by using less filler, but the tensile properties will suffer in case of SBR/BR used as polymer matrix. Furthermore, good dispersion of the nano-sized aggregates is the key to obtain rubber composites with superior overall properties. With the selected measurement parameters for dynamic analysis and for the LAT-100, no correlation of the hysteresis at 0 – 20 °C with the side force coefficient was found for both series.

The influence of physical and chemical filler-polymer bonds on the tire performance indicators is investigated in **Chapter 4**. Silica is compounded with 1,6-bis-(triethoxysilyl)hexane (TESH), to obtain interactions similar to those which exist between

carbon black and rubber. The bound rubber content data confirm this. Introduction of physical interactions instead of chemical bonds radically decreases the values of the tensile strength because of inertness of the silica surface. The dynamic properties of the samples measured at low temperature again do not correspond with the wet skid resistance as measured by the LAT-100. Replacement of physical bonds (TESH) by chemical interactions (TESPT) between rubber and fillers increases the values of side force coefficient measured with the LAT-100. Consequently, chemical bonds are preferred for good wet skid resistance of the tire treads. The assumption that under the influence of energy resulting from skidding, polymer molecules physically bonded to the filler surface can easily be displaced, what should increase the energy dissipation and as a consequence increase the wet skid resistance, is not correct. Furthermore, the experiments performed by Heinz (M. Heinz, J. Rubb. Res., 13 (2010) 91) show strong correlations between the values of the side force coefficient measured on the LAT 100 and (wet) skid values obtained during road tests. At the same time he points out that no correlation exists between dynamic measurements and road tests. As a consequence, a correlation between LAT-100 and dynamic measurements does not exist. The contradiction between the higher hysteresis of the compounds at 0 – 20 °C but yet lower values of the side force coefficient measured with the LAT-100 found in the present study concur with the tests done by Heinz. The author of this thesis inclines towards the use of the LAT-100 as a decisive tool during assessment of the wet skid potential of a rubber compound.

Bis-(dimethylethoxysilylpropyl) tetrasulfide (DMESPT), a silane with the potential of higher utilization of the silanol groups available on the silica surface, is investigated in **Chapter 5**. Providing just one ethoxy-group instead of three in the silane coupling agent, improves both, wet skid and rolling resistance. An explanation of these effects is a more rigid filler-polymer interface in the case of DMESPT, compared to TESPT with three ethoxy-groups, which generate ethanol. The alcohol remains partially adsorbed on the interface between filler and polymer and thus influences the properties of the material. Both silanes, TESPT and DMESPT, bind the same number of silanol groups available on the silica surface as measured by the Payne effect of the green compounds. Therefore, the low steric hindrance caused by absence of lateral ethoxy-groups in the

DMESPT molecule does not result in a higher number of bonded silanol-groups than in the case of TESPT. The filler-polymer interactions determine the peak height of the  $\tan \delta = f(T)$  curve: the more restricted the polymer movements on the filler surface, the lower the height of the peak, as the immobilized polymer acts more filler-like than polymer-like. In the case of DMESPT, the polymer-filler interface is more rigid in comparison to TESPT: The latter possesses secondary ethoxy-groups, which react when the material heated up during further processing, and splits off ethanol which partially remains accumulated at the interface, softening the interface and thus increasing the energy loss (indicated by  $\tan \delta$ ) by desorption and sliding of polymer chains at lower temperatures. Contrary to TESPT, for DMESPT the SFC of the samples increases with rising loading of this silane. More restricted movements of the polymer chains in the glassy layer cause increased stiffness of the compounds containing DMESPT. A higher local stiffness around the filler particles with high DMESPT concentrations results in higher wet skid resistance as indicated by the SFC.

The impact of the linker length which connects the silicone atom with the sulfidic moiety in the silane coupling agent is described in **Chapter 6**. Compounds containing a silane with longer linker, bis-(triethoxysilyldecyl) tetrasulfide (TESDeT) are characterized by a slightly higher elongation at break but similar tensile strength compared to the TESPT containing compounds. A longer and more flexible linker as in the case of TESDeT can accommodate higher strains without cracking. An increased linker length of the coupling agent reduces rolling resistance significantly, but does not change the wet skid resistance. The longer linker of TESDeT can accommodate higher strain amplitudes within the filler-polymer interphase occurring during deformation, instead of transferring them directly onto the filler surface. An increased linked length increases the hysteretic losses in the glass transition temperature range of the elastomer. A more flexible linker in the case of TESDeT leads to less restricted polymer movements at the filler-polymer interphase in comparison with the reference silane. Hence, more polymer can contribute to the energy dissipation phenomena at the glass transition temperature. By replacing TESPT by a silane with a longer linker, the rolling resistance of this material in a tire tread can be improved. However, the major drawback of TESDeT is its high molecular

weight: in order to obtain equimolar concentrations, higher amounts of TESDeT need to be applied compared to TESPT.

**Chapter 7** is dedicated to the influence of the reactivity of silane coupling agents towards the silica surface on the tire tread performance indicators. Two tailored silanes without lateral alkoxy-groups are synthesized: bis-(dimethylmethoxysilylpropyl) tetrasulfide (MMeOS) and bis-(dimethylmethoxyethoxysilylpropyl) tetrasulfide (MMeOEtOS), and compared in a tire tread compound with TESPT as reference. The clear advantage of these silanes compared to TESPT is a substantially lower alcohol-generation during the mixing process, what is not only a positive environmental aspect of the monoethoxy silanes, but also gives an improvement in processing of the rubber compounds. The type of alkoxy-groups of the silane coupling agents determines the type of alcohol-byproducts of the silanization reaction, and thus the kinetics of the silanization reaction, as well as the influence on compound processing and properties. The low boiling point of methanol leads to a relatively fast reaction with the silanol groups on the silica surface, and presumably a higher degree of utilization of silanol groups; this can be derived from the low Payne effect values of the corresponding uncured compounds. Apart from the boiling point, another important parameter concerning the alcohol evolved during silanization needs to be considered: the ability to form hydrogen bonds. The higher tendency of 2-methoxyethanol-containing silanes to form intra- and intermolecular hydrogen bonds in comparison to methanol- or ethanol-containing causes increased stiffness of the polymer-filler interface at lower temperatures, and as a result higher side force coefficient values in comparison to the materials containing MMeOS and TESPT. Due to the lack of lateral alkoxy-groups, both monomethoxy- and monomethoxyethoxy-silanes are also characterized by lower values of  $\tan \delta$  at 60 °C in comparison with TESPT. As a result of the lower amount of alcohol provided in the silane, less alcohol remains adsorbed onto the polymer-filler interphase. This decreases the probability of polymer segmental movements, what reduces energy losses. The more “rigid” polymer-filler interphase in the case of MMeOS and MMeOEtOS at lower temperatures increases the stiffness of the compound as measured with the storage modulus. The force necessary to deform the tread of a tire

into micro-cavities is higher for stiffer compounds and results in an improved, higher side force coefficient in comparison with TESPT.

The impact of three different sulfur vulcanization systems is described in **Chapter 8**. A maximum in tensile strength is most pronounced for the efficient curing system, and the least visible for the conventional vulcanization system. The samples with efficient vulcanization are also characterized by the highest values of the tensile strength, which can be caused by lower crack propagation ability of the material with lower overall crosslink density, together with a higher bond-energy of the mono- and disulfidic crosslinks. Increasing the overall crosslink density of the compounds causes a rise in the glass transition temperature by about 5 °C between the compounds with the efficient curing system and the conventional system. However, no major changes in the height of the  $\tan \delta$  peak are registered. Apparently, only variations in the polymer immobilization on the filler surface can lead to changes in the peak height, for instance in the case of silicas differing in specific surface area or different coupling agents. The values of  $\tan \delta$  at 60 °C are decreasing with increasing overall crosslink density of the compounds. This trend is independent of the crosslink types, as at the strain level applied during the measurement the ability towards recombination of longer poly-sulfidic crosslinks is not yet playing a role. The compounds with the different curing systems are characterized by only a small change in the LAT-100 SFC. This could be caused by minor differences in the storage and loss moduli of the compounds at low temperatures, for a similar value of hardness the efficient and semi-efficient curing systems give slightly higher values of the SFC in comparison with the conventional system.

---

## Samenvatting

---

Sinds de introductie van de "Green tire", is silica uitgegroeid tot een van de belangrijkste vulstoffen gebruikt in loopvlak rubbermengsels voor banden vanwege de bijdrage aan een beter milieu. Silica versterkte band-loopvlakken worden niet alleen gekenmerkt door een verlaagde rolweerstand, maar ook door verbeterde natte slip-weerstand in vergelijking met roet als vulmiddel. Echter de verwerking van silica-gevulde mengsels gaat gepaard met vele problemen als gevolg van het verschil in polariteit tussen silica en polymeer. Om deze polariteits-verschillen te overbruggen worden bi-functionele silaan koppelmiddelen (couplingagents) algemeen toegepast. Een typische silaan couplingagent is bis-(triethoxysilylpropyl) tetrasulfide (TESPT). De silaan chemie tijdens de verwerking van rubber is zeer ingewikkeld. Er vinden twee koppelingsreacties plaats, wanneer TESPT wordt gebruikt. De eerste reactie is een koppelingsreactie tussen het TESPT molecuul en het silica oppervlak, de zogenaamde silanisatie-reactie. Voor deze reactie is hydrolyse van TESPT met water vereist, aanwezig op het silica oppervlak. Silaniseren van het silica oppervlak verbetert de verwerking door een aanzienlijke verlaging van het aandrijf-koppel tijdens mengen. De tweede reactie is silaan-rubber koppeling, die bij voorkeur alleen tijdens het vulkaniseren moet plaatsvinden. Het is echter bekend dat TESPT kan functioneren als zwavel-donor tijdens de verwerking van rubber. Daarom kan voortijdige vernetting of aanvulkanisatie (gewoonlijk aangeduid met 'premature scorch') al plaatsvinden bij te hoge temperaturen in de menging. Grote zorg moet worden besteed aan silica compounding door deze te bedrijven in het temperatuurgebied waarin optimale silanisatie kan plaatsvinden en de scorch-reactie wordt geminimaliseerd. Al deze reacties kunnen gelijktijdig plaatsvinden tijdens silica rubberverwerking en derhalve is het versterkings mechanisme van silica veel ingewikkelder van roet.

Het proefschrift begint met een korte geschiedenis van synthetische rubber in **Hoofdstuk 1**, waarin de voordelen van silica t.o.v. roet als versterkende vulstoffen voor rubber en het effect van de couplingagents worden beschreven. In **Hoofdstuk 2** wordt



de invloed van verschillende versterkende vulstoffen, alsook van verschillende couplingagents en rubber-polymeermodificatie op de prestaties van banden gedocumenteerd.

In **Hoofdstuk 3** worden vijf soorten silica, verschillend in het specifieke CTAB oppervlak en aggregaat grootte, getest in een personenauto-band mengsel. Een van de silica's: SSA-200 (het getal geeft het CTAB specifieke oppervlak uitgedrukt in  $m^2/g$ ) heeft ook een andere structuur – de silica aggregaten zijn groter terwijl het specifieke oppervlak vergelijkbaar is met het type SSA-195. De types silica met kleinere totale afmetingen en groter specifiek oppervlak vertonen een hoger versterkend effect, zoals geïllustreerd in verbeterde treksterkte-eigenschappen. Echter, de mengbaarheid van deze silica is moeilijker dan voor de silica types met grotere aggregaten. Mengsels waarin SSA-195 wordt gebruikt, hebben superieure treksterkte-eigenschappen en de laagste verliesmodulus bij lagere temperaturen. Dit type silica resulteert in de hoogste waarden van de Side-Force Coëfficiënt (SFC) in LAT-100 testen, hetgeen de beste grip op nat wegdek indiceert. Aanpassing van de hoeveelheid voor het verkrijgen van een vergelijkbare hardheid van de vulkanisaten leidt tot een omgekeerde volgorde van de dynamische eigenschappen. Silica met de kleinste aggregaten is nog steeds superieur ten aanzien van de SFC. Echter, de trend zichtbaar voor constante silica belading is verdwenen. Dit toont aan dat met betrekking tot de natte grip of slip-weerstand vulstoffen met kleinere aggregaten beter voldoen en dat een hogere lengte-breedte verhouding van de vulstoffen zoals bij type SSA-200 niet bijdraagt tot de natte slipweerstand. Silicas met grotere aggregaten, SSA-80 en SSA-110 leiden tot lage hysteresis bij hoge temperaturen, maar hun lage versterkende werking maakt ze wel minder geschikt als versterkende vulstof voor loopvlak mengsels. De dynamische eigenschappen van materialen met hoog versterkende silica kunnen verder worden verbeterd door minder vulmiddel, maar de trek-rek eigenschappen worden nadelig beïnvloed bij SBR/BR als polymeermatrix. Verder is een goede dispersie van de nano-aggregaten de sleutel om rubbercomposieten met algeheel superieure eigenschappen te verkrijgen. Met de gebruikte meetparameters voor dynamische analyse en voor de

LAT-100, wordt geen correlatie gevonden van de hysteresis bij 0 - 20 °C met de SFC voor beide reeksen experimenten.

De invloed van fysische en chemische vulstof-polymeer bindingen op de performance indicatoren van banden worden onderzocht in **Hoofdstuk 4**. Silica wordt gemengd met 1,6-bis-(triethoxysilyl)hexaan (TESH), om interacties vergelijkbaar met die tussen roet en rubber te verkrijgen. De Bound Rubber Content gegevens bevestigen dit. Het aanbrengen van fysische interacties in plaats van chemische bindingen verlaagt de waarden van de treksterkte drastisch door de inertie van het silica oppervlak. De dynamische eigenschappen van de monsters gemeten bij lage temperatuur komen wederom niet overeen met de natte slipweerstand zoals gemeten met de LAT-100. Vervanging van fysische interacties (TESH) door chemische bindingen (TESPT) tussen rubber en vulstoffen verhoogt de waarden voor de SFC met de LAT-100. Bijgevolg hebben chemische bindingen de voorkeur voor een goede natte slipweerstand van de loopvlakken. De veronderstelling dat onder invloed van energie als gevolg van slippen, polymere moleculen fysisch gebonden aan het vulmiddel oppervlak zich gemakkelijk kunnen heroriënteren, waardoor de energiedissipatie en dus de natte slipweerstand zou toenemen, is niet correct. Daarnaast vertonen de experimenten uitgevoerd door Heinz (Heinz M., J. Rubb. Res., 13 (2010) 91) een sterke correlatie tussen de waarden van de SFC gemeten met LAT 100 en (natte) slip verkregen met weg-testen. Tegelijkertijd wijst hij erop dat er geen correlatie bestaat tussen dynamische metingen en testen op de weg. Bijgevolg bestaat er geen correlatie tussen LAT-100 en dynamische metingen. De tegenstelling tussen de hogere hysteresis van de mengsels bij 0 - 20 ° C, maar desalniettemin lagere waarden van de SFC gemeten met de LAT-100 in het huidige onderzoek, sluiten aan bij de tests gedaan door Heinz. De auteur van het huidige proefschrift neigt naar het gebruik van de LAT-100 als doorslaggevend hulpmiddel bij de beoordeling van het natte slip vermogen van een rubber mengsel.

Bis-(dimethylethoxysilylpropyl)tetrasulfide (DMESPT), een silaan met mogelijk hogere benutting van de silanolgroepen op het silica-oppervlak, wordt onderzocht in **Hoofdstuk 5**. De aanwezigheid van slechts één ethoxy-groep in plaats van drie in de silaan

couplingagent verbetert zowel de natte slip- als rol-weerstand. Een verklaring voor deze effecten is een stijver vulstof-polymeer-grensvlak bij DMESPT ten opzichte van de drie ethoxy-groepen in TESPT, die ethanol afgeven. Deze alcohol blijft gedeeltelijk geadsorbeerd op het grensvlak tussen vulstof en polymeer en beïnvloedt daardoor de eigenschappen van het materiaal. Beide silanen, TESPT en DMESPT, fixeren dezelfde aantallen silanol-groepen op het silica-oppervlak, zoals gemeten met het Payne effect van de onge vulkaniseerde mengsels. Daarom leidt de lagere sterische hindering veroorzaakt door afwezigheid van zijwaardse ethoxy-groepen in het molecuul DMESPT niet tot een hoger aantal gebonden silanol-groepen dan bij TESPT. De vulstof-polymeer wisselwerkingen bepalen de piekhoogte van de  $\tan\delta = f(T)$  curve: hoe geremder de polymeer beweeglijkheid aan het vulmiddel oppervlak, hoe lager de hoogte van de piek; het geïmmobiliseerde polymeer fungeert meer vulstof-achtig dan polymeer-achtig. Bij DMESPT is het polymeer-vulstof grensvlak stijver dan bij TESPT: deze bezit secundaire ethoxy-groepen, die reageren wanneer het materiaal weer wordt opgewarmd tijdens verdere verwerking en splitsen ethanol af, dat zich gedeeltelijk ophoopt aan het grensvlak en dus het energieverlies (aangeduid met  $\tan\delta$ ) verhoogt door desorptie en glijden van de polymeerketens bij lagere temperaturen. Anders dan bij TESPT neemt voor DMESPT de SFC van de monsters toe bij verhoogde silaan-dosering. Meer bewegingsbeperking van de polymeerketens in de glasachtige grenslaag veroorzaakt verhoogde stijfheid bij de mengsel met DMESPT. Een hogere lokale stijfheid rondom de vulstofdeeltjes met hoge DMESPT concentraties leidt tot hogere natte slipweerstand, zoals gemeten met de SFC.

Het effect van de linker-lengte die het siliciumatoom met het sulfidische deel in de silaan couplingagent verbindt, wordt beschreven in **Hoofdstuk 6**. Mengsels die een silaan bevatten met langere linker, bis-(triethoxysilyldecyl) tetrasulfide (TESDeT) worden gekenmerkt door een iets hogere rek bij breuk maar vergelijkbare treksterkte vergeleken met TESPT bevattende mengsels. Een langere en flexibeler linker als bij TESDeT kan grotere deformaties opvangen zonder te breken. Een verhoogde linker lengte van het koppelmiddel vermindert de rolweerstand aanzienlijk, maar niet de natte slipweerstand. De langere linker van TESDeT is geschikt voor hogere deformatie-amplitudes in het vulstof-polymeer grensvlak tijdens vervorming, in plaats van dat ze

deze direct overbrengen op het vulstof-oppervlak. Een langere linker-lengte verhoogt de hysteresis verliezen in het glasovergangstemperatuur bereik van het elastomeer. Een flexibeler linker bij TESDeT leidt tot minder belemmering in de polymeer- bewegingen aan het vulstof-polymeer grensvlak in vergelijking met de referentie silaan TESPT. Derhalve kan meer polymeer bijdragen aan de energiedissipatie verschijnselen op de glasovergangstemperatuur. Door TESPT te vervangen door een silaan met langere linker kan de rolweerstand van het materiaal in een loopvlak worden verbeterd. Echter, het belangrijkste nadeel van TESDeT is het hoge molecuulgewicht: om equimolaire concentraties te verkrijgen moeten grotere hoeveelheden TESDeT worden toegepast dan TESPT.

**Hoofdstuk 7** is gewijd aan de invloed van de reactiviteit van silaan couplingagents naar het silica oppervlak op de loopvlak indicatoren. Twee silanen zonder zijwaardse alkoxy-groepen worden op maat gesynthetiseerd: bis-(dimethylmethoxysilylpropyl)tetrasulfide (MMeOS) en bis-(dimethylmethoxyethoxysilylpropyl)tetrasulfide (MMeOEtOS), en vergeleken in een loopvlak mengsel met TESPT als referentie. Het duidelijke voordeel van deze silanen ten opzichte van TESPT is een aanzienlijk lagere alcohol ontwikkeling gedurende het mengproces, wat niet alleen een positief milieuaspect vertegenwoordigt van de mono-ethoxy silanen, maar ook een verbetering geeft van de verwerking in rubbermengsels. Het type alkoxy-groepen van de silaan couplingagents bepaalt het type alcohol-bijproducten van de silanisatie reactie en dus de kinetiek van de silaniserings-reactie, alsmede de invloed op mengsel verwerking en eigenschappen. Het lage kookpunt van methanol leidt tot een relatief snelle reactie van de genoemde silanen met de silanolgroepen op het silica-oppervlak en vermoedelijk een hogere mate van benutting van de silanolgroepen. Dit kan worden afgeleid uit de lage Payne effect waardes van de overeenkomstige ge vulcaniseerde mengsels. Naast het kookpunt moet een andere belangrijke parameter worden meegenomen betreffende de alcohol ontwikkeld gedurende de silanisering: het vermogen om waterstofbindingen te vormen. De grotere neiging van 2-methoxyethanol bevattende silanen om intra- en intermoleculaire waterstofbindingen te vormen in vergelijking met methanol- of ethanol-bevattende soorten veroorzaakt verhoogde stijfheid van het polymeer-vulstof-grensvlak bij lagere temperaturen, en daardoor hogere SFC-waardes in vergelijking met de

materialen die MMeOS of TESPT bevatten. Door het ontbreken van zijwaardse alkoxy-groepen worden beide monomethoxy- en monomethoxyethoxy-silanen gekenmerkt door lagere waarden van  $\tan\delta$  bij 60 °C ten opzichte van TESPT. Als gevolg van de lagere hoeveelheid alcohol die in de silaan aanwezig is blijft minder alcohol geadsorbeerd aan het polymeer-vulstof grensvlak. Dit vermindert de kans op polymeer korte-segment bewegingen, hetgeen energieverlies reduceert. Het stijvere polymeer-vulstof grensvlak bij MMeOS en MMeOEtOS bij lagere temperaturen verhoogt de stijfheid van het mengsel zoals gemeten met de opslagmodulus. De kracht die nodig is om het loopvlak van een band te vervormen in microholtes in het wegdek is hoger voor stijvere mengsels en resulteert in een verbeterde, hogere SFC ten opzichte van TESPT.

Het effect van drie verschillende zwavel vulkanisatiesystemen wordt beschreven in **Hoofdstuk 8**. Een maximale treksterkte is meest uitgesproken voor een efficiënt vulkanisatiesysteem, en het minst voor een conventioneel systeem. De hoogste waarden in treksterkte voor de monsters met efficiënte vulkanisatie, kunnen worden veroorzaakt door lagere scheurpropagatie van het materiaal met lagere totale crosslinkdichtheid, gecombineerd met een hogere bindings-energie van mono- en disulfidische crosslinks. Het verhogen van de algehele crosslinkdichtheid van de mengsels geeft een verhoging van de glasovergangstemperatuur van ongeveer 5 ° C tussen de mengsels met het efficiënte vs. conventionele vulkanisatie-systeem. Echter, geen grote veranderingen in de hoogte van de  $\tan\delta$ -piek worden waargenomen. Blijkbaar kunnen alleen veranderingen in de immobilisatie van het polymeer op het vulmiddel oppervlak leiden tot veranderingen in de piekhoogte, bijvoorbeeld in het geval van silica's verschillend in specifiek oppervlak of gebruik van verschillende couplingagents. De waarden van  $\tan\delta$  bij 60°C nemen af bij toenemende totale crosslinkdichtheid van de mengsels. Deze trend is onafhankelijk van de crosslink types, aangezien bij het rek-niveau toegepast in de meting het vermogen tot recombinate van langere poly-sulfidisch crosslinks nog geen rol speelt. De mengsels met de verschillende vulkanisatiesystemen worden gekenmerkt door slechts een kleine verandering in de LAT-100 SFC. Dit zou kunnen worden veroorzaakt door kleine verschillen in de opslag en verlies moduli van de mengsels bij lage temperaturen; bij vergelijkbare hardheid

geven de efficiënte en semi-efficiënte vulkanisatiesystemen iets hogere waardes van de SFC ten opzichte van het conventionele systeem.

**Publications and papers**

---

1. E. Cichomski, A. Blume, W.K. Dierkes, J.W.M. Noordermeer, T.V. Tolpekina, S. Schultz, "Influence of Silica-Polymer Bond Microstructure on Tire-Performance Indicators" *Kautschuk und Gummi Kunststoffe* 68 (2015) 38.
2. E. Cichomski, W.K. Dierkes, T.V. Tolpekina, S. Schultz, "Influence of physical and chemical polymer-filler bonds on tire wet-traction performance indicators for passenger car tire tread materials" *Kautschuk und Gummi Kunststoffe*, 67 (2014) 50.
3. E. Cichomski, T.V. Tolpekina, Steven Schultz, Jacques W.M. Noordermeer, W.K. Dierkes, Anke Blume 11<sup>th</sup> Fall Rubber Colloquium, 26-28 November 2014, Hannover, Germany.
4. W.K. Dierkes, E. Cichomski, T.V. Tolpekina, S. Schultz, A. Blume, J.W.M. Noordermeer "Influence of Silica Characteristics on Tire Performance Indicators" 185<sup>th</sup> Technical Meeting of the Rubber Division ACS, 14-16 October 2014, Nashville, Tennessee, USA.
5. W.K. Dierkes, E. Cichomski, W. Kawesakul, S.S. Sarkawi, S. Schultz, T.V. Tolpekina, K. Sahakaro, J.W.M. Noordermeer, "Filler - coupling agent - polymer interactions and their significance for tire performance" 15. Tagung der Bezirksgruppe Nord "automobil for the future" 28-29 November 2013, Hamburg, Germany.

6. E. Cichomski, T.V. Tolpekina, S. Schultz, W.K. Dierkes, J.W.M. Noordermeer, "Structural influences of silane coupling agents on the dynamic properties of a SBR / silica compound" 184<sup>th</sup> Technical Meeting of the Rubber Division ACS, 8-10 October 2013, Cleveland, Ohio, USA.
7. E. Cichomski, T.V. Tolpekina, S. Schultz, W.K. Dierkes, J.W.M. Noordermeer, "Influence of the silica surface area and structure on rolling and wet skid resistance of a passenger car tire tread" Eurofillers 2013, 25-29 August 2013, Bratislava, Slovakia.
8. E. Cichomski, T.V. Tolpekina, S. Schultz, W.K. Dierkes, J.W.M. Noordermeer, "Structural influences of silane coupling agents on the dynamic properties of a SBR / silica compound" 29<sup>th</sup> Polymer Processing Society, 15-19 July 2013, Nürnberg, Germany.
9. E. Cichomski, T.V. Tolpekina, S. Schultz, W.K. Dierkes, J.W.M. Noordermeer, "Influence of the structure of silane coupling agent on wet skid and rolling resistance of passenger car tire treads" European PhD Seminar, 13-14 June 2013, Łódź, Poland.
10. W.K. Dierkes, E. Cichomski, W. Kaewsakul, S.S. Sarkawi, S. Schultz, T.V. Tolpekina, K. Sahakaro, J.W.M. Noordermeer, "A scientific view on silica technology: filler - coupling agent - polymer interactions and their significance for tire performance" 183<sup>rd</sup> Technical Meeting of the Rubber Division ACS, 22-24 April 2013, Akron, Ohio, USA.
11. E. Cichomski, W.K. Dierkes, J.W.M. Noordermeer, T.V. Tolpekina, S. Schultz, "Influence of physical and chemical polymer-filler bonds on wet skid resistance and related properties of passenger car tire treads" Deutsche Kautschuk-Tagung 2012, 2-5 July 2012, Nürnberg, Germany.



12. E. Cichomski, W.K. Dierkes, J.W.M. Noordermeer, T. V. Tolpekina, S. Schultz  
"Influence of physical and chemical polymer-filler bonds on wet skid resistance of the passenger car tire treads" Elastomery 2011, 23-25 November 2011 Warsaw, Poland.
13. E. Cichomski "Influence of chemical or physical filler-polymer interactions on the wet skid resistance of silica filled SBR-BR blends" presentation at the PhD-workshop IPF/UT/MLU/TUL/ContiTech, 6-8 June 2011, Hannover, Germany.

---

## Symbols and abbreviations

---

| <b><u>Symbol</u></b> | <b><u>Abbreviation</u></b>                      |
|----------------------|---|
| H                    | hysteresis                                      |
| $\gamma$             | shear strain                                    |
| $\gamma(t)$          | sinusoidal shear deformation                    |
| $\omega$             | angular frequency                               |
| $\sigma(t)$          | sinusoidal shear stress response of a material  |
| $\gamma_0$           | maximum strain amplitude                        |
| $\sigma_0$           | shear response at maximum strain                |
| t                    | time  |
| G'                   | storage modulus                                 |
| G''                  | loss modulus                                    |
| $\delta$             | loss angle                                      |
| $\tan \delta$        | mechanical loss tangent                         |
| BR                   | butadiene rubber                                |
| CBS                  | N-cyclohexyl-2-benzothiazole sulphenamide       |
| TMTD                 | tetramethylthiuramdisulphide                    |
| DPG                  | diphenyl guanidine                              |
| EtO                  | ethoxy  |
| MeO                  | methoxy   |
| EtOH                 | ethanol   |
| MeOH                 | methanol  |
| NR                   | natural rubber                                  |
| phr                  | parts per hundred rubber                        |
| ppm                  | parts per million                               |
| C-BR                 | conventional vinyl content polybutadiene rubber |
| V-BR                 | high vinyl content polybutadiene rubber         |

|               |  |
|---------------|--|
| RPA           | rubber process analyser                      |
| T             | temperature                                  |
| TESPD         | bis(triethoxysilylpropyl) disulphide         |
| TESPT         | bis(triethoxysilylpropyl) tetrasulphide      |
| TMTD          | tetramethylthiuram disulphide                |
| TESH          | bis(triethoxysilyl)hexane                    |
| DMESPT        | bis-(dimethylethoxysilylpropyl) tetrasulfide |
| ZnO           | zinc oxide                                   |
| E-SBR         | emulsion styrene butadiene Rubber            |
| $T_g$         | glass transition temperature                 |
| LAT 100       | laboratory abrasion tester 100               |
| $\phi$        | volumetric concentration of the particles    |
| $\eta_0$      | viscosity of the pure liquid                 |
| $\eta$        | viscosity of the suspension                  |
| E             | elasticity modulus                           |
| $k_B$         | Boltzmann constant                           |
| $\nu$         | crosslink density                            |
| $M_{100}$     | stress at 100 % strain                       |
| $M_{300}$     | stress at 300 % strain                       |
| CV            | conventional vulcanization                   |
| S-EV          | semi-efficient vulcanization                 |
| EV            | efficient vulcanization                      |
| DSA           | dynamic strain deformation                   |
| H-bonds       | hydrogen bonds                               |
| $pK_a$        | logarithmic acid dissociation constant       |
| CTAB          | cetyl trimethylammonium bromide              |
| $\gamma_s$    | surface energy                               |
| $\gamma^d$    | dispersive surface energy                    |
| $\gamma^{sp}$ | specific surface energy                      |
| OE SBR        | oil extended styrene butadiene rubber        |
| MMT           | montmorillonite                              |

|       |   |
|-------|---|
| MBT   | mercaptobenzothiazyl                                  |
| MBTS  | mercaptobenzothiazyl disulfide                        |
| XNBR  | carboxylated nitrile butadiene rubber                 |
| DBP   | dibutyl phthalate adsorption                          |
| BET   | specific surface area measured by nitrogen adsorption |
| $k_a$ | primary kinetic rate constants                        |
| $k_b$ | secondary reaction rate constants                     |
| MPTMS | (3-mercaptopropyl) trimethoxysilane                   |
| THF   | tetrahydrofurane                                      |
| CHX   | cyclohexane   |
| AIBN  | azobisisobutyronitrile                                |
| DIN   | Deutsches Institut für Normung                        |

## ***Curriculum Vita***

Ernest Cichomski grew up together with two older sisters and their parents in Lodz, Poland. Due to his technical interest, he attended a school for motor vehicle engineering (high-school with technical specification) that he graduated from in 2003 as an automobile technician and obtained university entrance qualification with high final grade in chemistry.

2003 he started at the University of Technology in Lodz, Poland and graduated in 2009 with a master's degree in materials engineering with a major in polymer materials. His master thesis was on silica filled dental composites (silane coupling agents) and thus allowed him to gain in depth knowledge of polymer chemistry.

2010 he then had the chance to enter a PhD programme at the University of Twente in Enschede, Netherlands. Since then he has been working as a researcher at the university with a focus on engineering technology of elastomers. At the same time he supervised Master student in writing their thesis and supporting other fellow PhD candidates. Furthermore, he organized and attended multiple conferences, especially on polymer topics. In the past 4 years he has done extensive research on rubber compounding, working closely not only with the university but also with Apollo Global Tyres R&D in Enschede on project related with the improvement of the rolling resistance, tire wet-traction etc. with corresponding publications.

## ***Acknowledgments***

I would have never been able to finish my dissertation without guidance from my committee members, help from my friends, and support from my family. I would like to express my deepest gratitude to my co-promotor Dr. Dierkes, for her excellent guidance, caring and patience, and for providing me with the optimal atmosphere for doing research, not forgetting of course her persistent corrections of my writing. I would like to thank my promotor Professor Noordermeer, who helped me experience research beyond the textbooks and inspired me to develop good ideas and interpretations of my results. I would also like to thank Professor Blume for her valuable advice and the intellectual discussions during the final stage of the project.

I would like to thank my good friend Jacob Lopulissa, who was always willing to help by giving me his best suggestions not only on a professional level but also on a private plane. The lab would have been a lonely place without him. Special thanks go to André Louis and Nadia Vleugels, who were always supporting me with their friendship. Our discussions of work and research were provided with comic relief in jokes and light comments that resonated through our offices. I hope we will all meet again somewhere in the world of rubber.

I would also like to thank my parents and two sisters. They were always supporting me and encouraging me with their best wishes. Finally, I would like to thank my life partner, Rima Cortbawi. Thank you for your generous and loving support. You have always been there cheering me up and standing by my side through the good and bad times.